POLITECHNIKA WARSZAWSKA

BIOTECHNOLOGIA

NAUKI ŚCISŁE I PRZYRODNICZE

ROZPRAWA DOKTORSKA

mgr inż. Sylwia Pniewska

(z d. Karoń)

Opracowanie modyfikowalnych platform biosensorowych
do wieloparametrowej immunodetekcji wybranych
biomarkerów związanych z infekcjami wirusowymi

Promotor

prof. dr hab. inż. Elżbieta Malinowska

Promotor pomocniczy

dr inż. Marcin Drozd

WARSZAWA 2025

Badania będące podstawą niniejszej Rozprawy Doktorskiej zostały sfinansowane:

w ramach **projektu „Inicjatywa Doskonałości - Uczelnia Badawcza" (1820/102/Z01/2023)**

Konstrukcja uniwersalnego, przenośnego urządzenia mikrofluidycznego działającego w formacie pasywnego przepływu do szybkiej immunodetekcji zakażeń wirusowych i monitorowania wybranych biomarkerów odpowiedzi immunologicznej

projektu Narodowego Centrum Badań i Rozwoju

(POIR.01.01.01-00-0638/20)

Opracowanie konstrukcji i technologii wytwarzania miniaturowych urządzeń diagnostycznych do szybkiego wykrywania wirusa SARS-CoV-2 w trybie POCT

oraz programu Mobility PW

Składam serdeczne podziękowania moim Promotorom, **prof. dr hab. inż. Elżbiecie Malinowskiej** za ciepłe przyjęcie w Jej grupie badawczej, merytoryczne i duchowe wsparcie oraz cenne wskazówki naukowe.

oraz

dr inż. Marcinowi Drozdowi, bez którego ta praca nie miałaby szans powstać. Przede wszystkim za nieocenione wsparcie na każdym etapie realizowania rozprawy doktorskiej pod jego opieką naukową, chęć do pomocy, okazaną mi wyrozumiałość, codziennie towarzystwo i przekazaną wiedzę.

Dziękuję również

Polinie Ivanovej, **Adrianowi** Duszczykowi, **Ani** Szymczyk-Drozd, **Monice** Śmigielskiej, **Marcinowi** Filipiakowi oraz **Lorico** Lapitanowi za wsparcie emocjonalne, które mi okazali w trakcie „doktoratowej" drogi.

Pani **Ewie Szczygieł** oraz Pani **Renacie Jaczewskiej** za gotowość do rozwiązania każdej, nawet najbardziej zawiłej sprawy związanej ze Szkołą Doktorską.

Paulinie i **Maćkowi Trzaskowskim** za wspierające i serdeczne kuchenne rozmowy w CEZAMAT.

Grupie Badawczej z instytutu SITEC w Mediolanie– **Marcelli**, **Dario**, **Federice, Allessandro** i **Francesco** za umożliwienie odbycia mojego wyjazdu naukowego i cudowną atmosferę, którą tworzą w zespole.

Moim kochanym **Rodzicom Iwonce** i **Włodkowi** oraz **Babci Basi** za ich obecność, pamięć o ważnych sprawach i wspierające rozmowy.

A na koniec mojemu mężowi **Karolowi** – to dzięki Tobie mogłam zrealizować ten cel.

Streszczenie Rozprawy Doktorskiej

Opracowanie modyfikowalnych platform biosensorowych
do wieloparametrowej immunodetekcji wybranych
biomarkerów związanych z infekcjami wirusowymi

mgr inż. Sylwia Pniewska
Szkoła Doktorska Politechniki Warszawskiej,
Katedra Biotechnologii Medycznej, Wydział Chemiczny,
Politechnika Warszawska

Diagnostyka medyczna jest fundamentem współczesnej medycyny, a postęp technologiczny umożliwił opracowanie zaawansowanych platform diagnostycznych, które pozwalają na jednoczesne wykrywanie wielu biomarkerów użytecznych z punktu widzenia wczesnego wykrywania chorób. Takie wieloparametrowe podejście, określane jako *multiplex,* znajduje zastosowanie w testach realizowanych w miejscu opieki nad pacjentem (*Point-of-Care Testing*, POCT). Kluczowym elementem platform diagnostycznych są warstwy receptorowe, odpowiedzialne za selektywne wiązanie analitów z powierzchnią. Ich funkcjonalność i powtarzalność wytwarzania jest warunkiem osiągnięcia wiarygodnych rezultatów procedury analitycznej. Istotnym jest zatem zaproponowanie nowoczesnych metodyk wytwarzania testów diagnostycznych w formacie *multiplex,* łączących wysoką jakość uzyskiwanych warstw receptorowych oraz technologiczną wygodę ich wytwarzania, najlepiej w jednoetapowym procesie.

Celem niniejszej rozprawy doktorskiej było opracowanie nowoczesnych strategii wytwarzania i charakteryzacji białkowych warstw receptorowych dedykowanych multipleksowej detekcji biomarkerów związanych z zakażeniami wirusowymi. Realizacja tego celu obejmowała badania nad różnymi aspektami procesu immobilizacji białek i konstrukcji immunotestów, m. in. za pomocą rezonansu plazmonów powierzchniowych (*Surface Plasmon Resonance, SPR*).

Badania rozpoczęto od analizy opisanych w literaturze metod immobilizacji białek, umożliwiających unieruchamianie bioreceptorów na różnych podłożach. Z uwagi na oferowane możliwości wytwarzania macierzy warstw receptorowych zbudowanych z różnych białek z wykorzystaniem powinowactwa biologicznego w jednoetapowym procesie, jako wiodącą strategię wytypowano unieruchomienie za pomocą kotwic DNA (*DNA-directed*

immobilization, DDI). Wskazano luki badawcze w dotychczasowym stanie wiedzy na temat tej metody i przyjęto hipotezę, według której pogłębiona charakteryzacja różnych aspektów procesu wytwarzania warstw poprzez DDI może przyczynić się do uzyskania lepszej jakości warstw receptorowych zdolnych do bardziej efektywnego wychwytu cząsteczek analitu.

Podczas prac eksperymentalnych zweryfikowano istotność wpływu składu monowarstwy zawierającej sondy ssDNA oraz czystości i stechiometrii koniugatów DNA-białko na stabilność i gęstość powierzchniową warstw receptorowych. Wykazano, że jednoskładnikowe monowarstwy nie chronią skutecznie przed niespecyficzną adsorpcją białek, podczas gdy mieszanie sond z długołańcuchowymi ligandami może utrudniać zakotwiczenie koniugatów DNA-białko. Ponadto potwierdzono przewagę klasycznych sond DNA nad ich analogami. Badania przeprowadzono z użyciem modelowych receptorów należących do dwóch odrębnych grup białek; białka nukleokapsydu wirusa SARS-CoV-2 oraz przeciwciał klasy IgG. Wybór ten miał na celu zademonstrowanie uniwersalności projektowanej platformy pod względem diagnostycznym ze względu na specyficzne funkcje i właściwości wykrywanych biomarkerów.

Istotnym etapem badań było opracowanie nieniszczącej metody kontroli jakości białkowych warstw receptorowych, kompatybilną z SPRi w formacie mikromacierzowym. Zaproponowano nowatorską, do tej pory nieopisaną strategię odwracalnego znakowania białek na powierzchni barwnikami anionowymi takimi jak błękit brylantowy Coomassie G-250, czerń amidowa 10B czy róż Ponceau S. Udowodniono, że podejście to umożliwia mapowanie gęstości powierzchniowej receptorów i stanowi prostszą oraz bardziej ekonomiczną alternatywę dla klasycznego immunoznakowania białek.

Kolejny etap badań dotyczył zaprojektowania jednoetapowych strategii unieruchamiania receptorów białkowych na potrzeby testów diagnostycznych z detekcją znacznikową (enzymatyczną). Wykorzystano w tym celu amino- oraz DBCO-reaktywne kopolimery uzyskane w ramach współpracy naukowej z Instituto di Scienze e Tecnologie Chimiche w Mediolanie. Kopolimery te wykorzystano do powlekania folii PET a uzyskane reaktywne podłoża użyto w konstrukcji planarnych, elastycznych immunoplatform. Efektem zrealizowanych badań jest zweryfikowana użyteczność platform w analizie próbek rzeczywistych (surowicy krwi) na potrzeby diagnostyki serologicznej COVID-19. Zaprojektowany test immunoenzymatyczny na podłożu PET umożliwił wykrycie przeciwciał przeciwko nukleoproteinie wirusa SARS-CoV-2 oferując 100,0% czułość i 92,9% swoistość w ujęciu diagnostycznym. Dodatkowo, wykorzystując unieruchomienie receptorów za pomocą

DDI, zademonstrowano możliwość konstrukcji wieloparametrowych immunoplatform na podłożach PET.

W niniejszej pracy zintegrowano techniki detekcji znacznikowej i bezznacznikowej, wykorzystując SPR zarówno jako metodę detekcji, jak i skuteczne narzędzie charakteryzacji warstw immunoreceptorowych. Pozwoliło to na lepsze zrozumienie procesów zachodzących na powierzchni podczas etapów wytwarzania immunotestów i oddziaływania ze składnikami próbek. Takie nieoczywiste podejście może przyczynić się do postępu w tworzeniu powtarzalnych i funkcjonalnych warstw receptorowych, które mogą znaleźć zastosowanie zarówno w klasycznych platformach diagnostycznych, jak i w nowoczesnych urządzeniach POCT.

słowa kluczowe: diagnostyka medyczna**,** warstwy receptorowe, mikromacierze białkowe, immunoplatformy, rezonans plazmonów powierzchniowych, biomarkery serologiczne, kontrola jakości receptorów białkowych, gęstość powierzchniowa białek, reaktywne kopolimery

Summary of the Doctoral Thesis

Development of customizable biosensing platforms
for multiplex immunodetection of selected
biomarkers associated with viral infections

M.Sc. Eng. Sylwia Pniewska
Doctoral School of Warsaw University of Technology
Chair of Medical Biotechnology, Faculty of Chemistry,
Warsaw University of Technology

Medical diagnostics form the cornerstone of modern medicine, with technological advancements enabling the development of sophisticated diagnostic platforms capable of simultaneously detecting multiple biomarkers critical for early disease diagnosis. This multi-parameter approach, known as multiplexing, mainly applies to point-of-care testing (POCT). A crucial component of such diagnostic platforms is the receptor layer, which ensures the selective binding of analytes to the surface. The functionality and reproducible fabrication of these layers are essential for obtaining reliable analytical results. Therefore, developing innovative methodologies for producing multiplex diagnostic assays that combine high receptor layer quality with technological convenience is imperative, ideally through a streamlined, single-step process.

This dissertation focuses on developing novel strategies for fabricating and characterizing protein receptor layers tailored to detect multiplex viral infection biomarkers. The research encompassed various aspects of protein immobilization and immunoassay design, particularly on surface plasmon resonance (SPR) analysis.

The study commenced with a comprehensive review of protein immobilization strategies described in the literature for anchoring bioreceptors onto different substrates. Given the potential to generate a matrix of receptor layers composed of different proteins in a single step using biological affinity, DNA-directed immobilization (DDI) was selected as the primary approach. Research gaps in the existing state of the art were identified, leading to the hypothesis that a detailed characterization of DDI-based receptor layer fabrication could enhance the quality and efficiency of analyte capture.

Experimental investigations examined the impact of various factors on receptor layer stability and surface density, including the composition of monolayers containing single-

stranded DNA (ssDNA) probes and the purity and stoichiometry of DNA-protein conjugates. The findings demonstrated that single-component monolayers do not sufficiently prevent non-specific protein adsorption. At the same time, including long-chain ligands in mixed probes can hinder the anchoring of DNA-protein conjugates. Moreover, classical DNA probes were shown to outperform their analogues. Studies were conducted using model receptors representing two distinct groups of proteins: the nucleocapsid protein of SARS-CoV-2 and IgG-class antibodies. This selection aimed to demonstrate the versatility of the developed platform for diagnostic applications based on the unique functions and properties of the detected biomarkers.

A significant aspect of this research was developing a non-destructive quality control method for protein receptor layers compatible with SPR imaging (SPRi) in a microarray format. A novel, previously unreported strategy for reversibly labeling surface-bound proteins using anionic dyes—such as Coomassie Brilliant Blue G-250, Amido Black 10B, and Ponceau S—was introduced. This approach enabled precise mapping of receptor surface density, providing a more straightforward and cost-effective alternative to conventional protein immunolabeling techniques.

In the subsequent research phase, one-step strategies for protein receptor immobilization were designed for diagnostic assays employing enzymatic detection. This work was conducted in collaboration with the Instituto di Scienze e Tecnologie Chimiche in Milan and involved using amine- and DBCO-reactive copolymers to functionalize PET foils. These reactive substrates were then employed to construct planar, flexible immunoplatforms. The developed platforms were validated for real sample analysis, specifically in COVID-19 serological diagnostics. The immunoenzymatic assay on PET substrates demonstrated 100.0% sensitivity and 92.9% specificity in detecting antibodies against the SARS-CoV-2 nucleoprotein. The feasibility of constructing multi-parameter immunoplatforms on PET substrates using DDI-mediated receptor immobilization was also confirmed.

This research contributes to the advancement of multiplexed immunodiagnostics by proposing innovative receptor layer fabrication strategies that improve analytical reliability while simplifying production processes. The findings hold significant potential for enhancing POCT applications in infectious disease diagnostics.

keywords: medical diagnostics, receptor layers, protein microarrays, immunoplatforms, surface plasmon resonance, serological biomarkers, quality control of protein receptors, protein surface density, reactive copolymers

Spis treści

Wykaz publikacji będących podstawą Rozprawy Doktorskiej

mgr inż. Sylwia Pniewska
Identyfikator ORCID: 0000-0003-0125-3248
Identyfikator Scopus: 57223039505
Indeks Hirscha (h-index, wg Scopus): 3

P1 Recent Advancements in Receptor Layer Engineering for Applications in SPR-Based Immunodiagnostics. Drozd, M., Karoń, S., Malinowska, E., Sensors, 2021, 21(11), 3781, https://doi.org/10.3390/s21113781
IF_{2020} = 4.43

P2 A Careful Insight into DDI-Type Receptor Layers on the Way to Improvement of Click-Biology-Based Immunosensors. Karoń, S., Drozd, M., Malinowska, E., Biosensors, 2024, 14(3), 136, https://doi.org/10.3390/bios14030136
IF_{2023} = 5.18

P3 A Versatile Approach to Quality Control of Protein-based Receptor Layers by Reversible, Nonspecific Staining for Multiplex SPRi Immunosensing. Karoń, S., Porycka, K., Lapitan, Jr, L.D., Drozd, M., Pietrzak, M., Malinowska, E., Sensors and Actuators B: Chemical, 2024, 421, 136512, https://doi.org/10.1016/j.snb.2024.136512
IF_{2023} = 8.46

P4 PET Foils Functionalized with Reactive Copolymers as Adaptable Microvolume ELISA Spot Array Platforms for Multiplex Serological Analysis of SARS-CoV-2 Infections. Pniewska, S.; Drozd, M.; Mussida, A.; Brambilla, D.; Chiari, M.; Rastawicki, W.; Malinowska, E., Sensors 2024, 24, 7766, https://doi.org/10.3390/s24237766
IF_{2023} = 4.25

Wykaz skrótów

Ab – przeciwciało

ALP – fosfataza alkaliczna

APTES – (3-aminopropylo)trietoksysilan

BSA – albumina surowicy bydlęcej

CBB-G – Coomassie błękit brylantowy G-250

CCD – matryca elementów światłoczułych

CMD – karboksymetydekstran

DBCO – dibenzocyklooktyn

DDI – immobilizacja za pomocą kotwic DNA (*DNA-directed immobilization*)

DMA – N,N-dimetyloakrylamid

EDC – chlorowodorek N-(3-dimetyloaminopropylo)-N′-etylokarbodiimidu

ELISA – test immunoenzymatyczny

Gly – glicyna

HRP – peroksydaza chrzanowa

MAPS – metakrylan 3-(trimetoksysililo)propylu

MCH – 6-merkaptoheksanol

NAS – akryloiloksysukcynimid

NHS – N-hydroksysukcynimid

NP/N – białko nukleokapsydu

PBST – sól fizjologiczna buforowana fosforanami z dod. 0,05% Tween-20

PEG – poli(glikol etylenowy)

PET – poli(tereftalan etylenu)

PNA – kwas peptydonukleinowy

POCT – testy realizowane w miejscu opieki nad pacjentem

PS – róż Ponceau S

QCM – mikrowaga kwarcowa

QDs – kropki kwantowe

RBD – domena wiążąca receptor

RI – współczynnik załamania światła

S – białko kolca

SAM – samozorganizująca się monowarstwa

SERS – powierzchniowo wzmocniona spektroskopia ramanowska

SPR – rezonans plazmonów powierzchniowych

SPRi – rezonans plazmonów powierzchniowych z obrazowaniem

ssDNA – DNA jednoniciowe

ZNA – modyfikowane kwasy nukleinowe ZIP (z ang. *zip nucleic acid*)

Rozdział 1

1. Wprowadzenie w problematykę podjętych badań

Diagnostyka medyczna stanowi jeden z filarów współczesnej medycyny, umożliwiając wczesne wykrywanie chorób oraz monitorowanie ich przebiegu. Identyfikacja nowych biomarkerów, takich jak białka, stanowi ważne i aktualne wyzwanie w kontekście rozwoju diagnostyki medycznej. Analiza obecności oraz stężenia biomarkerów w płynach ustrojowych lub tkankach dostarcza informacji o stanie chorobowym, na przykład o trwającym stanie zapalnym, oraz pozwala na precyzyjne określenie etiologii danej jednostki chorobowej.

Obserwowany na przestrzeni ostatnich lat postęp technologiczny pozwolił na rozwój zaawansowanych platform diagnostycznych w formacie mikromacierzowym. Pozwalają one na jednoczesne wykrywanie wielu analitów w czasie jednej analizy, co czyni je szczególnie przydatnymi w kontekście szybkiej diagnostyki w miejscu opieki nad pacjentem (z ang. *Point-of-Care Testing, POCT*). Odpowiednio dobrane matryce warstw receptorowych, odpowiadających za selektywne wiązanie wykrywanych biomarkerów, stanowią kluczowy element wytwarzanych platform. Właściwe zaprojektowanie i wysoka jakość wytwarzanych warstw powinny zapewnić skuteczne wiązanie docelowych analitów oraz powtarzalność wyników.

Detekcja wieloparametrowa (z ang. *multiplex*) jest obiecującym kierunkiem nowoczesnej diagnostyki, jednak jej dalszy rozwój wymaga przezwyciężenia istotnych wyzwań technologicznych, w szczególności związanych z immobilizacją wielu receptorów na jednej matrycy. Mając na uwadze aktualny stan wiedzy, dostrzegam potrzebę znajdowania nowych rozwiązań i dalszego doskonalenia procesów wytwarzania warstw immuno-receptorowych podczas projektowania testów multipleksowych na potrzeby diagnostyki medycznej.

Wyniki badań stanowiących podstawę niniejszej rozprawy doktorskiej zostały przedstawione w ramach cyklu 4 artykułów naukowych. Przeprowadzone przeze mnie badania dotyczyły opracowania nowych oraz udoskonalania istniejących strategii unieruchamiania receptorów białkowych w nowatorskich immunoplatformach diagnostycznych do detekcji wieloparametrowej, jak również zaproponowania nowej, uniwersalnej metody kontroli ich jakości.

Na drodze do realizacji założonego celu przeanalizowane zostały dostępne metody immobilizacji białek. Do badań wybrano te, które umożliwiają unieruchamianie bioreceptorów na różnych podłożach w reakcji jednoetapowej, ze szczególnym uwzględnieniem immobilizacji za pomocą kotwic DNA (z ang. *DNA-directed immobilization, DDI*). Jako modelowe anality związane z zakażeniami wirusowymi wybrano białka wirusa SARS-CoV-2 (biomarkery antygenowe) oraz przeciwciała wytworzone przez gospodarza w odpowiedzi na infekcję (biomarkery serologiczne). W pierwszym etapie badań zweryfikowano istotność wpływu składu monowarstwy zawierającej kotwice ssDNA na stabilność i gęstość powierzchniową warstw receptorowych immobilizowanych poprzez DDI za pomocą rezonansu plazmonów powierzchniowych (z ang. *Surface Plasmon Resonance, SPR*) w wariancie z obrazowaniem (z ang. *Imaging, SPRi*). Następnie opracowano nowatorską, nieopisaną do tej pory w literaturze, metodę kontroli jakości warstw receptorowych mikromacierzy SPRi, wykorzystującą odwracalne znakowanie immobilizowanych białek barwnikami anionowymi. Końcowy etap pracy obejmował zaprojektowanie multipleksowych immunoplatform opartych na detekcji znacznikowej z wykorzystaniem enzymatycznego znakowania. Bazując na elastycznych podłożach, takich jak folie PET funkcjonalizowane reaktywnymi kopolimerami, opracowano rozwiązania kompatybilne z technologią *lab-on-a-foil*, co dodatkowo rozszerza możliwości ich zastosowań w nowoczesnej diagnostyce wieloparametrowej.

1.1 Diagnostyka medyczna infekcji wirusowych

Choroby zakaźne pozostają jedną z głównych przyczyn zgonów i zachorowań na świecie, przy czym istotną ich część stanowią infekcje wirusowe. W ostatnich dekadach zaobserwowano zarówno pojawianie się nowych typów patogenów, jak i powrót wcześniej znanych wirusów oraz związanych z nimi chorób. Przykładami są wirusy Ebola i Zika, a także niedawna pandemia SARS-CoV-2, która zakłóciła funkcjonowanie światowych systemów opieki zdrowotnej [1, 2]. Potrzeba opracowania szybkich, niezawodnych i czułych narzędzi diagnostycznych do wykrywania infekcji wirusowych stała się bardziej znacząca niż kiedykolwiek wcześniej. Wczesna identyfikacja zakażeń odgrywa kluczową rolę w zapobieganiu wybuchom epidemii, zapewnianiu odpowiedniego leczenia oraz prowadzeniu ukierunkowanych działań na rzecz zdrowia publicznego. Ze względu na ciągłą ewolucję wirusów, metody diagnostyczne wymagają stałego udoskonalania i adaptacji do nowych zagrożeń [3, 4]. Tradycyjne metody często trudno szybko dostosować do nowych analitów,

co ogranicza ich zastosowanie wobec pojawiających się szczepów wirusów. W odpowiedzi na te wyzwania, istniejące podejścia są systematycznie doskonalone, aby sprostać dynamicznie zmieniającym się potrzebom diagnostyki.

1.1.1 Biomarkery zakażeń wirusowych

Biomarkery zakażeń wirusowych dostarczają kluczowych informacji o zaawansowaniu infekcji, jej nasileniu oraz odpowiedzi immunologicznej gospodarza. Umożliwiają również ocenę ryzyka powikłań poinfekcyjnych, wspierając diagnostykę i leczenie [5]. Wirusy, mimo stosunkowo prostej budowy, ograniczonej do kwasów nukleinowych i białek strukturalnych, wywołują infekcje o złożonych i często dalekosiężnych skutkach [6, 7]. Skutkiem postępu infekcji u gospodarza są skomplikowane i zróżnicowane reakcje immunologiczne, które obejmują zarówno odporność wrodzoną, jak i adaptacyjną, prowadząc do rozwoju stanu zapalnego [8]. Do tej pory zidentyfikowano ponad 1500 wirusów ludzkich i zwierzęcych, które wykazują dużą różnorodność pod względem struktury, składu i genomu [9]. Liczba wirusów, złożoność procesów infekcji i wywoływanych przez nie odpowiedzi odpornościowych przekładają się na szeroką gamę dostępnych biomarkerów. Wśród nich znajdują się zarówno wirusowe białka i kwasy nukleinowe, jak i cząsteczki pochodzące od gospodarza, takie jak cytokiny [10], białka ostrej fazy [11, 12] miRNA [13] pęcherzyki zewnątrzkomórkowe [14] i różne klasy oraz podklasy immunoglobulin [15, 16].

Cząsteczki pochodzące bezpośrednio od wirusa są najbardziej oczywistymi wskaźnikami zakażenia. Obejmują one wirusowe DNA lub RNA i białka strukturalne, które ulegają ekspresji podczas replikacji i infekcji wirusowej. Testy molekularne, wykorzystujące technikę amplifikacji kwasów nukleinowych (z ang. *nucleic acid amplification tests, NAAT*), cechują się wysoką czułością i specyficznością. Stanowią one powszechnie stosowaną metodę wykrywania biomarkerów genetycznych wirusów [17]. Wśród nich możemy wyróżnić testy PCR (z ang. *polymerase chain reaction*), wykorzystywane do detekcji m. in. wirusowego DNA (np. herpeswirusów [18] wywołujących opryszczkę czy pokswirusów [19] odpowiedzialnych za ospę prawdziwą), lub RT-PCR (z ang. *reverse transcription PCR*), używane do wykrywania wirusowego RNA (np. wirusów wywołujących grypę [20] czy koronawirusów [21] Oprócz testów jakościowych, wirusowe kwasy nukleinowe o unikalnych sekwencjach mogą być oznaczane ilościowo za pomocą qPCR lub RT-qPCR (z ang. *quantitative PCR/RT-PCR*), czyli amplifikacji w czasie rzeczywistym [22]. Takie testy dostarczają informacji na temat wiremii -

kluczowego czynnika w monitorowaniu stopnia zaawansowania infekcji [23]. Na przykład, w diagnostyce HIV ilościowe oznaczanie wirusowego RNA służy do monitorowania postępu choroby oraz oceny skuteczności terapii antyretrowirusowej [24].

Białka strukturalne wirusów, takie jak białka nukleokapsydu (N) lub kolca (S), są powszechnie stosowane w testach diagnostycznych zarówno w roli analitów (testy antygenowe), jak i bioreceptorów (testy serologiczne). W przypadku wirusa SARS-CoV-2, białko S jest odpowiedzialne za wnikanie wirusa do komórek gospodarza. Białko N odgrywa kluczową rolę w upakowywaniu genomu wirusa, a jego ekspresja osiąga najwyższy poziom spośród wszystkich białek wirusa podczas infekcji. Ze względu na wysokie stężenie i występowanie wspomnianych białek już w początkowej fazie zakażenia, są one wiarygodnymi biomarkerami przydatnymi do wczesnego wykrywania infekcji [25-27]. Niemniej jednak, w przypadku wirusa SARS-CoV-2, białko N jest częściej wykorzystywane w różnego typu narzędziach diagnostycznych w porównaniu z białkiem S [28]. Podczas pandemii COVID-19 szybkie testy antygenowe, ukierunkowane na białko N lub S, były podstawowym, prostym narzędziem do identyfikacji zakażonych. Potencjalnymi biomarkerami mogą jednak być również inne białka strukturalne, takie jak białko otoczki (E) oraz błony (M), znane także jako białko macierzy. Białko E jest małym białkiem transmembranowym zaangażowanym w tworzenie struktury i uwalnianie wirusa, podczas gdy białko M odgrywa rolę w utrzymaniu integralności otoczki wirusowej [29]. W przypadku niektórych wirusów jednoczesne wykrywanie wielu białek strukturalnych (np. N oraz M) zwiększa czułość testów diagnostycznych [30].

Oprócz białek pochodzących bezpośrednio od wirusa, w wyniku reakcji gospodarza na infekcję dochodzi do wytworzenia szeregu różnych polipeptydów o charakterze biomarkerów. Cytokiny, małe białka regulujące odpowiedź immunologiczną i reakcje zapalne, działają jako sygnalizatory, koordynując rekrutację i aktywację komórek odpornościowych. Podczas infekcji wirusowych często obserwuje się podwyższony poziom prozapalnych cytokin, takich jak interleukina-6 (IL-6) [31], czynnik martwicy nowotworów alfa (TNF-α) [32] i interferon-gamma (IFN-γ) [33]. Białka ostrej fazy, takie jak dobrze poznane białko C-reaktywne (CRP), są istotnymi markerami stanu zapalnego. Podwyższone poziomy CRP oraz innych białek gospodarza, takich jak surowiczy amyloid A (SAA) [34], prokalcytonina (PCT) [35] czy ferrytyna [36] wskazują na ogólnoustrojowy stan zapalny i nasilenie choroby

w infekcjach wirusowych. PCT jest tradycyjnie stosowana jako marker do rozróżniania między infekcjami bakteryjnymi a wirusowymi [37].

Wykrywanie i oznaczanie poziomów cytokin oraz białek ostrej fazy dostarcza cennych informacji o nasileniu choroby, jednak ich mała specyficzność w ujęciu diagnostycznym uniemożliwia wykorzystanie ich jako samodzielnych biomarkerów infekcji wirusowych. Wzrost poziomu tych cząsteczek może być wynikiem różnych infekcji, zarówno wirusowych, jak i bakteryjnych, a także niezakaźnych stanów zapalnych. Aby uzyskać dokładną diagnozę, wspomniane białka wskaźnikowe mogą zostać wykorzystane w projektowaniu testów nastawionych na wykrywanie wielu analitów jednocześnie. Cytokiny i białka ostrej fazy stanowią wartościowe markery uzupełniające w połączeniu z bardziej specyficznymi biomarkerami zakażeń wirusowych, np. przeciwciałami, które są produkowane przez organizm gospodarza w odpowiedzi na infekcję [38].

Przeciwciała, czyli glikoproteiny wytwarzane w odpowiedzi na obce antygeny podczas infekcji wirusowych, pełnią rolę kluczowych biomarkerów wykorzystywanych do ich detekcji i monitorowania. Wykrywanie przeciwciał umożliwiają testy serologiczne, których zasada działania polega na wychwycie przeciwciał o określonej specyficzności z surowicy krwi przez antygen pełniący rolę receptora. Wszechstronność tych testów polega na możliwości zaprojektowania platform zdolnych do rozróżnienia konkretnych ich klas (IgG, IgA, IgM, IgE lub IgD [39]), a nawet poszczególnych podklas [40, 41]. Testy serologiczne, w przeciwieństwie do technik molekularnych, umożliwiają określanie stadium zakażenia oraz ocenę wcześniejszej ekspozycji na wirusa [42]. Różne infekcje mogą prowadzić do zróżnicowanej dystrybucji i proporcji poszczególnych podklas przeciwciał. W odpowiedzi na infekcje wirusowe częściej obserwuje się podwyższone poziomy IgG_1 i IgG_3 w porównaniu z IgG_2 i IgG_4. Wzorzec ten jest szczególnie wyraźny w przypadku zakażeń wirusami otoczkowymi, takimi jak HIV [43], wirus zapalenia wątroby typu C (HCV) [44] i SARS-CoV-2 [45, 46].

W poniższej tabeli przedstawiono przykłady biomarkerów różnorodnych typów (antygenowe, genetyczne i serologiczne), które posłużyły do wykrycia różnych rodzajów infekcji wirusowych.

Tabela 1. Przykłady biomarkerów służących do wykrywania różnych rodzajów infekcji wirusowych

Biomarker	Wirus	Próbka	Referencja
Przeciwciała IgG przeciwko domenie wiążącej receptor (RBD) w białku kolca (S)	SARS-CoV-2	surowica	[47]
RNA wirusa	HIV	nasienie	[48]
Przeciwciała IgM przeciwko białku nukleokapsydu (N)	Wirus Dengi	surowica	[49]
miRNA	Wirus Grypy typu B	wymaz z gardła	[50]
Przeciwciała IgM i IgG przeciwko antygenowi HBc	Wirus zapalenia wątroby typu C	surowica	[51]
Antygen P30	Wirus afrykańskiego pomoru świń	wymaz z nosa	[52]

1.1.2 Immunoplatformy analityczne

Spośród szeregu dostępnych metod oznaczania białek, niewiele z nich umożliwia detekcję indywidualnych biomarkerów białkowych w próbkach biologicznych o złożonej matrycy [53]. Różnego typu immunoplatformy wykorzystują swoistość przeciwciał poliklonalnych, monoklonalnych lub ich fragmentów jako podstawę do selektywnego wykrywania struktur antygenowych (epitopów) [54-56]. Dzięki oferowanemu przez przeciwciała wysokiemu powinowactwu (stała dysocjacji K_d często ≤ 1 nM) oraz możliwości uzyskania specyficzności wobec szerokiej puli epitopów o różnym pochodzeniu, możliwe jest dostosowywanie projektowanych platform do szerokiej puli wykrywanych cząsteczek, a co za tym idzie adaptacja wytwarzanych testów do nowopowstałych patogenów lub nowoodkrytych biomarkerów. Zdolność do selektywnego wiązania badanych białek sprawia, że metody immunodiagnostyczne są nieocenione w analizie złożonych próbek, takich jak krew [57], surowica [58] lub homogenaty tkanek [59]. Ponadto możliwość miniaturyzacji projektowanych testów pozwala na wdrażanie tego typu rozwiązań w szerokim spektrum zastosowań, od klasycznych testów laboratoryjnych po zaawansowane platformy w postaci mikrosystemów.

Techniki, takie jak spektrometria mas [60, 61], elektroforeza kapilarna [62] i techniki chromatograficzne [63] oferują wysoką czułość i specyficzność wykrywania białek

o charakterze biomarkerowym. Są one jednak czasochłonne i wymagają zastosowania złożonych procedur przygotowania próbki. Ponadto, używana do realizacji oznaczeń aparatura jest kosztowna i trudna w obsłudze. Z tego względu wyżej wspomniane metody są rzadko wdrażane do rutynowej diagnostyki klinicznej lub zastosowań w badaniach w miejscu opieki nad pacjentem, chociaż w ostatnich latach widoczne w literaturze są próby upraszczania procedur i miniaturyzacji sprzętu [64].

Zastosowanie aptamerów DNA do wykrywania biomarkerów białkowych, jako alternatywa dla przeciwciał, oferuje porównywalną specyficzność względem wykrywanych białek, przy jednocześnie niższym koszcie wytwarzania tego typu receptorów. Aptamery, czyli krótkie fragmenty kwasów nukleinowych, które wiążą się swoiście z docelową cząsteczką, mogą być syntetyzowane *in vitro* i selekcjonowane pod kątem powinowactwa do szerokiej gamy białek [65]. Jednak w warunkach klinicznych techniki wykorzystujące aptamery nie dorównały jeszcze testom immunologicznym pod względem niezawodności. Brak stabilności receptorów oligonukleotydowych w złożonych matrycach biologicznych wciąż stanowi przeszkodę w praktycznym wykorzystaniu aptamerów w narzędziach diagnostycznych do detekcji biomarkerów białkowych [66, 67].

Metody immunodiagnostyczne wiodą prym w zastosowaniach POCT, głównie dzięki swojej wszechstronności i łatwości ich adaptacji do różnych systemów detekcji. W zależności od mechanizmu działania i sposobu generowania sygnału, wśród metod immunodiagnostycznych można wyróżnić immunosensory, testy aglutynacji cząstek, a także homogeniczne i heterogeniczne testy immunologiczne. Podział tych ostatnich zależy od tego, czy w trakcie ich przeprowadzania konieczne jest zastosowanie etapów rozdzielania związanych i wolnych kompleksów antygen-przeciwciało. Rysunek 1 zestawia podstawowe różnice w mechanizmach poszczególnych rodzajów testów immunologicznych.

Testy aglutynacyjne to klasa testów immunologicznych, których zasada działania bazuje na widocznej agregacji cząstek. Efekt ten jest wywoływany interakcją antygen-przeciwciało, gdzie jedno z nich (pełniące rolę receptora) jest przyłączone do dużych cząstek, takich jak np. kulki lateksowe [68], czy czerwone krwinki [69]. Nośniki są dobierane tak, aby ich agregaty były widoczne gołym okiem (Rysunek 1A). Takie testy są szeroko stosowane ze względu na ich prostotę, niski koszt i szybkość uzyskania wyników, jednak charakteryzują się one niską czułością. Dodatkowym wyzwaniem w projektowaniu jednoetapowych testów aglutynacyjnych jest ryzyko fałszywie ujemnych wyników przy wysokim stężeniu analitu.

Jest to związane z saturacją większości miejsc wiążących przez analit obecny w wysokim stężeniu, bez wytworzenia struktury typu kanapkowego. Skutkuje to minimalną aglutynacją cząstek i nazywane jest „efektem haka” (z ang. *„Hook effect”* lub *„Prozone effect”*) [70].

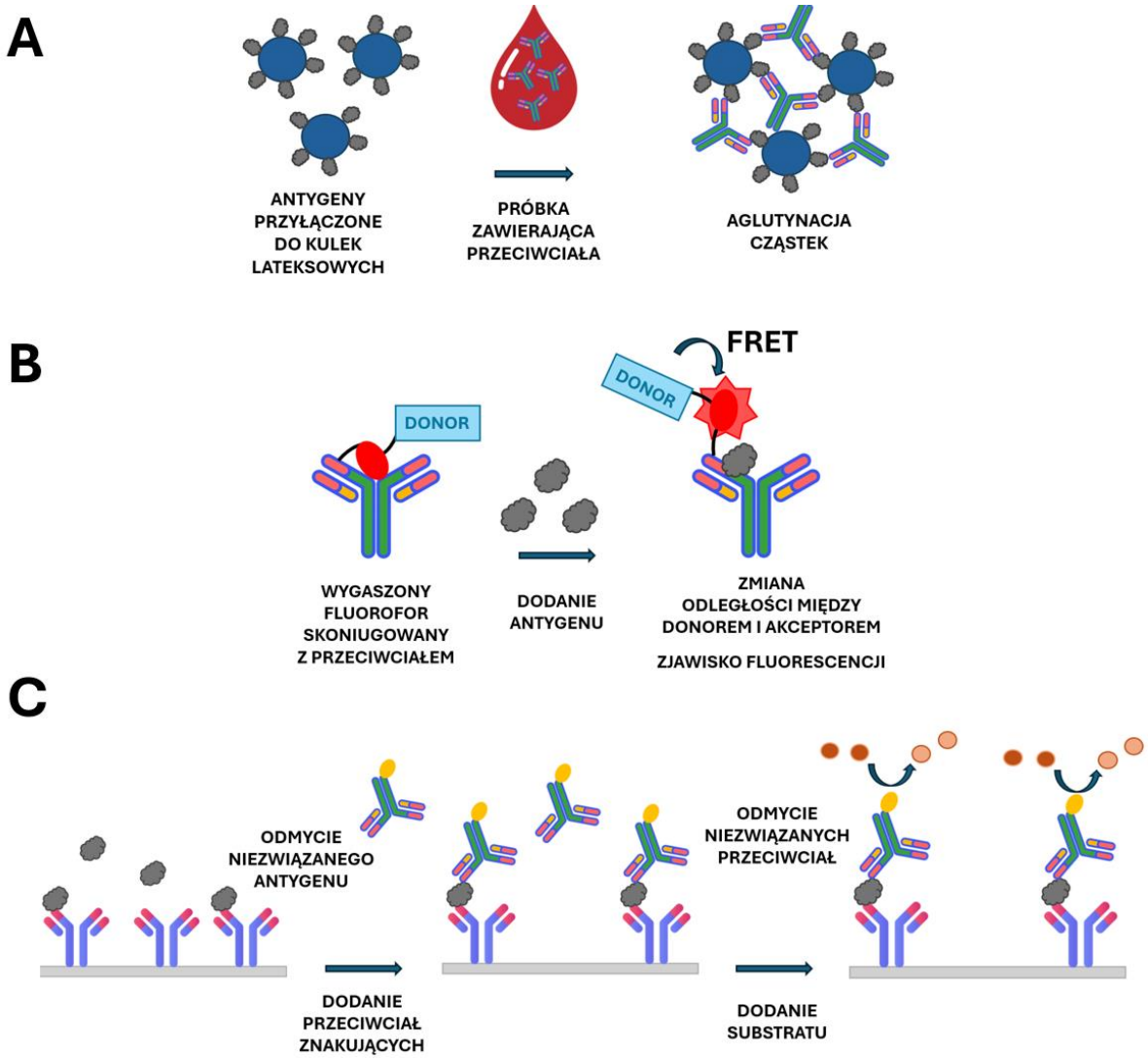

Rysunek 1. Podział testów immunologicznych; A. test aglutynacji cząstek, B. homogeniczny test wykorzystujący zjawisko FRET, C. heterogeniczny test typu ELISA.

Homogeniczne testy immunologiczne to testy jednofazowe, które nie wymagają oddzielania analitów związanych w postaci immunokompleksów od ich postaci niezwiązanych. Przykładem są testy immunologiczne z amplifikacją enzymatyczną (z ang. *enzyme-multiplied immunoassay technique, EMIT*). Technika ta wykorzystuje konkurencję między znakowanym

antygenem a analitem o wiązanie z przeciwciałem. Związanie znakowanego antygenu wywołuje zmianę konformacyjną, hamującą aktywność enzymu i zmniejszającą sygnał, który jest odwrotnie proporcjonalny do stężenia analitu w próbce. Takie rozwiązanie było jednym z pierwszych dostępnych na rynku komercyjnym i zostało opracowane przez firmę Syva w 1973 roku [71]. Innym przykładem testów typu homogenicznego są te, które wykorzystują rezonansowy transfer energii (z ang. *Resonance Energy Transfer, RET*). Test tego typu bazuje na fakcie, iż zdarzenie molekularne jakim jest wiązanie analitu, wywołuje zmianę odległości między cząsteczkami donora i akceptora energii (Rysunek 1B). Do odczytu wykorzystywane jest zjawisko fluorescencji (Försterowski rezonansowy transfer energii, w skrócie FRET) [72], chemiluminescencji (CRET) [73] lub bioluminescencji (BRET) [74].

Heterogeniczne testy immunologiczne wyróżnia konieczność realizacji sekwencyjnych etapów odmywania i separacji składników testu od kompleksów antygen-przeciwciało związanych z powierzchnią. Najbardziej znanym ich przykładem jest test immunoenzymatyczny (z ang. *enzyme-linked immunosorbent assay, ELISA*), gdzie antygen lub przeciwciało jest unieruchamiane na stałym podłożu studzienki mikropłytki wielodołkowej. W najprostszym formacie, tj. bezpośrednim, po dodaniu próbki z analitem następuje inkubacja, umożliwiająca tworzenie kompleksów antygen-przeciwciało. Po odmyciu niezwiązanego analitu dodaje się enzymatycznie znakowane przeciwciało, tworząc kompleks kanapkowy, co zilustrowano na Rysunku 1C. Kolejne odmywanie usuwa nadmiar przeciwciał, a dodany substrat reaguje z enzymem, generując sygnał proporcjonalny do stężenia analitu [75]. Zastosowanie enzymów jako znaczników katalitycznych w heterogenicznych testach immunologicznych przynosi istotną korzyść w postaci wzmocnienia sygnału, co wynika ze zwielokrotnienia w czasie ilości produktu będącego jego nośnikiem. Na podstawie prostej techniki ELISA możliwy jest rozwój bardziej zaawansowanych wariantów testów poprzez wprowadzanie innowacji, takich jak wykorzystanie w ich konstrukcji elastycznych podłoży (np. folii PET) [76] oraz platform papierowych [77]. Na popularności zyskują również testy, które wykorzystują koniugaty przeciwciał z nanomateriałami (z ang. *nano-linked immunosorbent assay, NLISA*), np. nanocząstkami katalitycznymi w roli mimetyków enzymów [78]. Ponadto, dzięki integracji immunodetekcji z mikrosystemami przepływowymi możliwa jest automatyzacja przeprowadzanych testów [79]. W nowoczesnej diagnostyce rośnie zapotrzebowanie na metody, które łączą prostotę i niski koszt testu ELISA z czułością

i szybkością współczesnych rozwiązań w formatach odpowiednich zarówno dla rutynowych zastosowań laboratoryjnych, jak narzędzi POCT.

Immunosensory to odrębna klasa platform diagnostycznych, które łączą wysoką specyficzność reakcji przeciwciało-antygen z zaawansowanymi metodami detekcji. Dzięki zintegrowanej części przetwornikowej możliwe jest przekształcenie sygnału biologicznego na mierzalny sygnał analityczny. Dodatkowo, w przeciwieństwie do jednorazowych immunotestów, immunosensory pozwalają na ich wielokrotne wykorzystanie, co zwiększa ich efektywność i obniża koszty analizy. Narzędzia te można sklasyfikować bazując na mechanizmie przetwarzania sygnału. Najpopularniejszymi typami są: immunosensory elektrochemiczne, gdzie powstanie kompleksu przeciwciało-antygen powoduje zmiany właściwości elektrycznych [80, 81], immunosensory optyczne, gdzie mierzone są zmiany właściwości światła (np. wykorzystujące zjawisko rezonansu plazmonów powierzchniowych [82]) oraz immunosensory piezoelektryczne działające na zasadzie pomiaru częstotliwości drgań spowodowanych zmianą masy związanej z powierzchnią [83, 84].

Testy homogeniczne, dzięki ograniczeniu liczby etapów inkubacji i przemywań, są prostsze w realizacji, jednak wymagają bardziej złożonych mechanizmów generowania sygnału. Z kolei testy heterogeniczne, choć obejmują więcej etapów, umożliwiają skuteczniejsze eliminowanie niepożądanych zjawisk poprzez odmywanie niezwiązanych cząsteczek. Ta kluczowa różnica sprawia, że testy heterogeniczne cechują się większą niezawodnością i szerszym zakresem dynamicznym, co jest istotne przy analizie próbek o wysokim stężeniu analitu. Ostateczny wybór metody immunodetekcji zależy od wymagań diagnostycznych, takich jak szybkość uzyskania wyniku, czułość, koszt, dostępność odczynników oraz złożoność próbki. Ostatnio rośnie również zainteresowanie technikami umożliwiającymi jednoczesną detekcję wielu analitów w jednej analizie, co stawia przed projektantami immunoplatform nowe wyzwania z tym związane.

1.1.3 Diagnostyka wieloparametrowa – *Multiplexing*

Detekcja wieloparametrowa (z ang. *multiplex*) umożliwia wykrywanie wielu biomarkerów wykorzystując tę samą próbkę w trakcie jednej analizy. To podejście minimalizuje ograniczenia związane z przepustowością tradycyjnych metod (z ang. *monoplex*), które zazwyczaj koncentrują się na pojedynczym analicie, co może prowadzić do niepełnych wniosków diagnostycznych lub wiąże się z koniecznością przeprowadzenia szeregu osobnych

analiz. Ponadto, z czysto praktycznego punktu widzenia, platformy wieloparametrowe skracają czas potrzebny na uzyskanie wyników, a także minimalizują potrzebną objętość próbki [85]. Porównanie zalet platform typu *multiplex* z testami tradycyjnymi zostało przedstawione w formie graficznej na Rysunku 2.

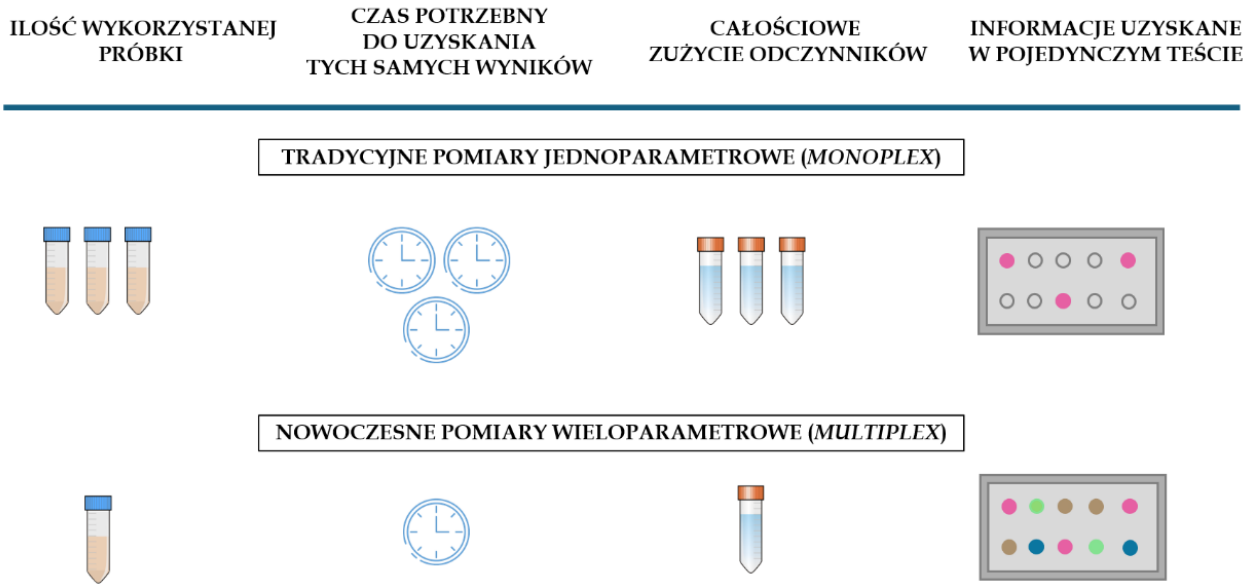

Rysunek 2. Porównanie klasycznych testów jednoparametrowych z testami multipleksowymi.

Infekcje wirusowe wywołują kaskadę procesów związanych z odpowiedzią odpornościową gospodarza, co bezpośrednio przekłada się na szeroką gamę potencjalnych biomarkerów zakażeń. Możliwość równoległego oznaczenia kilku z nich zapewnia bardziej kompleksowy obraz stanu zdrowia pacjenta. Takie podejście stanowi wstęp do rozwoju spersonalizowanej diagnostyki, umożliwiając dostosowanie opieki medycznej do konkretnego pacjenta. Jest to szczególnie istotne, gdyż osoby z podobnymi objawami klinicznymi mogą różnić się etiologią i patogenezą choroby [86, 87]. Efektem jest przyspieszenie ścieżki do wdrożenia odpowiedniego postępowania terapeutycznego. Dodatkowo szeroka pula wykrywanych analitów i możliwość ich ilościowego oznaczania pozwala na analizę korelacji pomiędzy nimi, a także umożliwia oszacowanie upływu czasu od momentu zakażenia i ocenę skuteczności szczepienia [88].

Rosnące zainteresowanie narzędziami do diagnostyki wieloparametrowej jest zgodne z rosnącym zapotrzebowaniem na wysokoprzepustowe badania w warunkach diagnostyki przyłóżkowej (POCT). Jest to szczególnie ważne w miejscach o wysokim wskaźniku

zachorowalności, gdzie dostęp do tradycyjnych laboratoriów jest ograniczony. Takie sytuacje obejmują pandemie oraz kraje rozwijające się, gdzie szybkie uzyskanie wyników w warunkach ograniczonych zasobów jest niezbędne do skutecznego zarządzania dużymi populacjami pacjentów [89].

Podsumowanie

Antygenowe i serologiczne biomarkery białkowe związane z zakażeniami wirusowymi odgrywają kluczową rolę w diagnostyce medycznej. W związku z tym, również receptory stosowane do ich wykrywania cechują się różnorodnością strukturalną. Na podstawie wniosków z bieżącego rozdziału, w badaniach nad projektowaniem warstw receptorowych opisanych w niniejszej pracy doktorskiej zastosowano modelowe receptory, tj. przeciwciała klasy IgG jako receptory antygenów oraz białka antygenowe, w tym białko nukleokapsydu (N) wirusa SARS-CoV-2 jako receptory wiążące przeciwciała surowicze. Opracowane w ramach tej pracy platformy analityczne bazują na heterogenicznych testach immunologicznych możliwych do realizacji w formacie *multiplex*. Wybór modelowych receptorów należących do różnych grup białek miał na celu zademonstrowanie uniwersalności projektowanych platform pod względem diagnostycznym. Proponowane podejście umożliwia wieloparametrową detekcję zarówno czynników zakaźnych, jak i ocenę odpowiedzi układu odpornościowego. Odpowiada to rosnącemu zapotrzebowaniu na rozwiązania typu POCT oraz potrzebie holistycznego podejścia do zdrowia pacjenta, co stanowi podstawę rozwoju medycyny spersonalizowanej.

1.2 Mikromacierze białkowe

Mikromacierze białkowe stanowią przykład narzędzia umożliwiającego immunodetekcję multipleksową [90]. Swoją nazwę zawdzięczają możliwości unieruchomienia wielu różnych białek receptorowych na wspólnym, stałym podłożu. Odpowiednie rozlokowanie przestrzenne zaimmobilizowanych białek jest kluczowym aspektem związanym z wytwarzaniem mikromacierzy i jednocześnie wyzwaniem technologicznym. Dzięki temu, jak również odpowiednim narzędziom odczytu (najczęściej optycznego, bazującego na obrazowaniu) możliwe jest symultaniczne monitorowanie poziomu różnych biomarkerów w trakcie jednej analizy. Graficzne przedstawienie mikromacierzy z odczytem fluorescencji zostało pokazane na Rysunku 3. Na przedstawionej mikromacierzy unieruchomionymi

białkami są nukleoproteina wirusa SARS-CoV-2 (białko testowe, kolor czerwony) oraz przeciwciało anty-koza (białko referencyjne, kolor zielony). Wykorzystane białko referencyjne jest sprzężone ze znacznikiem fluorescencyjnym (Alexa Fluor 488). Mikromacierz inkubowana była z próbką rzeczywistą – surowicą ludzką pobraną od pacjenta ze zdiagnozowanym COVID-19, a następnie znakowana przeciwciałami drugorzędowymi skoniugowanymi ze znacznikiem fluorescencyjnym (Cy5).

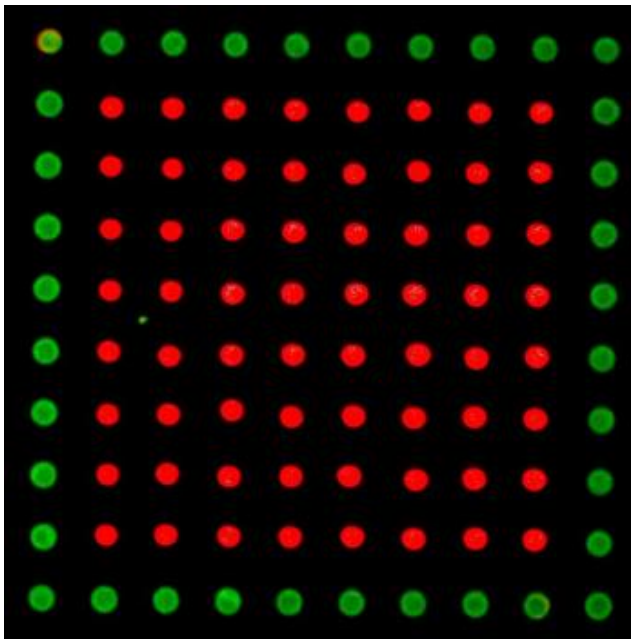

Rysunek 3. Mikromacierz białkowa wytworzona na chipie krzemowym. Zdjęcie wykonane przy użyciu skanera InnoScan 710 dzięki uprzejmości Instituto di Scienze e Tecnologie Chimiche w Mediolanie (zarejestrowane podczas wyjazdu naukowego w ramach programu Mobility PW IDUB - NAWA STER).

Jedną z najważniejszych zalet mikromacierzy białkowych jest ich potencjał do wykorzystania w badaniach o wysokiej przepustowości. Pojedyncza macierz może zawierać nawet tysiące różnych białek receptorowych, pozwalając na jednoczesną detekcję szerokiego spektrum analitów. Zminiaturyzowany format mikromacierzy pozwala na integrację z różnymi metodami detekcji, takimi jak odczyt fluorescencyjny, kolorymetryczny lub elektrochemiczny.

Mikromacierze białkowe, mimo wielu zalet, napotykają istotne wyzwania technologiczne, zwłaszcza w zakresie immobilizacji białek o zróżnicowanych właściwościach. Zachowanie biologicznej aktywności receptorów oraz uzyskanie jednolitej gęstości na polach

testowych jest niezbędne dla powtarzalności i czułości testu. Efektywne unieruchomienie wielu białek na jednym podłożu jest skomplikowane i stanowi istotne ograniczenie tej technologii.

1.2.1 Strategie unieruchamiana receptorów: immobilizacja nieodwracalna i odwracalna

Unieruchamianie białek na stałych podłożach jest istotnym etapem w tworzeniu funkcjonalnych warstw receptorowych w immunosensorach i mikromacierzach białkowych. Proces ten wymaga starannego doboru metod immobilizacji, aby zapewnić stabilność i aktywność biologiczną białek na powierzchni nośnika. Klasycznie sposoby immobilizacji białek opierają się na jednym z trzech mechanizmów: kowalencyjnym (chemicznym), adsorpcyjnym (fizycznym) oraz powinowactwa biologicznego [91]. Jednak ten konwencjonalny podział można dodatkowo skategoryzować i wyróżnić dwie główne strategie, tj. immobilizacje nieodwracalne i odwracalne. Odwracalność (regenerowalność) warstwy receptorowej definiowana jest jako zdolność do wielokrotnego wykorzystania tej samej warstwy receptorowej bez utraty jej funkcjonalności. Możliwość regeneracji warstwy receptorowej, a tym samym wielokrotnego użycia tego samego czujnika lub testu, pozwala uniknąć fałszywych wyników pomiarów spowodowanych niską jakością i brakiem powtarzalności wytwarzania mikromacierzy [92].

Regenerację warstwy receptorowej immunoplatform można osiągnąć za pomocą dwóch podejść. Pierwsze – rozumiane klasycznie, polega na dysocjacji kompleksu przeciwciało-antygen przy jednoczesnym zachowaniu możliwie nienaruszonej struktury i zdolności wiązania receptora unieruchomionego trwale na powierzchni. Drugie podejście obejmuje każdorazowe, całkowite usunięcie bioreceptora z powierzchni po zrealizowanym pomiarze, a następnie rekonstrukcję warstwy receptorowej przed następną analizą.

W przypadku pierwszego z wyżej wymienionych podejść dużym wyzwaniem jest fakt, że białkowa warstwa receptorowa jest wrażliwa na – często dość agresywne – warunki wymagane do zniszczenia wiązania przeciwciało-antygen [93]. Dysocjacja immunokompleksu bez uszkodzenia struktury receptora i osłabienia jego zdolności do ponownego wiązania analitu stanowi wyzwanie. Stosowanie buforów regeneracyjnych o skrajnych wartościach pH, często wzbogaconych detergentami lub środkami chaotropowymi, ma na celu zakłócenie interakcji molekularnych i usunięcie związanych cząsteczek analitu z powierzchni.

Jednak klasyczna regeneracja powierzchni, z zachowaniem warstwy receptorowej, wiąże się z ryzykiem uszkodzenia przetwornika, zmian właściwości fizycznych lub denaturacji zaimmobilizowanych białek receptorowych [94]. Aby ominąć te problemy często wykorzystuje się receptory, które zostały zmodyfikowane za pomocą technik biologii molekularnej, na przykład poprzez zmniejszenie powinowactwa zmodyfikowanego receptora do analitu [95, 96].

Atrakcyjną alternatywą dla klasycznej regeneracji w immunotestach jest każdorazowe usuwanie z powierzchni białek receptorowych i rekonstrukcja warstwy receptorowej z wykorzystaniem szybkich i łatwych do kontroli metod samoorganizacji molekularnej, takich jak immobilizacja białek z wykorzystaniem powinowactwa biologicznego. Oferują one takie zalety, jak łatwość sterowania gęstością powierzchniową, zachowanie natywnej formy receptora oraz odpowiednia ekspozycja miejsc wiążących, co nie jest możliwe w przypadku pasywnej adsorpcji czy kowalencyjnego sprzęgania [97].

Przykładem takiej regenerowalnej immobilizacji jest unieruchamianie białek za pomocą kotwic DNA (z ang. *DNA-directed immobilization, DDI*). Dzięki możliwości syntezy chemicznej na dużą skalę oraz stabilności DNA, cząsteczka ta wzbudziła zainteresowanie jako łącznik do powierzchniowego unieruchamiania białek. Metoda DDI wykorzystuje hybrydyzację zachodzącą pomiędzy nićmi DNA skoniugowanymi z białkami receptorowymi a komplementarnymi sekwencjami (sondami) na podłożu, który to proces jest niezależny od budowy i właściwości białka skoniugowanego z kotwicą DNA. Dzięki temu, metoda DDI charakteryzuje się uniwersalnością, pozwalając na unieruchamianie różnorodnych białek bez konieczności dostosowywania procedury do ich indywidualnych właściwości. DDI pozwala również na łatwą i szybką regenerację warstwy poprzez zerwanie wiązań wodorowych w dupleksie DNA-DNA, np. poprzez zmianę siły jonowej i/lub pH buforu [98]. Ponadto, metoda ta pozwala na łatwą kontrolę przestrzennego rozmieszczenia receptorów, co odgrywa kluczową rolę w konstrukcji mikromacierzy białkowych [99]. Mechanizm parowania zasad nici DNA gwarantuje na tyle wysoką specyficzność, że możliwe jest selektywne wiązanie docelowych białek jedynie w pożądanych strefach nawet w obecności szeregu różnych receptorów białkowych znakowanych kotwicami DNA o innej sekwencji.

Metoda DDI daje możliwość unieruchamiania receptorów na dwa sposoby, które można stosować w zależności od preferowanej technologii wytwarzania immunotestów. Pierwszy polega na przeprowadzaniu immobilizacji w warunkach przepływowych, gdzie odpowiednie przestrzenne rozmieszczenie różnych koniugatów białkowych uzyskuje się dzięki

wcześniejszemu lokalnemu rozmieszczeniu na powierzchni sond DNA o odpowiednio zaprojektowanych, różniących się sekwencjach. W drugim podejściu unieruchamianie bioreceptorów odbywa się *ex-situ* poprzez kontrolowane nanoszenie koniugatów białko-DNA w formie pól testowych (z ang. *spotting*), przy czym cała powierzchnia podłoża jest pokryta komplementarnymi sondami. Podejście *ex-situ* umożliwia wykorzystanie tej samej kotwicy DNA do unieruchamiania różnych białek. Dzięki temu proces immobilizacji jest uproszczony, co znacząco ułatwia przygotowanie mikromacierzy o zróżnicowanym zestawie receptorów. Możliwość regeneracji warstwy receptorowej jest istotna zarówno w immunoplatformach analitycznych do oznaczania różnych bioanalitów, jak i w biosensorach służących do badania kinetyki interakcji międzycząsteczkowych. Dzięki temu nie ma potrzeby tworzenia wielu identycznych pól testowych dla różnych stężeń biomolekuł, co upraszcza proces analizy [100]. Zestawienie innych popularnych strategii odwracalnej (regenerowalnej) immobilizacji receptorów białkowych wraz ze wskazaniem ich głównych wad i zalet znajduje się w Tabeli 2.

Tabela 2. Charakterystyka podstawowych strategii odwracalnej immobilizacji receptorów białkowych

Strategia immobilizacji regenerowalnej	**Wady**	**Zalety**	**Przykład wykorzystania**
Pasywna adsorpcja	Przypadkowa orientacja białka receptorowego, niestabilność wiązania z podłożem, agregacja receptorów	Kompatybilność z wieloma typami podłoży	[101]
DDI	Konieczność koniugacji białka z kotwicą oligonukleotydową	Możliwość unieruchomienia każdego rodzaju białka receptorowego	[102]
His-tag/Ni^{2+}-NTA	Dysocjacja receptora w trakcie analizy, konieczność stosowania rekombinowanych przeciwciał	Dostępność komercyjna podłoży i rekombinowanych antygenów białkowych	[103]
Białko A/G	Ograniczenie do przeciwciał klasy IgG, podatność uzyskanych warstw na niespecyficzne interakcje	Brak potrzeby modyfikacji receptora	[104, 105]
Mieszana	Długi czas i wysoki koszt procesu	Połączenie zalet różnych strategii	[106]

1.2.2 Nowe strategie unieruchamiana receptorów

Nowo opracowane strategie odwracalnego unieruchamiania receptorów często polegają na modyfikacjach i udoskonaleniach istniejących rozwiązań. Łączą one sprawdzone protokoły funkcjonalizacji powierzchni z nowymi możliwościami, jakie oferują koniugaty białek receptorowych z różnego rodzaju cząsteczkami kotwiczącymi.

Immobilizacja kowalencyjna

Bezpośrednie, kowalencyjne sprzęganie białek z powierzchnią poprzez ich grupy funkcyjne może powodować problemy, takie jak brak kontroli nad orientacją przestrzenną, czasochłonne i skomplikowane procedury modyfikacji powierzchni oraz ograniczenia w stosowaniu standardowych protokołów immobilizacji dla białek o zróżnicowanych właściwościach. Przykładowo, efektywność sprzęgania za pomocą karbodiimidów jest silnie zależna od ładunku powierzchniowego białka [107, 108]. Przeciwciała jako glikoproteiny z klasy globulin wykazują strukturalne i funkcjonalne podobieństwo, jednak fizykochemiczna różnorodność antygenów białkowych sprawia, że opracowanie uniwersalnych protokołów ich unieruchamiania jest trudniejsze. Niemniej jednak immobilizacja kowalencyjna pozostaje niezwykle popularna i niezastąpiona w wielu zastosowaniach, w których pasywna adsorpcja okazuje się niewystarczająca. Szczególnie sprawdza się w immunoplatformach jednokrotnego użytku, dzięki długoterminowej stabilności immobilizowanych cząsteczek oraz niskim kosztom wytwarzania [109].

Reaktywne kopolimery

Kowalencyjna immobilizacja białek z reguły wymaga uprzedniej modyfikacji podłoża w celu wprowadzenia odpowiednich grup reaktywnych, które selektywnie wiążą się z określonymi grupami funkcyjnymi aminokwasów w strukturze białek. Tradycyjne metody modyfikacji powierzchni, takie jak silanizacja, wprowadzanie grup epoksydowych czy wykorzystanie karbodiimidów i maleimidów, są powszechnie stosowane, ale charakteryzują się czasochłonnością i wieloetapowością. Z technologicznego punktu widzenia, procedury te nie są optymalne do seryjnej produkcji immunoplatform zintegrowanych w zaawansowane urządzenia diagnostyczne [110].

Atrakcyjną alternatywą do wyżej wymienionych podejść okazuje się być zastosowanie do funkcjonalizacji powierzchni reaktywnych kopolimerów [111-113]. Reaktywne kopolimery w wyniku chemicznego sieciowania tworzą warstwy zdolne do pokrywania różnych typów powierzchni i posiadające wprowadzone do swojej struktury grupy funkcyjne (np. aldehydowe, karboksylowe, czy aminowe), które ułatwiają kowalencyjne przyłączanie cząsteczek.

Przykład takiego kopolimeru na bazie pochodnych kwasu akrylowego został przedstawiony na Rysunku 4.

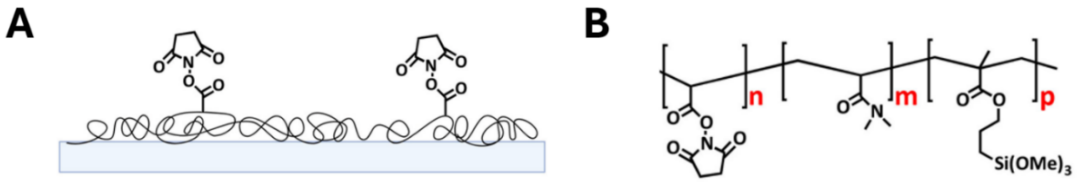

C

stosunek molowy monomerów		
DMA (m)	NAS (n)	MAPS (p)
97	2	1

Rysunek 4. Przykład reaktywnego kopolimeru na bazie pochodnych kwasu akrylowego. A. Powierzchnia pokryta kopolimerem z wyeksponowanymi grupami funkcyjnymi NHS (reaktywnymi względem grup aminowych), B. Schemat budowy kopolimeru MCP-2, C. Stosunek molowy monomerów wchodzących w skład kopolimeru MCP-2 (DMA- N,N-dimetyloakrylamid, NAS – akryloiloksysukcynimid oraz MAPS- metakrylan 3-(trimetoksysililo)propylu).

Wykorzystanie kopolimerów o różnych stosunkach monomerów pozwala na precyzyjną kontrolę gęstości powierzchniowej grup funkcyjnych, pozwalając na kontrolowaną immobilizację receptorów. Takie podejście niweluje ograniczenia związane z konwencjonalnymi sposobami funkcjonalizacji powierzchni. Kopolimery są dostosowane do szerokiej gamy podłoży, od chipów krzemowych [114], po szkło [115], polimery [116] i metale [117]. Umożliwia to ich potencjalne wykorzystanie w szerokim spektrum zastosowań, od konstrukcji jednorazowych testów, po zintegrowane urządzenia diagnostyczne [118]. Ponadto, możliwe jest wprowadzenie do struktury takich kopolimerów segmentów ułatwiających związanie z powierzchnią (np. reszty 3-(trimetoksysililo)propylu), czy elementów zapobiegających niespecyficznej adsorpcji, co pozwala na wytworzenie warstwy uniemożliwiającej płynom biologicznym nieswoiste oddziaływanie z podłożem [119].

Stworzenie już na etapie syntezy odpowiednio zaprojektowanego modyfikatora powierzchni o pożądanych funkcjonalnościach skraca czas i koszty wytworzenia zmodyfikowanej warstwy dzięki jednoetapowemu procesowi powlekania. Dodatkowo, wykorzystanie reaktywnych kopolimerów otwiera możliwość integracji różnych strategii immobilizacji. Przykładowo, kowalencyjne przyłączenie sond oligonukleotydowych do podłoża zmodyfikowanego reaktywnym polimerem, a następnie unieruchomienie receptorów białkowych poprzez DDI, łączy zalety powlekania powierzchni polimerem z korzyściami odwracalnej immobilizacji bazującej na powinowactwie biologicznym [99].

1.2.3 Kontrola jakości białkowych warstw receptorowych

Użyteczność biosensorów i biotestów w formacie *multiplex* w dużej mierze zależy od jakości wytworzonej warstwy receptorowej. Wyzwanie to staje się szczególnie istotne, gdy na tej samej powierzchni unieruchamia się wiele różnych białek. Jednorodność pól testowych warstwy receptorowej mikromacierzy wpływa na uzyskiwany sygnał, co podkreśla potrzebę opracowania metod kontroli ich jakości [120, 121].

Immobilizacja białek *ex-situ* w warunkach stacjonarnych (np. z wykorzystaniem zautomatyzowanego systemu nanoszenia) pozwala na jednoczesne unieruchamianie i przestrzenne rozmieszczenie wielu różnych receptorów na jednej matrycy, co maksymalizuje wykorzystanie dostępnej powierzchni przetwornika. Jednak proces ten ma istotne ograniczenia. W przeciwieństwie do immobilizacji w zamkniętym układzie mikroprzepływowym, podejście *ex situ* utrudnia kontrolę nad czasem interakcji między białkiem a podłożem oraz nie pozwala na śledzenie procesu wiązania z powierzchnią, co znacznie utrudnia oszacowanie gęstości powierzchniowej receptorów i ocenę jednorodności pól testowych. Powoduje to, że immobilizacja *ex-situ* wymaga szczególnej dbałości o standaryzację warunków procesu, aby minimalizować potencjalne różnice między poszczególnymi polami testowymi.

Jednym z głównych wyzwań, z punktu widzenia powtarzalności wytwarzania, jest unieruchomienie wielu białek na powierzchni przetwornika w postaci pól testowych o bardzo małych powierzchniach. Na powodzenie tego procesu ma wpływ szereg różnych czynników, jak chociażby wilgotność i temperatura otoczenia [122]. Wszelkie wahania podczas procesu immobilizacji mogą prowadzić do nierównomiernego rozmieszczenia białek. Przykładem jest nierównomierne wysychanie i powstawanie efektu pierścienia kawowego (ang. *coffee ring effect*), co często zdarza się przy nakładaniu pól testowych przy braku

odpowiedniej kontroli wilgotności powietrza. Aby zautomatyzować proces immobilizacji, stosuje się specjalistyczne plotery, które precyzyjnie nanoszą niewielkie objętości roztworów zawierających receptory. Dozowanie kropli odbywa się dzięki siłom kapilarnym w kontrolowanych warunkach, często z użyciem nawilżanych komór klimatycznych. Objętość nakładanego roztworu zależy od konstrukcji dyszy, lepkości roztworu, hydrofilowości podłoża oraz czasu kontaktu kapilary z podłożem [123].

Pomimo powszechnego obecnie wykorzystania zautomatyzowanych metod nanoszenia receptorów, problem niejednorodności pól testowych wciąż pozostaje aktualnym wyzwaniem technologicznym. Przykładowy efekt tego zjawiska został zilustrowany na Rysunku 5.

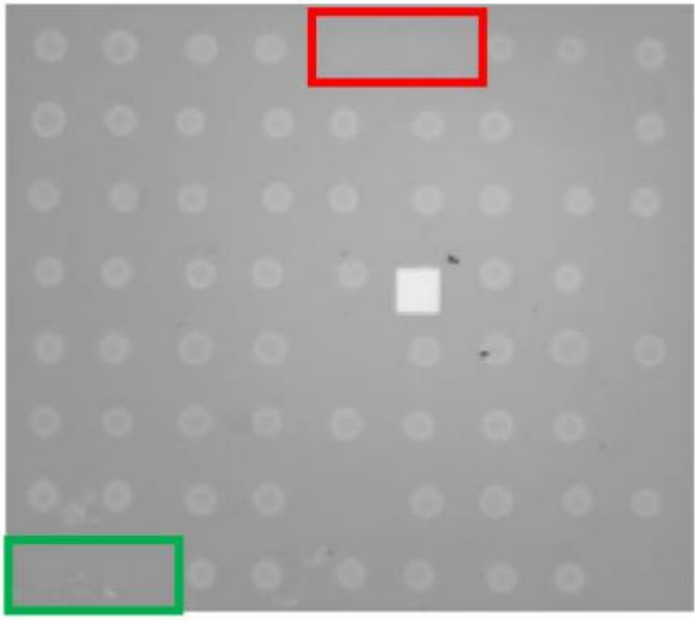

Rysunek 5. Zdjęcie przedstawiające mikromacierz wytworzoną techniką automatycznego nanoszenia z wykorzystaniem plottera [121].

W teorii, każde z pól testowych powinno cechować się w przybliżeniu jednakową gęstością powierzchniową. W rzeczywistości widać, że niektóre receptory nie zostały unieruchomione na powierzchni (czerwona ramka), bądź w wyniku nierównomiernego wysychania proces immobilizacji cechował się dużo niższą wydajnością (zielona ramka).

W obliczu trudnych do całkowitego wyeliminowania problemów z jednorodnością pól testowych masowo wytwarzanych mikromacierzy, zyskuje na znaczeniu potrzeba opracowania prostej metody kontroli ich wytwarzania [124]. Do tej pory nie opracowano jednak

uniwersalnej metody umożliwiającej ocenę jakości białkowych warstw receptorowych w układzie mikromacierzowym. Takie podejście umożliwiłoby rutynową ocenę jednorodności pól testowych jeszcze przed rozpoczęciem analizy, a co za tym idzie eliminację potencjalnych błędów z nich wynikających.

Jednym ze sposobów kontroli jakości warstwy receptorowej jest bezpośrednie monitorowanie procesu immobilizacji, co można osiągnąć poprzez wykorzystanie rezonansu plazmonów powierzchniowych (SPR) [125]. Technika ta pozwala na monitorowanie interakcji białka z podłożem w czasie rzeczywistym. Niestety w przypadku większości mikromacierzy takie podejście nie jest możliwe do zastosowania, ponieważ unieruchomienie receptorów zachodzi *ex-situ*, poza układem przepływowym.

Innym potencjalnym rozwiązaniem jest wykorzystanie specyficznego znakowania immunologicznego. Użycie przeciwciał (np. znakowanych fluorescencyjnie) skierowanych przeciwko białku receptorowemu pozwala na określenie efektywności immobilizacji biocząsteczek, a także na ocenę jednorodności gęstości powierzchniowej receptora w obrębie pól testowych. Istotne ograniczenie stanowi jednak fakt, iż dostępność znakowanych przeciwciał, zwłaszcza wobec nowych antygenów, jest ograniczona. Ponadto unieruchomienie wielu białek na wspólnym podłożu wymagałoby zastosowania różnych przeciwciał, co jest kosztowne i czasochłonne. Dodatkowo, specyficzne znakowanie warstwy receptorowej przeciwciałami uniemożliwiłoby ponowne użycie platformy bez wcześniejszej regeneracji.

Kolejną koncepcją jest również możliwość bezpośredniego znakowania receptorów przed procesem immobilizacji z wykorzystaniem znaczników (np. fluorescencyjnych) [124]. Niestety, takie podejście wiąże się ze skomplikowanym i czasochłonnym procesem koniugacji. Ponadto, sprzęganie receptora ze znacznikiem takim jak fluorofor, wiąże się z nieuniknioną utratą części białka w trakcie tej procedury a także potencjalnym obniżeniem jego zdolności wiążących na skutek chemicznej modyfikacji. Obecność znacznika związanego z receptorem może również komplikować odczyt sygnału (np. optycznego) podczas docelowej analizy.

Alternatywą dla powyższych metod jest poszukiwanie niespecyficznych znaczników białek, które umożliwiłyby ocenę jakości warstw złożonych z immobilizowanych receptorów. Choć podejście to jest bardziej uniwersalne, opracowanie takiej metody stanowi wyzwanie, ponieważ niespecyficzne znaczniki białek muszą wiązać się odwracalnie, aby nie zakłócać późniejszego rozpoznawania analitu przez receptor. Opisane wyżej metody kontroli jakości białkowych warstw receptorowych zostały przedstawione na Rysunku 6.

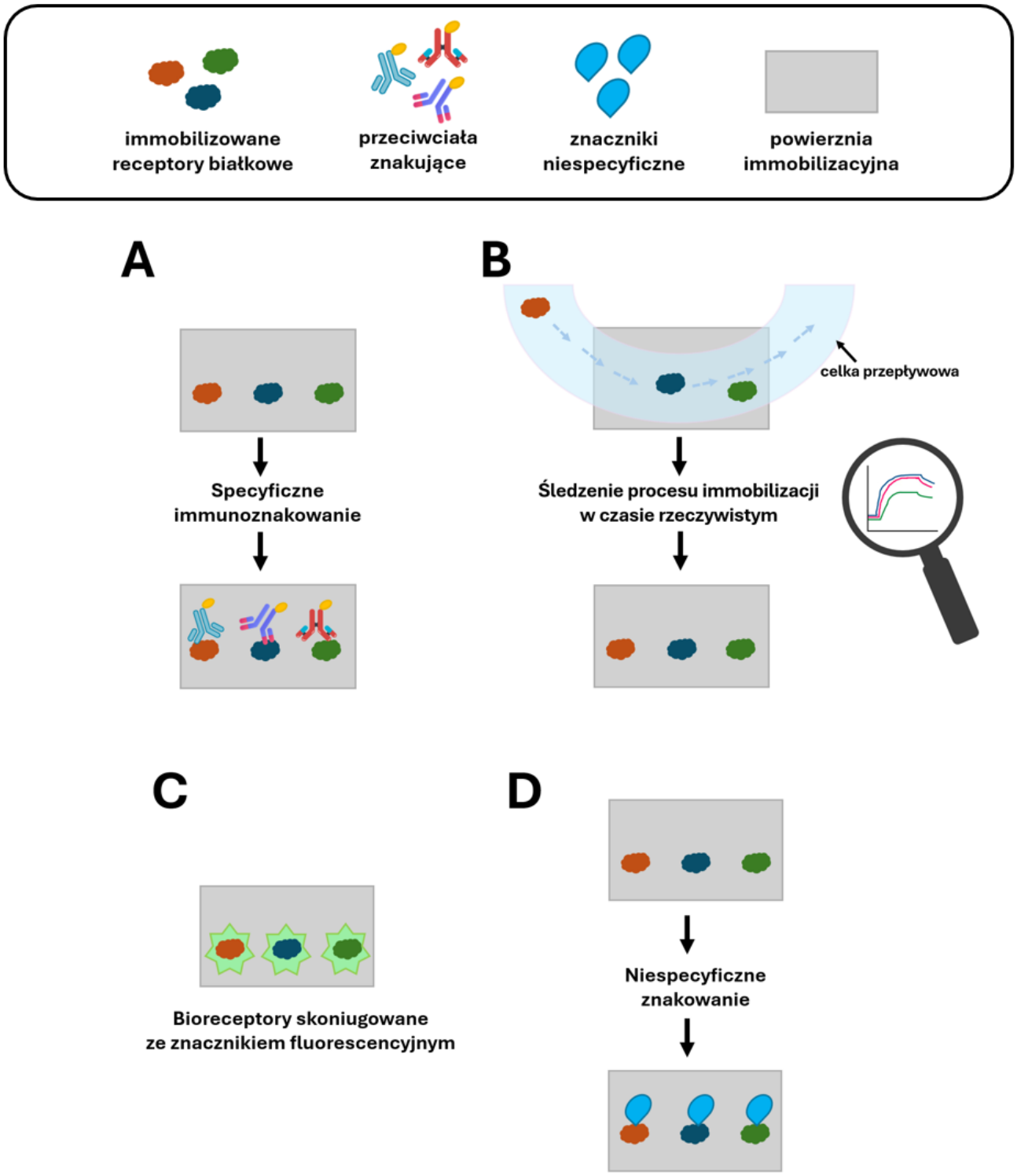

Rysunek 6. Metody kontroli jakości białkowych warstw receptorowych; A. Specyficzne znakowanie z wykorzystaniem przeciwciał, B. Monitorowanie procesu immobilizacji w czasie rzeczywistym, C. Wykorzystanie wyznakowanych bioreceptorów, D. Użycie niespecyficznych znaczników.

Podsumowanie

Unieruchomienie i przestrzenne rozmieszczenie białek w formie mikromacierzy na wspólnym podłożu to kluczowy etap w tworzeniu narzędzi analitycznych do detekcji wieloparametrowej. Proces ten wiąże się jednak z wyzwaniami technologicznymi, które wymagają odpowiedniego doboru metody immobilizacji w celu zapewnienia wysokiej jakości oraz powtarzalności warstw receptorowych. Na podstawie wniosków z niniejszego rozdziału, w ramach badań rozwijano kowalencyjne strategie unieruchamiania receptorów, ze szczególnym uwzględnieniem rozwiązań oferujących możliwość dowiązania białek w jednoetapowej reakcji, takich jak warstwy pośrednie zbudowane z reaktywnych kopolimerów. Podjęto również próby opracowania platform z regenerowalną warstwą receptorową poprzez unieruchomienie białek za pomocą kotwic oligonukleotydowych na podłożach złotych oraz transparentnych foliach PET. Proponowane podejście miało wykazać potencjalne przewagi metody DDI w zastosowaniach mikromacierzowych. Szczególną uwagę poświęcono analizie słabo poznanego dotychczas wpływu składu monowarstwy zawierającej kotwice ssDNA na stabilność i gęstość powierzchniową warstw receptorowych uzyskanych metodą DDI.

Analiza literatury wskazuje, iż istnieje problem braku powtarzalności uzyskiwanych gęstości powierzchniowych unieruchamianych receptorów białkowych i może on istotnie obniżać wiarygodność wyników analiz realizowanych za pomocą immunotestów w formacie *multiplex*. W pracy zidentyfikowano tę lukę badawczą i zaproponowano innowacyjne podejście – metodę mapowania gęstości receptorów w mikromacierzach SPRi z wykorzystaniem odwracalnego, niespecyficznego znakowania białek. Zaprezentowane rozwiązania odpowiadają na rosnące potrzeby diagnostyki wieloparametrowej oraz rozwój urządzeń POCT, wnosząc istotne innowacje w projektowanie nowoczesnych platform immunologicznych.

1.3 Strategie detekcji

Odpowiednia metoda detekcji sygnału, którą można zastosować do immunoplatform w formacie mikromacierzy, powinna oferować: (i) wysoki stosunek sygnału do szumu tła, (ii) w przypadku detekcji optycznej możliwość odczytu w trybie obrazowania lub skanowania, (iii) dobrą rozdzielczość przestrzenną, oraz (iv) odpowiednio wysoką stabilność odczytywanego sygnału [126]. W immunoplatformach do wykrywania oraz ilościowego

oznaczania bioanalitów, jak również do śledzenia oddziaływań biocząsteczkowych, stosowane są dwie podstawowe strategie: detekcja znacznikowa oraz detekcja bezznacznikowa.

1.3.1 Strategie wykorzystujące znaczniki

Strategie detekcji, w których odczytywany sygnał nie pochodzi bezpośrednio z interakcji białko receptorowe-analit, wykorzystują jako jego źródło dodatkowe znakowanie. Najczęściej spotykane jest wykorzystanie przeciwciał drugorzędowych skoniugowanych ze specjalną „metką" (z ang. *label* lub *tag*). Znacznik definiowany jest jako dowolna obca cząsteczka lub cząstka przyłączona do białka, umożliwiająca wykrycie obecności lub aktywności analitu w próbce. Odczyt sygnału jest możliwy dzięki wykorzystaniu szeregu technik analitycznych, w zależności od rodzaju znacznika, którego rolę mogą pełnić enzymy [127], barwniki fluorescencyjne [128], izotopy radioaktywne [129], znaczniki chemiluminescencyjne [130], kropki kwantowe [131], jak i nanocząstki [132].

Przykłady znaczników wykorzystanych w immunodetekcji biomarkerów wirusowych znajdują się w Tabeli 3.

Tabela 3. Przegląd znaczników stosowanych w immunotestach do wykrywania biomarkerów infekcji wirusowych

Rodzaj znacznika	Wykrywany analit	Strategia detekcji	Referencja
Peroksydaza chrzanowa (HRP)	Wirus Zika	Detekcja optyczna (utleniona TMB)	[133]
Fosfataza alkaliczna (ALP)	Wirus RSV	Detekcja optyczna (złote nanocząstki)	[134]
Kropki kwantowe	Antygen powierzchniowy wirusa zapalenia wątroby typu B	Detekcja optyczna-fluorescencja QDs	[135]

Złote nanogwiazdki	Wirus Zika oraz wirus dengi	Powierzchniowo wzmocniona spektroskopia ramanowska	[136]
Izotiocyjanian fluoresceiny (FITC)	Białko nukleokapsydu wirusa SARS-CoV-2	Detekcja optyczna - fluorescencja	[137]
Kropki kwantowe	CRP	Detekcja optyczna – fluorescencja QDs	[138]
Peroksydaza chrzanowa (HRP)	Przeciwciała skierowane przeciwko wirusowi afrykańskiego pomoru świń	Detekcja optyczna (utleniony luminol)	[139]
Złote nanocząstki jako nanozymy	Wirus grypy typu A	Detekcja optyczna (utleniona TMB)	[140]

Pierwsze immunotesty wykorzystujące znaczniki do detekcji sygnału pojawiły się pod koniec lat 50. XX wieku dzięki badaniom Rosalyn Yalow i Solomona Bersona [141]. Zastosowanie radioizotopów umożliwiło wykrywanie nano- i pikomolarnych stężeń związków w osoczu i tkankach, co przyczyniło się do rozwoju późniejszych technik, takich jak testy ELISA, w których radioizotopy zastąpiono enzymami.

W immunodetekcji znacznikowej stosuje się znakowanie bezpośrednie lub pośrednie, zwykle z koniugatem przeciwciała drugorzędowego. Każde z tych podejść odpowiada na inne potrzeby.

Znakowanie bezpośrednie upraszcza procedurę analityczną, redukując liczbę etapów w konstrukcji immunotestu. Eliminacja dodatkowej reakcji immunologicznej zmniejsza tym samym ryzyko reaktywności krzyżowej pomiędzy przeciwciałami [142, 143]. Konstrukcja

testu ze znakowaniem bezpośrednim polega na przyłączeniu znacznika sprzężonego z pierwszorzędowym przeciwciałem lub antygenem (tzw. znakującym), które bezpośrednio wiąże się z analitem (Rysunek 7A). Dzięki wytworzeniu znakowanego immunokompleksu w jednoetapowej reakcji metoda jest szybka i minimalizuje zużycie odczynników, co czyni ją korzystną w zastosowaniach wymagających natychmiastowych wyników. Należy jednak pamiętać, że ograniczona dostępność komercyjnych koniugatów przeciwciał często zmusza do uprzedniego, samodzielnego sprzęgania specyficznego bioreceptora ze znacznikiem.

Znakowanie pośrednie umożliwia stosowanie uniwersalnych koniugatów przeciwciał drugorzędowych, eliminując konieczność znakowania drogich i trudno dostępnych przeciwciał skierowanych przeciwko wykrywanym antygenom. W tym podejściu przeciwciało drugorzędowe, skoniugowane ze znacznikiem, wiąże się z przeciwciałem pierwszorzędowym lub antygenem, które pierwotnie związały się z docelowym analitem, tworząc układ kanapkowy (Rysunek 7B). Zastosowanie przeciwciał drugorzędowych, zwykle poliklonalnych, umożliwia wiązanie z wieloma epitopami receptora, co zwiększa efektywność znakowania i wzmacnia sygnał, czyniąc metodę bardziej czułą i uniwersalną. Jednakże, odbywa się to kosztem bardziej złożonego i wydłużonego procesu analitycznego. Mimo tej niedogodności, szeroka dostępność komercyjnych przeciwciał drugorzędowych stanowi istotną zaletę tej strategii.

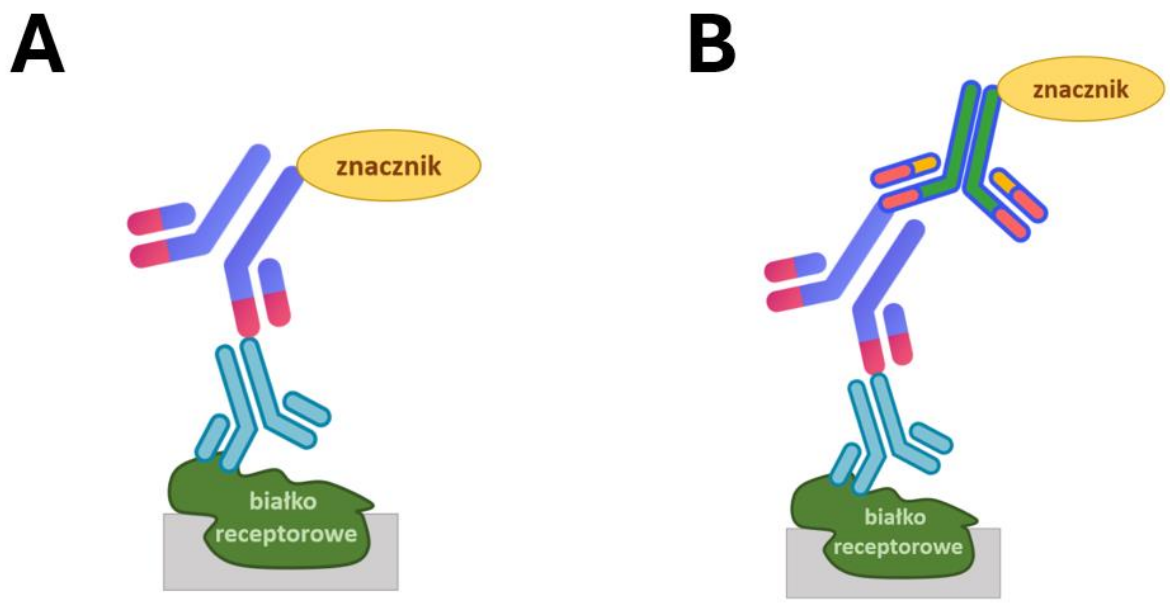

Rysunek 7. Schematyczne przedstawienie koncepcji znakowania w immunodetekcji znacznikowej: (A) znakowanie bezpośrednie, (B) znakowanie pośrednie.

1.3.2 Strategie bezznacznikowe

Alternatywną strategią detekcji sygnału w immunoplatformach jest bezpośredni pomiar zmian fizycznych wynikających z interakcji między receptorem a analitem. Metody te, bazujące na właściwościach biofizycznych, takich jak masa czy ładunek cząsteczki, eliminują potrzebę wtórnego znakowania, co umożliwia monitorowanie oddziaływań molekularnych w czasie rzeczywistym. Bezznacznikowe metody optyczne opierają się głównie na refraktometrii [144] lub reflektometrii, w tym rezonansie plazmonowym [145]. Natomiast najbardziej znanymi platformami akustycznymi są mikrowagi kwarcowe (QCM) [146]. Platformy wykorzystujące bezznacznikową transdukcję elektrochemiczną są mniej popularne niż ich odpowiedniki znacznikowe. Wynika to z faktu, że często wymagają zastosowania markerów redoks, które muszą być związane z receptorem lub obecne w roztworze [147].

Rezonans plazmonów powierzchniowych (SPR)

SPR jest jedną z najczęściej stosowanych technik detekcji bezznacznikowej. Technika ta została po raz pierwszy zastosowana w konstrukcji biosensora optycznego przez Liedberga i Nylandera w 1982 roku, a w ciągu kolejnych dziesięcioleci stała się niezwykle popularnym narzędziem do ilościowej charakteryzacji oddziaływań biocząsteczkowych [144].

W klasycznym formacie SPR immobilizacja białek receptorowych zachodzi bezpośrednio w celce mikrofluidycznej, co umożliwia śledzenie procesu unieruchamiania receptorów w czasie rzeczywistym a tym samym kontrolę ich gęstości powierzchniowej. Niestety takie rozwiązanie niesie za sobą praktyczne ograniczenie w konstrukcji biosensorów typu *multiplex,* gdyż w takim przypadku liczba potencjalnych białek receptorowych obecnych na jednym przetworniku jest zdeterminowana liczbą dostępnych celek przepływowych [148]. W praktyce ogranicza to możliwości konstrukcji macierzy SPR do maksymalnie 8 niezależnych pól testowych [149]. Alternatywą w takim przypadku jest SPR z obrazowaniem (z ang. *Surface Plasmon Resonance Imaging, SPRi*). Jest on pochodną klasycznego SPR i jego zasada działania bazuje na układzie mikromacierzowym. Z uwagi na przetwarzanie sygnału w postaci obrazu, cała powierzchnia przetwornika może zostać wykorzystana do unieruchomienia receptorów. Warto podkreślić jednak, że w przypadku SPRi immobilizacja zachodzi *ex-situ* poprzez nakraplanie roztworów bioreceptorów w określonych strefach poza systemem mikrofluidycznym urządzenia, co pozbawia SPRi możliwości śledzenia tego zjawiska w czasie

rzeczywistym. Schematy działania analizatorów SPRi oraz klasycznego SPR zostały przedstawione na Rysunku 8.

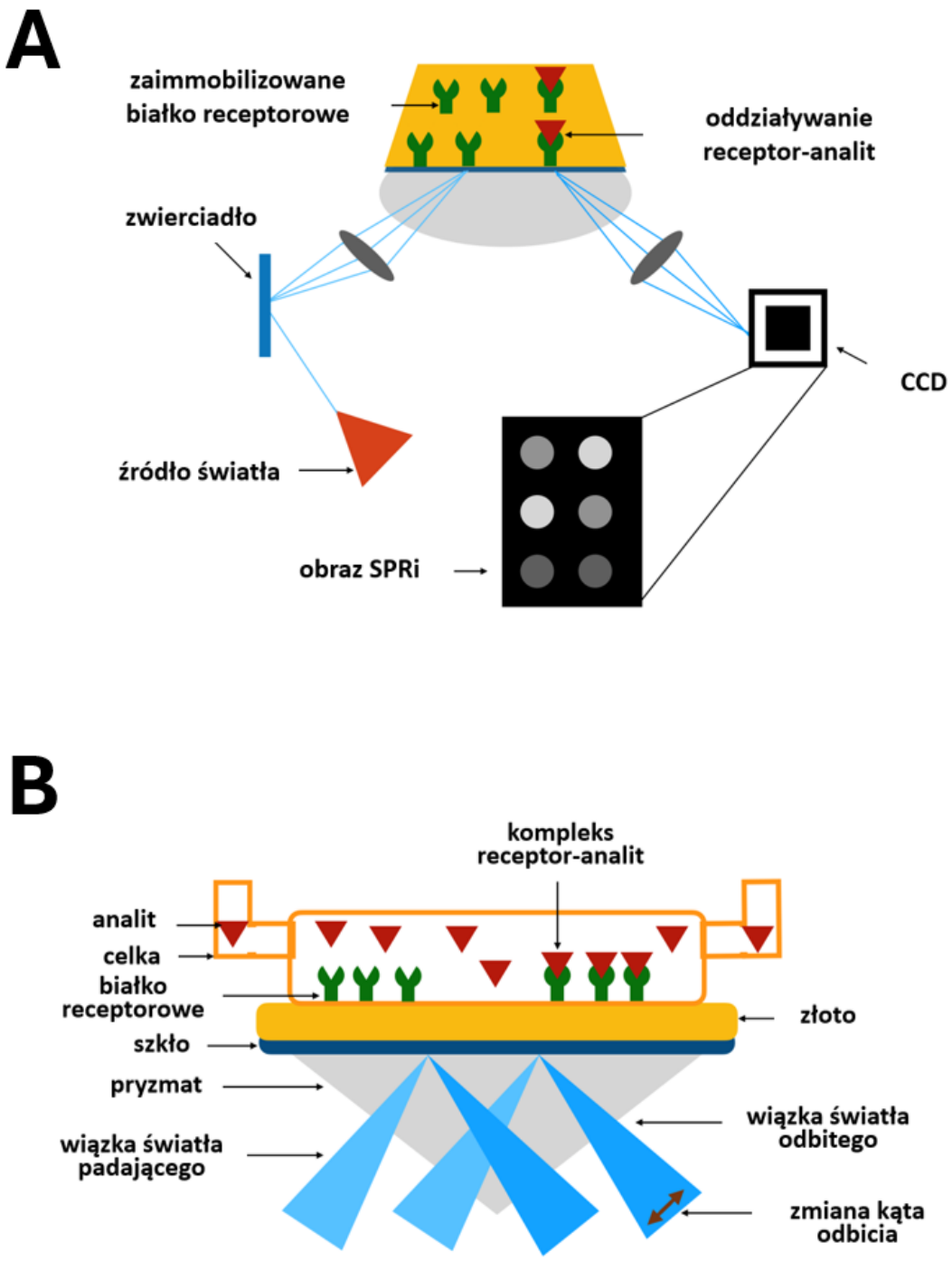

Rysunek 8. Schemat ukazujący różnice w konstrukcji analizatorów SPRi (A) oraz klasycznego SPR w trybie skanowania kątowego (B).

W technice SPR wykorzystuje się szklany przetwornik pokryty cienką warstwą metalu, najczęściej złota, na którym immobilizowane są białka receptorowe. Monochromatyczne, spolaryzowane światło pada na przetwornik, oddziałując z elektronami na powierzchni metalu i wzbudzając plazmony powierzchniowe w postaci fal elektromagnetycznych na granicy metalu i dielektryka [150]. Rezonans występuje, gdy częstotliwość światła odpowiada częstotliwości plazmonów, co prowadzi do maksymalnej absorpcji światła odbitego. Lokalne zmiany współczynnika załamania światła, zależne od masy przy powierzchni metalu, wpływają na obserwowane przesunięcie kąta rezonansowego. W SPRi (z ang. *imaging*) stały kąt padania światła umożliwia monitorowanie zmian intensywności promieniowania odbitego za pomocą kamery CCD (z ang. *charge-coupled device*), co pozwala na obserwację zaciemnień na obrazie różnicowym. Natężenie odbitego światła (reflektancja) zmienia się w czasie, co jest rejestrowane przez detektor. W klasycznym SPR pomiary mogą być prowadzone przy stałym kącie padania światła lub w trybie skanowania kątowego. Przesunięcie kąta rezonansowego jest proporcjonalne do masy cząsteczek związanych na powierzchni metalu w wyniku oddziaływań z unieruchomionymi receptorami [151].

1.3.3 Praktyczne porównanie strategii detekcji

Dobór strategii detekcji w immunotestach zależy zarówno od wymaganych do osiągnięcia parametrów analitycznych, wygody użytkownika jak i od kosztów analizatorów. Formaty znacznikowe charakteryzują się wysoką czułością, umożliwiającą wykrywanie analitów nawet na poziomie sub-pikomolarnym [152]. We wczesnych stadiach chorób stężenie biomarkerów w płynach ustrojowych bywa ekstremalnie niskie, co często uniemożliwia ich detekcję metodami bezznacznikowymi. Jednakże, zastosowanie znakowanych białek wiąże się z wyższymi kosztami produkcji takich imunotestów oraz wydłużonym czasem analizy. W diagnostyce POCT metody bezznacznikowe mogą stanowić korzystną alternatywę, ponieważ umożliwiają jednoetapowe pomiary w czasie rzeczywistym. W ostatnich latach obserwuje się wzrost liczby badań nad udoskonalaniem czujników bezznacznikowych, co świadczy o rosnącym zainteresowaniu tą technologią w diagnostyce medycznej [147, 153].

Analiza wieloparametrowa, umożliwiająca jednoczesną identyfikację wielu biomarkerów, odgrywa kluczową rolę w kompleksowej diagnostyce, na przykład w profilowaniu odpowiedzi immunologicznej. Choć metody znacznikowe są obecnie częściej stosowane, sensory bezznacznikowe również pozwalają na projektowanie takich platform

[154]. Jednakże ich zastosowanie jest ograniczone ze względu na niewielką liczbę technik oferujących jednocześnie odczyt bezznacznikowy i kompatybilność z formatem mikromacierzowym. Warto jednak podkreślić, że podejście bezznacznikowe umożliwia monitorowanie oddziaływań analitów z warstwą receptorową w czasie rzeczywistym, dostarczając tym samym więcej informacji o badanych oddziaływaniach międzycząsteczkowych, w tym o kinetyce wiązania [155, 156].

Podczas pracy ze złożonymi próbkami, takimi jak surowica, zasada generowania sygnału wykorzystywana w metodach bezznacznikowych może okazać się jednak znaczącą wadą, ponieważ składniki obecne w matrycy próbki mogą również wiązać się z powierzchnią czujnika, prowadząc do fałszywie dodatnich wyników [157]. W związku z tym, podczas projektowania tego typu formatów testów, konieczne jest zapewnienie maksymalnie wysokiej selektywności wiązania analitu z bioreceptorem.

W formatach wykorzystujących znaczniki sygnał tła oraz inne niepożądane efekty wynikające ze złożoności matrycy próbki są mniejsze, ponieważ rejestrowany sygnał pochodzi od znacznika, którego wiązanie jest w dużej mierze niezależne od składników matrycy [147]. Ponadto, w formacie kanapkowym (z ang. *sandwich format)* podwójnie rozpoznawanie molekularne przez receptor dodatkowo zwiększa selektywność znakowania. Niemniej jednak, ograniczeniem dla heterogenicznych formatów znacznikowych jest konieczność znalezienia kompatybilnych par receptorów (z ang. *matched pairs*) wykazujących powinowactwo do różnych epitopów wykrywanej cząsteczki, co często wymaga czasochłonnych testów optymalizacyjnych i może stanowić istotne wyzwanie w procesie projektowania takich platform. Dodatkowo, w przypadku metod znacznikowych analiza próbek o wysokim stężeniu analitu wiąże się z ryzykiem wystąpienia „efektu haka", które polega na uzyskiwaniu wyników fałszywie ujemnych z powodu nadmiaru analitu hamującego tworzenie kompleksów typu kanapkowego. Metody bezznacznikowe eliminują ryzyko wystąpienia tego zjawiska dzięki odmiennemu mechanizmowi działania, co czyni je bardziej niezawodnymi w analizie próbek o szerokim zakresie stężeń. W Tabeli 4 przedstawiono porównanie popularnych strategii detekcji wykorzystywanych w immunoplatformach z podziałem na znacznikowe i bezznacznikowe oraz oceną użyteczności poszczególnych technik w pomiarach multipleksowych oraz zautomatyzowanych analizatorach wysokoprzepustowych.

Tabela 4. Porównanie najczęściej wykorzystywanych znacznikowych i bezznacznikowych technik detekcji stosowanych w immunoplatformach

	Metoda detekcji	Koszt aparatury do odczytu sygnału	Możliwość pomiarów multipleksowych	Możliwość analiz wysokoprze-pustowych
Znacznikowe	Fluorescencja	Niski	Tak	Tak
	Chemiluminescencja	Niski	Tak	Tak
	Pomiary elektrochemiczne	Niski	Tak	Tak
	Znakowanie radioizotopami	Średni	Tak	Nie
	Znakowanie nanocząstkami	Niski	Tak	Tak
Bezznacznikowe	Mikrowaga kwarcowa (QCM)	Wysoki	Nie	Nie
	Rezonans plazmonów powierzchniowych (SPR)	Wysoki	Nie	Tak
	Rezonans plazmonów powierzchniowych z obrazowaniem (SPRi)	Wysoki	Tak	Tak
	Powierzchniowo wzmocniona spektroskopia ramanowska (SERS)	Bardzo wysoki	Tak	Tak

Podsumowanie

Metody znacznikowe, dzięki swojej wysokiej czułości, pozostają złotym standardem w diagnostyce medycznej. Z kolei strategie bezznacznikowe oferują unikalne możliwości monitorowania oddziaływań receptor-analit w czasie rzeczywistym, co pozwala na poznanie dynamiki oddziaływań cząsteczkowych bez potrzeby modyfikacji białek. Tradycyjnie w opisywanych w literaturze pracach badawczych, techniki bezznacznikowe i formaty wykorzystujące znakowanie są traktowane niezależnie jako dwie alternatywne strategie detekcji.

W niniejszej pracy doktorskiej zaproponowano podejście polegające na wykorzystaniu technik bezznacznikowych (SPR i SPRi) zarówno jako strategii detekcji w konstrukcji immunosensorów SPR, jak również jako uzupełniającego narzędzia do charakteryzacji oddziaływań, które jest szczególnie przydatne na początkowych etapach projektowania immunotestów. Takie wygodne narzędzie pomaga bardziej szczegółowo monitorować i lepiej zrozumieć procesy zachodzące na powierzchni. Zaproponowane podejście wykorzystujące system SPR pozwala na śledzenie oddziaływań wybranych receptorów z docelowymi analitami w czasie rzeczywistym, a także na kontrolę nad gęstością powierzchniową białek.

Rozdział 2

2. Cel i zakres pracy doktorskiej

Celem niniejszej pracy doktorskiej było opracowanie nowych strategii wytwarzania i charakteryzacji białkowych warstw receptorowych do multipleksowej detekcji biomarkerów związanych z zakażeniami wirusowymi.

Droga do realizacji tego celu w pierwszym etapie obejmowała badania nad różnymi aspektami procesu immobilizacji białek receptorowych przy użyciu kotwic DNA (DDI), m. in. za pomocą rezonansu plazmonów powierzchniowych (SPR). Ważnym zadaniem było również opracowanie innowacyjnej, nieopisanej do tej pory w literaturze, metody kontroli jakości warstw receptorowych w formacie mikromacierzy SPRi, do czego wykorzystano anionowe barwniki jako niespecyficzne znaczniki receptorów białkowych unieruchomionych na powierzchni przetwornika. Dalsze badania miały na celu opracowanie uniwersalnych strategii immobilizacji białek (zarówno odwracalnych jak i nieodwracalnych) na powierzchniach złotych oraz foliach PET i sprawdzenie możliwości ich wykorzystania w konstrukcji immunotestów. Modelowe receptory obejmowały przeciwciała klasy IgG oraz białka o charakterze antygenowym, w tym białko nukleokapsydu (N) wirusa SARS-CoV-2.

Opracowane podejście miało na celu zapewnienie możliwości unieruchomienia obu grup modelowych receptorów, niezależnie od ich struktury i właściwości, a następnie łatwą implementację wybranego rozwiązania do formatów multipleksowych.

Na drodze do osiągnięcia zaplanowanego celu scharakteryzowano wybrane strategie (pasywną adsorpcję, immobilizację kowalencyjną oraz DDI) wykorzystując bezznacznikową detekcję SPR. Ostatnim z celów cząstkowych pracy było zaprojektowanie platform diagnostycznych do wykrywania biomarkerów infekcji wirusowych w diagnostyce serologicznej. Korzystając z reaktywnych kopolimerów jako warstw przejściowych, skonstruowano immunotesty na elastycznych podłożach PET z detekcją w oparciu o znakowanie enzymatyczne. Ich potencjalną użyteczność zweryfikowano na końcowym etapie badań, analizując rzeczywiste próbki surowic pobranych od pacjentów pod kątem diagnostyki COVID-19.

W ramach pracy doktorskiej zaplanowano następujące, szczegółowe zadania badawcze, których realizacja stała się podstawą cyklu 4 artykułów naukowych:

- analiza dostępnych metod immobilizacji białek umożliwiających ich unieruchamianie na różnych podłożach (głównie złotych i polimerowych);
- weryfikacja istotności wpływu składu monowarstwy zawierającej sondy ssDNA oraz czystości i stechiometrii koniugatów DNA-białko na stabilność i gęstość powierzchniową białkowych warstw receptorowych immobilizowanych poprzez DDI;
- opracowanie nowej, łagodnej dla unieruchomionych białek i kompatybilnej z techniką SPRi w formacie mikromacierzowym metody kontroli jakości warstwy receptorowej z wykorzystaniem odwracalnego znakowania barwnikami anionowymi;
- zaprojektowanie strategii unieruchamiania receptorów białkowych na potrzeby konstrukcji immunotestów w oparciu o detekcję znacznikową (znakowanie enzymatyczne) z wykorzystaniem elastycznych podłoży i reaktywnych kopolimerów;
- weryfikacja użyteczności wytworzonych platform w analizie próbek rzeczywistych (surowica krwi) na potrzeby diagnostyki serologicznej COVID-19.

Główne zadania badawcze zostały przedstawione w formie graficznej na Rysunku 9.

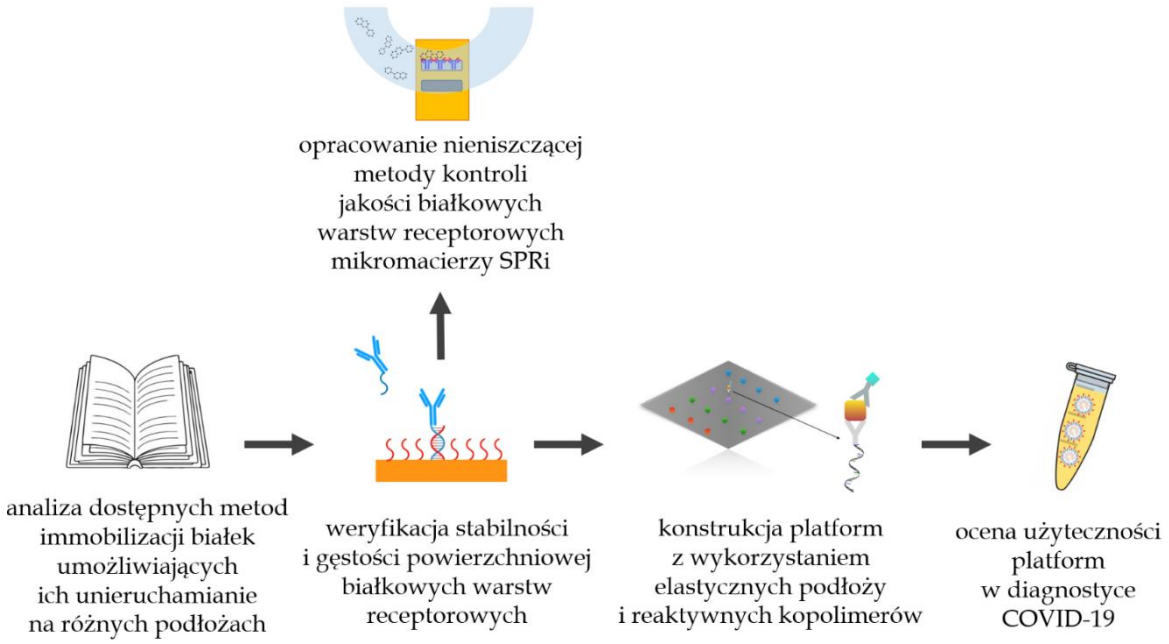

Rysunek 9. Zadania badawcze wyznaczone w ramach cyklu czterech artykułów naukowych stanowiących podstawę rozprawy doktorskiej.

Rozdział 3

3. Komentarz do cyklu artykułów naukowych będących podstawą rozprawy doktorskiej

Cykl publikacji naukowych, które składają się na niniejszą rozprawę doktorską, przedstawia opis badań nad rozwojem nowoczesnych immunoplatform umożliwiających multipleksową detekcję biomarkerów związanych z zakażeniami wirusowymi z wykorzystaniem dwóch systemów detekcji – bezznacznikowej detekcji SPRi oraz detekcji spektrofotometrycznej w oparciu o znakowanie enzymatyczne. Są to cztery publikacje naukowe, z których pierwsza (P1) ma charakter przeglądowy, a pozostałe trzy (P2, P3, P4) prezentują wyniki oryginalnych badań eksperymentalnych.

3.1 Projektowanie warstw receptorowych do zastosowań w immunodiagnostyce [P1]

We wprowadzeniu literaturowym (w podrozdziale *1.3 Strategie detekcji*) wykazano, że immunosensory z zastosowaniem rezonansu plazmonów powierzchniowych (SPR) wyróżnia zdolność do bezpośredniego monitorowania oddziaływań pomiędzy biocząsteczkami w czasie rzeczywistym bez konieczności stosowania znaczników. Ta cecha czyni SPR szczególnie atrakcyjnym i przydatnym narzędziem w projektowaniu warstw receptorowych platform biosensorowych.

Projektowanie białkowych warstw receptorowych odpowiednich do analizy próbek rzeczywistych i kompatybilnych z formatami multipleksowymi wymaga dogłębnej analizy dostępnych strategii immobilizacji oraz zrozumienia kluczowych wyzwań technologicznych, które mogą wpływać na proces detekcji. Warstwy te powinny charakteryzować się adaptowalnością, czyli łatwością ich dostosowania do nowych typów receptorów, a także możliwością regeneracji, co pozwala na wielokrotne użycie czujnika czy immunotestu bez znaczącego pogorszenia jego parametrów analitycznych.

A artykule **P1** przedstawiono przegląd literatury dotyczący najnowszych osiągnięć i istniejących wyzwań w zakresie konstrukcji warstw receptorowych immunosensorów SPR. Stanowi on niezbędne wprowadzenie do badań eksperymentalnych opisanych w kolejnych pracach wchodzących w skład tej rozprawy. W artykule **P1** przeanalizowano i porównano różnorodne metody wytwarzania białkowych warstw receptorowych, akcentując wpływ

wybranej strategii unieruchamiania receptorów na potencjalne możliwości zastosowań diagnostycznych uzyskanego immunosensora. Wykonany przegląd literatury (**P1**) pozwala wyróżnić dwie wiodące grupy metod unieruchamiania receptorów białkowych. Pierwsza z nich obejmuje wykorzystanie fizycznej adsorpcji bądź chemicznej funkcjonalizacji powierzchni skutkujące losową orientacją wiązanych receptorów, z kolei druga obejmuje metody ukierunkowanej immobilizacji wykorzystujące powinowactwo biologiczne.

W artykule **P1** podkreślono fundamentalne różnice pomiędzy strategiami immobilizacji oraz zawarto szczegółowe omówienie różnych podejść do tego zagadnienia, w tym metod fizycznych, takich jak adsorpcja elektrostatyczna, i chemicznych, które zapewniają trwałe połączenie, ale mogą wpływać na konformację i aktywność białek związanych z powierzchnią. Zwrócono szczególną uwagę na nowatorskie podejścia umożliwiające immobilizację białek (zarówno przeciwciał, jak i receptorów antygenowych, w tym białek rekombinowanych) z zachowaniem ich stabilności i aktywności biologicznej, takie jak immobilizacja z wykorzystaniem bakteriofagów, bakteryjnych superantygenów czy immobilizacja za pomocą kotwic DNA (DDI). Wykonany przegląd literaturowy wskazuje na rosnące zainteresowanie badaczy możliwością monitorowania procesów zachodzących na powierzchni sensora w czasie rzeczywistym oraz wykorzystania metod immobilizacji w oparciu o powinowactwo biologiczne.

W publikacji **P1** podsumowano główne ograniczenia w zastosowaniu immunosensorów SPR do diagnostyki medycznej. Jest to m.in. adsorpcja składników złożonych matryc biologicznych, które mogą negatywnie wpływać na wiarygodność uzyskiwanych wyników. Wartym podkreślenia wnioskiem jest również fakt, iż stabilność chemiczna oraz powtarzalność procesu wytwarzania warstw receptorowych ciągle pozostają wyzwaniami technologicznymi, które mogą negatywnie wpływać na wiarygodność i odtwarzalność uzyskiwanych wyników. Te wyzwania pozostają również aktualne względem innych rodzajów immunotestów czy sensorów działających w formacie detekcji *multiplex*, co podkreśla uniwersalny charakter przedstawionej problematyki. Aby sprostać tym wyzwaniom, konieczne jest rozwijanie nowatorskich metod wytwarzania i charakteryzacji warstw immunoreceptorowych, co stało się podstawą badań nad metodą kontroli ich jakości, opisanych w artykule **P3**. Z kolei propozycja odpowiedzi na wspominane wyzwania związane z niespecyficzną adsorpcją składników próbek klinicznych i wydajnością procesu immobilizacji przedstawione zostały w publikacji **P4**.

W pracy przeglądowej **P1** podkreślono, że spośród metod wykorzystujących powinowactwo biologiczne, DDI wyróżnia się możliwością precyzyjnej kontroli gęstości powierzchniowej białek na powierzchni. Ponadto, strategia ta umożliwia efektywną regenerację warstw kotwiczących poprzez zniszczenie dupleksów DNA-DNA stanowiących główny mechanizm kotwiczenia receptorów białkowych. Z uwagi na wspomniane zalety strategia DDI została wybrana do dalszych badań, opisanych w artykule **P2**.

Należy w tym miejscu podkreślić jednak fakt, że w istniejących doniesieniach literaturowych podejmujących temat wytwarzania białkowych warstw receptorowych z wykorzystaniem DDI stosunkowo niewielką uwagę przykłada się do optymalizacji składu warstwy kotwiczącej koniugaty DNA-białko (typowo monowarstwy mieszanej zawierającej sondy ssDNA i czynnik blokujący powierzchnię, tzw. „wypełniacz") oraz oczyszczania uzyskanych koniugatów DNA-białko z nadmiaru reagentów, w szczególności niezwiązanych nici DNA. W obliczu doniesień wskazujących na stosunkowo niewielką wydajność sprzęgania nici DNA z grupami aminowymi białka, a co za tym idzie konieczność stosowania nadmiaru DNA w reakcji koniugacji, jego obecność może stanowić istotny, acz jak dotąd niezauważony problem wpływający negatywnie na efektywność wiązania koniugatów przez warstwę kotwiczącą [158]. Zbadanie literatury przedmiotu przedstawione w pracy **P1** umożliwiło dostrzeżenie niszy badawczej, jaką jest ulepszenie metodologii wytwarzania białkowych warstw receptorowych z wykorzystaniem DDI. Spostrzeżenie to stanowiło również asumpt do sformułowania i późniejszej weryfikacji hipotezy badawczej dotyczącej możliwości poprawy gęstości powierzchniowej receptorów białkowych, a tym samym czułości immunosensorów konstruowanych w oparciu o DDI, poprzez optymalizację składu warstwy kotwiczącej oraz wykorzystanie odpowiednio oczyszczonych koniugatów DNA-białko o preferowanej stechiometrii 1:1.

Zgodnie z przyjętymi celami badawczymi, przegląd literatury w artykule **P1** stanowił niezbędne wprowadzenie do badań nad projektowaniem białkowych warstw receptorowych, ukierunkowując je na wybór bardziej zaawansowanych strategii immobilizacji i wskazując na potrzebę optymalizacji parametrów tego procesu.

3.2 Badania nad warstwami receptorowymi w oparciu o hybrydyzację DNA jako fundament rozwoju adaptowalnych platform multipleksowych [P2]

Mając na uwadze sformułowany cel niniejszej rozprawy doktorskiej, jakim było opracowanie adaptowalnych białkowych warstw receptorowych przeznaczonych do multipleksowej detekcji biomarkerów związanych z zakażeniami wirusowymi, praca **P2** odgrywa kluczową rolę w jego realizacji. Opisane w niej badania koncentrują się na szczegółowym zrozumieniu procesów towarzyszących immobilizacji białek za pomocą kotwic DNA oraz ich optymalizacji na potrzeby konstrukcji nowoczesnych platform diagnostycznych opartych na tej technologii.

Przeprowadzone badania miały na celu między innymi weryfikację hipotezy badawczej dotyczącej wpływu stechiometrii i czystości koniugatów białko-DNA na wydajność ich immobilizacji na warstwach kotwiczących pokrytych sondami zbudowanymi z jednoniciowych kwasów nukleinowych. W pierwszym etapie badań opisanych w artykule **P2** skoniugowano dwa rodzaje modelowych receptorów – białko nukleokapsydu wirusa SARS-CoV-2 oraz przeciwciało przeciwko ludzkiemu białku C-reaktywnemu – z kotwicami DNA, a następnie przeprowadzono oczyszczenie mieszaniny poreakcyjnej za pomocą chromatografii jonowymiennej. Metoda ta wykorzystuje różnice w czasach retencji składników mieszaniny uzyskanej po koniugacji, które wynikają z innych ładunków rozdzielanych biomolekuł. Dzięki chromatograficznemu oczyszczaniu udało się oddzielić niepożądane komponenty pozostające w mieszaninie reakcyjnej po reakcji sprzęgania (**Rysunek 1** w publikacji **P2** oraz **Rysunek S1** w suplemencie do tego artykułu), takie jak wolne, nieskoniugowane białka oraz DNA. Wpływ stopnia oczyszczenia koniugatów DNA-przeciwciało na kinetykę procesu DDI został zbadany przy użyciu SPR, a sensogramy będące wynikiem przeprowadzonych analiz zestawiono na **Rysunku 2** artykułu **P2.** Krzywe asocjacji (wynikające z hybrydyzacji kotwic DNA z komplementarnymi sondami unieruchomionymi na powierzchni chipa) zarówno wolnego DNA, jak i koniugatów białkowych przed i po oczyszczaniu chromatograficznym, przedstawione na **Rysunek 2A** potwierdzają hipotezę, iż niepożądane komponenty mieszaniny w znaczący sposób zakłócają proces immobilizacji receptorów białkowych. Charakter oddziaływania nieoczyszczonych koniugatów z warstwą jest zbliżony do oddziaływania wolnego DNA, co wynika z dużego stężenia tej niewielkiej biocząsteczki w roztworze i przypuszczenia, iż jej przyłączanie jest faworyzowane kinetycznie względem wiązania dużych struktur DNA-białko. Przypuszczenie to znalazło dodatkowe potwierdzenie w wyznaczonych

stałych kinetycznych charakteryzujących oba wspomniane oddziaływania (**Rysunki 2B i 2C** oraz **Rysunek S3** w suplemencie publikacji **P2**). Oddziaływanie kotwic z wolnym DNA cechowała zarówno wyższa szybkość asocjacji (k_a = 1,51 · 10^5 M^{-1} · s^{-1}) oraz niższa stała dysocjacji kompleksu (K_D = 1,95 mM) w porównaniu do parametrów opisujących wiązanie koniugatu DNA-przeciwciało (odpowiednio k_a = 1,13 · 10^5 M^{-1} · s^{-1} i K_D = 5,19 nM). Wnioski z tych doświadczeń jednoznacznie wskazują na potrzebę dokładnego oczyszczania mieszaniny poreakcyjnej z niezwiązanych nici DNA.

W toku dalszych badań nad poprawą efektywności i stabilności wiązania koniugatów DNA-białko przez warstwy kotwiczące w strategii DDI porównano różne rodzaje sond oligonukleotydowych unieruchomionych na powierzchni złota na drodze chemisorpcji, w tym klasyczne DNA oraz jego analogi, tj. PNA (z ang. *peptide nucleic acid*) i ZNA® (z ang. *zip nucleic acid)* (**Rysunek 3** w publikacji **P2**). W przypadku PNA standardowy szkielet cukrowo-fosforanowy został zastąpiony neutralnym chemicznie łańcuchem poliamidowym (polimerem opartym na N-(2-aminoetylo)glicynie), natomiast w ZNA oligonukleotydy są sprzężone z kationowymi jednostkami sperminy. Obie modyfikacje miały na celu zmniejszenie odpychania elektrostatycznego pomiędzy komplementarnymi nićmi kwasów nukleinowych, co by potencjalnie zwiększyło stabilność uzyskanych dupleksów. Przeprowadzone badania efektywności hybrydyzacji immobilizowanych analogów z DNA w roztworze ujawniły, że ZNA® pozwala osiągnąć blisko dwukrotnie wyższą efektywność hybrydyzacji w porównaniu do klasycznych sond DNA, podczas gdy w przypadku PNA nie obserwowano wiązania komplementarnej sekwencji (**Rysunek 3B** w publikacji **P2**).

Bazując na wynikach pomiarów ζ-potencjału powierzchni wskazujących na odmienny ładunek powierzchniowy warstw kotwiczących zawierających sondy DNA i ZNA® (odpowiednio -38,2 mV dla DNA i +47,8 mV dla ZNA®) wysnuto hipotezę, że zastosowanie kationowej warstwy ZNA® może korzystnie wpływać na stabilność dupleksów z DNA, a tym samym na stabilność koniugatów białek receptorowych unieruchomionych w wyniku DDI. Wykorzystując technikę SPR sprawdzono prawdziwość takiego założenia (**Rysunek 5** w publikacji **P2**). Co jednak zaskakujące, poza wcześniej zaobserwowaną, wyższą wydajnością tworzenia dupleksu ZNA®-DNA, nie zaobserwowano podwyższonej stabilności tego typu hybryd względem klasycznych hybryd DNA-DNA w warunkach niskiej siły jonowej. Podsumowanie badań dotyczących typów sond oligonukleotydowych, w tym efektywności unieruchamiania sond, wpływu analogów na tworzenie dupleksów, koszt syntezy analogów,

a także ich wpływ na ładunek powierzchni zostało zawarte w **Tabeli S2** suplementu publikacji **P2**. Wnioski z niej płynące wskazują na zauważalnie wyższą efektywność hybrydyzacji sond ZNA w porównaniu do klasycznych sond DNA, przy jednocześnie znacząco wyższych kosztach ich syntezy. W obliczu braku istotnych zalet z punktu widzenia stabilności dupleksów ZNA®-DNA, w szczególności braku odporności na obniżoną siłę jonową roztworu (co pozwoliłoby obniżyć wymagania względem składu buforów stosowanych w konstrukcji immunotestów w oparciu o DDI, m. in. na etapach przemywania), w dalszych badaniach wykorzystywano warstwy kotwiczące zawierające sondy DNA.

Kolejnym krokiem w kierunku optymalizacji składu warstw kotwiczących do DDI był dobór odpowiedniego czynnika wypełniającego. W tym celu porównano trzy polarne ligandy różniące się wielkością i elastycznością strukturalną, tj. 6-merkaptoheksanol oraz tiolowane pochodne poli(glikolu etylenowego) o ciężarze cząsteczkowym odpowiednio 800 i 3000 Da. Odpowiedzi SPRi zestawione na **Rysunku 6** w artykule **P2** wskazują, iż PEG o ciężarze cząsteczkowym 800 Da działa skutecznie jako czynnik zabezpieczający przed niespecyficzną adsorpcją białka obecnego we wprowadzonej do układu próbce oraz generuje mniejsze przeszkody steryczne podczas procesu wiązania DNA w porównaniu z PEG o ciężarze 3 kDa. Jednocześnie sprawdzono również wpływ gęstości powierzchniowej sond na uzyskiwane sygnały SPR pochodzące od hybrydyzacji z DNA. W celu uzyskania warstw kotwiczących o różnych gęstościach powierzchniowych sond DNA, były one współimmobilizowane z tiolowanym PEG-800 jako środkiem rozcieńczającym w różnych stosunkach molowych. Wnioski z doświadczenia zilustrowanego na **Rysunku 6F** wskazują, że „rozcieńczona" warstwa uzyskana przez koadsorpcję sondy DNA z PEG-800 w stosunku molowym 1:4 wykazywała o ponad 120% lepszą zdolność wiązania komplementarnej nici DNA niż analogiczna warstwa utworzona przez „nierocieńczoną" sondę.

Celem sprawdzenia, czy warstwa kotwicząca o uprzednio zoptymalizowanym składzie zapewnia odpowiednie warunki do wydajnego i specyficznego unieruchomienia koniugatów DNA-przeciwciało poprzez DDI, przeprowadzono sekwencyjne doświadczenie w ramach którego unieruchomiono początkowo wolną nić DNA, a następnie koniugaty białko-DNA a oba procesy były zakończone regeneracją z wykorzystaniem 50 mM roztworu NaOH (**Rysunek 7** w publikacji **P2**). Wykazano wysoką skuteczność regeneracji, zarówno na etapie zerwania wiązań w dupleksie DNA, jak i usunięcia powstałych immunokompleksów po etapie immunoznakowania zaimmobilizowanych koniugatów białek receptorowych. Z kolei brak

obserwowanych zmian sygnału SPRi w obszarach stanowiących referencję świadczy o wysokiej selektywności immobilizacji (ograniczonej wyłącznie do wcześniej przygotowanych pól testowych zawierających komplementarne sondy DNA), jak również wskazuje na brak adsorpcji niespecyficznej białka receptorowego. Wnioski te wskazują na możliwość wykorzystania opracowanego w ramach badań protokołu unieruchamiania receptorów białkowych poprzez DDI również w warunkach przepływowych.

Podsumowując, badania opisane w pracy **P2** dowiodły, iż szczegółowa analiza szeregu parametrów, takich jak czystość koniugatów białkowych, rodzaj i gęstość powierzchniowa sond DNA oraz rodzaj czynnika wypełniającego wykazują istotny wpływ na efektywność wiązania przez warstwę kotwiczącą koniugatów DNA-białko. Opisane powyżej innowacje wprowadzone do procedur immobilizacji stanowią nową wiedzę, ważną z punktu widzenia dalszego rozwoju zaawansowanych platform diagnostycznych w oparciu o DDI.

3.3 Nieniszcząca metoda kontroli jakości białkowej warstwy receptorowej w formacie mikromacierzy SPRi [P3]

We wstępie literaturowym artykułu **P3**, jak również szerzej we wprowadzeniu niniejszej Rozprawy (podrozdział *1.2.3*) nakreślono potrzebę poszukiwania metod kontroli jakości białkowych warstw receptorowych w formatach mikromacierzowych wytwarzanych w procesach immobilizacji *ex situ*. Podkreślono, że brak dokładnych i nieinwazyjnych narzędzi do oceny takich warstw stanowi ograniczenie z punktu widzenia ich rutynowego stosowania.

W części doświadczalnej artykułu **P3** zaprezentowano wyniki badań nad zaproponowanym nowatorskim podejściem do kontroli jakości warstw receptorowych w systemach SPRi, które wykorzystuje odwracalne znakowanie powierzchniowo unieruchomionych białek barwnikami anionowymi. Wstępna selekcja barwników, polegająca na zbadaniu kinetyki ich wiązania z zaimmobilizowanym na powierzchni przeciwciałem króliczym za pomocą SPRi, wykazała, że z puli badanych sześciu barwników jednynie Ponceau S (PS), czerń amidowa 10B (Amido Black 10B, AB) oraz błękit brylantowy G-250 (Coomassie Brilliant Blue G-250, CBB-G) wykazują zdolność do odwracalnego wiązania z białkiem (**Rysunki S1 i S2** suplementu artykułu **P3**).

Schemat przyjętej procedury badawczej zilustrowany na **Rysunku 1A** obejmuje w pierwszym etapie unieruchomienie modelowych białek – transferyny i przeciwciała króliczego klasy IgG – przy użyciu klasycznego SPR na powierzchni złotego przetwornika.

Proces ten pozwolił na monitorowanie procesu immobilizacji w czasie rzeczywistym oraz wyznaczenie gęstości powierzchniowej zaimmobilizowanych białek. Korzystając z **Równania 1** przedstawionego w publikacji **P3,** wiążącego zmianę kąta rezonansowego i ilość zasocjowanej na powierzchni masy, możliwe było każdorazowo dokładne określenie gęstości powierzchniowej zaimmobilizowanych receptorów. Przetwornik z unieruchomionymi receptorami o znanej gęstości powierzchniowej przenoszono następnie do aparatu SPRi, gdzie prowadzano dalsze badania nad ich odwracalnym znakowaniem za pomocą barwników. Sensogram różnicowy SPRi pokazany na **Rysunku 1C** ilustruje odwracalność oddziaływania wybranych barwników anionowych z przeciwciałem króliczym unieruchomionym na powierzchni. Obraz CCD uchwycony przed i po znakowaniu potwierdza możliwość wizualizacji receptorów na powierzchni i niespecyficzny charakter oddziaływań barwników z białkami (zarówno przeciwciałami, jak i antygenami). Z kolei brak zauważalnej zmiany sygnału SPRi dla stref w których nie zostało zaimmobilizowane białko świadczy o braku oddziaływań między barwnikami a podłożem, co potwierdza selektywność wybranych znaczników względem białek. Jako alternatywną metodę kontroli jakości białkowych warstw receptorowych w przedstawionych badaniach wybrano specyficzne znakowanie białek za pomocą odpowiednio dobranych względem nich przeciwciał (**Rysunek S1B** w publikacji **P3**).

W kolejnym etapie prac skupiono się na optymalizacji metody celem uzyskania możliwie wysokiej czułości znakowania za pomocą wybranych barwników. **Rysunek 2A** w publikacji **P3** ilustruje wpływ pH medium na czułość odpowiedzi SPRi dla PS, AB oraz CBB-G. Zaobserwowano, że najbardziej efektywne wiązanie wszystkich trzech barwników zachodzi w środowisku kwaśnym, zaś za optymalne dla PS i CBB-G przyjęto pH 2,0 (bufor glicyna-HCl) z kolei w przypadku AB – pH 4,0 (bufor octanowy). Celem dokładniejszego poznania mechanizmu oddziaływania barwnik-białko w poszczególnych przypadkach, zbadano wpływ siły jonowej (stężenia NaCl) na odpowiedzi SPRi dla AB oraz CBB-G (**Rysunek 2B**). W przypadku czerni amidowej, wraz ze wzrostem stężenia soli zaobserwowano istotny spadek czułości znakowania, co potwierdziło kluczową rolę oddziaływań elektrostatycznych w wiązaniu tego barwnika z białkami. W przypadku błękitu brylantowego, którego wiązanie opiera się głównie na oddziaływaniach hydrofobowych, zmiana siły jonowej nie miała tak znaczącego wpływu na czułość odpowiedzi.

Jako, że opracowana metoda mapowania białek powierzchniowych powinna być nieniszcząca dla unieruchomionych receptorów, w toku dalszych badań oceniono wpływ

oddziaływania roztworu barwnika na zachowanie zdolności immobilizowanego białka do tworzenia immunokompleksów oraz ogólną stabilność warstwy receptorowej. Jest to o tyle istotne, że sam proces znakowania za pomocą PS i CBB-G jest prowadzony w roztworze o niskim pH, typowo stosowanym do regeneracji białkowych warstw receptorowych (bufor glicyna-HCl, pH 2,0). Na **Rysunku 3** w publikacji **P3** przedstawiono analizę zmian odpowiedzi biosensora SPRi na przestrzeni sześciu cykli, w ramach których nastrzyki roztworu CBB-G poprzedzane były specyficznym immunoznakowaniem jednego z białek receptorowych (króliczego IgG). Pomiędzy specyficznym i niespecyficznym znakowaniem wprowadzono etapy regeneracji warstwy. W przypadku obu modelowych białek można zauważyć, że warstwa receptorowa tylko nieznacznie traci swoją zdolność wiązania. Zarówno w przypadku immunoznakowania, jak i oddziaływania z barwnikiem, zauważono niewielkie spadki odpowiedzi (w obu przypadkach spadki po 6 cyklu nie przekraczały 30% względem wyjściowego sygnału). Te zmiany zostały przypisane naturalnemu, stopniowemu procesowi degradacji i desorpcji warstwy. Rezultaty badań wykazały, że nastrzyki roztworu barwnika CBB-G w buforze o pH 2,0 nie wywołują istotnej degradacji czy utraty aktywności immobilizowanych kowalencyjnie receptorów białkowych, co potwierdza nieniszczący dla warstwy receptorowej charakter proponowanej metody kontroli jakości.

Zbadano także korelację między sygnałem SPRi uzyskanym w wyniku oddziaływania barwnik-białko a gęstością powierzchniową receptorów. Pozwoliło to na ocenę użyteczności metody pod kątem analiz ilościowych. Wykresy przedstawiające uzyskane zależności dla znakowania transferyny i IgG za pomocą trzech wybranych barwników oraz dla immunoznakowania (jako metody referencyjnej) zostały przedstawione na **Rysunku 4** w publikacji **P3**. Analiza uzyskanych wyników wykazała, że dla wszystkich trzech badanych barwników, a także dla mapowania z wykorzystaniem przeciwciał, możliwe jest wyznaczenie w określonych zakresach liniowej zależności opisującej relację odpowiedzi SPRi i gęstości powierzchniowej białek. Zdecydowanie najwyższą czułość ilościowego oznaczenia białek powierzchniowych (odpowiednio 6,6 RU/ng · mm^{-2} dla IgG i 4,4 RU/ng · mm^{-2} dla transferyny) uzyskano przy pomocy znakowania CBB-G. Należy jednak zwrócić uwagę, że uzyskane różnice w czułościach względem obydwu białek w przypadku znakowania danym rodzajem barwnika wskazują na konieczność wstępnej kalibracji metody na potrzeby analiz ilościowych. Uzyskane wyniki potwierdziły hipotezę, że przedstawiona metoda może być stosowana do ilościowej oceny gęstości powierzchniowej unieruchomionych receptorów.

W toku dalszych badań wstępnie zweryfikowano potencjał zastosowania opracowanej metody do mapowania białek unieruchomionych na komercyjnym podłożu CMD. Podłoże takie, w przeciwieństwie do wcześniej badanych monowarstw na powierzchni Au stanowi trójwymiarową matrycę umożliwiającą uzyskanie znacząco wyższych gęstości powierzchniowych unieruchomionych białek, co opisywano szerzej w publikacji **P1**. Dzięki temu podłoża CMD stanowią złoty standard w analizach białek za pomocą techniki SPR. **Rysunek 5** w publikacji **P3** przedstawia zależność sygnału SPRi uzyskanego w wyniku oddziaływania barwnik-białko (**Rysunek 5A** dla króliczego IgG, **Rysunek 5B** dla transferyny) lub immunoznakowania tych receptorów zaimmobilizowanych na slajdzie CMD. Do immobilizacji wykorzystano roztowry białek o stężeniach: 100 μg/ml - oznaczone jako stężenie wysokie (H) lub 5 μg/ml - oznaczone jako stężenie niskie (L). Aby dokładniej ocenić ilościowe zależności, obliczono stosunki sygnału SPRi uzyskane dla tych dwóch stężeń dla każdego z białek. Przyjęto, że im bliższy jest stosunek odpowiedzi SPRi do stosunku gęstości powierzchniowych uzyskanych w wyniku kowalencyjnej immobilizacji w warunkach przepływowych, tym dokładniej dany barwnik odzwierciedla przedstawione korelacje.

Wartości uzyskanych współczynników opisujących relacje pomiędzy sygnałem a gęstością powierzchniową białka podsumowane w **Tabeli 1** w publikacji **P3** jednoznacznie wskazują, że proporcje pomiędzy różnymi gęstościami powierzchniowymi białek na slajdzie CMD zdecydowanie najlepiej odwzorowuje ich znakowanie za pomocą barwnika PS. Przypuszczalnym wytłumaczeniem obserwowanego zjawiska jest bardzo szybka kinetyka jego asocjacji, skutkująca łatwością wysycenia dostępnych miejsc wiążących w strukturze białek, nawet w przypadku ich dużego upakowania na powierzchni. Uzyskane rezultaty stanowią przesłankę świadczącą o dużej uniwersalności zaproponowanej metody, jednak jej implementacja do kontroli jakości białkowych warstw receptorowych uzyskiwanych na innych podłożach wymaga dalszych, bardziej szczegółowych badań.

Końcowym etapem walidacji opracowanej metody była ocena użyteczności w zastosowaniach mikromacierzowych. W tym celu przygotowano platformę o architekturze mikromacierzy na chipie SPRi z unieruchomionymi *ex-situ* transferyną oraz przeciwciałem króliczym w postaci pól testowych o zróżnicowanej gęstości powierzchniowej. Różnice te osiągnięto poprzez nanoszenie różnych stężeń białek (od 2 do 200 μg/ml) na wspólne podłoże. Na **Rysunku 6A** w publikacji **P3** przedstawiono zależności pomiędzy rejestrowanymi zmianami sygnałów SPRi w wyniku oddziaływania barwnik-białko (lub immunoznakowania

jako metody referencyjnej), a stężeniami receptorów użytych do immobilizacji. Ich analiza potwierdziła, że każdy z trzech wybranych do badań barwników umożliwia wizualizację, a także (w określonych zakresach, dla których zaobserwowano liniowe odpowiedzi) również ilościową ocenę gęstości powierzchniowej białek receptorowych unieruchomionych na powierzchni CMD. Brak obserwowanych zmian sygnału dla pól testowych bez zaimmobilizowanego białka oraz możliwość wizualizacji obu białek w jednym doświadczeniu potwierdzają dodatkowo pożądany, niespecyficzny charakter oddziaływania barwnik-białko. Wspomniane zalety stanowią przewagę proponowanego rozwiązania nad immunoznakowaniem.

Podsumowując, badania opisane w artykule **P3** dowodzą, że odwracalne znakowanie barwnikami anionowymi jest skuteczną i nieniszczącą metodą kontroli jakości białkowych warstw receptorowych w systemach SPRi. Wykorzystanie niespecyficznego znakowania umożliwia szybką wizualizację receptorów oraz ilościową ocenę ich gęstości powierzchniowej. Opracowana metodyka, będąca najważniejszym osiągnięciem opisanym w tej publikacji, jest nowatorskim narzędziem wspierającym rozwój platform biosensorycznych w układach mikromacierzowych.

W tym miejscu chciałabym wspomnieć, że badania dotyczące wykorzystania barwników anionowych do mapowania białkowych warstw receptorowych biosensorów SPRi w formacie *multiplex* były kontynuowane. Prace te ukierunkowano na sprawdzenie możliwości adaptacji opracowanej metodyki do charakteryzacji warstw receptorowych uzyskanych innymi metodami, ze szczególnym uwzględnieniem immobilizacji z wykorzystaniem powinowactwa biologicznego. Pokazano, że jest możliwe zastosowanie wybranych barwników do kontroli jakości warstw receptorowych bazujących na metodzie DDI (opracowanych w ramach publikacji **P2)** oraz z wykorzystaniem powinowactwa kaptawidyna-biotyna. Potwierdzono również, że znakowanie białek anionowymi barwnikami (na przykładzie CBB-G) może zostać skutecznie wykorzystane do kontroli gęstości powierzchniowej białek receptorowych unieruchomionych kowalencyjnie na podłożach karboksylowanych o zróżnicowanych architekturach powierzchni. Wyniki zebrano i przedstawiono w manuskrypcie o roboczym tytule „*Practical and Mechanistic Insights into Receptor Layer Quality Control in Label-free SPRi Biosensors Using Click-Biology Approaches*”, który jest obecnie na końcowym etapie przygotowania i nie może być włączony do cyklu publikacji będących podstawą przedłożonej rozprawy doktorskiej.

3.4 Platformy immunoenzymatyczne skonstruowane na bazie elastycznych podłoży PET i reaktywnych kopolimerów [P4]

W tym etapie prac badawczych skoncentrowano się na opracowaniu elastycznych immunoplatform kompatybilnych z formatem *multiplex* w oparciu o znakowanie enzymatyczne. Punkt wyjścia stanowić miały funkcjonalizowane reaktywnymi kopolimerami folie PET, zaś celem było uzyskanie zminiaturyzowanych, elastycznych podłoży testowych do wykrywania różnych klas i podklas immunoglobulin w surowicy pacjentów pod kątem diagnostyki zakażeń SARS-CoV-2. Wyzwanie badawcze podjęte w artykule **P4** wpisuje się w aktualne trendy diagnostyki medycznej, łącząc rozwój mikroobjętościowych testów ELISA z możliwościami miniaturyzacji i integracji z platformami typu *lab-on-a-foil.*

Prekursory do wytwarzania warstw reaktywnych kopolimerów pozyskano w ramach współpracy naukowej z instytutem SCITEC w Mediolanie (grupa badawcza prof. Marcelli Chiari). Reaktywne kopolimery zawierały w swojej strukturze odpowiednie grupy funkcyjne (odpowiednio: - estry N-hydroksysukcynimidowe w polimerze MCP-2 oraz grupy azydkowe w polimerze Copoly Azide), co umożliwiało kontrolowaną immobilizację cząsteczek posiadających w strukturze grupy aminowe i reszty dibenzocyklooktynowe (DBCO) [159]. Struktura i szczegółowy skład kopolimerów wykorzystanych w badaniach oraz mechanizm immobilizacji cząsteczek na ich powierzchni zostały przedstawione na **Rysunku S1** w suplemencie publikacji **P4**.

Multipleksowe platformy diagnostyczne powinny umożliwiać wykrywanie różnych przeciwciał przeciwko wybranym antygenom. W związku z tym, badania rozpoczęto od selekcji antygenu wirusa SARS-CoV-2, w ramach której stwierdzono, że platformy wykorzystujące nukleoproteinę (NP) lub domenę wiążącą receptor (RBD) jako receptory białkowe, oferują zbliżoną i wysoką czułość immunotestów serologicznych. Z uwagi na omawianą szerzej we wstępie literaturowym (podrozdział *1.1.1 Biomarkery zakażeń wirusowych*) immunogenność oraz wysoki poziom ekspresji NP, białko to zostało ostatecznie wybrane do dalszych badań jako modelowy antygen.

Aby ocenić wpływ rodzaju podłoża i sposobu immobilizacji antygenu na czułość serologicznych testów immunologicznych oraz niespecyficzną adsorpcję składników surowicy, porównano różne materiały polimerowe w roli podłoży immunotestów. Podczas eksperymentów zaobserwowano, iż w przypadku unieruchamiania rekombinowanych antygenów podłoże i metoda ich immobilizacji mają o wiele większy wpływ na uzyskiwaną

czułość immunotestu niż w przypadku immobilizowanych przeciwciał (**Rysunek 1, P4**). Dlatego tym bardziej zasadne wydało się poszukiwanie rozwiązań pozwalających na uzyskanie stabilnego i efektywnego dowiązania białek do różnych podłoży, w tym materiałów elastycznych i cienkowarstwowych kompatybilnych z technologiami mikrofluidycznymi. W odpowiedzi na sformułowany problem badawczy, do opracowania miniaturowych platform do testów immunoenzymatycznych wykorzystano podłoża z folii PET modyfikowane warstwą kopolimeru MCP-2 reaktywnego względem grup aminowych białek.

Potwierdzono przewagę kowalencyjnej immobilizacji na podłożu PET modyfikowanym MCP-2 nad pasywną adsorpcją, wykazując wyższą czułość testu serologicznego w obu stosowanych strategiach znakowania – pośrednim i bezpośrednim (**Rysunek 2, P4**). Format pośredni dodatkowo pozwolił na uzyskanie przeciętnie o ponad 30% wyższych sygnałów dla tej samej próbki surowicy zawierającej przeciwciała IgG przeciwko nukleoproteinie SARS CoV-2, dzięki dodatkowej amplifikacji sygnału przez koniugat przeciwciała drugorzędowego.

Kolejnym etapem badawczym było zastosowanie immunoplatformy PET opartej na MCP-2 do analizy ilościowej. Przedstawione na **Rysunku 3** w artykule **P4** zależności zarejestrowanych sygnałów w funkcji rozcieńczeń surowicy (**3A**) oraz stężeń przeciwciała monoklonalnego przeciwko białku N SARS CoV-2 (**3B**) w obu przypadkach cechują szerokie zakresy zarówno dynamicznej, jak i liniowej odpowiedzi. Stanowi to dowód, iż platformy skonstruowane na foliach PET pokrytych MCP-2 dają możliwość ilościowej analizy próbek pod kątem zawartości przeciwciał anty-SARS-CoV-2. Dodatkowo, na podstawie krzywej kalibracyjnej (**Rysunek 3B)** wyznaczono parametry analityczne testu w formacie bezpośrednim i uzyskano odpowiedź liniową w zakresie stężeń 5-200 ng/ml komercyjnych mysich przeciwciał monoklonalnych anty-SARS-CoV-2, przy dolnej granicy wykrywalności wynoszącej 2,73 ng/ml.

W celu weryfikacji użyteczności diagnostycznej, immunoplatforma na podłożu PET została zastosowana najpierw do wykrywania podklas przeciwciał IgG (IgG1, IgG2, IgG3 i IgG4) w surowicy pacjenta z potwierdzonym COVID-19, a następnie do przetestowania 28 próbek surowicy od pacjentów z dodatnim i ujemnym wynikiem testu na COVID-19 pod kątem zawartości specyficznych przeciwciał klas IgG i IgA (**Rysunek 4** w publikacji **P4**). Przedstawione wykresy pokazują, że dla obu wykrywanych klas specyficznych przeciwciał uzyskane sygnały (wartości absorbancji) dla surowic dodatnich są znacznie wyższe niż dla próbek ujemnych, przekraczając przyjętą wartość odcięcia (stanowiącą średnią z sygnałów

dla próbek ujemnych zwiększoną o podwojone odchylenie standardowe). Podstawowe parametry diagnostyczne testu dla klas IgA i IgG (**Tabela 1**, publikacja **P4**) określono na podstawie wszystkich 28 próbek. Czułość w ujęciu diagnostycznym wyniosła 100% (14/14 próbek pozytywnych poprawnie sklasyfikowanych), a swoistość 92,9% (1/14 próbek negatywnych błędnie sklasyfikowano jako pozytywną).

Reasumując, dotychczas opisane badania w artykule **P4** dotykają szeregu aspektów aplikacyjnych, dotyczących wytwarzania podłoży i konstruowania miniaturowych platform multipleksowych z detekcją immunoenzymatyczną. Niemniej jednak, zaproponowana metodyka kowalencyjnej immobilizacji z wykorzystaniem reaktywnego kopolimeru MCP-2, choć wykazuje istotne przewagi względem dotychczas wykorzystywanych rozwiązań, nie jest w stanie w pełni sprostać wyzwaniom wynikającym z różnorodności strukturalnej antygenów. Uzyskane wyniki potwierdziły wcześniejszą hipotezę dotyczącą konieczności poszukiwania bardziej uniwersalnych podejść do immobilizacji białek, tj. takich, które pozwalają na efektywne unieruchomienie receptorów bez brania pod uwagę ich indywidualnej budowy. Takim podejściem jest DDI, co zostało omówione w artykule **P1** i **P2**.

Na podstawie powyższych wniosków, jak również metodyki opisanej w publikacji **P2** postanowiono sprawdzić możliwość konstrukcji testu immunoenzymatycznego w formacie multipleksowym na folii PET w oparciu o metodę DDI.

Do badań nad implementacją DDI na foliach PET wykorzystano reaktywny kopolimer Copoly Azide, który umożliwia reakcję typu „*click chemistry*" z biocząsteczkami posiadającymi grupy dibenzocyklooktynowe (DBCO). W ramach badań wstępnych potwierdzono selektywność procesu kowalencyjnej immobilizacji modyfikowanych DBCO sond ssDNA na powierzchni reaktywnego kopolimeru Copoly Azide (**Rysunek 5A**, publikacja **P4**). Technika rezonansu plazmonów powierzchniowych z obrazowaniem (SPRi) umożliwiła śledzenie w czasie rzeczywistym oddziaływania komplementarnego DNA i koniugatów DNA-białko z tak wytworzonymi warstwami kotwiczącymi. Badanie wykazało, że Copoly Azide skutecznie zapobiega niespecyficznej adsorpcji biomolekuł i umożliwia stabilne unieruchomienie sond DNA oraz immobilizację koniugatów DNA-białko poprzez hybrydyzację, co czyni ten kopolimer odpowiednim do zastosowania jako warstwę przejściową w procesie DDI na folii PET.

Zarejestrowane zmiany sygnałów na skutek wiązania koniugatów DNA-białko widoczne na sensogramach SPRi (**Rysunek 5B**, publikacja **P4**) potwierdziły skuteczność immobilizacji obydwu modelowych białek receptorowych (nukleoproteiny oraz przeciwciał

przeciwko ludzkim IgG). Co szczególnie istotne, uzyskano gęstości powierzchniowe receptorów na bardzo podobnym poziomie, niezależnie od ich struktury, co stanowić miało jedną z hipotetycznych przewag metody DDI nad kowalencyjnym dowiązaniem.

Ostatnim elementem prac badawczych, ważnym z punktu widzenia celu niniejszej rozprawy, było przeniesienie strategii immobilizacji receptorów białkowych za pomocą hybrydyzacji kotwic DNA na podłoża PET kompatybilne z detekcją znacznikową. W celu weryfikacji poprawności działania skonstruowanego testu przeprowadzono ilościowy test serologiczny przy użyciu ludzkiej surowicy w różnych rozcieńczeniach (**Rysunek 6A** w publikacji **P4**). W pierwszym kroku pozytywnie zweryfikowana została specyficzność wiązania analitów przez warstwę receptorową immobilizowaną poprzez DDI.

Dalsze szczegółowe badania potwierdzające postulowany przebieg procesu immobilizacji poprzez DDI (**Rysunek S3** w suplemencie publikacji **P4**) wykazały, że unieruchomienie receptora białkowego na folii zmodyfikowanej Copoly Azide zachodzi prawie wyłącznie poprzez tworzenie dupleksu DNA-DNA. Potwierdza to fakt, iż nie zaobserwowano niespecyficznej adsorpcji koniugatów na podłożu pozbawionym komplementarnych sond oligonukleotydowych. Następne doświadczenie stanowiło weryfikację hipotezy badawczej dotyczącej możliwości tworzenia platform multipleksowych w oparciu o znakowanie immunoenzymatyczne przy pomocy metody DDI jako podstawowej strategii immobilizacji. Jednoczesna immobilizacja dwóch różnych receptorów białkowych pozwoliła na wykrywanie przeciwciał zarówno w próbkach syntetycznych zawierających przeciwciała IgG ze źródeł komercyjnych, jak i w próbkach rzeczywistych (**Rysunek 6B** w publikacji **P4**). Co szczególnie ważne, niezależnie od składu matrycy próbki, w każdym z przypadków obserwowano jedynie śladowy sygnał pochodzący z próbek kontrolnych.

Wyniki zawarte w publikacji **P4** dowodzą, że stanowiące główny element nowości w niniejszej pracy folie PET funkcjonalizowane reaktywnymi kopolimerami w roli podłoży testów immunoenzymatycznych mogą stanowić ważne ogniwo w rozwoju nowoczesnych platform multipleksowych do diagnostyki serologicznej. Prostota procesu wytwarzania podłoży modyfikowanych kopolimerami akrylowymi z reaktywnymi grupami funkcyjnymi (na przykładzie MCP-2 i Copoly Azide) oraz ich kompatybilność z różnymi metodami immobilizacji stanowi istotny aspekt sprzyjający opracowaniu nowoczesnych, przenośnych systemów diagnostycznych. Mogą one znaleźć zastosowanie zarówno w warunkach klinicznych, jak i systemach typu POCT.

Rozdział 4

4. Podsumowanie

Niniejsza rozprawa doktorska, będąca cyklem powiązanych tematycznie artykułów naukowych, przedstawia wyniki badań dotyczące projektowania nowoczesnych platform immunodiagnostycznych do multipleksowej detekcji biomarkerów związanych z zakażeniami wirusowymi. W ramach pracy przeprowadzono analizę dotychczas wykorzystywanych metod immobilizacji bioreceptorów i zdefiniowano kluczowe wyzwania z nimi związane w kontekście możliwości ich zastosowania w konstrukcji platform w formacie macierzy białkowych.

Wykazano, że metoda DDI może zostać z powodzeniem wykorzystana do realizowanego w jednoetapowym procesie unieruchamiania zróżnicowanych pod względem struktury białek, takich jak przeciwciała i antygeny rekombinowane. Udowodniono, iż kluczowe znaczenie dla zapewnienia odpowiedniej gęstości powierzchniowej warstw immunoreceptorowych uzyskiwanych poprzez DDI miało zastosowanie oczyszczonych chromatograficznie koniugatów DNA-białko o kontrolowanej stechiometrii w roli receptorów. Badania potwierdziły, że dobór odpowiednich komponentów monowarstwy kotwiczącej, w tym składników niereceptorowych takich jak wypełniacze powierzchni, wpływa na szereg parametrów związanych z jej funkcjonowaniem. Wybór jako wypełniacza pochodnej PEG o ciężarze cząsteczkowym około 800 Da okazał się dobrym kompromisem pomiędzy zachowaniem przez warstwę zdolności wiązania koniugatów białko-DNA a zapewnieniem ochrony przed niespecyficzną adsorpcją białek. Przeprowadzone badania z wykorzystaniem techniki SPR i SPRi udowodniły, iż DDI jako strategia immobilizacji pozwala na szybkie i odwracalne unieruchomienie różnych białek receptorowych na powierzchni złota w formacie macierzowym. Zastosowanie powinowactwa biologicznego umożliwia również efektywną regenerację warstw receptorowych na skutek dysocjacji dupleksów kotwic DNA z koniugatami DNA-białko.

Opracowana metoda mapowania i kontroli jakości białkowych warstw receptorowych za pomocą odwracalnego znakowania białek barwnikami anionowymi umożliwiła ilościową i jakościową charakteryzację warstw receptorowych w formacie mikromacierzy SPRi, zachowując aktywność biologiczną receptorów. Każdy z finalnie wytypowanych do tego celu barwników wykazywał unikatowe zalety, takie jak: wysoka czułość w przypadku Coomassie

G-250, łagodne warunki znakowania (pH 4,0) w przypadku czerni amidowej 10B oraz duża labilność kompleksu barwnik-białko, ułatwiająca jego szybkie odmycie z warstwy, obserwowana w przypadku Ponceau S. Wykazano, iż opracowane metody znakowania białek powierzchniowych są kompatybilne z różnymi podłożami typowo stosowanymi do kowalencyjnej immobilizacji białek na przetwornikach SPR (w tym z monowarstwami typu SAM i warstwami 3D z hydrożelu karboksymetylodekstranu). Należy podkreślić, że po odpowiedniej modyfikacji opracowane metody dają szansę ich stosowania również w przypadku niekowalencyjnych strategii immobilizacji (takich jak DDI), co było obiektem dalszych badań, których wyniki nie zostały ujęte w niniejszej rozprawie.

Zaprojektowano i przetestowano elastyczne immunoplatformy uzyskane z wykorzystaniem folii PET funkcjonalizowanych kopolimerami MCP-2 oraz Copoly Azide. Przeprowadzona za pomocą bezpośredniego immunoznakowania analiza porównawcza warstw receptorowych złożonych z immobilizowanych antygenów białkowych potwierdziła, iż kowalencyjna immobilizacja białek na powierzchni folii PET pokrytej MCP-2 pozwala osiągnąć kilkukrotnie wyższe gęstości powierzchniowe receptorów w porównaniu do pasywnej adsorpcji, co przekłada się na większą stabilność warstwy receptorowej oraz redukcję niespecyficznych oddziaływań w testach serologicznych. Badania wykazały, że zastosowane polimery umożliwiają efektywną i stabilną immobilizację receptorów białkowych, zarówno w formacie znacznikowym (wykorzystującym znakowanie enzymatyczne), jak i bezznacznikowym (z detekcją SPR). Zaprojektowane platformy pozwoliły na skuteczną i wiarygodną analizę różnych klas i podklas przeciwciał w surowicach pacjentów po przebyciu COVID-19. Na podstawie wyników analiz 28 próbek rzeczywistych stwierdzono, iż immunoplatformy PET cechują się 100% czułością diagnostyczną oraz 92,9% swoistością w wykrywaniu przeciwciał anty-SARS-CoV-2, co potwierdza ich potencjał aplikacyjny w diagnostyce serologicznej. Zaimplementowanie strategii DDI na elastycznych podłożach PET potwierdziło jej wszechstronność w kontekście detekcji multipleksowej. Zademonstrowano, iż elastyczne podłoża polimerowe w połączeniu z nowoczesnymi metodami immobilizacji i znakowania mogą być wykorzystane do rozwoju przenośnych testów diagnostycznych typu POCT, umożliwiających szybkie i skuteczne wykrywanie zakażeń wirusowych.

Niniejsza praca dostarcza nowych rozwiązań w zakresie projektowania białkowych warstw receptorowych oraz wskazuje kluczowe czynniki wpływające na ich jakość

i funkcjonalność. Uzyskane wyniki stanowią solidny fundament do dalszych badań nad immunoplatformami zgodnymi z wymaganiami nowoczesnej diagnostyki multipleksowej i systemów typu *point-of-care.*

Najważniejsze osiągnięcia badawcze:

- Wykazanie przewagi DDI nad klasycznymi metodami immobilizacji pod względem uniwersalności i łatwości unieruchamiania receptorów białkowych na różnych podłożach.
- Opracowanie i optymalizacja metody DDI do unieruchamiania przeciwciał i rekombinowanych antygenów białkowych na podłożach złotych i polimerowych.
- Zaprojektowanie nieniszczącej metody kontroli jakości warstw receptorowych, umożliwiającej mapowanie gęstości powierzchniowej białek w mikromacierzowych platformach SPRi.
- Stworzenie immunoplatform na bazie folii PET funkcjonalizowanych reaktywnymi kopolimerami do diagnostyki serologicznej oraz wdrożenie strategii DDI na modyfikowanych podłożach PET w konstrukcji immunoplatform multipleksowych.

Bibliografia

[1] A. H. Rishu et al., ‘Time required to initiate outbreak and pandemic observational research’, J Crit Care, vol. 40, pp. 7–10, 2017, doi: 10.1016/j.jcrc.2017.02.009.

[2] R. Filip, R. Gheorghita Puscaselu, L. Anchidin-Norocel, M. Dimian, and W. K. Savage, ‘Global Challenges to Public Health Care Systems during the COVID-19 Pandemic: A Review of Pandemic Measures and Problems’, J Pers Med, vol. 12, no. 8, 2022, doi: 10.3390/jpm12081295.

[3] A. Stern and R. Andino, Viral Evolution: It is All About Mutations. 2016. doi: 10.1016/B978-0-12-800964-2.00017-3.

[4] S. Subramanian, ‘The long-term evolutionary history of gradual reduction of cpg dinucleotides in the sars-cov-2 lineage’, Biology (Basel), vol. 10, no. 1, pp. 1–9, 2021, doi: 10.3390/biology10010052.

[5] E. S. Mayne, J. A. George, and S. Louw, Assessing Biomarkers in Viral Infection, vol. 1412. 2023. doi: 10.1007/978-3-031-28012-2_8.

[6] E. G. S. James H. Strauss, ‘CHAPTER 2 - The Structure of Viruses’, in Viruses and Human Disease, Second Edition., E. G. S. James H. Strauss, Ed., Academic Press, 2008, pp. 35–62. doi: 10.1016/B978-0-12-373741-0.50005-2.

[7] M. G. Rossmann, ‘Structure of viruses: A short history’, Q Rev Biophys, vol. 46, no. 2, pp. 133–180, 2013, doi: 10.1017/S0033583513000012.

[8] T. Aoshi, S. Koyama, K. Kobiyama, S. Akira, and K. J. Ishii, ‘Innate and adaptive immune responses to viral infection and vaccination’, Curr Opin Virol, vol. 1, no. 4, pp. 226–232, 2011, doi: 10.1016/j.coviro.2011.07.002.

[9] G. E. Greening and J. L. Cannon, ‘Human and Animal Viruses in Food (Including Taxonomy of Enteric Viruses)’, in Viruses in Foods, Springer International Publishing, 2016, pp. 5–57. doi: 10.1007/978-3-319-30723-7_2.

[10] Y. Vázquez et al., ‘Cytokines in the respiratory airway as biomarkers of severity and prognosis for respiratory syncytial virus infection: An update’, Front Immunol, vol. 10, no. JUN, 2019, doi: 10.3389/fimmu.2019.01154.

[11] D. Vasileva and A. Badawi, ‘C-reactive protein as a biomarker of severe H1N1 influenza’, Inflammation Research, vol. 68, no. 1, pp. 39–46, 2019, doi: 10.1007/s00011-018-1188-x.

[12] A. Waris et al., ‘Evaluation of serum procalcitonin level as a biomarker for disease severity in COVID-19 patients’, New Microbes New Infect, vol. 43, 2021, doi: 10.1016/j.nmni.2021.100922.

[13] D. Loureiro, I. Tout, S. Narguet, S. M. Benazzouz, A. Mansouri, and T. Asselah, ‘Mirnas as potential biomarkers for viral hepatitis b and c’, Viruses, vol. 12, no. 12, 2020, doi: 10.3390/v12121440.

[14] A. O. Ipinmoroti and Q. L. Matthews, ‘Extracellular vesicles: Roles in human viral infections, immune-diagnostic, and therapeutic applications’, Pathogens, vol. 9, no. 12, pp. 1–20, 2020, doi: 10.3390/pathogens9121056.

[15] Z. R. Korobova et al., ‘Changes in Anti-SARS-CoV-2 IgG Subclasses over Time and in Association with Disease Severity’, Viruses, vol. 14, no. 5, 2022, doi: 10.3390/v14050941.

[16] T. Wasiluk et al., ‘Analysis of the IgG subclass profile and IgG sum-total discrepancy in COVID-19 convalescent plasma donors: A single-centre prospective cohort study’, Transfusion and Apheresis Science, vol. 62, no. 1, 2023, doi: 10.1016/j.transci.2022.103527.

[17] T. Kang, J. Lu, T. Yu, Y. Long, and G. Liu, ‘Advances in nucleic acid amplification techniques (NAATs): COVID-19 point-of-care diagnostics as an example’, Biosens Bioelectron, vol. 206, 2022, doi: 10.1016/j.bios.2022.114109.

[18] M. W. Pandori, J. Lei, E. H. Wong, J. Klausner, and S. Liska, ‘Real-time PCR for detection of herpes simplex virus without nucleic acid extraction’, BMC Infect Dis, vol. 6, 2006, doi: 10.1186/1471-2334-6-104.

[19] L. Luciani et al., ‘A novel and sensitive real-time PCR system for universal detection of poxviruses’, Sci Rep, vol. 11, no. 1, 2021, doi: 10.1038/s41598-021-81376-4.

[20] H. Cui et al., ‘Rapid detection of influenza A viruses using a real-time reverse transcription recombinase-aided amplification assay’, Front Cell Infect Microbiol, vol. 12, 2023, doi: 10.3389/fcimb.2022.1071288.

[21] H. Tombuloglu et al., ‘Multiplex real-time RT-PCR method for the diagnosis of SARS-CoV-2 by targeting viral N, RdRP and human RP genes’, Sci Rep, vol. 12, no. 1, 2022, doi: 10.1038/s41598-022-06977-z.

[22] W. Song et al., ‘Development of a multiplex reverse transcription-quantitative PCR (qPCR) method for detecting common causative agents of swine viral diarrhea in China’, Porcine Health Manag, vol. 10, no. 1, 2024, doi: 10.1186/s40813-024-00364-y.

[23] K. Hagman et al., ‘Prevalence and clinical relevance of viraemia in viral respiratory tract infections: a systematic review’, Lancet Microbe, 2024, doi: 10.1016/j.lanmic.2024.100967.

[24] A. Wiegand and F. Maldarelli, Single-copy quantification of HIV-1 in clinical samples, vol. 1087. 2014. doi: 10.1007/978-1-62703-670-2_20.

[25] M. Barlev-Gross et al., 'Spike vs nucleocapsid SARS-CoV-2 antigen detection: application in nasopharyngeal swab specimens', Anal Bioanal Chem, vol. 413, no. 13, pp. 3501–3510, 2021, doi: 10.1007/s00216-021-03298-4.

[26] W. Wu, Y. Cheng, H. Zhou, C. Sun, and S. Zhang, 'The SARS-CoV-2 nucleocapsid protein: its role in the viral life cycle, structure and functions, and use as a potential target in the development of vaccines and diagnostics', Virol J, vol. 20, no. 1, 2023, doi: 10.1186/s12985-023-01968-6.

[27] R. Ren et al., 'Multiplexed detection of viral antigen and RNA using nanopore sensing and encoded molecular probes', Nat Commun, vol. 14, no. 1, 2023, doi: 10.1038/s41467-023-43004-9.

[28] K. Vashisht et al., 'Exploring the Immunodominant Epitopes of SARS-CoV-2 Nucleocapsid Protein as Exposure Biomarker', Cureus, Feb. 2023, doi: 10.7759/cureus.34827.

[29] B. Boson et al., 'The SARS-CoV-2 envelope and membrane proteins modulate maturation and retention of the spike protein, allowing assembly of virus-like particles', Journal of Biological Chemistry, vol. 296, 2021, doi: 10.1074/jbc.RA120.016175.

[30] P. Jian-umpunkul et al., 'Improved sensitivity of influenza A antigen detection using a combined NP, M, and NS1 sandwich ELISA', J Virol Methods, vol. 185, no. 1, pp. 24–31, 2012, doi: 10.1016/j.jviromet.2012.05.021.

[31] Z. S. Ulhaq and G. V. Soraya, 'Interleukin-6 as a potential biomarker of COVID-19 progression', Med Mal Infect, vol. 50, no. 4, pp. 382–383, 2020, doi: 10.1016/j.medmal.2020.04.002.

[32] R. González-Amaro et al., 'Induction of tumor necrosis factor α production by human hepatocytes in chronic viral hepatitis', Journal of Experimental Medicine, vol. 179, no. 3, pp. 841–848, 1994, doi: 10.1084/jem.179.3.841.

[33] L. Li and A. P. Dufour, 'Using IFN-γ as a biomarker for detecting exposure to viral pathogens', Curr Microbiol, vol. 56, no. 1, pp. 84–88, 2008, doi: 10.1007/s00284-007-9044-1.

[34] H. Li et al., 'Serum Amyloid A is a biomarker of severe Coronavirus Disease and poor prognosis', Journal of Infection, vol. 80, no. 6, pp. 646–655, 2020, doi: 10.1016/j.jinf.2020.03.035.

[35] S. Gautam et al., ‘Severe respiratory viral infection induces procalcitonin in the absence of bacterial pneumonia’, Thorax, vol. 75, no. 11, pp. 974–981, 2020, doi: 10.1136/thoraxjnl-2020-214896.

[36] S. Shukla, S. M. Jadhav, Y. K. Gurav, D. Parashar, and K. Alagarasu, ‘Serum ferritin level as a prognostic biomarker for predicting dengue disease severity: A systematic review and meta-analysis’, Rev Med Virol, vol. 33, no. 5, 2023, doi: 10.1002/rmv.2468.

[37] I. S. Kamat, V. Ramachandran, H. Eswaran, D. Guffey, and D. M. Musher, ‘Procalcitonin to distinguish viral from bacterial pneumonia: A systematic review and meta-analysis’, Clinical Infectious Diseases, vol. 70, no. 3, pp. 538–542, 2020, doi: 10.1093/cid/ciz545.

[38] Y. Guo et al., ‘Different Profiles of Antibodies and Cytokines Were Found Between Severe and Moderate COVID-19 Patients’, Front Immunol, vol. 12, 2021, doi: 10.3389/fimmu.2021.723585.

[39] H. W. Schroeder and L. Cavacini, ‘Structure and function of immunoglobulins’, Journal of Allergy and Clinical Immunology, vol. 125, no. 2 SUPPL. 2, pp. S41–S52, 2010, doi: 10.1016/j.jaci.2009.09.046.

[40] M. Sällberg, H. Norder, and L. O. Magnius, ‘Comparison of class and subclass distribution of antibodies to the hepatitis B core and B e antigens in chronic hepatitis B’, J Med Virol, vol. 30, no. 1, pp. 1–6, 1990, doi: 10.1002/jmv.1890300102.

[41] J. L. Yates et al., ‘Serological analysis reveals an imbalanced IgG subclass composition associated with COVID-19 disease severity’, Cell Rep Med, vol. 2, no. 7, 2021, doi: 10.1016/j.xcrm.2021.100329.

[42] K. Abu Jabal and M. Edelstein, ‘Using SARS-CoV-2 anti-S IgG levels as a marker of previous infection: example from an Israeli healthcare worker cohort.’, International Journal of Infectious Diseases, vol. 120, pp. 22–24, 2022, doi: 10.1016/j.ijid.2022.04.010.

[43] J. M. Marcelino et al., ‘Envelope-specific antibody response in HIV-2 infection: C2V3C3-specific IgG response is associated with disease progression’, AIDS, vol. 22, no. 17, pp. 2257–2265, 2008, doi: 10.1097/QAD.0b013e3283155546.

[44] M. R. Walker, A. A. Eltahla, M. M. Mina, H. Li, A. R. Lloyd, and R. A. Bull, ‘Envelope-specific IgG3 and IgG1 responses are associated with clearance of acute hepatitis C virus infection’, Viruses, vol. 12, no. 1, 2020, doi: 10.3390/v12010075.

[45] J. K. Iles et al., ‘Determination of IgG1 and IgG3 SARS-CoV-2 Spike Protein and Nucleocapsid Binding—Who Is Binding Who and Why?’, Int J Mol Sci, vol. 23, no. 11, 2022, doi: 10.3390/ijms23116050.

[46] M. J. Bolton et al., ‘IgG3 subclass antibodies recognize antigenically drifted influenza viruses and SARS-CoV-2 variants through efficient bivalent binding’, Proc Natl Acad Sci U S A, vol. 120, no. 35, 2023, doi: 10.1073/pnas.2216521120.

[47] S. Avivi-Mintz, Y. Lustig, V. Indenbaum, E. Schwartz, and A. Danielli, ‘Highly sensitive and specific SARS-CoV-2 serological assay using a magnetic modulation biosensing system’, Biosensors (Basel), vol. 12, no. 1, 2022, doi: 10.3390/bios12010007.

[48] P. Halfon et al., ‘Semen may harbor hiv despite effective haart: Another piece in the puzzle’, PLoS One, vol. 5, no. 5, 2010, doi: 10.1371/journal.pone.0010569.

[49] S. Vazquez, G. Hafner, D. Ruiz, N. Calzada, and M. G. Guzman, ‘Evaluation of immunoglobulin M and G capture enzyme-linked immunosorbent assay Panbio kits for diagnostic dengue infections’, Journal of Clinical Virology, vol. 39, no. 3, pp. 194–198, 2007, doi: 10.1016/j.jcv.2007.04.003.

[50] F. Peng et al., ‘Identification of microRNAs in throat swab as the biomarkers for diagnosis of influenza’, Int J Med Sci, vol. 13, no. 1, pp. 77–84, 2016, doi: 10.7150/ijms.13301.

[51] Y. Cheng, N. Dubovoy, M. E. Hayes-Rogers, J. Stewart, and D. Shah, ‘Detection of IgM to hepatitis B core antigen in a reductant containing, chemiluminescence assay’, J Immunol Methods, vol. 230, no. 1–2, pp. 29–35, 1999, doi: 10.1016/S0022-1759(99)00128-3.

[52] C. Chen, H. Lai, H. Liang, Y. He, G. Guo, and L. Li, ‘A New Method for Detection African Swine Fever Virus: Time-resolved Fluorescence Immunoassay’, J Fluoresc, vol. 31, no. 5, pp. 1291–1296, 2021, doi: 10.1007/s10895-021-02754-9.

[53] X. Terzapulo, A. Kassenova, and R. Bukasov, ‘Immunoassays: Analytical and Clinical Performance, Challenges, and Perspectives of SERS Detection in Comparison with Fluorescent Spectroscopic Detection’, Int J Mol Sci, vol. 25, no. 4, 2024, doi: 10.3390/ijms25042080.

[54] A. González-Techera, H. J. Kim, S. J. Gee, J. A. Last, B. D. Hammock, and G. González-Sapienza, ‘Polyclonal antibody-based noncompetitive immunoassay for small analytes developed with short peptide loops isolated from phage libraries’, Anal Chem, vol. 79, no. 23, pp. 9191–9196, 2007, doi: 10.1021/ac7016713.

[55] Y. Gao, X. Huang, Y. Zhu, and Z. Lv, ‘A brief review of monoclonal antibody technology and its representative applications in immunoassays’, J Immunoassay Immunochem, vol. 39, no. 4, pp. 351–364, 2018, doi: 10.1080/15321819.2018.1515775.

[56] Y. Wang and Y. Xianyu, ‘Nanobody and Nanozyme-Enabled Immunoassays with Enhanced Specificity and Sensitivity’, Small Methods, vol. 6, no. 4, 2022, doi: 10.1002/smtd.202101576.

[57] H. Torul et al., ‘Microfluidic-based blood immunoassays’, J Pharm Biomed Anal, vol. 228, 2023, doi: 10.1016/j.jpba.2023.115313.

[58] Z. Zhong, J. Dong, L. Xia, J. He, and G. Li, ‘A self-driven microfluidic immunosensor for rapid separation, enrichment, and detection of biomarkers in serum’, Anal Bioanal Chem, 2024, doi: 10.1007/s00216-024-05490-8.

[59] U. Weissenstein et al., ‘Protein chip based miniaturized assay for the simultaneous quantitative monitoring of cancer biomarkers in tissue extracts’, Proteomics, vol. 6, no. 5, pp. 1427–1436, 2006, doi: 10.1002/pmic.200500078.

[60] J. Villanueva, O. Yanes, E. Querol, L. Serrano, and F. X. Aviles, ‘Identification of protein ligands in complex biological samples using intensity-fading MALDI-TOF mass spectrometry’, Anal Chem, vol. 75, no. 14, pp. 3385–3395, 2003, doi: 10.1021/ac020644k.

[61] A. Scherl, ‘Clinical protein mass spectrometry’, Methods, vol. 81, pp. 3–14, 2015, doi: 10.1016/j.ymeth.2015.02.015.

[62] Z. Yu et al., ‘Real-time and quantitative protein detection via polyacrylamide gel electrophoresis and online intrinsic fluorescence imaging’, Anal Chim Acta, vol. 1291, 2024, doi: 10.1016/j.aca.2024.342219.

[63] L. Nováková and H. Vlčková, ‘A review of current trends and advances in modern bio-analytical methods: Chromatography and sample preparation’, Anal Chim Acta, vol. 656, no. 1–2, pp. 8–35, 2009, doi: 10.1016/j.aca.2009.10.004.

[64] S. Lee, D. S. Kulyk, S. O. Afriyie, K. Badu, and A. K. Badu-Tawiah, ‘Malaria Diagnosis Using Paper-Based Immunoassay for Clinical Blood Sampling and Analysis by a Miniature Mass Spectrometer’, Anal Chem, vol. 94, no. 41, pp. 14377–14384, 2022, doi: 10.1021/acs.analchem.2c03105.

[65] M. Domsicova, J. Korcekova, A. Poturnayova, and A. Breier, ‘New Insights into Aptamers: An Alternative to Antibodies in the Detection of Molecular Biomarkers’, Int J Mol Sci, vol. 25, no. 13, 2024, doi: 10.3390/ijms25136833.

[66] M. Famulok, J. S. Hartig, and G. Mayer, ‘Functional aptamers and aptazymes in biotechnology, diagnostics, and therapy’, Chem Rev, vol. 107, no. 9, pp. 3715–3743, 2007, doi: 10.1021/cr0306743.

[67] M. Bauer, M. Strom, D. S. Hammond, and S. Shigdar, ‘Anything you can do, i can do better: Can aptamers replace antibodies in clinical diagnostic applications?’, Molecules, vol. 24, no. 23, 2019, doi: 10.3390/molecules24234377.

[68] S. Esmail et al., ‘Rapid and accurate agglutination-based testing for SARS-CoV-2 antibodies’, Cell Reports Methods, vol. 1, no. 2, 2021, doi: 10.1016/j.crmeth.2021.100011.

[69] N. U. Ertesvåg et al., ‘A rapid antibody screening haemagglutination test for predicting immunity to SARS-CoV-2 variants of concern’, Communications Medicine, vol. 2, no. 1, 2022, doi: 10.1038/s43856-022-00091-x.

[70] D. R. Peaper and M. L. Landry, Laboratory diagnosis of viral infection, vol. 123. 2014. doi: 10.1016/B978-0-444-53488-0.00005-5.

[71] A. Dasgupta, ‘Chapter 1 - Immunoassay Design and Mechanism of Biotin Interference’, in Biotin and Other Interferences in Immunoassays, Elsevier, 2019, pp. 1–15. doi: 10.1016/B978-0-12-816429-7.00001-0.

[72] T. Li, J.-Y. Byun, B. B. Kim, Y.-B. Shin, and M.-G. Kim, ‘Label-free homogeneous FRET immunoassay for the detection of mycotoxins that utilizes quenching of the intrinsic fluorescence of antibodies’, Biosens Bioelectron, vol. 42, no. 1, pp. 403–408, 2013, doi: 10.1016/j.bios.2012.10.085.

[73] F. Mehrabi, B. Ranjbar, M. Hosseini, N. Sadeghi, J. Mohammadi, and M. R. Ganjali, ‘CRET-based immunoassay on magnetic beads for selective and sensitive detection of Nanog antigen as a key cancer stem cell marker’, Microchimica Acta, vol. 191, no. 7, 2024, doi: 10.1007/s00604-024-06505-y.

[74] R. Takahashi, T. Yasuda, Y. Ohmuro-Matsuyama, and H. Ueda, ‘BRET Q-Body: A Ratiometric Quench-based Bioluminescent Immunosensor Made of Luciferase-Dye-Antibody Fusion with Enhanced Response’, Anal Chem, vol. 93, no. 21, pp. 7571–7578, 2021, doi: 10.1021/acs.analchem.0c05217.

[75] S. Aydin, ‘A short history, principles, and types of ELISA, and our laboratory experience with peptide/protein analyses using ELISA’, Peptides (N.Y.), vol. 72, pp. 4–15, 2015, doi: 10.1016/j.peptides.2015.04.012.

[76] M. Drozd et al., ‘Printer toner-assisted immobilization of antibodies on PET for genuinely-2D, flexible ELISA spot arrays’, Sens Actuators B Chem, vol. 403, 2024, doi: 10.1016/j.snb.2023.135173.

[77] F. Li et al., ‘Paper-based point-of-care immunoassays: Recent advances and emerging trends’, Biotechnol Adv, vol. 39, 2020, doi: 10.1016/j.biotechadv.2019.107442.

[78] P. Ivanova, M. Drozd, K. Michrowski, S. Karoń, M. Mazurkiewicz-Pawlicka, and M. Pietrzak, ‘Au-X (X=Pt/Ru)-decorated magnetic nanocubes as bifunctional nanozyme labels in colorimetric, magnetically-enhanced, one-step sandwich CRP immunoassay’, Biosens Bioelectron, vol. 237, 2023, doi: 10.1016/j.bios.2023.115511.

[79] C. Coarsey, B. Coleman, M. A. Kabir, M. Sher, and W. Asghar, ‘Development of a flow-free magnetic actuation platform for an automated microfluidic ELISA’, RSC Adv, vol. 9, no. 15, pp. 8159–8168, 2019, doi: 10.1039/c8ra07607c.

[80] I. Ashur et al., ‘Rapid electrochemical immunodetection of SARS-CoV-2 using a pseudo-typed vesicular stomatitis virus model’, Talanta, vol. 239, 2022, doi: 10.1016/j.talanta.2021.123147.

[81] L. C. T. Shoute et al., ‘Label-free impedimetric immunosensor for point-of-care detection of COVID-19 antibodies’, Microsyst Nanoeng, vol. 9, no. 1, 2023, doi: 10.1038/s41378-022-00460-5.

[82] V. Lisyte, A. Kausaite-Minkstimiene, B. Brasiunas, A. Popov, and A. Ramanaviciene, ‘Surface Plasmon Resonance Immunosensor for Direct Detection of Antibodies against SARS-CoV-2 Nucleocapsid Protein’, Int J Mol Sci, vol. 25, no. 16, 2024, doi: 10.3390/ijms25168574.

[83] M. Bisoffi, V. Severns, D. W. Branch, T. L. Edwards, and R. S. Larson, ‘Rapid detection of human immunodeficiency virus types 1 and 2 by use of an improved piezoelectric biosensor’, J Clin Microbiol, vol. 51, no. 6, pp. 1685–1691, 2013, doi: 10.1128/JCM.03041-12.

[84] D. Mandal, M. M. Indaleeb, A. Younan, and S. Banerjee, ‘Piezoelectric point-of-care biosensor for the detection of SARS-COV-2 (COVID-19) antibodies’, Sens Biosensing Res, vol. 37, 2022, doi: 10.1016/j.sbsr.2022.100510.

[85] H. Ahsan, ‘Monoplex and multiplex immunoassays: approval, advancements, and alternatives’, Comp Clin Path, vol. 31, no. 2, pp. 333–345, 2022, doi: 10.1007/s00580-021-03302-4.

[86] F. Illanes-álvarez, D. Márquez-Ruiz, M. Márquez-Coello, S. Cuesta-Sancho, and J. A. Girón-González, ‘Similarities and differences between hiv and sars-cov-2’, Int J Med Sci, vol. 18, no. 3, pp. 846–851, 2021, doi: 10.7150/ijms.50133.

[87] C. Geismar et al., ‘Symptom profiles of community cases infected by influenza, RSV, rhinovirus, seasonal coronavirus, and SARS-CoV-2 variants of concern’, Sci Rep, vol. 13, no. 1, 2023, doi: 10.1038/s41598-023-38869-1.

[88] D. Wilkins et al., ‘Validation and performance of a multiplex serology assay to quantify antibody responses following SARS-CoV-2 infection or vaccination’, Clin Transl Immunology, vol. 11, no. 4, 2022, doi: 10.1002/cti2.1385.

[89] S. K. Vashist, P. B. Luppa, L. Y. Yeo, A. Ozcan, and J. H. T. Luong, ‘Emerging Technologies for Next-Generation Point-of-Care Testing’, Trends Biotechnol, vol. 33, no. 11, pp. 692–705, 2015, doi: 10.1016/j.tibtech.2015.09.001.

[90] S. Beck et al., ‘A Protein Microarray-Based Respiratory Viral Antigen Testing Platform for COVID-19 Surveillance’, Biomedicines, vol. 10, no. 9, 2022, doi: 10.3390/biomedicines10092238.

[91] F. Rusmini, Z. Zhong, and J. Feijen, ‘Protein immobilization strategies for protein biochips’, Biomacromolecules, vol. 8, no. 6, pp. 1775–1789, 2007, doi: 10.1021/bm061197b.

[92] S. Choi and J. Chae, ‘A regenerative biosensing surface in microfluidics using electrochemical desorption of short-chain self-assembled monolayer’, Microfluid Nanofluidics, vol. 7, no. 6, pp. 819–827, 2009, doi: 10.1007/s10404-009-0440-7.

[93] K. Gajos, A. Orzech, K. Sanocka, P. Petrou, and A. Budkowski, ‘Covalent and Non-covalent In-Flow Biofunctionalization for Capture Assays on Silicon Chips: White Light Reflectance Spectroscopy Immunosensor Combined with TOF-SIMS Resolves Immobilization Stability and Binding Stoichiometry’, Langmuir, vol. 39, no. 29, pp. 10216–10229, 2023, doi: 10.1021/acs.langmuir.3c01181.

[94] N. Fornsted, ‘Affinity Chromatographic studies on antigen-antibody dissociation’, FEBS Lett, vol. 177, no. 2, pp. 195–199, 1984, doi: 10.1016/0014-5793(84)81282-X.

[95] J.-M. Park, M. Y. Kim, J. Jose, and M. Park, ‘Covalently immobilized regenerable immunoaffinity layer with orientation-controlled antibodies based on Z-domain autodisplay’, Int J Mol Sci, vol. 23, no. 1, 2022, doi: 10.3390/ijms23010459.

[96] C. Fercher, M. L. Jones, S. M. Mahler, and S. R. Corrie, ‘Recombinant Antibody Engineering Enables Reversible Binding for Continuous Protein Biosensing’, ACS Sens, vol. 6, no. 3, pp. 764–776, 2021, doi: 10.1021/acssensors.0c01510.

[97] J. E. Butler et al., ‘The physical and functional behavior of capture antibodies adsorbed on polystyrene’, J Immunol Methods, vol. 150, no. 1–2, pp. 77–90, 1992, doi: 10.1016/0022-1759(92)90066-3.

[98] R. Meyer, S. Giselbrecht, B. E. Rapp, M. Hirtz, and C. M. Niemeyer, ‘Advances in DNA-directed immobilization’, 2014. doi: 10.1016/j.cbpa.2013.10.023.

[99] D. Brambilla, L. Sola, and M. Chiari, ‘Advantageous antibody microarray fabrication through DNA-directed immobilization: A step toward use of extracellular vesicles in diagnostics’, Talanta, vol. 222, 2021, doi: 10.1016/j.talanta.2020.121542.

[100] A. C. Crisostomo et al., ‘Kinetic analysis of IgG antibodies to beta-amyloid oligomers with surface plasmon resonance’, Anal Biochem, vol. 481, pp. 43–54, 2015, doi: 10.1016/j.ab.2015.03.032.

[101] P. Chen et al., ‘Paper-based Vertical Flow Immunoassay (VFI) for detection of bio-threat pathogens’, Talanta, vol. 191, pp. 81–88, 2019, doi: 10.1016/j.talanta.2018.08.043.

[102] N. L. Ünlü, F. E. Kanik, E. Seymour, J. H. Connor, and M. S. Ünlü, DNA-directed antibody immobilization for robust protein microarrays: Application to single particle detection ‘DNA-directed antibody immobilization, vol. 1571. 2017. doi: 10.1007/978-1-4939-6848-0_12.

[103] L. Xu, H. Cao, C. Huang, and L. Jia, ‘Oriented immobilization and quantitative analysis simultaneously realized in sandwich immunoassay via his-tagged nanobody’, Molecules, vol. 24, no. 10, 2019, doi: 10.3390/molecules24101890.

[104] J. U. McDonald, J. Ekeruche-Makinde, M. M. Ho, J. S. Tregoning, and O. Ashiru, ‘Development of a custom pentaplex sandwich immunoassay using Protein-G coupled beads for the Luminex® xMAP® platform’, J Immunol Methods, vol. 433, pp. 6–16, 2016, doi: 10.1016/j.jim.2016.02.018.

[105] Z. Rahmati, M. Roushani, H. Hosseini, and H. Choobin, ‘Electrochemical immunosensor with Cu<inf>2</inf>O nanocube coating for detection of SARS-CoV-2 spike protein’, Microchimica Acta, vol. 188, no. 3, 2021, doi: 10.1007/s00604-021-04762-9.

[106] Y. Jung, M. L. Jeong, H. Jung, and H. C. Bong, ‘Self-directed and self-oriented immobilization of antibody by protein G-DNA conjugate’, Anal Chem, vol. 79, no. 17, 2007, doi: 10.1021/ac070484i.

[107] Q. Yu, Q. Wang, B. Li, Q. Lin, and Y. Duan, ‘Technological Development of Antibody Immobilization for Optical Immunoassays: Progress and Prospects’, Crit Rev Anal Chem, vol. 45, no. 1, pp. 62–75, 2015, doi: 10.1080/10408347.2014.881249.

[108] M. Drozd, E. Kobylska, M. Żmieńko, and M. Chudy, ‘Sensitive and label-free SPR biosensing platforms for high-throughput screening of plasma membrane receptors interactions with insulin-like targets of hypoglycaemic activity’, Talanta, vol. 274, 2024, doi: 10.1016/j.talanta.2024.125914.

[109] J. E. Butler, ‘Solid supports in enzyme-linked immunosorbent assay and other solid-phase immunoassays’, Methods, vol. 22, no. 1, pp. 4–23, 2000, doi: 10.1006/meth.2000.1031.
[110] A. Shakeri, N. A. Jarad, A. Leung, L. Soleymani, and T. F. Didar, ‘Biofunctionalization of Glass- and Paper-Based Microfluidic Devices: A Review’, Adv Mater Interfaces, vol. 6, no. 19, 2019, doi: 10.1002/admi.201900940.
[111] M. Cretich, G. Pirri, F. Damin, I. Solinas, and M. Chiari, ‘A new polymeric coating for protein microarrays’, Anal Biochem, vol. 332, no. 1, pp. 67–74, 2004, doi: 10.1016/j.ab.2004.05.041.
[112] D. Sung, D. H. Shin, and S. Jon, ‘Toward immunoassay chips: Facile immobilization of antibodies on cyclic olefin copolymer substrates through pre-activated polymer adlayers’, Biosens Bioelectron, vol. 26, no. 9, pp. 3967–3972, 2011, doi: 10.1016/j.bios.2011.03.005.
[113] J. Zhao et al., ‘Oriented Antibody Immobilization and Immunoassay Based on Boronic Acid-containing Polymer Brush’, Chinese Journal of Polymer Science (English Edition), vol. 36, no. 4, pp. 472–478, 2018, doi: 10.1007/s10118-018-2031-0.
[114] P. S. Petrou, M. Chatzichristidi, A. M. Douvas, P. Argitis, K. Misiakos, and S. E. Kakabakos, ‘A biomolecule friendly photolithographic process for fabrication of protein microarrays on polymeric films coated on silicon chips’, Biosens Bioelectron, vol. 22, no. 9–10, pp. 1994–2002, 2007, doi: 10.1016/j.bios.2006.08.036.
[115] D. Sung, S. Park, and S. Jon, ‘Facile immobilization of biomolecules onto various surfaces using epoxide-containing antibiofouling polymers’, Langmuir, vol. 28, no. 9, pp. 4507–4514, 2012, doi: 10.1021/la204898y.
[116] D. Sung, S. Yang, J. W. Park, and S. Jon, ‘High-density immobilization of antibodies onto nanobead-coated cyclic olefin copolymer plastic surfaces for application as a sensitive immunoassay chip’, Biomed Microdevices, vol. 15, no. 4, pp. 691–698, 2013, doi: 10.1007/s10544-012-9732-x.
[117] J. S. Mitchell, ‘Spin-coated methacrylic acid copolymer thin films for covalent immobilization of small molecules on surface plasmon resonance substrates’, Eur Polym J, vol. 47, no. 1, pp. 16–23, 2011, doi: 10.1016/j.eurpolymj.2010.10.028.
[118] A. E. Ongaro et al., ‘Engineering a sustainable future for point-of-care diagnostics and single-use microfluidic devices’, Lab Chip, vol. 22, no. 17, pp. 3122–3137, 2022, doi: 10.1039/d2lc00380e.
[119] H. Vaisocherová et al., ‘Functionalizable surface platform with reduced nonspecific protein adsorption from full blood plasma-Material selection and protein immobilization

optimization', Biosens Bioelectron, vol. 24, no. 7, pp. 1924–1930, 2009, doi: 10.1016/j.bios.2008.09.035.
[120] Y. Liu and J. Yu, 'Oriented immobilization of proteins on solid supports for use in biosensors and biochips: a review', 2016. doi: 10.1007/s00604-015-1623-4.
[121] E. Chiodi et al., 'A reliable, label free quality control method for the production of dna microarrays with clinical applications', Polymers (Basel), vol. 13, no. 3, pp. 1–13, 2021, doi: 10.3390/polym13030340.
[122] S. K. S. Patel, V. C. Kalia, J.-H. Choi, J.-R. Haw, I.-W. Kim, and J. K. Lee, 'Immobilization of laccase on SiO<inf>2</inf> nanocarriers improves its stability and reusability', J Microbiol Biotechnol, vol. 24, no. 5, pp. 639–647, 2014, doi: 10.4014/jmb.1401.01025.
[123] R. T. Aggarwal, L. Lai, and H. Li, 'Microarray fabrication techniques for multiplexed bioassay applications', Anal Biochem, vol. 683, 2023, doi: 10.1016/j.ab.2023.115369.
[124] M. A. Campanero-Rhodes, E. Llobet, J. A. Bengoechea, and D. Solís, 'Bacteria microarrays as sensitive tools for exploring pathogen surface epitopes and recognition by host receptors', RSC Adv, vol. 5, no. 10, pp. 7173–7181, 2015, doi: 10.1039/c4ra14570d.
[125] S. K. Vashist, C. K. Dixit, B. D. MacCraith, and R. O'Kennedy, 'Effect of antibody immobilization strategies on the analytical performance of a surface plasmon resonance-based immunoassay', Analyst, vol. 136, no. 21, pp. 4431–4436, 2011, doi: 10.1039/c1an15325k.
[126] A. Syahir, K. Usui, K. Tomizaki, K. Kajikawa, and H. Mihara, 'Label and Label-Free Detection Techniques for Protein Microarrays', Microarrays, vol. 4, no. 2, pp. 228–244, Apr. 2015, doi: 10.3390/microarrays4020228.
[127] X.-M. Li, X.-Y. Yang, and S.-S. Zhang, 'Electrochemical enzyme immunoassay using model labels', TrAC - Trends in Analytical Chemistry, vol. 27, no. 6, pp. 543–553, 2008, doi: 10.1016/j.trac.2008.04.002.
[128] G. U. Nienhaus and K. Nienhaus, Fluorescence Labeling. 2017. doi: 10.1002/9783527687732.ch4.
[129] R. Liu, S. Zhang, C. Wei, Z. Xing, S. Zhang, and X. Zhang, 'Metal Stable Isotope Tagging: Renaissance of Radioimmunoassay for Multiplex and Absolute Quantification of Biomolecules', Acc Chem Res, vol. 49, no. 5, pp. 775–783, 2016, doi: 10.1021/acs.accounts.5b00509.

[130] C. Wang, J. Wu, C. Zong, J. Xu, and H.-X. Ju, 'Chemiluminescent immunoassay and its applications', Fenxi Huaxue/ Chinese Journal of Analytical Chemistry, vol. 40, no. 1, pp. 3–10, 2012, doi: 10.1016/S1872-2040(11)60518-5.
[131] R. C. Castro, M. L. M. F. S. Saraiva, J. L. M. Santos, and D. S. M. Ribeiro, 'Multiplexed detection using quantum dots as photoluminescent sensing elements or optical labels', Coord Chem Rev, vol. 448, 2021, doi: 10.1016/j.ccr.2021.214181.
[132] M. Seydack, 'Nanoparticle labels in immunosensing using optical detection methods', Biosens Bioelectron, vol. 20, no. 12, pp. 2454–2469, 2005, doi: 10.1016/j.bios.2004.11.003.
[133] L. Zhang et al., 'Development and characterization of double-antibody sandwich ELISA for detection of zika virus infection', Viruses, vol. 10, no. 11, 2018, doi: 10.3390/v10110634.
[134] L. Zhan, W. B. Wu, L. Yang, and C. Z. Huang, 'Sensitive detection of respiratory syncytial virus based on a dual signal amplified plasmonic enzyme-linked immunosorbent assay', Anal Chim Acta, vol. 962, pp. 73–79, 2017, doi: 10.1016/j.aca.2017.01.023.
[135] J. Shen et al., 'Immunochromatographic assay for quantitative and sensitive detection of hepatitis B virus surface antigen using highly luminescent quantum dot-beads', Talanta, vol. 142, pp. 145–149, 2015, doi: 10.1016/j.talanta.2015.04.058.
[136] M. Sánchez-Purrà, M. Carré-Camps, H. De Puig, I. Bosch, L. Gehrke, and K. Hamad-Schifferli, 'Surface-Enhanced Raman Spectroscopy-Based Sandwich Immunoassays for Multiplexed Detection of Zika and Dengue Viral Biomarkers', ACS Infect Dis, vol. 3, no. 10, pp. 767–776, 2017, doi: 10.1021/acsinfecdis.7b00110.
[137] G. Mao et al., 'Ratiometric fluorescence immunoassay of SARS-CoV-2 nucleocapsid protein via Si-FITC nanoprobe-based inner filter effect', Nano Res, vol. 16, no. 4, pp. 5383–5390, 2023, doi: 10.1007/s12274-022-4740-5.
[138] P. Zhang, Y. Bao, M. S. Draz, H. Lu, C. Liu, and H. Han, 'Rapid and quantitative detection of C-reactive protein based on quantum dots and immunofiltration assay', Int J Nanomedicine, vol. 10, pp. 6161–6173, 2015, doi: 10.2147/IJN.S89307.
[139] Y. Yang et al., 'Development of a chemiluminescence immunoassay to accurately detect African swine fever virus antibodies in serum', J Virol Methods, vol. 298, 2021, doi: 10.1016/j.jviromet.2021.114269.
[140] S. Oh et al., 'Magnetic Nanozyme-Linked Immunosorbent Assay for Ultrasensitive Influenza A Virus Detection', ACS Appl Mater Interfaces, vol. 10, no. 15, pp. 12534–12543, 2018, doi: 10.1021/acsami.8b02735.

[141] S. Glick, ‘Rosalyn Sussman Yalow (1921-2011)’, Nature, vol. 474, no. 7353, p. 580, 2011, doi: 10.1038/474580a.
[142] J. T. Dias, L. Lama, J. Gantelius, and H. Andersson-Svahn, ‘Minimizing antibody cross-reactivity in multiplex detection of biomarkers in paper-based point-of-care assays’, Nanoscale, vol. 8, no. 15, pp. 8195–8201, 2016, doi: 10.1039/c5nr09207h.
[143] D. Juncker, S. Bergeron, V. Laforte, and H. Li, ‘Cross-reactivity in antibody microarrays and multiplexed sandwich assays: Shedding light on the dark side of multiplexing’, Curr Opin Chem Biol, vol. 18, no. 1, pp. 29–37, 2014, doi: 10.1016/j.cbpa.2013.11.012.
[144] M.-C. Estevez, M. A. Otte, B. Sepulveda, and L. M. Lechuga, ‘Trends and challenges of refractometric nanoplasmonic biosensors: A review’, Anal Chim Acta, vol. 806, pp. 55–73, 2014, doi: 10.1016/j.aca.2013.10.048.
[145] P. Fechner, G. Gauglitz, and G. Proll, ‘Through the looking-glass - Recent developments in reflectometry open new possibilities for biosensor applications’, TrAC - Trends in Analytical Chemistry, vol. 156, 2022, doi: 10.1016/j.trac.2022.116708.
[146] J. Zhang, X. Zhang, X. Wei, Y. Xue, H. Wan, and P. Wang, ‘Recent advances in acoustic wave biosensors for the detection of disease-related biomarkers: A review’, Anal Chim Acta, vol. 1164, 2021, doi: 10.1016/j.aca.2021.338321.
[147] B. E. Rapp, F. J. Gruhl, and K. Länge, ‘Biosensors with label-free detection designed for diagnostic applications’, Anal Bioanal Chem, vol. 398, no. 6, pp. 2403–2412, 2010, doi: 10.1007/s00216-010-3906-2.
[148] K. Subramanian, C. J. Fee, R. Fredericks, R. S. Stubbs, and M. T. Hayes, ‘Insulin receptor-insulin interaction kinetics using multiplex surface plasmon resonance’, Journal of Molecular Recognition, vol. 26, no. 12, pp. 643–652, 2013, doi: 10.1002/jmr.2307.
[149] Bruker, karta katalogowa aparatu Triceratops SPR #64’ [Internet, dostęp 07.02.2025] https://www.bruker.com/en/news-and-events/news/2024/bruker-introduces-the-ingenious-novel-triceratops-spr-64-surface-plasmon-resonance-system.html
[150] A. Gade, A. Sharma, N. Srivastava, and S. J. S. Flora, ‘Surface plasmon resonance: A promising approach for label-free early cancer diagnosis’, Clinica Chimica Acta, vol. 527, pp. 79–88, 2022, doi: 10.1016/j.cca.2022.01.023.
[151] R. Peltomaa, B. Glahn-Martínez, E. Benito-Peña, and M. C. Moreno-Bondi, ‘Optical Biosensors for Label-Free Detection of Small Molecules’, Sensors (Basel), vol. 18, no. 12, 2018, doi: 10.3390/s18124126.

[152] D. M. Rissin et al., ‘Single-molecule enzyme-linked immunosorbent assay detects serum proteins at subfemtomolar concentrations’, Nat Biotechnol, vol. 28, no. 6, pp. 595–599, 2010, doi: 10.1038/nbt.1641.

[153] T. Yang, S. Chen, X. He, H. Guo, and X. Sun, ‘How to convincingly measure low concentration samples with optical label-free biosensors’, Sens Actuators B Chem, vol. 306, 2020, doi: 10.1016/j.snb.2019.127568.

[154] S. K. Vashist, ‘Trends in multiplex immunoassays for in vitro diagnostics and point-of-care testing’, Diagnostics, vol. 11, no. 9, 2021, doi: 10.3390/diagnostics11091630.

[155] A. Kussrow, C. S. Enders, and D. J. Bornhop, ‘Interferometric methods for label-free molecular interaction studies’, Anal Chem, vol. 84, no. 2, pp. 779–792, 2012, doi: 10.1021/ac202812h.

[156] P. Jahanshahi, Q. Wei, Z. Jie, M. Ghomeishi, S. D. Sekaran, and F. R. Mahamd Adikan, ‘Kinetic analysis of IgM monoclonal antibodies for determination of dengue sample concentration using SPR technique’, Bioengineered, vol. 8, no. 3, pp. 239–247, 2017, doi: 10.1080/21655979.2016.1223413.

[157] E. Stern et al., ‘Label-free biomarker detection from whole blood’, Nat Nanotechnol, vol. 5, no. 2, pp. 138–142, 2010, doi: 10.1038/nnano.2009.353.

[158] Y. S. Ang and L. L. Yung, ‘Protein-DNA Conjugates with a Discrete Number of Oligonucleotide Strands for Highly Reproducible Protein Quantification by the DNA Proximity Assay’, Anal Chem, vol. 95, no. 32, pp. 12071–12079, 2023, doi: 10.1021/acs.analchem.3c02033.

[159] L. Sola, F. Damin, and M. Chiari, ‘Array of multifunctional polymers for localized immobilization of biomolecules on microarray substrates’, Anal Chim Acta, vol. 1047, pp. 188–196, 2019, doi: 10.1016/j.aca.2018.10.006.

Oświadczenia współautorów publikacji

Warszawa, dn. 26.02.2025r.

prof. dr hab. inż. Elżbieta Malinowska
Katedra Biotechnologii Medycznej
Wydział Chemiczny
i
Centrum Zaawansowanych Materiałów i Technologii CEZAMAT
Politechnika Warszawska

OŚWIADCZENIE

Niniejszym oświadczam, że w ~~pracy~~/pracach:

P1 "Recent Advancements in Receptor Layer Engineering for Applications in SPR-Based Immunodiagnostics" Sensors, Drozd, M., Karoń, S., Malinowska, E., 2021, 21(11), 3781, DOI:10.3390/s21113781

P2 "A Careful Insight into DDI-Type Receptor Layers on the Way to Improvement of Click-Biology-Based Immunosensors" Biosensors, Karoń, S., Drozd, M., Malinowska, E., 2024, 14(3), 136, DOI:10.3390/bios14030136

P3 "A Versatile Approach to Quality Control of Protein-based Receptor Layers by Reversible, Nonspecific Staining for Multiplex SPRi Immunosensing" Sensors and Actuators B: Chemical, Karoń, S., Porycka, K., Lapitan, Jr. L.D., Drozd, M., Pietrzak, M., Malinowska, E, 2024, 421, 136512, DOI:10.1016/j.snb.2024.136512

P4 "PET Foils Functionalized with Reactive Copolymers as Adaptable Microvolume ELISA Spot Array Platforms for Multiplex Serological Analysis of SARS-CoV-2 Infections" Sensors, Pniewska, S.; Drozd, M.; Mussida, A.; Brambilla, D.; Chiari, M.; Rastawicki, W.; Malinowska, E., 2024, 24, DOI:10.3390/s24237766

Mój wkład pracy polegał na współudziale w opracowaniu metodologii prowadzonych prac, zapewnieniu finansowania i wsparcia merytorycznego podczas ogółu prowadzonych badań, dyskusji merytorycznej otrzymanych wyników, współredagowaniu manuskryptów otrzymanych od współautorów przed ich wysłaniem oraz kluczowej roli przy wyborze czasopism, w których prace zostały opublikowane.

Warszawa, dn. 26.02.2025

Dr inż. Marcin Drozd
Katedra Biotechnologii Medycznej
Wydział Chemiczny
i
Dział Diagnostyki Medycznej
Centrum Zaawansowanych Materiałów i Technologii CEZAMAT
Politechnika Warszawska

OŚWIADCZENIE

Niniejszym oświadczam, że w pracy/pracach:

P1 "Recent Advancements in Receptor Layer Engineering for Applications in SPR-Based Immunodiagnostics" Sensors, Drozd, M., Karoń, S., Malinowska, E., 2021, 21(11), 3781, DOI:10.3390/s21113781

Mój wkład pracy polegał na opracowaniu ogólnej koncepcji przeglądu, napisaniu podrozdziałów 1.1, 1.3, rozdziału 2 oraz podsumowania, zapoznaniu się z literaturą przedmiotu i zebraniu literatury stanowiącej podstawę wskazanych rozdziałów, bezpośredniemu przygotowaniu edytorskiemu manuskryptu przed wysłaniem do czasopisma oraz prowadzeniu korespondencji z edytorem i recenzentami.

P2 "A Careful Insight into DDI-Type Receptor Layers on the Way to Improvement of Click-Biology-Based Immunosensors" Biosensors, Karoń, S., Drozd, M., Malinowska, E., 2024, 14(3), 136, DOI:10.3390/bios14030136

Mój wkład pracy polegał na współautorstwie koncepcji badawczej, pomocy przy wyznaczaniu kinetyki oddziaływania DNA i ich koniugatów z warstwą kotwiczącą, bieżącym wsparciu merytorycznym doktorantki podczas prowadzonych badań, bezpośredniemu przygotowaniu edytorskiemu manuskryptu przed wysłaniem do czasopisma oraz prowadzeniu korespondencji z edytorem i recenzentami.

P3 "A Versatile Approach to Quality Control of Protein-based Receptor Layers by Reversible, Nonspecific Staining for Multiplex SPRi Immunosensing" Sensors and Actuators B: Chemical, Karoń, S., Porycka, K., Lapitan, Jr, L.D., Drozd, M., Pietrzak, M., Malinowska, E, 2024, 421, 136512, DOI:10.1016/j.snb.2024.136512

Mój wkład pracy polegał na współautorstwie koncepcji badawczej, zaplanowaniu doświadczeń dotyczących optymalizacji metody znakowania białek powierzchniowych za pomocą trzech wybranych barwników oraz demonstrujących jej użyteczność w analizie ilościowej i kontroli jakości mikromacierzy SPRi. Wspólnie z mgr inż. S Pniewską pełniłem opiekę nad pracą inżynierską której część badawcza stanowiła element badań

Drozd

wykorzystanych w manuskrypcie (jako kierujący pracą dyplomową). Byłem również odpowiedzialny za bezpośrednie przygotowanie edytorskie manuskryptu przed wysłaniem do czasopisma oraz prowadzenie korespondencji z edytorem i recenzentami na etapie zgłoszenia i obu etapach rewizji.

P4 "PET Foils Functionalized with Reactive Copolymers as Adaptable Microvolume ELISA Spot Array Platforms for Multiplex Serological Analysis of SARS-CoV-2 Infections" Sensors, Pniewska, S.; Drozd, M.; Mussida, A.; Brambilla, D.; Chiari, M.; Rastawicki, W.; Malinowska, E., 2024, 24, DOI:10.3390/s24237766

Mój wkład pracy polegał na współautorstwie koncepcji badawczej, zaplanowaniu części doświadczeń obejmujących wykorzystanie platform do analizy próbek rzeczywistych (rozszerzenie wcześniejszej współpracy z NIZP PZH – PIB), koordynacji prowadzonych prac, bezpośredniemu przygotowaniu edytorskiemu manuskryptu przed wysłaniem do czasopisma oraz prowadzeniu korespondencji z edytorem i recenzentami. Byłem również autorem wniosku projektowego i kierownikiem projektu IDUB YOUNG PW, w ramach którego zapewniono finansowanie części badań w publikacji.

Marcin Drozd

dr hab. inż. Mariusz Pietrzak, prof. PW
(stopień/tytuł naukowy, imię i nazwisko)
Wydział Chemiczny, Katedra Biotechnologii Medycznej
(Wydział/Katedra/Zakład)
Politechnika Warszawska
(Uczelnia)

Warszawa, dn. 24.02.2025 r.

OŚWIADCZENIE

Niniejszym oświadczam, że w pracy:

[P3] **A versatile approach to quality control of protein based receptor layers by reversible, nonspecific staining for multiplex SPRi immunosensing** Sensors and Actuators B: Chemical. Karoń, S., Porycka, K., Lapitan, L.D., Drozd, M., Pietrzak, M., & Malinowska, E., 2024, DOI:10.1016/j.snb.2024.136512.

Mój wkład pracy polegał na nadzorowaniu prac badawczych, ich częściowym finansowaniu oraz korekcie manuskryptu.

[wtasnoręczny podpis współautora]

Warsaw, 31.01.2025

Dr. Lorico Lapitan Jr
Department of Medical Diagnostics
Center for Advanced Materials and Technologies
Warsaw University of Technology

STATEMENT OF CO-AUTHORSHIP

I confirm that in the joint publication with S. Pniewska

[P3] Karoń, S., Porycka, K., Lapitan, L.D., Drozd, M., Pietrzak, M., & Malinowska, E. (2024). A versatile approach to quality control of protein-based receptor layers by reversible, nonspecific staining for multiplex SPRi immunosensing. Sensors and Actuators B: Chemical. https://doi.org/10.1016/j.snb.2024.136512

I was responsible for preparing carboxylic acid-PEG Self-Assembled (SAM) monolayers on Au chips and conjugating rabbit IgG via EDC/NHS coupling.

Dr. Lorico Lapitan Jr

Consiglio Nazionale delle Ricerche

Istituto di Scienze e Tecnologie Chimiche (SCITEC) "Giulio Natta"

Milan, 31.01.2025

STATEMENT OF CO-AUTHORSHIP

I, Dr. Dario Brambilla, confirm that in the joint publication with S. Pniewska

[P4] Pniewska, S.; Drozd, M.; Mussida, A.; Brambilla, D.; Chiari, M.; Rastawicki, W.; Malinowska, E. **PET Foils Functionalized with Reactive Copolymers as Adaptable Microvolume ELISA Spot Array Platforms for Multiplex Serological Analysis of SARS-CoV-2 Infections.** *Sensors* 2024, *24*, 7766. https://doi.org/10.3390/s24237766

I was responsible for optimizing the protocol for conjugating antibodies with ssDNA sequences, reviewing the manuscript and producing part of the pictures.

Dario Brambilla

Signature

Consiglio Nazionale
delle Ricerche

Istituto di Scienze e Tecnologie Chimiche (SCITEC) "Giulio Natta"

Milan, 31.01.2025

STATEMENT OF CO-AUTHORSHIP

I, Dr. Mussida Alessandro, confirm that in the joint publication with S. Pniewska

[P4] Pniewska, S.; Drozd, M.; Mussida, A.; Brambilla, D.; Chiari, M.; Rastawicki, W.; Malinowska, E. **PET Foils Functionalized with Reactive Copolymers as Adaptable Microvolume ELISA Spot Array Platforms for Multiplex Serological Analysis of SARS-CoV-2 Infections.** *Sensors* 2024, 24, 7766. https://doi.org/10.3390/s24237766

I was responsible for the synthesis and the optimization of the polymers employed for the coating of the PET substrates.

Alessandro Mussida
Signature

CNR - Istituto di Scienze e Tecnologie Chimiche (SCITEC) "G. Natta"
Via Alfonso Corti n. 12, I-20133 Milano

Warszawa, dn. 26.02.2025

mgr inż. Karolina Porycka
Szkoła Doktorska Politechniki Warszawskiej

OŚWIADCZENIE

Niniejszym oświadczam, że w pracy:

[P3] **A versatile approach to quality control of protein based receptor layers by reversible, nonspecific staining for multiplex SPRi immunosensing**. Sensors and Actuators B: Chemical. Karoń, S., Porycka, K., Lapitan, L.D., Drozd, M., Pietrzak, M., & Malinowska, E., 2024, DOI:10.1016/j.snb.2024.136512.

Mój wkład pracy polegał na przeprowadzeniu części badań opisanych w publikacji oraz opracowaniu uzyskanych wyników (w ramach realizacji pracy dyplomowej inżynierskiej). Obejmowały one wstępną selekcję barwników i podstawowe badania ich oddziaływań z immobilizowanymi białkami za pomocą SPRi.

Karolina Porycka

Warszawa, dn. 25.02.2025r.
Mgr inż. Sylwia Pniewska
Wydział Chemiczny
Katedra Biotechnologii Medycznej
Politechnika Warszawska

WYKAZ **OPUBLIKOWANYCH PRAC NAUKOWYCH DOTYCZĄCYCH BEZPOŚREDNIO DYSCYPLINY ROZPRAWY DOKTORSKIEJ** WRAZ Z OŚWIADCZENIEM OSOBY UBIEGAJĄCEJ SIĘ O STOPIEŃ DOKTORA O SWOIM MERYTORYCZNYM UDZIALE W POWSTANIE TYCH PUBLIKACJI

P1 "Recent Advancements in Receptor Layer Engineering for Applications in SPR-Based Immunodiagnostics" Sensors, Drozd, M., Karoń, S., Malinowska, E., 2021, 21(11), 3781, DOI:10.3390/s21113781

Udział merytoryczny: zapoznanie siautorstwie koncepcji ę z literaturą przedmiotu i napisanie podrozdziału *1.2 Antibodies as Affinity Bioreceptors—History and Recent Trends* oraz rozdziału *3. Affinity-Based, Oriented Ab Immobilization Strategies* (podrozdziały *3.1. Mediating Proteins: A, G, and A/G, 3.2. Bacteriophages, 3.3. Biotin—(Strept)Avidin Affinity, 3.4. DNA- and Antibody Directed Immobilization*), *3.5. Bivalent Ion-Mediated Chelation of His-Tagged Receptors,* udział w zebraniu literatury stanowiącej podstawę publikacji oraz korekta tekstu na etapie *revision*.

P2 "A Careful Insight into DDI-Type Receptor Layers on the Way to Improvement of Click-Biology-Based Immunosensors" Biosensors, Karoń, S., Drozd, M., Malinowska, E., 2024, 14(3), 136, DOI:10.3390/bios14030136

Udział merytoryczny: współtworzenie koncepcji badawczej, przeprowadzenie doświadczeń, których wyniki zostały przedstawione w pracy, w tym wdrożenie w laboratorium niewykorzystywanego wcześniej w pracach tam prowadzonych protokołu sprzęgania białek z DNA oraz chromatograficznego oczyszczania koniugatów, opracowanie wyników otrzymanych podczas prowadzonych badań, ich analiza oraz interpretacja, stworzenie części rysunków zawartych w publikacji, przygotowanie początkowej wersji manuskryptu, korekta tekstu na etapie *revision*.

P3 "A Versatile Approach to Quality Control of Protein-based Receptor Layers by Reversible, Nonspecific Staining for Multiplex SPRi Immunosensing" Sensors and Actuators B: Chemical, Karoń, S., Porycka, K., Lapitan, Jr, L.D., Drozd, M., Pietrzak, M., Malinowska, E, 2024, 421, 136512, DOI:10.1016/j.snb.2024.136512

Udział merytoryczny: współtworzenie koncepcji badawczej, przeprowadzenie większości doświadczeń, których wyniki zostały wykorzystane w pracy (tj. wszystkich, z

wyłączeniem wstępnej charakteryzacji i selekcji barwników oraz przygotowania warstw receptorowych o różnych gęstościach powierzchniowych), opracowanie wyników otrzymanych podczas prowadzonych badań, ich analiza oraz interpretacja, stworzenie części rysunków zawartych w publikacji, przygotowanie początkowej wersji manuskryptu, korekta tekstu na etapie *revision*.

P4 "PET Foils Functionalized with Reactive Copolymers as Adaptable Microvolume ELISA Spot Array Platforms for Multiplex Serological Analysis of SARS-CoV-2 Infections" Sensors, Pniewska, S.; Drozd, M.; Mussida, A.; Brambilla, D.; Chiari, M.; Rastawicki, W.; Malinowska, E., 2024, 24, DOI:10.3390/s24237766

Udział merytoryczny: nawiązanie współpracy z międzynarodowym zespołem badawczym odpowiedzialnym za syntezę wykorzystanych kopolimerów (współpraca zainicjowana podczas stażu naukowego zrealizowanego przez doktorantkę i kontynuowana po jej powrocie), współtworzenie koncepcji badawczej, przeprowadzenie wszystkich doświadczeń, których wyniki zostały przedstawione w pracy, opracowanie wyników otrzymanych podczas prowadzonych badań, ich analiza oraz interpretacja, stworzenie większości rysunków zawartych w publikacji, przygotowanie początkowej wersji manuskryptu, korekta tekstu na etapie *revision*.

Sylwia Pniewska

Podpis doktorantki

Cykl publikacji stanowiących Rozprawę Doktorską

Publikacja P1:

Recent Advancements in Receptor Layer Engineering for Applications in SPR-Based Immunodiagnostics

sensors

MDPI

Review

Recent Advancements in Receptor Layer Engineering for Applications in SPR-Based Immunodiagnostics

Marcin Drozd [1,2,*], Sylwia Karoń [1,2] and Elżbieta Malinowska [1,2,*]

[1] Faculty of Chemistry, The Chair of Medical Biotechnology, Warsaw University of Technology, Noakowskiego 3, 00-664 Warsaw, Poland; sylwia.karon.dokt@pw.edu.pl
[2] Center for Advanced Materials and Technologies, Warsaw University of Technology, Poleczki 19, 02-822 Warsaw, Poland
* Correspondence: marcin.drozd2@pw.edu.pl (M.D.); e.malinowska@cezamat.eu (E.M.); Tel.: +48-22-234-75-73 (M.D.); +48-22-182-11-45 (E.M.)

Abstract: The rapid progress in the development of surface plasmon resonance-based immunosensing platforms offers wide application possibilities in medical diagnostics as a label-free alternative to enzyme immunoassays. The early diagnosis of diseases or metabolic changes through the detection of biomarkers in body fluids requires methods characterized by a very good sensitivity and selectivity. In the case of the SPR technique, as well as other surface-sensitive detection strategies, the quality of the transducer-immunoreceptor interphase is crucial for maintaining the analytical reliability of an assay. In this work, an overview of general approaches to the design of functional SPR-immunoassays is presented. It covers both immunosensors, the design of which utilizes well-known and often commercially available substrates, as well as the latest solutions developed *in-house*. Various approaches employing chemical and passive binding, affinity-based antibody immobilization, and the introduction of nanomaterial-based surfaces are discussed. The essence of their influence on the improvement of the main analytical parameters of a given immunosensor is explained. Particular attention is paid to solutions compatible with the latest trends in the development of label-free immunosensors, such as platforms dedicated to real-time monitoring in a *quasi*-continuous mode, the use of in situ-generated receptor layers (elimination of the regeneration step), and biosensors using recombinant and labelled protein receptors.

Keywords: SPR; immunosensor; antibody immobilization; medical diagnostics; gold functionalization; non-specific interactions; self-assembled monolayers

Citation: Drozd, M.; Karoń, S.; Malinowska, E. Recent Advancements in Receptor Layer Engineering for Applications in SPR-Based Immunodiagnostics. *Sensors* 2021, 21, 3781. https://doi.org/10.3390/s21113781

Academic Editor: Nicole Jaffrezic-Renault

Received: 6 May 2021
Accepted: 26 May 2021
Published: 29 May 2021

1. Introduction

1.1. Advantages of SPR-Based Immunosensing

SPR detection is classified as a label-free approach in which the generation of a measurable signal is directly related to the act of binding the analyte by the receptor layer. This attribute bestows the universality of SPR biosensors, since each molecule bound to the surface, regardless of its chemical character, can be considered as a specific signal carrier. Thus, direct detection of interactions by monitoring changes in the surface plasmon resonance seems to be perfectly tailored to the signal transduction of affinity sensors, with immunosensors at the forefront. This is an undoubted advantage over the methods typically used in medical diagnostics, like immunoassays labelled with enzymes, fluorophores, radioisotopes, and nanomaterials, since in these methods, the introduction of an additional labelling is inevitable. The need for the conjugation and purification of secondary bioreceptor complicates and extends the whole analysis. In turn, the extra steps of antibody/conjugate binding and enzymatic or catalytic reaction are often required [1]. What is more, for the most common sandwich assay format, the use of a previously selected and matched antibody pair is required, which is not always achievable for small or unusual antigens. In such cases, the advantages of SPR-based approaches are the most visible.

Label-free methods are easier to design, thanks to the simplicity of a sensing mechanism that naturally mimics the occurring interactions of antibodies with specific antigens. In turn, the affinity-based mass association on the sensor surface, which induces the change in the local refractive index is convenient for optical signal acquisition by tracking the associated SPR resonant angle in a label-free and real time format. Thereby, the analysis of interactions with layers of immobilized antibodies or antigens on SPR transducers also provides auxiliary information about the thermodynamic aspects of the immunoreaction and binding kinetics. Thanks to this, over 30 years from its first application (1990), SPR has become the gold standard for studying biological interactions and—apart from being used for direct signal transduction—also acts as a reference tool, which is indispensable in the development of other classes of affinity biosensors [2].

Molecules within the range of the SPR evanescent wave generated at the interface between metal (typically gold) and the dielectric (typically a liquid medium—buffer or tested sample) are responsible for the change of the refractive index (RI), and thus, the SPR signal depends, to a certain extent, on several factors [3]. The main factor is related to the molecular mass of the bound object, which is mirrored in changes of the local RI. The distance of the captured molecule from the Au surface is also important. The effect of analyte binding on the change in the SPR resonant angle is the most prominent in the immediate vicinity of the metal, and it decays exponentially as it moves away from the plasmonic metal surface. For this reason, an analytically useful range of SPR is not more than 200 nanometers for the classic SPR wave generated on macroscopic, flat transducers [4] and several tens of nm (~30 nm) for the localized SPR occurring at the surface of nanoparticles [5].

Modern medical diagnostics, ranging from screening tests for the rapid detection of civilization diseases' biomarkers to the detection of viral and bacterial infections, is largely based on the detection of specific, rare proteins [6–10]. A common feature of most of these types of molecular targets is their relatively large mass and wide availability of high-affinity antibodies for their detection. Both features make protein biomarkers attractive SPR targets, providing the possibility for their direct determination. In a classic format, antibodies play the role of ligands, and an analytical signal results directly from the act of the specific binding of the target antigen. This is the preferred format, as it enables detection directly in samples without additional steps, either during the sample preparation or during the analysis. However, this does not change the fact that in many cases, it is possible to use indirect formats, such as a sandwich or competitive/inhibition SPR assay. In most cases, it is dictated by the low molecular weight of the analyte or its very low concentration, resulting in an insufficient sensitivity of the direct assay [11]. However, the immobilization of an antigen is not always forced by circumstances, and it can be chosen, e.g., when this format allows for its convenient attachment, which is often the case with labelled recombinant proteins. Due to the high availability of universal coupling agents and protein conjugation methods, it is possible to easily adapt the format of the SPR assay, depending on the requirements of the specific analysis.

SPR detectors, like most of the label-free ones available today, do not distinguish specifically bound analytes from randomly adsorbed interferents. For this reason, SPR biosensors are particularly prone to problems with non-specific binding during analyses of complex samples and the determination of the ultra-low concentration level of the analytes, which are common for medical immunodiagnostics. Problems with the adsorption of body fluid sample components may be reflected in the deterioration of key performance parameters, such as baseline stability, limit of detection (LOD), and lifetime [12]. An insufficient fouling resistance of the immunosensing layer disturbs the sensitivity and selectivity of the assay defined in biomedical terms, which is understood as the percentage of false positive and false negative results and may result in a failure of their validation. This is why so much attention is paid to the appropriate quality of SPR intermediate immunosurfaces for application in medical diagnostics in the literature [13].

Since its first application, a number of methods have been developed to employ SPR for the sensitive detection of bioanalytes in complex samples. The current and main trends in the development of the SPR-related techniques for biosensing are focused on:

- the development of universal substrates for immunosensing, enabling the simple and cheap fabrication of high-quality receptor layers, aimed at improving the sensitivity and selectivity of sensors [14];
- novel approaches to signal amplification, which are particularly important in the case of the determination of bioanalytes occurring at ultra-low concentration levels and low molecular weight targets [15];
- new strategies of plasmonic signal transduction (single-particle and transmission LSPR sensors, Extraordinary Optical Transmission (EOT)-based sensors utilizing plasmonic nanopores, or sensors using meta-surfaces and metamaterials) [16–18];
- possibility for the simultaneous determination of more than one analyte (multiplexing);
- miniaturization of detectors, development of portable SPR systems for the *on-site* detection and adaptation of commonly available instruments to the role of detectors (e.g., integration of SPR platforms with smartphones) [19];

The ongoing development of SPR-based biosensors, both in the context of improving key parameters of receptor layers, as well as methods and instruments for data acquisition, expands the application possibilities of SPR and related techniques in medical analysis. These aspects are comprehensively discussed in recent reviews [1,5,15] and graphically summarized in Figure 1.

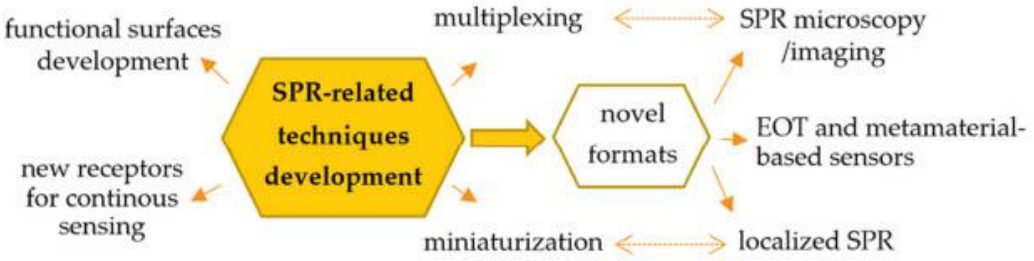

Figure 1. Current major trends in the development of plasmon-based immunosensors.

1.2. *Antibodies as Affinity Bioreceptors—History and Recent Trends*

Immunological receptors are commonly believed to be the most powerful recognition elements for biosensing. Due to their unsurpassed affinity and specificity of interaction with a variety of molecular targets and universality, antibodies have become the flagship biological receptors, with by far the broadest application in clinical analysis and biosensors construction [20]. In 1890, von Behring and Kitasato reported the existence of an agent in the blood capable of neutralizing diphtheria toxins, and they called it "Antikörper", which was later translated as "antibody." Antisomatogen is the name given to the material that causes the formation of antibodies, and the word "antigen" is a contraction of this expression. More than a century of research into the structure and function of antibodies has highlighted their complexities. Antibodies possess many unique properties, such as a high diversity (binding to a wide range of targets), specificity, and structural integrity. While individual immunoglobulins bind a narrow and limited set of ligands, as a population, they are capable of binding to an almost infinite number of antigens of little or no similarity [21]. Immunosensors are based on the concept of forming complexes, which are a product of the interaction between antibodies and their targets. Antibodies were first used in sensing applications in the late 1950s. Their rapid kinetics, specificity, and ability of antigen-binding in both artificial media and real samples caused their extreme popularity as major parts

of receptor layers [22]. Antibody–antigen binding is mediated by the existence of amino acids at the paratope–epitope interface. It has long been debated whether the interaction between the paratope of the immunoglobulin and antigen epitope is predictable, as this breakthrough would completely change medical biotechnology. Nevertheless, this is currently unknown [23]. The most frequently utilized antibody isotype is immunoglobulin G (IgG), both mono- and polyclonal. The first one, which is able to bind only a single epitope, had been the most expensive and desired for years. Nowadays, it has changed due to the development of genetic engineering techniques and worldwide concern for animal rights, which resulted in them becoming cheaper. By contrast, polyclonal antibodies are becoming rarer. Moreover, to avoid batch-to-batch variations, which are common for antibodies produced in animals, antigen-binding fragments (Fab) produced in bacteria are used, instead of whole immunoglobulins [24,25]. The expansion of alternatives to classical antibodies led to the development of novel techniques for their manufacturing, isolation, and selection, such as phage display [26], artificial cell surface constructs and production in plants [27], generation of single-chain fragment variable (scFv) [28], among others [29]. Moreover, new types of protein binders have emerged, such as affimers, which are able to withstand a wide range of temperatures and pH levels [30], or camelid nanobodies—the smallest naturally-derived fragments, which can bind an antigen [31]. While there are more replacements for classical or recombinant antibodies and their fragments, such as aptamers [32], common immunoglobulins are still on top. Their main advantages are their availability, cheapness, and facility of their conjugation and tagging.

The number of articles that are published on the topic of SPR immunosensors has rapidly grown in the last few years. The dataset retrieved from the Web of Science database on 22 May 2021 was based on the following search terms: (*SPR* OR *surface plasmon resonance* AND *immunosensor* OR *immunosensing*). It includes 7803 references over the last 5 years (2017–2021), of which most are in the last 2 years (nearly 2000 each). The advancements in the field of nanomaterial-based LSPR immunosensors, new formats, and designs of receptor layers, as well as methods of signal enhancement for sensitive plasmon-based sensing, are behind this intense increase in scientific output.

1.3. Main Challenges for SPR Immunosensors in Biomedical Diagnostics

Biosensing in body fluids, such as serum or blood plasma, is challenging due to the occurrence of an undesirable non-specific adsorption, resulting from the complexity of the sample matrix [12,33]. To provide clinically relevant results, numerous strategies to improve the analytical parameters of SPR sensors are currently being developed, among which two main trends can be distinguished. The first utilizes the amplification of the affinity-based signal by introducing additional labelling steps (e.g., with secondary antibodies, bioconjugates of plasmonic nanoparticles, and other particles capable of generating changes in the local refractive index). This strategy has very good results in the case of low-molecular mass analytes, but it takes place at the cost of an increased complexity of the measurement procedure and the label-free detection format. The second approach is focused on the broadly understood improvement of the properties of substrates and layers that play the role of a transducer-receptor interphase. A number of examples have been described in the literature, in which the appropriate architecture of the receptor layer's substrate affects various aspects of the SPR sensors, starting from the improvement of the sensitivity of detection (increase of SPR angle shift), through extending the surface available for bioreceptor binding, and ending with lowering background signals by developing layers with an ultra-low nonspecific adsorption [12,34,35]. The surface-related approach seems to be a challenge of particular importance from the point of view of SPR immunosensors, as it allows the most convenient, label-free working principle to be maintained. The development of high-quality immunosensing platforms allows us to fully reveal their greatest potential, i.e., their application for rapid and real-time diagnostic purposes.

The selection of an adequate immobilization strategy is vital for the success of the whole SPR biosensing platform. The receptor layer for applications in the analysis of

complex samples, which meets the requirements of modern medical diagnostics, must be a compromise between various aspects affecting its analytical and working parameters. The most important issues cover:

(I) The metal-receptor interphase thickness—the introduction of linkers/spacers ensuring the separation of the immunoreceptor from the surface has a positive effect on the thermodynamics and kinetics of the antibody–antigen interaction. It also facilitates the surface passivation and minimization of the impact of non-specific binding. However, an excessive distance of the biosensitive layer from SPR-active surface results in a significant decrease in sensitivity.

(II) The surface density and architecture of bioreceptors—a high receptor density represented by protein binding capacity of the interphase is always desirable due to the increased sensitivity of the immunosensor. However, the use of very dense receptor layers with an extensive 3D architecture may generate steric hindrances and problems with mass transport, affecting the response time and the ability of sensor regeneration.

(III) The method of the immobilization of recognition elements—compounds used to passivate the transducer surface should also offer the possibility of a robust, covalent attachment of the Ab receptor layer. On the other hand, site-oriented immobilization via affinity interactions (the use of recombinant/tagged receptors or auxiliary proteins, such as superantigen-like proteins A, G, and A/G) supports the preservation of the native form of receptors and the appropriate orientation and exposure of binding sites.

Both the classic SPR on the surface of macroscopic transducers, multiplexed SPR imaging (SPRi) assays, and the newest plasmonic technique—localized SPR on the surface of nanomaterials—have become attractive platforms for the construction of immunosensors for medical diagnostics [17,36]. The mentioned methodologies of SPR-based immunosensing, regardless of the receptor layer design, offer specific advantages and have different limitations in terms of detection performance. Classic SPR sensors, thanks to the possibility of differential analysis with the use of a reference cell, enable the efficient suppression of various types of interferences, both instrumental and related to surface processes. In addition, such devices typically work in the angular scan mode, which offers the best sensitivity to detect shifts in the resonance angle in a wide range. However, it can be achieved at the expense of the complexity of the detection system. SPRi immunosensors provide attractive platforms for the simultaneous detection of multiple analytes, with the spatially resolved detection of reflectivity changes. It is typical for this type of device detection systems, which are based on the analysis of images captured by a CCD camera, to offer a slightly lower detection sensitivity than an angular scan. In turn, the main advantage of immunosensors based on the localized plasmon resonance of nanostructures (LSPR) is the simplicity of the detection system based on transmission measurements by recording the absorbance spectrum or even by tracking changes in the absorbance intensity at a fixed wavelength. The analysis of the shift of the LSPR maxima requires a high resolution of detectors, but they are much easier to miniaturize. Unfortunately, due to the short range of the LSPR phenomenon, the possibilities of designing immunosurfaces with a high anti-fouling resistance are limited. However, thanks to the appropriate modification and use of signal amplification, it is possible to detect small and low-abundant analytes by means of LSPR immunosensors [5,18].

Biosensors exploiting the unique plasmonic properties of gold, regardless of the employed format and the signal generation and detection mechanism, require a careful design of the receptor layer. Therefore, apart from the intensively developed new detection formats, such as the use of gold nanoparticles as plasmonic transducers in LSPR biosensing, the design of new functional immunosurfaces is still one of the main scientific challenges. It is worth noting that in recent years many types of label-free immunosensing platforms founded on Au, Ag, or metal oxides have been developed. These cover, e.g., piezoelectric biosensors based on quartz crystal microbalance, and ultra-sensitive optical sensors employing surface-enhanced Raman scattering. The SERS phenomenon, thanks to the

strong amplification of the signal of specific molecules on the sensor substrate by plasmonic effects, enables the construction of sensors for the detection of bioanalytes characterized by very low detection limits [7,8].

In a further part of this review, the current state of the art of gold surface modifications for SPR and other plasmonic-based immunosensing platforms is discussed. The review focuses on the solutions developed in recent years and the most popular previously developed approaches in the field of SPR intermediate layers for antibodies and antigens immobilization—ranging from commercial solutions, through novelties in the field of self-assembled monolayers, the latest achievements in the field of chemical and affinity-based immobilization, and nanomaterial-based layers for SPR signal amplification, to smart layers for multiplex immunosensing. The latest developments and trends in the field of universal platforms for semi-continuous plasmonic biosensors will be also discussed. Special attention will be paid to design solutions for and applications of SPR immunosensors in a direct and competitive format for the direct detection of bioanalytes of high biomedical importance, such as protein biomarkers, metabolites, or toxins in complex samples, such as body fluids.

2. Functional Surfaces and Non-Oriented Ab Immobilization Strategies for SPR Immunosensing

A consistent classification of the currently available methodologies for the design of functional SPR immunosurfaces is not an easy task, because the engineering of such interphases is a multistep process. Beyond the type of molecules and other components, there are numerous methodologies for attaching them to the surface of bare gold chips. Additionally, a number of protein receptor attachment strategies are offered, including non-oriented immobilization via adsorption, non-oriented immobilization via chemical coupling, and affinity-based, oriented immobilization of native and labelled receptors. The type of intermediate layer used was chosen as the basic classification criterion within this work. However, in the case of solutions that are difficult to classify (e.g., hybrid approaches, such as a combination of monolayers and affinity-based immobilization), the review goes beyond the adopted framework, and the described solutions are discussed in a broader context. In order to compare the most significant and recent research developments in this field, methods based on physical/chemical interactions and affinity-based approaches have been compiled in separate tables that summarize the individual groups of subchapters.

2.1. Passive and Non-Covalent Adsorption

Methods based on the adsorption of antibodies and antigenic receptors on surfaces are widely used in the construction of immunoassays due to their simplicity of implementation. Even a bare gold surface shows the ability to bind immunoglobulins and their fragments [37,38]. A much wider range of possibilities for protein adsorption is offered by transducers pre-modified with cationic SAMs and polymer layers, e.g., cysteamine, APTES, and PDDA [39,40]. The binding of receptors to the surface is mainly determined by electrostatic interactions between the oppositely charged terminal ammonium and carboxylate residues of aminoacids, as well as coordination-type interactions. In another approach, a mechanism based on the interaction of hydrophobic protein domains allowed for the immobilization of antibodies on SPR substrates coated with hydrophobic polymers. Thin polystyrene layers were used in the construction of SPR immunosensors to bind antibodies and selected types of antigens (e.g., virus particles) by Wan der Waals hydrophobic forces [41]. However, due to the high risk of the inactivation of sensitive protein recognition elements, as a result of conformational changes during adsorption on the surface, as well as difficulties in the fabrication of repeatable and homogeneous layers with a high resistance to non-specific adsorption, such approaches are losing importance in SPR-based applications. Towards the development of durable and resistant immunolayers dedicated to applications in flow conditions commonly used in SPR, methods using random immobilization via chemical coupling and oriented affinity-based immobilization are currently dominating [42].

2.2. Covalent Anchoring and Surface Passivation through Self-Assembled Monolayers (SAMs)

While antibodies themselves have the ability to spontaneously adsorb on the Au surface and chemisorb through terminal cysteine residues (previously converted to the more chemically active reduced form or after the previous derivatization of terminal lysine residues by means of Traut's reagent [38,43]), these methods are quite rarely used in the construction of SPR sensors. The main disadvantage of such an approach is the deterioration of the Ab binding capacity due to conformational changes caused by the multidentate interaction with the surface of gold. What is more, such layers are characterized by a poor homogeneity, moderate reproducibility, and tendency to desorb under shear stress in microfluidic conditions. Therefore, intermediate layers that allow for covalent coupling with functional groups of a protein receptor are commonly used [44]. Primary amine residues, which are more abundant and less demanding in terms of the coupling reaction conditions than thiol/disulfide moieties, are most often employed for this purpose.

The easiest approach to the formation of functional SPR interphases reactive in amine-coupling reactions is the use of the self-assembly of bifunctional, -COOH terminated thiols [45]. Due to the better passivating properties and ability to form highly ordered molecular assemblies without pinholes and defects, the most commonly used are linkers with a long aliphatic chain—mercaptoundecanoic acid (MUA) or mercaptohexadecanoic acid (MHDA) [46–50]. Detailed considerations on the impact of the used *n*-alkanethiolate chain on the capacity of antibody immobilization and antigen-binding efficiency can be found in the research provided by Bhadra et al. [51].

Beyond ω-mercaptocarboxylic acids, in the design of SPR immunosensors, thiol-terminated amine-reactive prolinkers with terminal NHS ester groups, such as Cr5B and DSP (disuccinimido dithiobispropionate), are also exploited. The formation of such SAMs can be followed by a single-step immobilization of antibodies, without the need for prior activation [52,53]. Apart from bifunctional molecules, simple *n*-alkanethiols are also used in the construction of SPR sensors. Layers based on *n*-octanethiol were employed to passivate a gold surface or immobilize low-molecular, non-polar inhibitors, and antigens of non-protein nature by hydrophobic interactions [54,55]. Various strategies exploiting thiol-based SAMs in the construction of immunosensors for the detection of clinically relevant analytes are presented in Figure 2.

Even better passivating and protecting properties against non-specific binding to the sensor surface are demonstrated by ligands with an internal, polar spacer, such as linear PEG6 [56], dithiolalkanearomatic PEG (S_2PEGCOOH) [57], and thiolated PEG linker DSPEG2 [58]. Thanks to their complex structure, containing both linear aliphatic segments and flexible or bulky segments, such as a PEG/aromatic ring, such compounds combine the ability of alkanethiols to form highly oriented, dense assemblies, with flexibility and hydrophilicity and thus an anti-fouling capacity of ethylene glycol oligomers. This promotes the immobilization of antibodies by reducing the negative influence of steric hindrance [59]. Another way to optimally adjust the surface density of anchoring groups for the efficient immobilization of antibodies is the use of mixed monolayers, in which ω-mercaptoalcohols play the role of a diluent and a surface backfilling. Their presence reduces the surface charge density, thus facilitating its formation without the negative impact on the performance of the Ab coupling reaction, even for -OH/-COOH ratios significantly greater than 1:1, reaching even 1:10. Typically used compounds include mercaptoalcohols with an aliphatic chain length equal or lower than the length of mercaptocarboxylic linkers [60] or mixed layers of functional PEGs, like HS-PEG-OH/-COOH [57,61,62]. This approach facilitates the access of high-molecular-mass receptors (such as antibodies) to the surface. Terminal hydroxyl groups are responsible for the formation of hydration layers. Hydrogen bonds that form in contact with the aqueous samples effectively counteract the adsorption of matrix proteins. Backfilling agents of a longer chain than carboxylate anchors are rarely used and are mainly used for the immobilization of small receptors (immunosensors in a competitive format) and in biosensors requiring a very effective suppression of surface fouling. It should be stressed that long and flexible PEG chains, apart from the natural

hydrophilic barrier, also create a steric barrier, which, additionally, hinders the organization of layers on the surface due to entropy effects [12]. A detailed discussion of the influence of SAM composition on the availability of anchoring groups on the surface and the relation between the design of the SAM surface chemistry and sensitivity of the competitive immunoassay for the detection of small analytes can be found in the work authored by Castiello et al. [56].

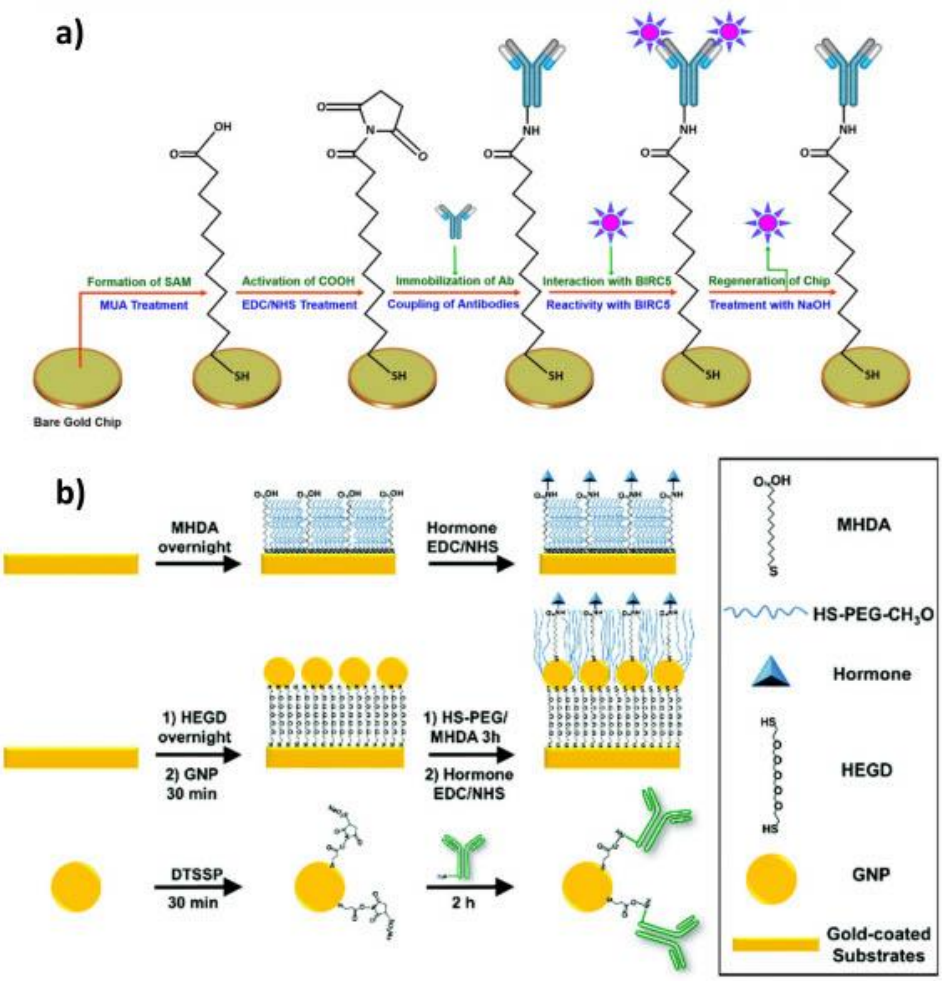

Figure 2. Examples of the utilization of various *n*-alkanethiolate and mixed SAMs in SPR immunosensing. (**a**) Schematic representation of ω-carboxylic acid-based SPR immunosensor fabrication with the use of EDC/NHS coupling, (**b**) various bifunctional linkers used for gold surface functionalization: MHDA/mercaptoundecanol mixed SAM (top), HEGD SAM for AuNPs self-assembly (middle), and DTSSP linker-mediated conjugation to AuNPs. Adapted with permission from Jena et al. [49] (under the terms and conditions of the Creative Commons CC BY License) and Castiello et al. [53] (Copyright © (2019) Royal Society of Chemistry).

The same group developed two competitive SPRi immunosensor configurations for the detection of insulin, glucagon, and somatostatin. In the first approach, antigen was immobilized on a mixed thiolate SAM. To obtain a high passivation and thus antifouling properties, 16-mercaptohexadecanoic acid (MHDA) molecules were used as anchors, and thiol-terminated PEG (CH_3O-PEG-SH) was introduced as a surface backfiller. The second format covers an additional introduction of the auxiliary layer of gold nanoparticles anchored by a hexa(ethylene glycol) dithiol (HEGD) monolayer on gold to enhance the sensitivity by plasmonic coupling (Figure 2b). Both approaches were aimed at the formation of surfaces compatible with the EDC/NHS immobilization chemistry and resistant to non-specific adsorption, thus enabling an ultra-sensitive, indirect detection of pancreatic hormones [53,56].

Another method of coupling antibodies/antigens to the SPR chip surface is the use of SAMs with terminal amino groups. In this approach, 2-aminoethanethiol (cysteamine) is by far the most commonly used building block (Figure 3a) [63–65]. Despite the inability to form well-defined layers due to the insufficient length of the aliphatic chain, this ligand finds an application in the construction of immunosensors characterized by a validated reliability in typical medical samples. Terminal amino groups on the transducer surface open up a number of possibilities for the adsorptive and covalent attachment of protein receptors. The most important coupling agents compatible with -NH_2-terminated interphases include glutaraldehyde (coupling with lysine residues through imine bond formation), EDC/NHS (coupling with carboxyl residues on C-terminal and the acidic amino acids of the protein), and maleimide (coupling with the thiol residues of cysteine in a reduced form) [66]. The limited resistance of amino-terminated SAMs towards protein adsorption is often associated with the necessity of using additional treatments, such as blocking of the immunosurface with polymers and proteins or the addition of anti-fouling agents (like dextrans and albumins) to the matrix buffers [46,47]. However, higher aliphatic aminothiols and functional aminothiols with oligoethylene glycol segments are not commonly used [67]. The smaller variety of the components used in the amino-SAMs can be explained by the significantly lower availability and high price of the higher aliphatic aminothiols, compared to their carboxyl counterparts.

Except for the simple, bifunctional thiol-based SAMs, bioinspired monolayers were also utilized in several examples of SPR interphases. An interesting approach is the use of monolayers of a short bifunctional peptide, 3-mercaptopropionic acid-His-His-His-Asp-Asp-COOH (3-MPA-HHHDD-OH). Such an oligopeptide has been introduced to reduce nonspecific adsorption in SPR-based PSA immunosensors, as described by Breault-Turcot et al. [68]. In a different approach, for the construction of universal biosensor platforms with a high resistance to non-specific protein binding, the synthetic layer of the carboxymethyl-terminated and disulfide-cored peptide was elaborated [69]. Short oligopeptides can be employed not only as a surface passivating agent. Islam et al. described the application of hexameric peptide ligands showing an affinity to human IgG as a foundation for an SPR immunosensor layer assembly. The authors demonstrated the Ab-binding capacity of the devised anchor to be similar to the well-known antibody-binding compound, protein A [67].

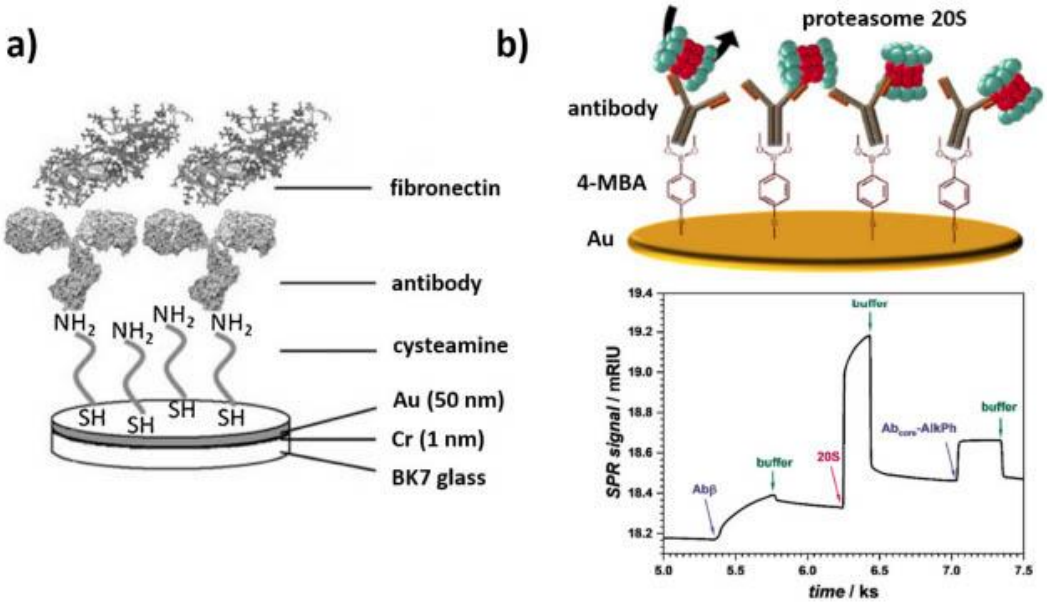

Figure 3. (a) The architecture of the oligopeptide SAM-based SPR immunosensor, (b) the mechanism of antibody immobilization through the interaction of carbohydrate residue with boronic acid SAM. Adapted with permission from Sankiewicz et al. [70] (Copyright © (2018) Elsevier) and Barsan et al. [71] (under the terms and conditions of the Creative Commons CC BY License).

To minimize the risk of the abovementioned inactivation of antibodies due to the attachment via amine groups (abundant in the Fab region of immunoglobulins), other antibody functional groups were also harnessed as surface anchors. A very intuitive method described in the literature is based on the employment of EDC/NHS chemistry in an inverted format. Gorodkiewicz's group used cysteamine SAMs for the construction of SPRi immunosensors. Carboxylic groups of antibodies in solution were first subjected to chemical activation, leading to the formation of reactive N-hydroxysuccinimide esters. Then, the pre-activated receptors react spontaneously with the surface amino groups [70,72]. Another method for the partially oriented immobilization of immunoglobulin G is the interaction of carbohydrates with phenylboronic acids (Figure 3b). IgG antibodies, as glycoproteins, contain N-glycan residues, located mainly in the Fc region, away from the binding sites. Such a configuration allows the appropriate spatial orientation of the immunoreceptors on the surface to be maintained [73]. SAMs composed of 4-mercaptophenylboronic acid (4-MBA) formed directly on gold [71] and 3-aminophenylboronic acid, immobilized on modified SPR transducers using graphene oxide carboxyl groups, have been described as compounds directly responsible for the capture of antibodies [74]. Additionally, amine-terminated ligands can be employed for carbohydrate-mediated immobilization through the previous oxidation of polysaccharide residues to aldehydes, followed by Schiff base formation [75].

2.3. Polymer-Based SPR Immunosensing Surfaces

Besides the abovementioned heterobifunctional thiols and short peptides, other compounds are also widely used as robust backfilling agents. Zwitterionic agents—both low-molecular-weight and polymeric—benefit from their well-defined charge distribution, ensuring a high hydrophilicity and suppressive properties against electrostatic interactions with proteins. Polymers such as betain and phosphorylcholine effectively fulfill

their protective function, ensuring a very low, even undetectable level of protein adsorption (<10 ng/mm^2) from samples such as serum or blood plasma [76]. However, their implementation in functional platforms for antibody immobilization is difficult, as it requires the preparation of mixed-type layers by thiolated anchor grafting [77]. Another approach is to use copolymers with zwitterionic segments, e.g., carboxybetaine acrylamide [78] and thiolated hyaluronic acid (HA) grafted with the zwitterionic CPPPPEKEKEKEK peptide [79]. Riedel et al. described the use of a coating with poly[(N-(2-hydroxypropyl)methacrylamide)-co-(carboxybetaine methacrylamide)] in the construction of a SPR sensor to detect hepatitis B antibodies in saliva. Previously grafted ω-mercaptoundecyl residuals were used as anchors to the chip surface and the antigen was attached using carbodiimide chemistry to the carboxylate terminal groups of the copolymer [78].

A number of hydrophilic polymers with functional groups capable of binding to a gold surface or groups that enable the chemical coupling of immunological receptors have been employed as interphases in SPR biosensors for clinically relevant analytes, including grafted hyaluronic acids [79,80], poly(N-isopropylacrylamide) (PNIPAAM) [63], poly(2-hydroxyethyl methacrylate) (pHEMA) [81], polysaccharides, and poly(β-peptoid)s. Hyperbranched polymers and dendrimers were also used as multifunctional immobilization platforms characterized by excellent anti-fouling properties. In work by Becherer et al., carboxymethylated dendritic polyglycidol grafted with thioctic amine was employed in the design of a sensor for the detection of anti-amyloid beta (Aβ) 1–40 antibodies [82]. In turn, D.E.P. Souto et al. introduced a self-made 3D matrix based on the PAMAM dendrimer with an ethylenediamine core for antigen immobilization in the competitive SPR immunoassay [83]. Due to the development of the surface available for the immobilization of the C1 protein (acting as immobilized antigen) by the introduction of the dendrimer, a significantly improved immobilization efficiency was achieved. According to the authors, the immunosensors in the 3D layers showed more than twice the sensitivity of the assay, compared to the classic immobilization on cysteamine SAM via glutaraldehyde chemistry.

Another example of an amine-terminated polymer coating for the immobilization of antibodies has been described by Makhneva et al. The plasma polymerization of cyclopropylamine resulted in the coverage of the SPR slide surface with a polymer coating rich in nitrogen-containing functional groups. The surfaces were activated with glutaraldehyde, and after the subsequent immobilization of the antibodies, the obtained SPR immunosensor was employed to detect microbial cells. As shown in Figure 4a, the developed methodology for amine-bearing polymer coating can be successfully applied for oriented Ab immobilization via protein A or the amine/thiol-reactive linker, SMCC [84]. By changing the polymerization precursors to an acetylene-maleic anhydride mixture [85] and 1,2,4-trivinylcyclohexane (TVC)-tetrahydrofurfuryl methacrylate (THFMA) [86], the same group also synthesized carboxyl-rich copolymer films and used them as matrices for covalent antibody immobilization. It was confirmed that the binding capacity of such layers exceeds mercaptocarboxylic acid SAMs and is comparable to commercial CMD layers, and the obtained LODs for HSA detection were similar to MUA and 3D dextran-based sensors.

In another approach, a thin film of in situ polymerized dopamine was introduced as a passivating layer of an SPRi transducer (Figure 4b). The oxidative, UV irradiation-mediated polymerization of the deposited dopamine allowed a layer with catechol and quinone moieties to be obtained. Due to their reactivity in the Michael addition and formation of Shiff bases, this substrate can be used to effectively immobilize proteins through sulfhydryl and amino groups, without the need for prior pre-activation [87]. The authors showed the applicability of this substrate for the immobilization of the protein antigen-ochratoxin A (OTA) conjugate in the construction of a sensor to detect specific antibodies [88]. A similar layer, but obtained by electropolymerization, has also been applied for the SPR immunosensing of prostate-specific antigen [89].

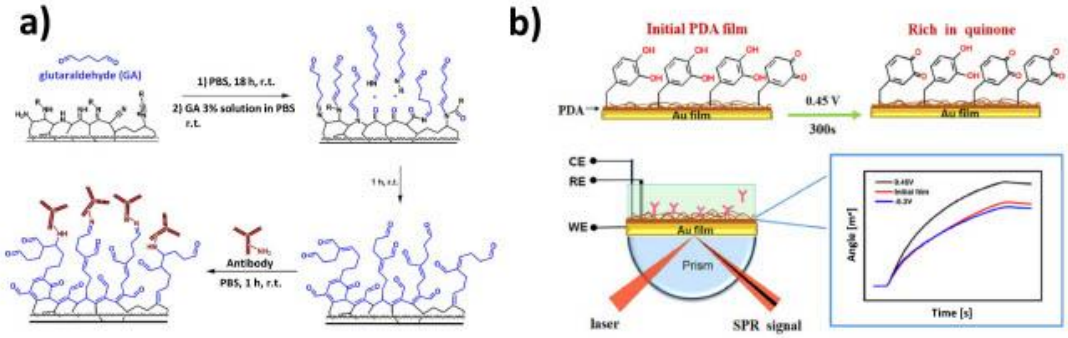

Figure 4. Examples of polymeric interphases employed in SPR immunosensors. (a) amine-terminated cyclopropylamine plasma polymer, (b) quinone-terminated polydopamine film. Adapted with permission from Makhneva et al. [84] (Copyright © (2018) Elsevier) and Chen et al. [89] (Copyright © (2018) Elsevier).

2.4. Carboxymethyldextran Hydrogels and Planar CMD Surfaces

Carboxymethyldextran (CMD) 3D hydrogels and planar CMD surfaces are considered the gold standard within matrices for SPR immunosensing and thus deserve a separate discussion. Dextran coatings owe their commercial success to the ease of maintaining the form of a hydrophilic hydrogel, the facility of a controlled introduction of carboxyl groups into the structure and thus the regulation of the binding capacity, as well as the ability to control the polymer morphology. Thanks to this, it is possible to obtain universal hydrogel CMD coatings with different densities, degrees of branching, and surface charges. CMD-modified substrates are highly compatible with EDC/NHS surface chemistry. Thanks to the possibility of using a pH-adjustable protein preconcentration on the surface of previously activated sensors, it is possible to additionally increase the efficiency of covalent immobilization. In turn, the possibility of using zwitterionic CMD matrixes of a low charge density enables the efficient immobilization of negatively charged molecules. Another easily tunable parameter is the length of the dextran chains. For the detection of high-mass analytes, planar matrices are typically used. In the case of the detection of small molecules, to increase the receptors' surface density (which determines the sensitivity of the assay), brush-like, 3D matrices with chain lengths of up to 700 nm can be employed. In such sensors, the hydrogel layer swells. An extensive spatial structure of the polymer matrix promotes the possibility of target association within a 3D brushed structure and thus enhances the RI changes responsible for the SPR angle shift as much as possible. Other examples of hydrogel materials that found applications as antifouling matrices of a high binding capacity include oligo(ethylene glycol) methacrylates, e.g., MeOEGMA, gelatin-based polymers, and linear polycarboxylates [90]. The use of CMD matrices, despite the obvious benefits of commercial availability and a high binding capacity, carry some risks. It is reported that CMD polymer substrates are characterized by a noticeable heterogeneity, resulting in the formation of regions of uneven affinities and inhomogeneity in terms of mass transport processes [91]. For this reason, the conscious selection of the substrate architecture in terms of the surface density and length of polymer chains is so important from the point of view of both characterizations of molecular interactions and SPR-based biosensing.

CMD substrates can be used as platforms for the immobilization of both antibodies and protein antigens, as well as for small molecule receptors used in indirect assay formats [92,93]. For example, He et al. employ the classic carboxymethyldextran (CM5) medium and EDC/NHS activation to immobilize the carrier protein conjugate (ovalbumin) with antigen 3-Nitrotyrosine (3-NT). The as-prepared receptor layer allowed for the SPR-

based detection of this inflammatory biomarker in the competitive assay. The analytical parameters offered by SPR biosensors exceeded the parallelly developed ELISA [94]. The robustness of the covalent immobilization, together with the a capability of an efficient regeneration, results in the wide application of CMD polymer substrates for the detection of multiple analytes important from the point of view of medical diagnosis [95].

2.5. 2D Nanomaterials—SPR Interphases as Enhancers of the Plasmonic Signal

The unique optoelectronic properties of graphene have found numerous applications in modern bioanalytics, including the improvement of signal transduction in SPR biosensing. Ultra-thin layers of graphene offer numerous benefits for SPR sensors due to their high in-plane electron mobility and zero-band gap properties [96]. Covering the surface of the gold transducer with a thin layer of this material (e.g., by chemical vapor deposition) enables a significant increase of the SPR signal due to its capability to amplify refractive index changes. At the same time, the graphene surface plays a role in acting as a convenient platform for the immobilization of antibodies. The developed bifunctional linkers are based on pyrene derivatives implying a $\pi-\pi$ interaction with aromatic rings of the graphene substrate. The use of the commercially available linkers, 1-pyrenebutyric acid or its NHS ester, enables a useful way to obtain amine-reactive surfaces for the rapid immobilization of antibodies [97]. Graphene can also be functionalized both chemically as well as by adsorption, thus opening a way to directly or passively immobilize through interactions of the hydrophobic protein domain [98,99]. Several methods for the oriented immobilization of antibodies/antigens on graphene, assisted by carrier proteins, such as A/G protein or avidin-biotin interaction, have been recently developed [64]. The introduction of water-dispersible graphene derivatives, such as GO and GO-COOH, simplifies the preparation of their layers on gold by enabling the deposition of the nanosheets directly from aqueous solutions [100]. To attach GO nanoflakes to the Au surface, cationic adhesive layers are commonly used, such as cysteamine, 3-mercapto-1-propane-sulfonate and cationic polymer PDDA [64,74,101–103]. The binding mechanism involves electrostatic interactions and reactions of GO epoxy groups with terminal amino groups on SAM-functionalized gold [64]. Examples of applications of 2D nanomaterial layers as plasmonic enhancers in the construction of SPR immunosensors are illustrated in Figure 5.

Apart from graphene and its derivatives, molybdenum disulfide (MoS_2) has become another 2D material that significantly promotes plasmonic phenomena at the metal-dielectric interface. MoS_2 is over two times more efficient than graphene in terms of optical absorption. This nanomaterial has been recently used in several SPR-based approaches [104]. SPR immunosensors were developed for the detection of biomarker proteins using both direct immobilization [105], coupling via terminal -COOH groups introduced through sulphur vacancies [106], and the decoration of nanomaterial deposited in the form of nanoflowers on the surface of the SPR transducer with gold nanoparticles [107].

2D Nanomaterials with a structure similar to graphene, which has attracted tremendous attention in recent years are transition metal carbides/carbonitrides (MXenes). Due to the high content of oxygen functional groups, MXenes are convenient substrates for the immobilization of biomolecules and, at the same time, make a significant contribution to SPR signal amplification [108]. The first applications of Ti_3C_2 MXene nanosheets in SPR immunosensors were described in 2019 and 2020 by Cui's group. They developed sandwich-type SPR biosensors for the ultra-sensitive determination of carcinoembryonic antigen. The proposed, sophisticated mechanism of amplification and detection of plasmonic signals covered the decoration of MXenes by gold nanoparticles [109] or hollow nanoshells [110], followed by the protein A-assisted immobilization of *anti*-CEA antibody. The additional labelling step provided in sandwich assay format allowed the authors to determine CEA at the clinically relevant levels with a high sensitivity. Examples of the harnessing of selected 2D nanomaterials as substrates and signal enhancers in SPR immunosensors are depicted in Figure 5.

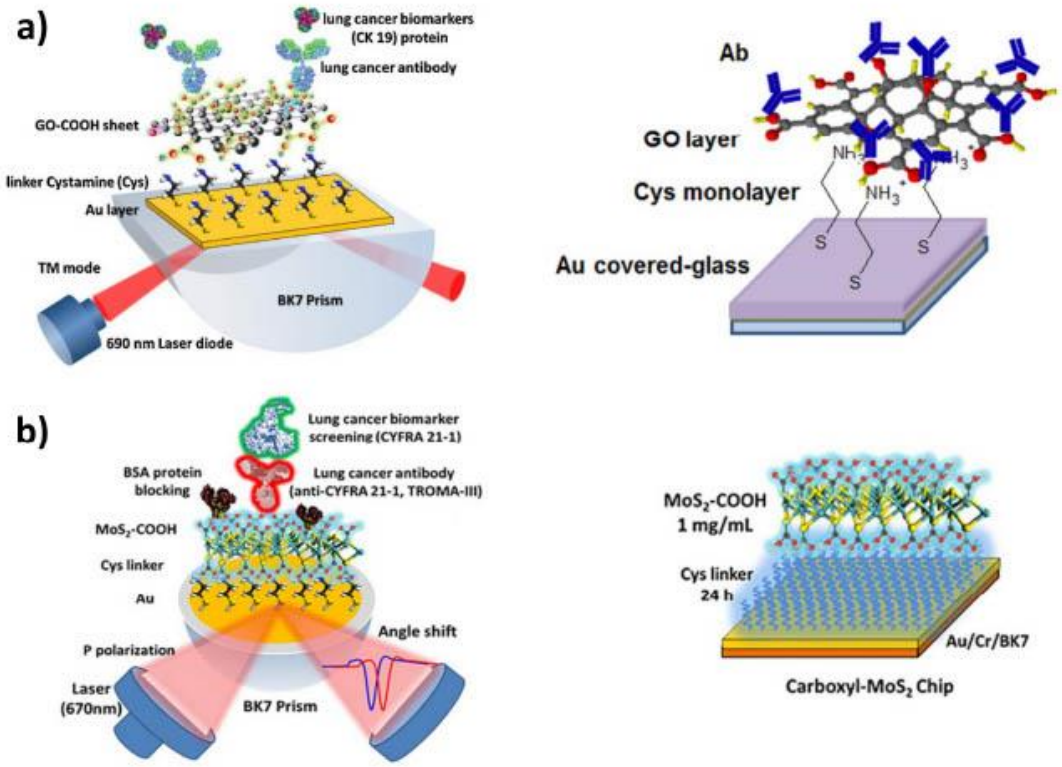

Figure 5. Carboxylated 2D nanomaterial layers as plasmonic enhancers in the construction of SPR immunosensors: (**a**) carboxylated graphene oxide, (**b**) carboxylated MoS2. Adapted with permission from Chiu et al. [98] (Copyright © (2018) Elsevier), Miyazaki et al. [102] (Copyright © (2018) Elsevier), and Chiu and Yang et al. [106] (under the terms and conditions of the Creative Commons CC BY License).

3. Affinity-Based, Oriented Ab Immobilization Strategies

As is well known, covalent immobilization carries an obvious risk of deteriorating the binding properties of immunoreceptors. What is more, chemical coupling through specific protein functional groups, such as -NH_2, -COOH, or -SH, requires the use of high-purity antibodies/antigens and often results in the need for additional purification by the user. Therefore, methods involving chemical or biological affinity have become an interesting alternative to non-selective, chemical, or physical immobilization. The mild and targeted attachment helps to ensure the optimal spatial orientation of the recognition element, facilitates the control of their surface density, and gives greater freedom in the choice of reaction medium [111,112]. Over the years, many strategies of oriented antibody or recombinant antigen immobilization have been developed. Most of them have been implemented in the construction of SPR sensors from other methodologies. This was the case for the methods adapted from affinity chromatography for the purification of antibodies (proteins A, G, A/G) [113] and recombinant proteins (nitrilotriacetic acid—bivalent ion chelation via terminal His-tag). Other affinity-based methods, such as attachment via biotin tags or ssDNA anchor sequences, require the post-synthetic labelling of bioreceptors. Very good, critical discussions on various aspects of the design of immunosurfaces for plasmonic sensing have been presented in several reviews, including works provided by De Angelis [66],

Mauriz [42], and Cheng [35]. The possibilities offered by affinity-based methodologies in the construction of SPR immunosensors for medical diagnostics, primarily in terms of universality, miniaturization, and multiplexing, will be discussed in the following sections.

3.1. Mediating Proteins: A, G, and A/G

Proteins A and G are derived from bacteria and possess a strong binding activity for IgGs. That is why these biomolecules—commonly known as superantigens—offer the convenient, site-oriented immobilization of immunoreceptors [114]. Regardless of the specificity of Fab regions, it is possible to obtain highly bioactive layers with exposed binding sites. Bacterial protein A is a five-binding-domain protein isolated from *Staphylococcus aureus*. It captures the Fc portion of humans' and domestic animals' antibodies, leaving the Fab fragment accessible for the detection of the antigen [112]. Streptococcal protein G, which is similar in terms of functionality, contains repetitively arranged domains, where the COOH-terminal domains bind IgG, and the NH_2 half residue was found to attach to human serum albumin. Thus, protein G has a broader spectrum of binding activity than protein A [115]. Nevertheless, native protein G is able to bind the Fab region of the antibody, but with an affinity 10 times lower than that towards the Fc region [116]. At first, these molecules were widely used in affinity chromatography for immunoglobulin purification. Therefore, their usage for the directed immobilization of antibodies was just a matter of time. As a non-specific binding between the surface of the metal and bare protein A is likely to appear, unmodified protein is not a preferable method for immobilization, and other chemical approaches typically need to be employed. The possibility of manipulating its affinity to antibodies and gold surfaces through genetic engineering, as well as its compatibility with various pre-immobilization strategies (e.g., carbodiimide coupling, thiolate, and dithiocarbamate self-assemblies), are behind the widespread use of this bacterial protein in the construction of plasmonic biosensors and commercial SPR substrates [66].

In 2003, Lee et al. fabricated an immunosensor that determined bovine serum albumin in a probe. The device was based on a self-assembled monolayer of modified protein A, where the surface group of the compound was substituted with thiol functionality. The modified layer resulted in an increased antibody binding capacity and, with this, showed a better capture of the antigen [117]. Bakhmachuk et al. developed a biosensor that was dependent on the recombinant Staphylococcal protein A, with an added cysteine residue. Genetic engineering enabled the introduction of the attachment site into an expendable part of the protein, which increased the immobilization level of the molecule. The interaction between the thiol group and the surface of the gold sensor chip is much stronger and more reliable than physical adsorption [118]. Juan-Franco et al. also investigated the ability of modified protein A to form an appropriate layer for enhanced immunosensing. The staphylococcal immunoglobulin-binding domains were fused with a gold-binding peptide (GBP) forming PAG—the protein A gold-binding domain. This modification provided an easy and directed immobilization of the antibodies against human growth hormone, where Fab fragments remained freely exposed to the epitopes [119]. Schmid et al. used thiol-based homobifunctional cross-linker dithiobissuccinimide propionate (DSP) to covalently immobilize protein A on a gold surface. A sterically accessible, stable, and uniform antibody coating was achieved (Figure 6a) [120]. Sohn et al. also formed a layer of protein A on a chip modified with (3-aminopropyl)triethoxysilane (APTES), using a cross-linker (EDC-NHS) for the site-directed immobilization of the antibodies, and compared the results with non-activated protein A and a self-assembled monolayer [121]. The greatest sensitivity of the chip was obtained with protein A activated already with the cross-linker. The use of a cross-linker is relatively easier in comparison to engineered protein G or A, and it allows for antigen detection at very low concentrations. Streptococcal protein G was utilized by Hsu et al. to form a covalently attached layer for the immobilization of monoclonal antibodies. Three types of antibodies against pentamer C-reactive protein (CRP) and modified CRP were used for the subsequent detection of these molecules. No

false signals were observed, and a sufficient sensitivity for the detection of this biomarker in biomedical samples was acquired [122].

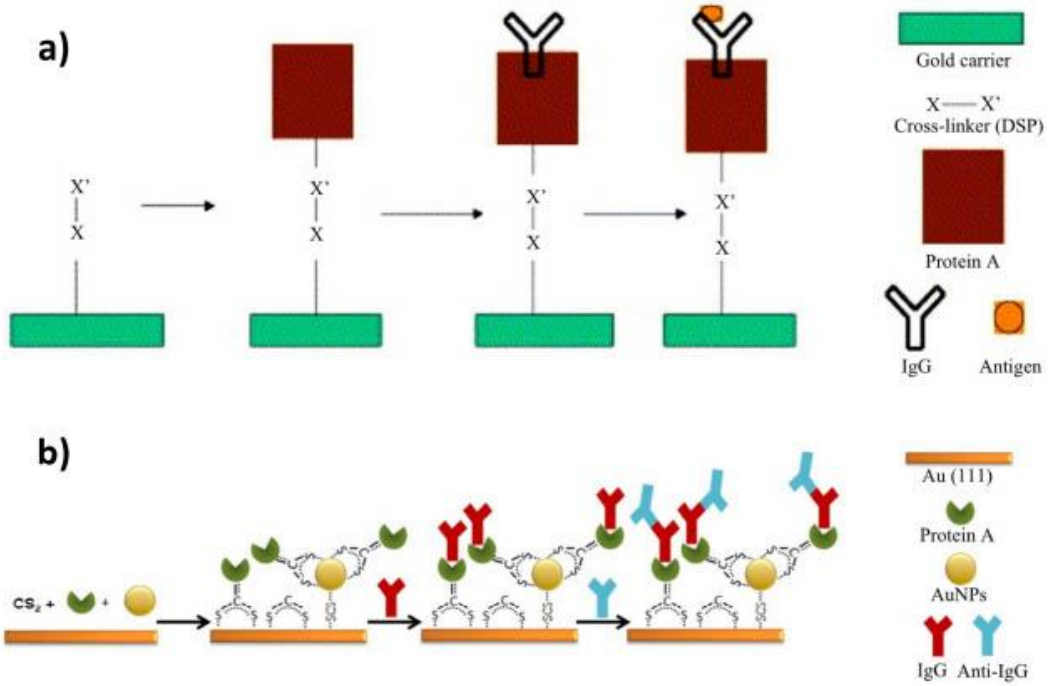

Figure 6. (a) Scheme of an SPR immunosensor construction based on the attachment of protein A to a gold surface through bifunctional DSP as a cross-linker, (b) functionalization of the terminal amino groups of protein A with carbon disulfide and direct immobilization of the carrier on gold by means of a dithiocarbamate assembly. Adapted with permission from Schmid et al. [120] (Copyright © (2006) Elsevier) and Paiva et al. [123] (Copyright © (2017) Elsevier).

In another approach, to increase the affinity of protein A to a gold surface without the need for a complex chemical modification or the use of recombinant protein, a simple, one-pot covalent immobilization via dithiocarbamate (DTC) chemistry was proposed [123,124]. In this strategy, the carrier protein was reacted with aqueous, alkaline carbon disulfide, which converts primary and secondary amino groups of protein A to dithiocarbamate. This simple functionalization allowed DTC-terminated molecules capable of bivalent interactions with gold to be obtained, involving the introduced sulphur atoms. The use of protein A functionalized the DTC chemisorption on flat transducers [124] and on the surface modified by introducing gold nanoparticles [123], which paved a way to the efficient immobilization of model antihuman IgG antibody and the use of an as-obtained platform in SPR-immunosensing (Figure 6b). This method has been also considered for the attachment of another intermediate protein—avidin—to a gold surface [66]. However, to date, it has not been used for the direct immobilization of protein receptors.

Bacterial mediator proteins and their bioconjugates are often applied in combination with other strategies aimed at improving the versatility or performance of SPR immunsurfaces [42]. Jung et al. developed a biolinker, which was a conjugate of protein G and DNA for the site-directed immobilization of antibodies. Single-stranded DNA oligonucleotides were attached to a gold surface, which enabled the hybridization of the complimentary oligonucleotide coupled with protein G. This form of immobilization resulted in a better

oriented layer and greater ability to bind an antigen in comparison to the chip, where protein G was immobilized via chemical bonding [125]. More examples of spatially resolved protein attachment via DNA-directed immobilization is contained in chapter 3.4. Oh et al. fabricated a monolayer of protein G due to the chemical binding on a gold surface, which was modified with 11-mercaptoundecanoic acid (MUA). Antibody immobilization through protein G resulted in the construction of immunosensors for the detection of four kinds of the pathogens: *E. coli*, *Y. enterocolitica*, *S. typhimurium*, and *L. pneumophila* [126].

To further improve the anti-fouling properties of an antibody layer immobilized through thiolated protein A and backfilled with 3-mercapto-1-propanol, an additional, post-immobilization surface passivation with a cationic lipid membrane composed of ethylphosphocholine (EPC+) was also employed. The devised receptor layer combines the advantages of oriented antibody immobilization with an improved resistance to the adsorption of components of undiluted human plasma. The applicability of such an immunosensor for the detection of IgG antibody and cholera toxin in plasma samples was confirmed [127]. Biomimetic immunosensing interfaces based on lipid bilayers have also been implemented to functionalize SPR transducers. Almeida et al. described a layer made of common, amine-terminated phospholipids and cholesterol, which exhibits a high resistance to non-specific adsorption. The deposition of an appropriate composition of previously prepared lipid vesicles allowed for a rapid formation of bilayers, which are flexible but stable enough to be implemented in SPR measurement conditions. The additive of 5% decanethiol was responsible for the anchoring of the bilayer to the gold substrate, while exposed phosphate groups enabled the immobilization of protein through amine coupling, with the use of EDC/NHS chemistry [128].

3.2. Bacteriophages

Bacteriophages, also known as phages, are viruses that infect bacteria and the most abundant form of life on the planet [129]. They are extremely stable, and it is very easy to modify them, both genetically and chemically [130]. Due to these characteristics, they have become of considerable interest as probes for biosensing. Non-lytic and filamentous phages (those which do not lyse bacteria immediately after infection, are able to incorporate their genome into the host cell, and remain latent for a very long time) can be used as scaffolds for the binding of target moieties after chemical or physical functionalization. Both lytic and non-lytic genetically engineered phages were fabricated as an element of a biorecognition layer, and they can thus be successfully implemented in the construction of affinity biosensors [131].

Phage-derived biorecognition elements, such asphage-display peptides (the most recent) and elder, phage receptor-binding proteins or whole viral cells, are becoming more and more popular due their easy production, simple immobilization, rigidness, and ability to withstand very harsh conditions, such as high temperatures [132]. It is possible to insert the gene encoding the protein of interest into the phage's genome, and then this particle is displayed as a fusion protein in the coating of the bacteriophage. Phage display is widely used for screening, but this technique is also suitable for biosensing as-obtained phage clones demonstrate peptides, proteins, and antibodies with the desired affinity for the target. It has been shown that phage display-identified peptides frequently bind to functional sites of the target proteins, rather than incidentally. Thus, non-specific interactions are rare [133]. Moreover, as there is a charge difference between the head of the bacteriophage (negative) and its tail fibers (positive) the site-directed binding using electrostatic forces is one of the most popular approaches of phage immobilization, after covalent coupling [134]. The general application of bacteriophages towards biosensors may be grouped into three categories: (a) specific peptides displayed on the surface of non-lytic phages' coats due to genetic engineering for target analyte detection; (b) lytic bacteriophages that disrupt the host, causing a release of bacterial cell markers and, afterwards, their detection (phage acts like an antibody); and (c) phages as scaffolding material for the immobilization of functional molecules [135].

Nanduri et al. developed a real-time biosensor, which was based on the layer of phage 1G40 immobilized on the gold surface of an SPR chip via physical adsorption. The detection of beta-galactosidase was possible due to the specificity of filamentous bacteriophage to this model antigen [136]. In the same year, they examined an SPR immunosensor for the identification of L. monocytogenes. Bacteriophage Lm P4:A8, which expressed a single-chain variable fragment antibody against transmembrane protein exposed on the bacterial surface, was immobilized on the chip due to physical adsorption. Low detection limits were achieved, and the whole process was effective and simple, as it did not require additional reagents or complex chemistry [137]. Karoonuthaisiri et al. used filamentous phage M13, which expressed 12-mer peptides for the detection of *Salomonella* [138]. Naidoo et al. studied a similar approach, and they used immobilized phages T4 and P22 for bacterial detection. Nevertheless, the adsorption to the surface was highly heterogeneous due to the phage clustering at higher surface densities, which ultimately limited the ability to capture the target [139].

Unluckily, phage display is a laborious and time-consuming technique requiring skilled researchers and additional equipment. Therefore, phage-based layers used in SPR immunosensors are not common and well-studied yet. However, their simplicity, robustness, rigidness, and stability make them a valuable and promising approach. However, there is a phage for each bacteria. Thus, bacteriophages are a cheap alternative to antibodies. Nonetheless, an attractive aspect is the possibility of using phages in the current development of immunosensors. Phage displays are gaining popularity as tools for the selection of synthetic antibodies or for screening antibody-biomarker interactions for both therapeutic applications and immunosensing [140,141].

3.3. Biotin—(Strept)Avidin Affinity

Biotin (Bt), also known as vitamin H, is a tiny water soluble molecule produced by many prokaryotic organisms and plants [142]. Biotin/avidin or biotin/streptavidin interlinkage is a non-covalent method of substrate immobilization to the chip surface with a high affinity. Biotinylation—attachment of the biotin to a protein, such as an antibody—can be done both in vivo and in vitro [143]. Biotinylation in vivo is accomplished at the genetic level by fusing the gene encoding the protein of interest to the gene-coding biotin, i.e., the desired fusion tag. This phenomenon uses microbial vectors and tools of genetic engineering. Tagging in vitro can be obtained through the usage of chemical reagents or enzymes, such as biotin ligase from *E. coli* [144]. Streptavidin (Sa) and avidin (Av) are thermostable homotetramers that bind molecules of biotin with $K_d \sim 10^{-14}$ M (streptavidin) and $K_d \sim 10^{-15}$ M (avidin). The first one is derived from *Streptomyces avidinii*. It is resistant to a high pH and is intransigent to degradation when exposed to enzymes and denaturing agents. Avidin is extracted from the oviparous vertebrates' eggs. The non-covalent interaction between biotin and these proteins is of great strength and specificity. It is approximately 10^3 to 10^6 times greater than antigen–antibody binding [145,146]. As avidin possess additional carbohydrate moieties—three N-acetyl glucosamine residues and four mannose in each unit—its pI is higher, resulting in a positive charge of the physiological pH, which causes a non-specific binding to the surfaces and molecules of the negative electrical charge, even though its interaction with biotin is the strongest biological binding ever described [147,148]. The immobilization of the protein of interest on the chip surface through the biotin/(strept)avidin interaction is simpler in comparison to covalent coupling [149], and (strept)avidin-coated sensor chips are commercially available (Biacore, Reichert Technologies, XanTec, Sofchip).

Dutra et al. used a carboxymethyldextran-modified gold chip covered with covalently coupled streptavidin forming a monolayer for the attachment of biotin-tagged anti-troponin T monoclonal antibodies. An immobilized layer together with an SPR apparatus served as an immunosensor for human cardiac troponin T. This method enables identification in real-time, with a detection limit around 0.01 ng/mL, which is comparable to ELISA methods [150]. There are many other approaches where biotin/streptavidin interactions

were used together with SPR to form an immunosensor for the detection of moieties of biological origin or for studying the interplays between them, e.g., markers [151], heparin [152], hormones [153], and viruses [154,155]. An example of a hybrid architecture combining the use of oligo(ethylene glycol) methyl ether methacrylate backfilling and affinity-based immobilization via avidin-biotin interaction is the SPR biosensor described by Parrillo et al. The employment of a thick polymer brush reduced non-specific adsorption, thus enabling analysis of blood plasma. At the same time, the biotin tag, which has been easily introduced by alkyne-azide cycloaddition, opened the way to the fast and effective anchoring of labelled immunoreceptors (Figure 7) [90].

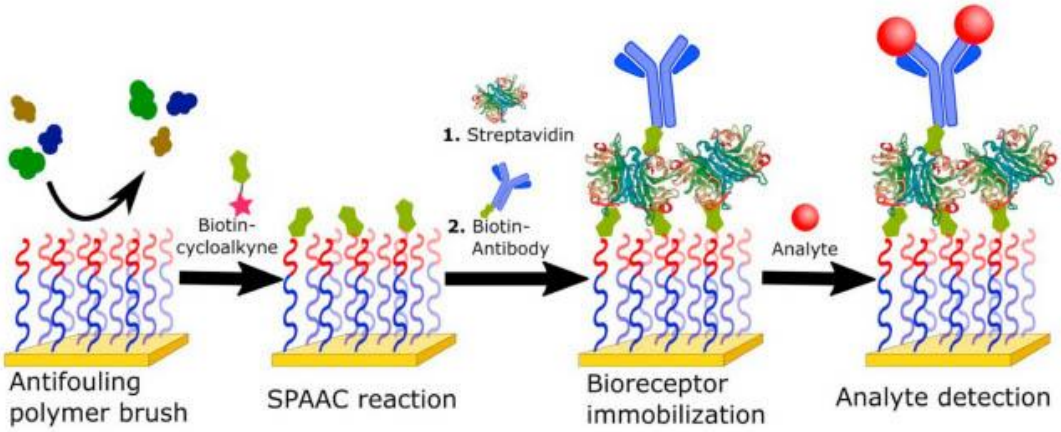

Figure 7. Schematic of a hybrid, multilayer SPR substrate composed of an antifouling polymer brush and biotin-captured streptavidin for the immobilization of biotinylated antibody. Adapted with permission from Parrillo et al. [90] (Copyright © (2017) Elsevier).

Beyond receptor immobilization, biotin/streptavidin interactions are also used to increase SPR signals [156–159]. Usually, the use of a dextran matrix results in its enhancement, but it does not affect the improvement of the sensitivity. Thus, analytes of a low molecular mass become undetectable. Pei et al. checked that the biotinylated protein-streptavidin complex is massive enough to amplify the response signal, inducing a boost of the detection sensitivity. In their studies, human immunoglobulins were detected at a level of 5 ng/mL [158].

In 2020, Sun et al. proposed another strategy, using biotin/streptavidin interlinkage to enhance the SPR signal. They applied "one-pot"-prepared bioconjugates of streptavidin-tagged antibodies and biotin-labeled phenylalanine nanoparticles. They prepared biotinylated phenylalanine monomers, which, in mild conditions, were able to self-assemble into nanoparticles. Subsequently, these nanoparticles were used as transporters of the complexes of antibodies tagged with streptavidin due to the strong biotin/SA interaction. Because of the high molecular weight of the conjugates, the SPR signal was amplified. Prostate-specific antigens were used to determine goal concentrations as low as 1 pg/mL [160].

Due to the high binding affinity of biotin and streptavidin, the process of their dissociation is extremely difficult. Consequently, reusing streptavidin-modified surfaces is practically unachievable. Li et al. described a new approach that enables the reuse of a streptavidin-coated SPR biosensor chip. They tagged an antibody against mature bovine prion protein with a nano-tag and streptavidin-binding protein (SBP) [161]. A nano-tag is a dozen amino acids of long protein that possess a constant dissociation below 17 nM while binding to streptavidin [162]. SBP is a 38 amino acid tag of K_d ~2.5 nM, which

can be eluted natively with biotin, enabling conditions for the purification of the proteins [163]. As both proteins have a weaker capacity of the streptavidin attachment, but they remain highly specific, it is possible to perform repeatable regenerations with a diluted NaOH solution, without losing the activity of the chip [161]. Another approach utilizes captavidin—a derivative of avidin that possess nitrated tyrosine in the site-binding biotin. While the specificity of the interaction remains the same, this modification enables the easy dissociation of the complex at pH 10.0. Garcia-Aljaro et al. showed that captavidin can be immobilized on the surface of the SPR sensor chip and then effectively take up to nine serial capturing and regeneration steps [148]. Regenerable (strept)avidin has become of great interest, and nowadays, researchers are discovering new mutants for the best combination of the properties, such as a high binding capacity, low level of nonspecific adsorption, and good stability [164].

The attachment of the biotin molecule to antibodies typically requires a separate, in vitro reaction, with the use of previously purified immunoglobulin. Despite this complication, the unmatched robustness of this interaction, as well as the multivalence of the avidin molecule (containing four binding sites), opens up many possibilities of using both simple (Av-modified surface + biotinylated receptor) and sandwich formats (Bt-modified surface + regenerable avidin + biotinylated receptor—see Figure 7). As shown above, a particularly interesting trend increasing the suitability of the platform for future SPR-based diagnostic applications is the use of an Av-Bt interaction, in combination with other solutions, with the aim of improving the performance parameters of immunosensors, including site-oriented immobilization, fouling-resistant layers, and SPR sensitivity enhancement.

3.4. DNA- and Antibody Directed Immobilization

Along with the development of automation and the progressive miniaturization of plasmonic sensors, new aspects have been playing an increasingly important role in recent years. The possibility of the fabrication of universal and fully regenerable receptor layers seems to be at the forefront. This idea allows the difficulties related to the sensitivity of the immunoreceptor layer to—often harsh—conditions required to destroy the antibody-antigen interaction to be overcome. In such a case, an attractive alternative to regeneration is the removal of the entire receptor layer and its reconstruction with the use of rapid and controllable methods of molecular self-assembly, such as "click biology". Beyond the already mentioned regenerable avidin, this strategy can be also accomplished by means of DNA- and antibody-directed immobilization [165].

Immobilization of the proteins through DNA was first described in the early 1990s. Due to the large-scale production and physicochemical stability of this molecule, and therefore its easy storage and widespread usage, DNA has become of interest in relation to site-directed immobilization on solid supports. This nucleic acid does not affect the biological activity of the protein, and the process of the conjugation requires mild conditions. Moreover, DNA is a great anchor, because it behaves like a rigid elastic rod in hydrated ionic liquids [165,166]. Oligonucleotides carrying thiol groups can be simply attached to the gold surface of an SPR chip, and then Watson-Crick base pairing enables the hybridization of a complimentary oligonucleotide, resulting in the immobilization of the DNA-tagged protein of interest. The main advantages of DNA-directed immobilization (DDI) are its specificity, stability, effortlessness, versatility, high surface coating density, and the possibility of regeneration via a simple denaturation protocol [165].

In 2004, Ladd et al. constructed an SPR biosensor with a functionalized surface for multichannel detection. The self-assembled monolayer of oligoethylene glycol and biotinylated alkanethiol on the gold chip enabled the coupling of single-stranded DNA through a streptavidin bridge. The DNA-tagged antibody against human chorionic gonadotropin (hCG) was immobilized on the surface by a hybridization process [167]. Four years later, they used a similar approach for the simultaneous detection of the DNA and proteins in the probe. Instead of additionally using a biotin-streptavidin bridge, thiolated oligos were used for micro-spotting. The biosensor consisted of eighteen spots for the identification of

four different DNA sequences and for two proteins: human chorionic gonadotropin (hCG) and follicle stimulating hormone (FSH). For the detection of hormones, conjugates of an appropriate antibody and complimentary DNA were used [168]. Bombera et al. designed and constructed a DNA-DNA-antibody SPR biochip for real-time cell sorting. Using the same device, it was possible to investigate both molecular and cellular interactions. Anti-CD19 and anti-CD90 IgGs were chosen for capturing B and T lymphocytes, respectively. The utilization of restriction endonucleases enabled the enzymatic cleavage of DNA-protein conjugates, resulting in the monitored release of the cells [169]. Leroy et al. examined an analogous approach to DDI for cell sorting. Additionally, a sensor chip was assembled in a microfluidic device, which was integrated with SPRi. Targeted release was possible due to the laser-induced heating [170]. Piliarik et al. has described the SPR immunosensor exploiting site-selective DNA-directed immobilization of antibodies against human chorionic gonadotropin (hCG) and activated leukocyte cell adhesion molecule (ALCAM), as biomarkers abundant in blood plasma [171]. DNA conjugates of low-molecular-weight antigens were also employed in the construction of SPR biosensors in a competitive format, as in the case of the immunosensor described by Tort et al., where a steroid–oligonucleotide conjugates line was used as recognition elements [172].

A similar system based on antibody-directed immobilization (ADI), which offers the rapid regeneration of the receptor layer dependent on the reversible antibody–antigen interaction was described by Kim et al. The developed immunoreceptor layer for the real-time monitoring of biomarkers involves the Ca^{2+} ion-dependent binding of the calcium-binding protein (CBP) conjugate and a monoclonal antibody specific to creatine kinase-MB. The Ca^{2+}-switchable capturing of CBP by an auxiliary, surface-tethered antibody enabled the facile and reversible control of the engagement and disengagement of the captured antibody conjugate on the SPR chip surface. This approach does not require the use of harsh conditions during the regeneration step and thus preserves the long-term viability of the receptor layer. The authors provide an universal system based on the exchangeable capture antibody for semi-continuous immunosensing [173]. Another example of antibody-directed immobilization is the use of *anti*-his-tag antibodies. Such versatile immunosurfaces show the ability to bind a wide range of recombinant proteins and antibodies, while offering the simplicity of their replacement by means of conventional regeneration methods known from antibody–antigen interactions. This solution is currently used in the SPR screening of new variants of polyhistidine-tagged scFvs [174]. However, in the near future, it will also be possible to implement it for immunosensing. The selected formats and applications of DDI and ADI in plasmonic immunosensing are shown in Figure 8.

The prospect of creating multiplex immunoassays is of exceptional value, as the conventional fabrication of arrays for the detection of dissimilar proteins requires different chemistries of the surface. The greatest challenge of DDI that has to be faced is to find the method of oligo-protein conjugation that possess a high efficiency and, subsequently, has a simple and rapid purification. Additionally, the coupling of multiple DNA strands to a single protein is unlikely to be avoided. Thus, the technique for obtaining the highest yields from mono-conjugated products is costly. In recent years, "click" reaction copper-free alkyneeazide cycloaddition using cyclooctyne (DBCO) reagents turned out to be a promising alternative to the classic carbodiimide and maleimide coupling in the biofunctionalization of protein receptors using various components and tags (including ssDNA) [90,175,176]. Together with the dedicated systems of chromatographic purification, this enabled the popularization of DNA-protein conjugates in the construction of immunoarrays and their use in commercial systems for studying intermolecular interactions [177,178].

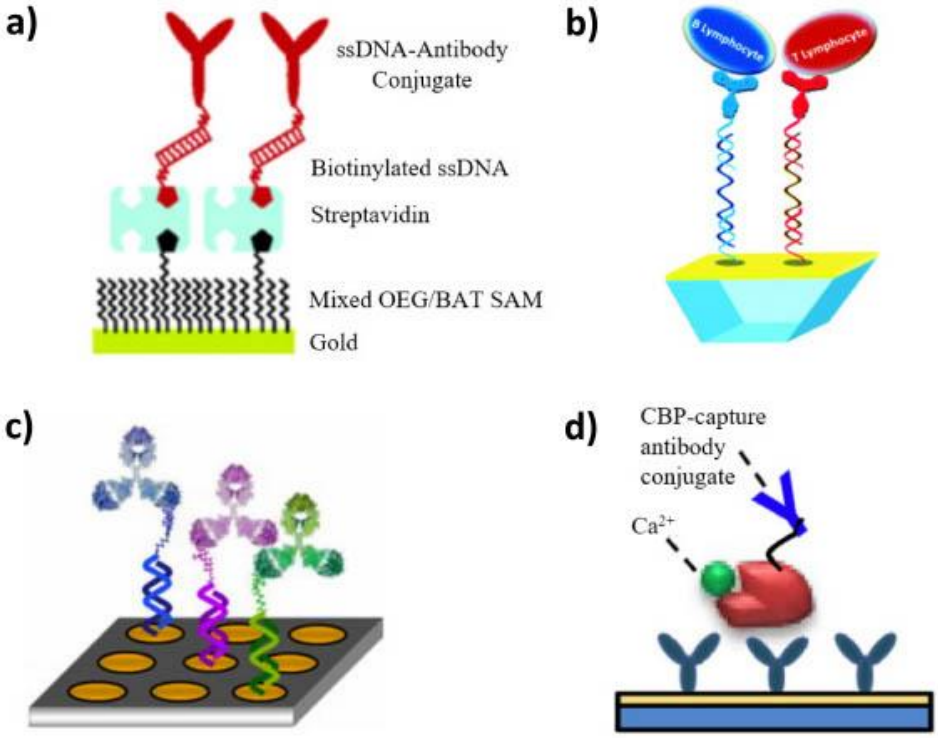

Figure 8. Various concepts of DNA-directed immobilization in the construction of SPR immunosensors: (**a**) immunosensor based on DNA anchoring via Av-Bt affinity, (**b**) direct SPRi assay for the detection of lymphocytes, employing DNA hybridization in sandwich-like format, (**c**) competitive SPRi immunoassay with the use of DNA-steroid conjugates, (**d**) immunosensor using Ca^{2+}-dependent antibody-directed immobilization. Adapted with permission from Ladd et al. [167] (Copyright © (2004) American Chemical Society), Leroy et al. [170] (Copyright © (2004) Royal Society of Chemistry), Tort et al. [172] (Copyright © (2012) American Chemical Society), and Kim et al. [173] (Copyright © (2017) Elsevier).

3.5. Bivalent Ion-Mediated Chelation of His-Tagged Receptors

Affinity tags have multiple advantages, such as having mild conditions for capturing, the capacity for site-directed immobilization, low price (usually), and the possibility of regeneration the chip. At the same time, they require the use of genetic engineering techniques. Apart from the use of substrates functionalized with super-antigenic proteins (proteins A, G, and A/G), another approach adapted from the methods of protein purification is immobilization with the use of a polyhistidine tag through bivalent ion-nitrilotriacetic acid (NTA) complexes [179]. This pathway is particularly convenient in the case of designing immunosensors in a competitive format, where recombinant proteins or synthetic oligopeptides are involved in the receptor layer. Importantly, when the receptor/analyte-binding mechanism is well known, it is also possible to design and deliberately insert a his-tag into such a region of the receptor, which will facilitate the process of oriented immobilization, without negatively affecting the binding sites [180].

Kimple et al. studied the protein–protein interactions in heterotrimeric G-protein biology using a His6 fusion tag for direct nonrandom immobilization [181]. Fischer et al. compared the attachment of a substrate-binding protein (SiaP) to the NTA surface of the sensor chip via C-terminal hexa-histidine (His), N-terminal deca-His, and N-terminal double-His

tags. SiaP derived from *H. influenzae* possess a high affinity to N-acetylneuraminic acid, which is a metabolic marker during the progression of coronary artery disease [182]. The hexa-His tagged protein could not be stably anchored even at low flow rates and a low concentration of the protein, and the immobilization of highly concentrated deca-His tagged SiaP resulted in a baseline drift. The double-His tagged approach was preferred, as it provided a reliable baseline and prompt regeneration of the chip [183]. Chu et al. tagged the protein, CXCR5 (chemokine receptor), with 6xHis and an HPC4 tandem tag for the facilitation of both the purification of the protein and its immobilization on the chip. HPC4 is a 12 amino acid sequence, which encodes some of the residues of the protein C heavy chain. A monoclonal antibody kinetics assay was performed, and this peptide-based binding assay was further applied for the capture of virus-like particles [184].

Due to the non-covalent and reversible mechanism of Ni^{2+}-dependent complexation (high K_D values in physiological media), the disadvantage of this approach is the gradual dissociation of the receptor from the surface. An important improvement in the Ni^{2+}-NTA-based immobilization of recombinant proteins was proposed by Wang et al. An additional step of the covalent affixation of bioreceptors with carboxymethyldextran-NTA residues via EDC/NHS coupling prevented the gradual degradation of the layer, while maintaining the homogeneous receptor orientation, which is determined by the previous chelation of His-tag-terminated sites. Thanks to this, it was possible to combine the advantages of covalent immobilization with the possibility of using a pre-concentration of tagged ligands on the surface and maintaining control over their orientation. This enables the construction of a competitive SPR biosensor for studying the interaction of non-small-cell lung cancer biomarker t-DARRP with a specific antibody [185]. To improve the stability of the receptor immobilization using the His-tag—in particular, the resistance to desorption in plasma samples—the Lammertyn and Vanhoorelbecke group proposed the chelation of the protein antigen on the fiber optic SPR sensor surface using Co^{3+}, instead of Ni^{2+}. The superiority of the Co^{3+}-dependent His-tagged receptor chelation, relative to Ni^{2+}, in terms of a better stability and sensitivity, was confirmed for the detection of autoantibodies, as a marker of autoimmunological disease [186]. In turn, the reversible, Co^{2+}-dependent chelation of recombinant, His_6-tagged single-chain variable fragments of *anti*-SARS receptor-binding domain (RBD) antibodies were used in the construction of a fiber-optic SPR biosensor. The authors confirmed the full reusability of the sensor probes on NTA media using various types of His-tagged bioreceptors, including recombinant antibody fragments and antigens [187]. Both Co-dependent mechanisms of the attachment of the His-tagged proteins are depicted in Figure 9.

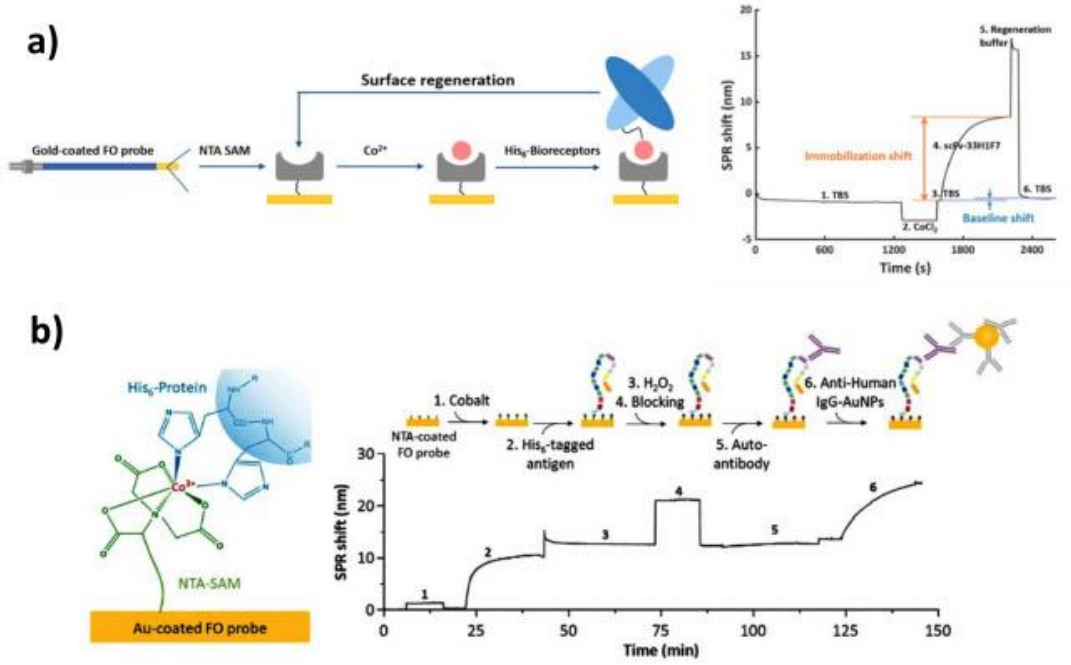

Figure 9. The application of cobalt ion-nitrilotriacetic acid complexes in SPR substrates for the immobilization of recombinant proteins. (**a**) Easily regenerable immobilization with a Co^{2+} ion, (**b**) robust chelation with a Co^{3+} ion. Adapted with permission from Qu et al. [187] (under the terms and conditions of the Creative Commons CC BY License) and Horta et al. [186] (Copyright © (2020) American Chemical Society).

3.6. Other Affinity-Based Methods for the Attachment of Recombinant Receptors

Recent trends in immunoreceptor engineering cover the development of receptors characterized by well-defined kinetic parameters [188,189]. The wide capabilities of the SPR and SPRi platforms would be fully exhibited in the case of their adaptation to biosensors operating in a continuous or *semi*-continuous mode. The monitoring of the concentrations of clinically relevant analytes, without the need for periodic receptor layer regeneration, requires the use of receptors characterized by fast association and dissociation kinetics (k_a and k_d) and thus a relatively low affinity (high equilibrium constant K_D, expressed as k_d/k_a). Classic methods of the selection and production of antibodies do not offer the possibility of the isolation of such receptors. However, the progress in the development and isolation of recombinant antibodies and their fragments open up completely new possibilities for the construction of SPR immunosensors capable of working in the real-time and continuous modes. In the case of the availability of sufficiently high-quality receptor-transducer interphases, *semi*-continuous immunosensing can be successfully introduced into routine medical and companion diagnostics [190]. It is worth emphasizing that for applications in *semi*-continuous plasmonic biosensors, fast and spatially resolved immobilization methodologies are desirable. They should enable the quick patterning of immunoreceptor arrays, as well as refreshing them through a simple exchange of the receptor layer. For this reason, site-oriented immobilization, which is based on affinity interactions (in particular, "chick chemistry" and "click biology"), seem to be ideally suited both to the needs of modern and flexible SPR and SPRi platforms for rapid screening, as well as the monitoring of clinically relevant analytes [191].

To increase the intrinsic affinity of antibody fragments to a bare gold surface, it is possible to fuse scFs fragments with gold-binding polypeptides by genetic engineering. Such a construct shows a rapid and oriented immobilization ability on the chip surface through an Au-S bond formation. Zhou et al. described recombinant hybrid fragments of anti-CFP-10 antibodies with histidine$_6$-tagged gold-binding protein (6His-GBP) in an SPR immunosensor for the detection of *Mycobacterium tuberculosis*. Owing to the controlled orientation of the bioreceptor and the proximity of the Au surface, as well as the use of gold-magnetic nanoparticles, a significant amplification of the signal was noticed [192]. Ha et al. developed an SPR-based immunoarray, where antibodies (human IgGs) were immobilized on the glutathione-modified gold chip surface, which was covered with immunoglobulin-binding domains tagged with glutathione S-transferase (GST). The potential of GST-tagged proteins, as anchors for the site-directed immobilization of antibodies, was compared with the conventional covalent coupling method. It turned out that the SPR response of immobilized IgGs, as well as the capability of binding with the antigen, was greatly enhanced in the case of the first method [193]. Binding via a his-tag-NTA is less specific than via a GST-tag, but it is cheaper and broadly available [194]. While immobilization via tags is not a newly discovered approach in protein anchoring, its fusion with antibodies, such as nano- or affibody, or the use of brand-new affinity tags is a cutting edge. In 2020, Boonen et al. developed an SPR immunoassay for the investigation of interactions between chemokine receptor CXCR4 and a nanobody fused with an Fc fragment. This chemokine receptor is highly expressed in numerous types of tumor cells. These cells hijack its pathway, which enables the metastasis of the tumor in distinct sites of the organs. CXCR4 was tagged with a C-terminal histidine$_{10}$ and successfully immobilized on a nitrilotriacetic acid sensor chip, which enabled the detection of nanobodies in the sample. The immobilized particles were stable and active for at least 12 h, the acquired kinetic data were reliable, and the surface was susceptible to removal during regeneration [194]. In 2017, Hussack et al. developed an antibody screening assay through SPR analyses. They used a new camelid-derived affinity tag, called ABTAG, which captures bovine serum albumin with a picomolar binding affinity. The immunization of llamas with carcinoembryonic antigen-related cell adhesion molecule 6 (CEACAM6) resulted in the production of heavy chain antibodies and then their use as a template for phage-displayed single-domain antibodies (sdAbs) against this protein. After panning (affinity selection technique in phage display), the expressed sdAbs were fused with ABTAG. Anti-CEACAM6-ABTAG conjugates were bound to the surface covered with BSA. The binding of the antigen to the complex enabled the determination of kinetic and affinity constants, as well as the read-out of the fusion protein expression level [195]. Examples of other promising receptors for applications in modern SPR immunosensing cover, e.g., recombinant antibodies and antibody fragments (polyhistidine-tagged scFvs [174], Fc-tagged scFvs [196], camelidae IgG-like molecules [197], nanobody-Fc (Nb-Fc) ligands [194], Fc-tagged chimeric proteins [198]), and mediating proteins (affinity-engineered staphylococcal Protein A and protein A fused with a gold-binding peptide [199]).

4. Conclusions

SPR and other plasmonic immunosensors in medical diagnostics are typically compared to other immunodetection methods. Biosensors with an SPR readout, as flagship representatives of label-free techniques, offer advantages in terms of detection time and simplicity in relation to methods employing enzyme immunolabeling, e.g., ELISA assays. Despite decades of SPR use in the detection of clinically relevant bioanalytes in real samples, the development of functional transducer-receptor interphases is still one of the main directions in the development of plasmonic immunosensors. Meanwhile, antibodies, as elements capable of the specific recognition of bioanalytes in complex samples, are still the gold standard.

The main research topics outlined in this review are focused on the development of high-quality immunoreceptor layers. They should guarantee an appropriate efficiency in

the immobilization of protein receptors, optimal spatial orientation, good sensitivity to changes in the local refractive index, and minimization of the effects associated with the non-specific adsorption from samples like body fluids. Since both the design of intermediate layers and the method of immobilizing biological receptors play an important role in achieving the abovementioned objectives, a thorough description of the recent and most exploited approaches in the field has been provided. This paper introduces and classifies approaches to the design of immunosensing platforms with the use of both random and site-oriented immobilization strategies. Additionally, hybrid methodologies—although difficult to clearly classify—were presented in this review. They usually combine the advantages of 3D substrates with site-oriented immobilization and the introduction of agents, ensuring ultra-low nonspecific binding capacity. Such versatile platforms turned out to be the most promising from the point of view of their feasibility in the field of medical diagnostics.

The continuous development of immunoreceptors is aimed at improving their affinity and compatibility with typical transducers. Antibodies characterized by ultra-fast kinetics of interaction with a target molecule, as well as the implementation of recombinant proteins as recognition elements, also opens up new possibilities for SPR immunosensors. The current trends, focused on the miniaturization and multiplexing of SPR platforms, as well as on the possibility of working in a (semi)continuous mode, pose new challenges in terms of the robustness and versatility of the design of sensor substrates. This results in the development of novel strategies, such as the fabrication of easily designable and regenerable layers via affinity-directed immobilization or the immobilization of recombinant, tagged receptors. Therefore, in the coming years, a great deal of scientific effort will be focused on the improvement of current and the design of new types of plasmon-based immunosensors. The constant pursuit of adapting SPR interphases to the possibilities offered by new receptors, like recombinant proteins and antibody fragments, aims to meet the requirements of modern medical diagnostics.

Author Contributions: Conceptualization, M.D. and S.K.; writing—original draft preparation, M.D. and S.K.; writing—review and editing, E.M., S.K., and M.D.; visualization, M.D. and S.K., formal analysis, E.M.; supervision, E.M.; funding acquisition, E.M. All authors have read and agreed to the published version of the manuscript.

Funding: This work has been supported by the Warsaw University of Technology. We would like to acknowledge the financial support from the Ministry of Education and Science, Poland, grant number 7015/IA/SP/2019.

Institutional Review Board Statement: Not applicable.

Informed Consent Statement: Not applicable.

Data Availability Statement: Not applicable.

Conflicts of Interest: The authors declare no conflict of interest.

Abbreviations

Ab	antibody
ADI	antibody-directed immobilization
ALCAM	activated leukocyte cell adhesion molecule
APTES	(3-aminopropyl)triethoxysilane
Av	avidin
Bt	biotin
CBP	calcium-binding protein
CEA	carcinoembryonic antigen
CEACAM6	carcinoembryonic antigen-related cell adhesion molecule 6
CFP	culture filtrate protein
CMD/CM5	carboxymethyldextran
DDI	DNA-directed immobilization

DSP	disuccinimido dithiobispropionate
DTC	dithiocarbamate
EDC	N-(3-dimethylaminopropyl)-N′-ethylcarbodiimide hydrochloride
EOT	extraordinary optical transmission
EPC	ethylphosphocholine
Fab	antigen-binding fragments
Fc	fragment crystallizable
FSH	follicle-stimulating hormone
GBP	gold-binding peptide
GO	graphene oxide
GST	glutathione S-transferase
HA	hyaluronic acid
HSA	human serum albumin
hCG	human chorionic gonadotropin
HEGD	hexa(ethylene glycol) dithiol
His	histidine
LSPR	localized surface resonance
MBA	mercaptophenylboronic acid
MeOEGMA	poly[oligo(ethylene glycol) methyl ether] methacrylate
MHDA	mercaptohexadecanoic acid
MPA	mercaptopropionic acid
MUA	mercaptoundecanoic acid
Nb	nanobody
NHS	N-hydroxysuccinimide
NT	nitrotyrosine
NTA	nitrilotriacetic acid
OTA	ochratoxin A
PAG	protein A gold-binding domain
PAMAM	poly(amidoamine)
PDDA	poly(diallyldimethylammonium chloride)
pHEMA	poly(2-hydroxyethyl methacrylate)
PNIPAAM	poly(N-isopropylacrylamide)
RBD	receptor-binding domain
RI	refractive index
Sa	streptavidin
SAM	self-assembled monolayer
SBP	streptavidin-binding protein
scFv	single-chain fragment variable
sdAbs	single-domain antibodies
SiaP	sialic acid-binding periplasmic protein
SMCC	succinimidyl 4-(N-maleimidomethyl)cyclohexane-1-carboxylate
THFMA	tetrahydrofurfuryl methacrylate
TVC	1,2,4-trivinylcyclohexane

References

1. Choi, J.H.; Lee, J.H.; Son, J.; Choi, J.W. Noble Metal-Assisted Surface Plasmon Resonance Immunosensors. *Sensors* **2020**, *20*, 1003. [CrossRef]
2. Homola, J. Surface Plasmon Resonance Sensors for Detection of Chemical and Biological Species. *Chem. Rev.* **2008**, *108*, 462–493. [CrossRef]
3. Nguyen, H.; Park, J.; Kang, S.; Kim, M. Surface Plasmon Resonance: A Versatile Technique for Biosensor Applications. *Sensors* **2015**, *15*, 10481–10510. [CrossRef] [PubMed]
4. Su, Y.-W.; Wang, W. Surface Plasmon Resonance Sensing: From Purified Biomolecules to Intact Cells. *Anal. Bioanal. Chem.* **2018**, *410*, 3943–3951. [CrossRef] [PubMed]
5. Qu, J.H.; Dillen, A.; Saeys, W.; Lammertyn, J.; Spasic, D. Advancements in SPR Biosensing Technology: An Overview of Recent Trends in Smart Layers Design, Multiplexing Concepts, Continuous Monitoring and In Vivo Sensing. *Anal. Chim. Acta* **2020**, *1104*, 10–27. [CrossRef] [PubMed]
6. Falkowski, P.; Lukaszewski, Z.; Gorodkiewicz, E. Potential of Surface Plasmon Resonance Biosensors in Cancer Detection. *J. Pharm. Biomed. Anal.* **2021**, *194*, 113802. [CrossRef] [PubMed]

7. Keshavarz, M.; Kassanos, P.; Tan, B.; Venkatakrishnan, K. Metal-Oxide Surface-Enhanced Raman Biosensor Template towards Point-of-Care EGFR Detection and Cancer Diagnostics. *Nanoscale Horiz.* **2020**, *5*, 294–307. [CrossRef]
8. Keshavarz, M.; Rezaul Haque Chowdhury, A.K.M.; Kassanos, P.; Tan, B.; Venkatakrishnan, K. Self-Assembled N-Doped Q-Dot Carbon Nanostructures as a SERS-Active Biosensor with Selective Therapeutic Functionality. *Sens. Actuators B Chem.* **2020**, *323*, 128703. [CrossRef]
9. Raymundo-Pereira, P.A.; De Oliveira Pedro, R.; Carr, O.; Melendez, M.E.; Gobbi, A.L.; Helena De Oliveira Piazzetta, M.; Carvalho, A.L.; Reis, R.M.; Miranda, P.B.; Oliveira, O.N. Influence of the Molecular Orientation and Ionization of Self-Assembled Monolayers in Biosensors: Application to Genosensors of Prostate Cancer Antigen 3. *J. Phys. Chem. C* **2021**, *125*, 498–506. [CrossRef]
10. Soares, J.C.; Soares, A.C.; Pereira, P.A.R.; Rodrigues, V.D.C.; Shimizu, F.M.; Melendez, M.E.; Scapulatempo Neto, C.; Carvalho, A.L.; Leite, F.L.; Machado, S.A.S.; et al. Adsorption according to the Langmuir-Freundlich Model Is the Detection Mechanism of the Antigen p53 for Early Diagnosis of Cancer. *Phys. Chem. Chem. Phys.* **2016**, *18*, 8412–8418. [CrossRef]
11. Mariani, S.; Minunni, M. Surface Plasmon Resonance Applications in Clinical Analysis. *Anal. Bioanal. Chem.* **2014**, *406*, 2303–2323. [CrossRef]
12. Mauriz, E. Low-Fouling Substrates for Plasmonic Sensing of Circulating Biomarkers in Biological Fluids. *Biosensors* **2020**, *10*, 63. [CrossRef] [PubMed]
13. Masson, J.F. Surface Plasmon Resonance Clinical Biosensors for Medical Diagnostics. *ACS Sens.* **2017**, *2*, 16–30. [CrossRef]
14. Fattahi, Z.; Khosroushahi, A.Y.; Hasanzadeh, M. Recent Progress on Developing of Plasmon Biosensing of Tumor Biomarkers: Efficient Method towards Early Stage Recognition of Cancer. *Biomed. Pharmacother.* **2020**, *132*, 110850. [CrossRef]
15. Nangare, S.N.; Patil, P.O. Affinity-Based Nanoarchitectured Biotransducer for Sensitivity Enhancement of Surface Plasmon Resonance Sensors for In Vitro Diagnosis: A Review. *ACS Biomater. Sci. Eng.* **2021**, *7*, 2–30. [CrossRef]
16. Hassan, M.M.; Sium, F.S.; Islam, F.; Choudhury, S.M. Plasmonic Metamaterial Based Virus Detection System: A Review. *arXiv* **2020**, arXiv:2012.00551.
17. Petryayeva, E.; Krull, U.J. Localized Surface Plasmon Resonance: Nanostructures, Bioassays and Biosensing-A Review. *Anal. Chim. Acta* **2011**, *706*, 8–24. [CrossRef] [PubMed]
18. Lopez, G.A.; Estevez, M.C.; Soler, M.; Lechuga, L.M. Recent Advances in Nanoplasmonic Biosensors: Applications and Lab-on-a-Chip Integration. *Nanophotonics* **2017**, *6*, 123–136. [CrossRef]
19. Liu, Y.; Liu, Q.; Chen, S.; Cheng, F.; Wang, H.; Peng, W. Surface Plasmon Resonance Biosensor Based on Smart Phone Platforms. *Sci. Rep.* **2015**, *5*, 12864. [CrossRef]
20. Crivianu-Gaita, V.; Thompson, M. Aptamers, Antibody scFv, and Antibody Fab' Fragments: An Overview and Comparison of Three of the Most Versatile Biosensor Biorecognition Elements. *Biosens. Bioelectron.* **2016**, *85*, 32–45. [CrossRef]
21. Schroeder, H.W.; Cavacini, L. Structure and Function of Immunoglobulins. *J. Allergy Clin. Immunol.* **2010**, *125*, S41–S52. [CrossRef]
22. Lim, S.A.; Ahmed, M.U. CHAPTER 1: Introduction to Immunosensors. *RSC Detect. Sci.* **2019**, 1–20. [CrossRef]
23. Akbar, R.; Robert, P.A.; Pavlović, M.; Jeliazkov, J.R.; Snapkov, I.; Slabodkin, A.; Weber, C.R.; Scheffer, L.; Miho, E.; Haff, I.H.; et al. A Compact Vocabulary of Paratope-Epitope Interactions Enables Predictability of Antibody-Antigen Binding. *Cell Rep.* **2021**, *34*, 108856. [CrossRef]
24. Bedford, R.; Tiede, C.; Hughes, R.; Curd, A.; McPherson, M.J.; Peckham, M.; Tomlinson, D.C. Alternative Reagents to Antibodies in Imaging Applications. *Biophys. Rev.* **2017**, *9*, 299–308. [CrossRef] [PubMed]
25. König, J.; Hust, M.; van den Heuvel, J. Validation of the Production of Antibodies in Different Formats in the HEK 293 Transient Gene Expression System. *Methods Mol. Biol.* **2021**. [CrossRef]
26. Alfaleh, M.A.; Alsaab, H.O.; Mahmoud, A.B.; Alkayyal, A.A.; Jones, M.L.; Mahler, S.M.; Hashem, A.M. Phage Display Derived Monoclonal Antibodies: From Bench to Bedside. *Front. Immunol.* **2020**, *11*, 1986. [CrossRef] [PubMed]
27. Listek, M.; Hönow, A.; Gossen, M.; Hanack, K. A Novel Selection Strategy for Antibody Producing Hybridoma Cells Based on a New Transgenic Fusion Cell Line. *Sci. Rep.* **2020**, *10*, 1664. [CrossRef]
28. Ahmad, Z.A.; Yeap, S.K.; Ali, A.M.; Ho, W.Y.; Alitheen, N.B.M.; Hamid, M. ScFv Antibody: Principles and Clinical Application. *J. Immunol. Res.* **2012**, 980250. [CrossRef]
29. Zhao, L.; Wu, Q.; Song, R.; Yun, Z. Genetic Engineering Antibody: Principles and Application. *IOP Conf. Ser. Mater. Sci. Eng.* **2019**, *612*, 022045. [CrossRef]
30. Tans, R.; van Rijswijck, D.M.H.; Davidson, A.; Hannam, R.; Ricketts, B.; Tack, C.J.; Wessels, H.J.C.T.; Gloerich, J.; van Gool, A.J. Affimers as an Alternative to Antibodies for Protein Biomarker Enrichment. *Protein Expr. Purif.* **2020**, *174*, 105667. [CrossRef] [PubMed]
31. Yang, E.Y.; Shah, K. Nanobodies: Next Generation of Cancer Diagnostics and Therapeutics. *Front. Oncol.* **2020**, *10*, 1182. [CrossRef]
32. Sun, L.; Wu, L.; Zhao, Q. Aptamer Based Surface Plasmon Resonance Sensor for Aflatoxin B1. *Microchim. Acta* **2017**, *184*, 2605–2610. [CrossRef]
33. Gorodkiewicz, E.; Lukaszewski, Z. Recent Progress in Surface Plasmon Resonance Biosensors (2016 to Mid-2018). *Biosensors* **2018**, *8*, 132. [CrossRef] [PubMed]
34. Guo, L.; Jackman, J.A.; Yang, H.H.; Chen, P.; Cho, N.J.; Kim, D.H. Strategies for Enhancing the Sensitivity of Plasmonic Nanosensors. *Nano Today* **2015**, *10*, 213–239. [CrossRef]
35. Hinman, S.S.; McKeating, K.S.; Cheng, Q. Surface Plasmon Resonance: Material and Interface Design for Universal Accessibility. *Anal. Chem.* **2018**, *90*, 19–39. [CrossRef]

36. Scarano, S.; Mascini, M.; Turner, A.P.F.; Minunni, M. Surface Plasmon Resonance Imaging for Affinity-Based Biosensors. *Biosens. Bioelectron.* **2010**, *25*, 957–966. [CrossRef]
37. Crivianu-Gaita, V.; Thompson, M. Immobilization of Fab' Fragments onto Substrate Surfaces: A Survey of Methods and Applications. *Biosens. Bioelectron.* **2015**, *70*, 167–180. [CrossRef]
38. Mai, Z.; Zhang, J.; Chen, Y.; Wang, J.; Hong, X.; Su, Q.; Li, X. A Disposable Fiber Optic SPR Probe for Immunoassay. *Biosens. Bioelectron.* **2019**, *144*, 111621. [CrossRef]
39. Vashist, S.K.; Lam, E.; Hrapovic, S.; Male, K.B.; Luong, J.H.T. Immobilization of Antibodies and Enzymes on 3-Aminopropyltriethoxysilane-Functionalized Bioanalytical Platforms for Biosensors and Diagnostics. *Chem. Rev.* **2014**, *114*, 11083–11130. [CrossRef]
40. Kim, H.-S.; Jung, S.-H.; Kim, S.-H.; Suh, I.-B.; Kim, W.J.; Jung, J.-W.; Yuk, J.S.; Kim, Y.-M.; Ha, K.-S. High-Throughput Analysis of Mumps Virus and the Virus-Specific Monoclonal Antibody on the Arrays of a Cationic Polyelectrolyte with a Spectral SPR Biosensor. *Proteomics* **2006**, *6*, 6426–6432. [CrossRef]
41. Beketov, G.; Shynkarenko, O.; Apatska, M. Towards Improving ELISA Surfaces: SPR Assessment of Polystyrene Modification Efficiency for Promoting Immobilization of Biomolecules. *Anal. Biochem.* **2021**, *618*, 114101. [CrossRef]
42. Mauriz, E.; García-Fernández, M.C.; Lechuga, L.M. Towards the Design of Universal Immunosurfaces for SPR-Based Assays: A Review. *Trends Anal. Chem.* **2016**, *79*, 191–198. [CrossRef]
43. Ben Haddada, M.; Hu, D.; Salmain, M.; Zhang, L.; Peng, C.; Wang, Y.; Liedberg, B.; Boujday, S. Gold Nanoparticle-Based Localized Surface Plasmon Immunosensor for Staphylococcal Enterotoxin A (SEA) Detection. *Anal. Bioanal. Chem.* **2017**, *409*, 6227–6234. [CrossRef] [PubMed]
44. Matharu, Z.; Bandodkar, A.J.; Gupta, V.; Malhotra, B.D. Fundamentals and Application of Ordered Molecular Assemblies to Affinity Biosensing. *Chem. Soc. Rev.* **2012**, *41*, 1363–1402. [CrossRef] [PubMed]
45. Vericat, C.; Vela, M.E.; Benitez, G.; Carro, P.; Salvarezza, R.C. Self-Assembled Monolayers of Thiols and Dithiols on Gold: New Challenges for a Well-Known System. *Chem. Soc. Rev.* **2010**, *39*, 1805–1834. [CrossRef] [PubMed]
46. Uludag, Y.; Tothill, I.E. Cancer Biomarker Detection in Serum Samples Using Surface Plasmon Resonance and Quartz Crystal Microbalance Sensors with Nanoparticle Signal Amplification. *Anal. Chem.* **2012**, *84*, 5898–5904. [CrossRef]
47. Martinez-Perdiguero, J.; Retolaza, A.; Bujanda, L.; Merino, S. Surface Plasmon Resonance Immunoassay for the Detection of the TNFα Biomarker in Human Serum. *Talanta* **2014**, *119*, 492–497. [CrossRef] [PubMed]
48. Masdor, N.; Altintas, Z.; Tothill, I. Surface Plasmon Resonance Immunosensor for the Detection of *Campylobacter jejuni*. *Chemosensors* **2017**, *5*, 16. [CrossRef]
49. Jena, S.C.; Shrivastava, S.; Saxena, S.; Kumar, N.; Maiti, S.K.; Mishra, B.P.; Singh, R.K. Surface Plasmon Resonance Immunosensor for Label-Free Detection of BIRC5 Biomarker in Spontaneously Occurring Canine Mammary Tumours. *Sci. Rep.* **2019**, *9*, 1–12. [CrossRef] [PubMed]
50. Taheri, R.A.; Rezayan, A.H.; Rahimi, F.; Mohammadnejad, J.; Kamali, M. Evaluating the Potential of an Antibody against Recombinant OmpW Antigen in Detection of Vibrio Cholerae by Surface Plasmon Resonance (SPR) Biosensor. *Plasmonics* **2017**, *12*, 1493–1504. [CrossRef]
51. Bhadra, P.; Shajahan, M.S.; Bhattacharya, E.; Chadha, A. Studies on Varying N-Alkanethiol Chain Lengths on a Gold Coated Surface and Their Effect on Antibody-Antigen Binding Efficiency. *RSC Adv.* **2015**, *5*, 80480–80487. [CrossRef]
52. Zhu, Z.; Li, H.; Xiang, Y.; Koh, K.; Hu, X.; Chen, H. Pyridinium Porphyrins and AuNPs Mediated Bionetworks as SPR Signal Amplification Tags for the Ultrasensitive Assay of Brain Natriuretic Peptide. *Microchim. Acta* **2020**, *187*, 1–9. [CrossRef]
53. Castiello, F.R.; Tabrizian, M. Gold Nanoparticle Amplification Strategies for Multiplex SPRi-Based Immunosensing of Human Pancreatic Islet Hormones. *Analyst* **2019**, *144*, 2541–2549. [CrossRef] [PubMed]
54. Haes, A.J.; Chang, L.; Klein, W.L.; Van Duyne, R.P. Detection of a Biomarker for Alzheimer's Disease from Synthetic and Clinical Samples Using a Nanoscale Optical Biosensor. *J. Am. Chem. Soc.* **2005**, *127*, 2264–2271. [CrossRef] [PubMed]
55. Ołdak, Ł.; Sankiewicz, A.; Żelazowska-Rutkowska, B.; Cylwik, B.; Lukaszewski, Z.; Skoczylas, M.; Gorodkiewicz, E. Two SPRi Biosensors for the Determination of Cathepsin S in Blood Plasma. *Talanta* **2021**, *225*, 121900. [CrossRef]
56. Castiello, F.R.; Tabrizian, M. Multiplex Surface Plasmon Resonance Imaging-Based Biosensor for Human Pancreatic Islets Hormones Quantification. *Anal. Chem.* **2018**, *90*, 3132–3139. [CrossRef]
57. Reiner, A.T.; Fossati, S.; Dostalek, J. Biosensor Platform for Parallel Surface Plasmon-Enhanced Epifluorescence and Surface Plasmon Resonance Detection. *Sens. Actuators B Chem.* **2018**, *257*, 594–601. [CrossRef]
58. Yu, H.; Han, R.; Su, J.; Chen, H.; Li, D. Multi-Marker Diagnosis Method for Early Hepatocellular Carcinoma Based on Surface Plasmon Resonance. *Clin. Chim. Acta* **2020**, *502*, 9–14. [CrossRef] [PubMed]
59. Wang, B.; Park, B.; Chen, J.; He, X. Rapid and Label-Free Immunosensing of Shiga Toxin Subtypes with Surface Plasmon Resonance Imaging. *Toxins* **2020**, *12*, 280. [CrossRef]
60. Wang, G.; Wang, C.; Yang, R.; Liu, W.; Sun, S. A Sensitive and Stable Surface Plasmon Resonance Sensor Based on Monolayer Protected Silver Film. *Sensors* **2017**, *17*, 2777. [CrossRef] [PubMed]
61. Jing, W.; Wang, Y.; Yang, Y.; Wang, Y.; Ma, G.; Wang, S.; Tao, N. Time-Resolved Digital Immunoassay for Rapid and Sensitive Quantitation of Procalcitonin with Plasmonic Imaging. *ACS Nano* **2019**, *13*, 8609–8617. [CrossRef] [PubMed]
62. Karczmarczyk, A.; Reiner-Rozman, C.; Hageneder, S.; Dubiak-Szepietowska, M.; Dostálek, J.; Feller, K.H. Fast and Sensitive Detection of Ochratoxin A in Red Wine by Nanoparticle-Enhanced SPR. *Anal. Chim. Acta* **2016**, *937*, 143–150. [CrossRef]

63. Ashaduzzaman, M.; Deshpande, S.R.; Murugan, N.A.; Mishra, Y.K.; Turner, A.P.F.; Tiwari, A. On/off-Switchable LSPR Nano-Immunoassay for Troponin-T. *Sci. Rep.* **2017**, *7*, 44027. [CrossRef] [PubMed]
64. Wang, Q.; Wang, B. Sensitivity Enhanced SPR Immunosensor Based on Graphene Oxide and SPA Co-Modified Photonic Crystal Fiber. *Opt. Laser Technol.* **2018**, *107*, 210–215. [CrossRef]
65. Szymańska, B.; Lukaszewski, Z.; Hermanowicz-Szamatowicz, K.; Gorodkiewicz, E. A Biosensor for Determination of the Circulating Biomarker CA125/MUC16 by Surface Plasmon Resonance Imaging. *Talanta* **2020**, *206*, 120187. [CrossRef]
66. Oliverio, M.; Perotto, S.; Messina, G.C.; Lovato, L.; De Angelis, F. Chemical Functionalization of Plasmonic Surface Biosensors: A Tutorial Review on Issues, Strategies, and Costs. *ACS Appl. Mater. Interfaces* **2017**, *9*, 29394–29411. [CrossRef]
67. Islam, N.; Shen, F.; Gurgel, P.V.; Rojas, O.J.; Carbonell, R.G. Dynamic and Equilibrium Performance of Sensors Based on Short Peptide Ligands for Affinity Adsorption of Human IgG Using Surface Plasmon Resonance. *Biosens. Bioelectron.* **2014**, *58*, 380–387. [CrossRef]
68. Breault-Turcot, J.; Poirier-Richard, H.P.; Couture, M.; Pelechacz, D.; Masson, J.F. Single Chip SPR and Fluorescent ELISA Assay of Prostate Specific Antigen. *Lab Chip* **2015**, *15*, 4433–4440. [CrossRef]
69. Dhawan, S.; Sadanandan, S.; Haridas, V.; Voelcker, N.H.; Prieto-Simón, B. Novel Peptidylated Surfaces for Interference-Free Electrochemical Detection of Cardiac Troponin I. *Biosens. Bioelectron.* **2018**, *99*, 486–492. [CrossRef]
70. Sankiewicz, A.; Romanowicz, L.; Pyc, M.; Hermanowicz, A.; Gorodkiewicz, E. SPR Imaging Biosensor for the Quantitation of Fibronectin Concentration in Blood Samples. *J. Pharm. Biomed. Anal.* **2018**, *150*, 1–8. [CrossRef] [PubMed]
71. Barsan, M.M.; Sanz, C.G.; Onea, M.; Diculescu, V.C. Immobilized Antibodies on Mercaptophenylboronic Acid Monolayers for Dual-Strategy Detection of 20S Proteasome. *Sensors* **2021**, *21*, 2702. [CrossRef]
72. Sankiewicz, A.; Hermanowicz, A.; Grycz, A.; Łukaszewski, Z.; Gorodkiewicz, E. An SPR Imaging Immunosensor for Leptin Determination in Blood Plasma. *Anal. Methods* **2021**, *13*, 642–646. [CrossRef]
73. Duval, F.; Van Beek, T.A.; Zuilhof, H. Key Steps towards the Oriented Immobilization of Antibodies Using Boronic Acids. *Analyst* **2015**, *140*, 6467–6472. [CrossRef] [PubMed]
74. Primo, E.N.; Kogan, M.J.; Verdejo, H.E.; Bollo, S.; Rubianes, M.D.; Rivas, G.A. Label-Free Graphene Oxide-Based Surface Plasmon Resonance Immunosensor for the Quantification of Galectin-3, a Novel Cardiac Biomarker. *ACS Appl. Mater. Interfaces* **2018**, *10*, 23501–23508. [CrossRef]
75. Acero Sánchez, J.L.; Fragoso, A.; Joda, H.; Suárez, G.; McNeil, C.J.; O'Sullivan, C.K. Site-Directed Introduction of Disulfide Groups on Antibodies for Highly Sensitive Immunosensors. *Anal. Bioanal. Chem.* **2016**, *408*, 5337–5346. [CrossRef] [PubMed]
76. Chou, Y.N.; Sun, F.; Hung, H.C.; Jain, P.; Sinclair, A.; Zhang, P.; Bai, T.; Chang, Y.; Wen, T.C.; Yu, Q.; et al. Ultra-Low Fouling and High Antibody Loading Zwitterionic Hydrogel Coatings for Sensing and Detection in Complex Media. *Acta Biomater.* **2016**, *40*, 31–37. [CrossRef]
77. Yang, W.; Xue, H.; Li, W.; And, J.Z.; Jiang, S. Pursuing "zero" protein Adsorption of Poly(carboxybetaine) from Undiluted Blood Serum and Plasma. *Langmuir* **2009**, *25*, 11911–11916. [CrossRef] [PubMed]
78. Riedel, T.; Hageneder, S.; Surman, F.; Pop-Georgievski, O.; Noehammer, C.; Hofner, M.; Brynda, E.; Rodriguez-Emmenegger, C.; Dostálek, J. Plasmonic Hepatitis B Biosensor for the Analysis of Clinical Saliva. *Anal. Chem.* **2017**, *89*, 2972–2977. [CrossRef]
79. Ye, H.; Che, J.; Huang, R.; Qi, W.; He, Z.; Su, R. Zwitterionic Peptide Enhances Protein-Resistant Performance of Hyaluronic Acid-Modified Surfaces. *Langmuir* **2020**, *36*, 1923–1929. [CrossRef]
80. Liu, X.; Huang, R.; Su, R.; Qi, W.; Wang, L.; He, Z. Grafting Hyaluronic Acid onto Gold Surface to Achieve Low Protein Fouling in Surface Plasmon Resonance Biosensors. *ACS Appl. Mater. Interfaces* **2014**, *6*, 13034–13042. [CrossRef]
81. Vaisocherová, H.; Ševců, V.; Adam, P.; Špačková, B.; Hegnerová, K.; de los Santos Pereira, A.; Rodriguez-Emmenegger, C.; Riedel, T.; Houska, M.; Brynda, E.; et al. Functionalized Ultra-Low Fouling Carboxy- and Hydroxy-Functional Surface Platforms: Functionalization Capacity, Biorecognition Capability and Resistance to Fouling from Undiluted Biological Media. *Biosens. Bioelectron.* **2014**, *51*, 150–157. [CrossRef]
82. Becherer, T.; Grunewald, C.; Engelschalt, V.; Multhaup, G.; Risse, T.; Haag, R. Polyglycerol Based Coatings to Reduce Non-Specific Protein Adsorption in Sample Vials and on SPR Sensors. *Anal. Chim. Acta* **2015**, *867*, 47–55. [CrossRef] [PubMed]
83. Souto, D.E.P.; Fonseca, A.M.; Barragan, J.T.C.; Luz, R.d.C.S.; Andrade, H.M.; Damos, F.S.; Kubota, L.T. SPR Analysis of the Interaction between a Recombinant Protein of Unknown Function in *Leishmania infantum* Immobilised on Dendrimers and Antibodies of the Visceral Leishmaniasis: A Potential Use in Immunodiagnosis. *Biosens. Bioelectron.* **2015**, *70*, 275–281. [CrossRef] [PubMed]
84. Makhneva, E.; Farka, Z.; Skládal, P.; Zajíčková, L. Cyclopropylamine Plasma Polymer Surfaces for Label-Free SPR and QCM Immunosensing of *Salmonella*. *Sens. Actuators B Chem.* **2018**, *276*, 447–455. [CrossRef]
85. Makhneva, E.; Farka, Z.; Pastucha, M.; Obrusník, A.; Horáčková, V.; Skládal, P.; Zajíčková, L. Maleic Anhydride and Acetylene Plasma Copolymer Surfaces for SPR Immunosensing. *Anal. Bioanal. Chem.* **2019**, *411*, 7689–7697. [CrossRef]
86. Makhneva, E.; Barillas, L.; Farka, Z.; Pastucha, M.; Skládal, P.; Weltmann, K.D.; Fricke, K. Functional Plasma Polymerized Surfaces for Biosensing. *ACS Appl. Mater. Interfaces* **2020**, *12*, 17100–17112. [CrossRef]
87. Wu, Q.; Sun, Y.; Zhang, D.; Li, S.; Zhang, Y.; Ma, P.; Yu, Y.; Wang, X.; Song, D. Ultrasensitive Magnetic Field-Assisted Surface Plasmon Resonance Immunoassay for Human Cardiac Troponin I. *Biosens. Bioelectron.* **2017**, *96*, 288–293. [CrossRef] [PubMed]
88. Mei, Y.; Li, L.; Chen, N.; Zhong, C.; Hu, W. A Microwell Array Structured Surface Plasmon Resonance Imaging Gold Chip for High-Performance Label-Free Immunoassay. *Analyst* **2020**, *145*, 6395–6400. [CrossRef]

89. Chen, D.; Mei, Y.; Hu, W.; Li, C.M. Electrochemically Enhanced Antibody Immobilization on Polydopamine Thin Film for Sensitive Surface Plasmon Resonance Immunoassay. *Talanta* **2018**, *182*, 470–475. [CrossRef] [PubMed]
90. Parrillo, V.; de los Santos Pereira, A.; Riedel, T.; Rodriguez-Emmenegger, C. Catalyst-Free "click" Functionalization of Polymer Brushes Preserves Antifouling Properties Enabling Detection in Blood Plasma. *Anal. Chim. Acta* **2017**, *971*, 78–87. [CrossRef]
91. Zhao, H.; Gorshkova, I.I.; Fu, G.L.; Schuck, P. A Comparison of Binding Surfaces for SPR Biosensing Using an Antibody-Antigen System and Affinity Distribution Analysis. *Methods* **2013**, *59*, 328–335. [CrossRef] [PubMed]
92. Wang, J.; Yao, W.; Meng, F.; Wang, P.; Wu, Y.; Wang, B. A Surface Plasmon Resonance Immunoassay for the Rapid Analysis of Methamphetamine in Forensic Oral Fluid. *J. Clin. Lab. Anal.* **2019**, *33*, e22993. [CrossRef] [PubMed]
93. Wang, Y.; Partridge, A.; Wu, Y. In Situ Surface Protein Conjugation of Small Molecules for SPR Immunoassays. *Anal. Biochem.* **2017**, *539*, 149–151. [CrossRef] [PubMed]
94. He, Q.; Chen, Y.; Shen, D.; Cui, X.; Zhang, C.; Yang, H.; Zhong, W.; Eremin, S.A.; Fang, Y.; Zhao, S. Development of a Surface Plasmon Resonance Immunosensor and ELISA for 3-Nitrotyrosine in Human Urine. *Talanta* **2019**, *195*, 655–661. [CrossRef]
95. Xia, Y.; Zhang, P.; Yuan, H.; Su, R.; Huang, R.; Qi, W.; He, Z. Sequential Sandwich Immunoassay for Simultaneous Detection in Trace Samples Using Single-Channel Surface Plasmon Resonance. *Analyst* **2019**, *144*, 5700–5705. [CrossRef]
96. Patil, P.O.; Pandey, G.R.; Patil, A.G.; Borse, V.B.; Deshmukh, P.K.; Patil, D.R.; Tade, R.S.; Nangare, S.N.; Khan, Z.G.; Patil, A.M.; et al. Graphene-Based Nanocomposites for Sensitivity Enhancement of Surface Plasmon Resonance Sensor for Biological and Chemical Sensing: A Review. *Biosens. Bioelectron.* **2019**, *139*, 111324. [CrossRef]
97. Singh, M.; Holzinger, M.; Tabrizian, M.; Winters, S.; Berner, N.C.; Cosnier, S.; Duesberg, G.S. Noncovalently Functionalized Monolayer Graphene for Sensitivity Enhancement of Surface Plasmon Resonance Immunosensors. *J. Am. Chem. Soc.* **2015**, *137*, 2800–2803. [CrossRef]
98. Chiu, N.F.; Lin, T.L.; Kuo, C.T. Highly Sensitive Carboxyl-Graphene Oxide-Based Surface Plasmon Resonance Immunosensor for the Detection of Lung Cancer for Cytokeratin 19 Biomarker in Human Plasma. *Sens. Actuators B Chem.* **2018**, *265*, 264–272. [CrossRef]
99. He, L.; Pagneux, Q.; Larroulet, I.; Serrano, A.Y.; Pesquera, A.; Zurutuza, A.; Mandler, D.; Boukherroub, R.; Szunerits, S. Label-Free Femtomolar Cancer Biomarker Detection in Human Serum Using Graphene-Coated Surface Plasmon Resonance Chips. *Biosens. Bioelectron.* **2017**, *89*, 606–611. [CrossRef]
100. Nurrohman, D.T.; Chiu, N.-F. A Review of Graphene-Based Surface Plasmon Resonance and Surface-Enhanced Raman Scattering Biosensors: Current Status and Future Prospects. *Nanomaterials* **2021**, *11*, 216. [CrossRef]
101. Chiu, N.F.; Fan, S.Y.; Yang, C.D.; Huang, T.Y. Carboxyl-Functionalized Graphene Oxide Composites as SPR Biosensors with Enhanced Sensitivity for Immunoaffinity Detection. *Biosens. Bioelectron.* **2017**, *89*, 370–376. [CrossRef]
102. Miyazaki, C.M.; Camilo, D.E.; Shimizu, F.M.; Ferreira, M. Improved Antibody Loading on Self-Assembled Graphene Oxide Films for Using in Surface Plasmon Resonance Immunosensors. *Appl. Surf. Sci.* **2019**, *490*, 502–509. [CrossRef]
103. Omar, N.; Fen, Y.; Saleviter, S.; Daniyal, W.; Anas, N.; Ramdzan, N.; Roshidi, M. Development of a Graphene-Based Surface Plasmon Resonance Optical Sensor Chip for Potential Biomedical Application. *Materials* **2019**, *12*, 1928. [CrossRef] [PubMed]
104. Nurrohman, D.T.; Wang, Y.-H.; Chiu, N.-F. Exploring Graphene and MoS_2 Chips Based Surface Plasmon Resonance Biosensors for Diagnostic Applications. *Front. Chem.* **2020**, *8*, 728. [CrossRef]
105. Kaushik, S.; Tiwari, U.K.; Deep, A.; Sinha, R.K. Two-Dimensional Transition Metal Dichalcogenides Assisted Biofunctionalized Optical Fiber SPR Biosensor for Efficient and Rapid Detection of Bovine Serum Albumin. *Sci. Rep.* **2019**, *9*, 1–11. [CrossRef]
106. Chiu, N.-F.; Yang, H.-T. High-Sensitivity Detection of the Lung Cancer Biomarker CYFRA21-1 in Serum Samples Using a Carboxyl-MoS_2 Functional Film for SPR-Based Immunosensors. *Front. Bioeng. Biotechnol.* **2020**, *8*, 234. [CrossRef] [PubMed]
107. Zhao, P.; Chen, Y.; Chen, Y.; Hu, S.; Chen, H.; Xiao, W.; Liu, G.; Tang, Y.; Shi, J.; He, Z.; et al. A MoS_2 nanoflower and Gold Nanoparticle-Modified Surface Plasmon Resonance Biosensor for a Sensitivity-Improved Immunoassay. *J. Mater. Chem. C* **2020**, *8*, 6861–6868. [CrossRef]
108. Zhu, X.; Zhang, Y.; Liu, M.; Liu, Y. 2D Titanium Carbide MXenes as Emerging Optical Biosensing Platforms. *Biosens. Bioelectron.* **2021**, *171*, 112730. [CrossRef]
109. Wu, Q.; Li, N.; Wang, Y.; Liu, Y.; Xu, Y.; Wei, S.; Wu, J.; Jia, G.; Fang, X.; Chen, F.; et al. A 2D Transition Metal Carbide MXene-Based SPR Biosensor for Ultrasensitive Carcinoembryonic Antigen Detection. *Biosens. Bioelectron.* **2019**, *144*, 111697. [CrossRef] [PubMed]
110. Wu, Q.; Li, N.; Wang, Y.; Xu, Y.; Wu, J.; Jia, G.; Ji, F.; Fang, X.; Chen, F.; Cui, X. Ultrasensitive and Selective Determination of Carcinoembryonic Antigen Using Multifunctional Ultrathin Amino-Functionalized Ti_3C_2-MXene Nanosheets. *Anal. Chem.* **2020**, *92*, 3354–3360. [CrossRef] [PubMed]
111. Shen, M.; Rusling, J.F.; Dixit, C.K. Site-Selective Orientated Immobilization of Antibodies and Conjugates for Immunodiagnostics Development. *Methods* **2017**, *116*, 95–111. [CrossRef] [PubMed]
112. Liu, Y.; Yu, J. Oriented Immobilization of Proteins on Solid Supports for Use in Biosensors and Biochips: A Review. *Microchim. Acta* **2016**, *183*, 1–19. [CrossRef]
113. Tsekenis, G.; Chatzipetrou, M.; Massaouti, M.; Zergioti, I. Comparative Assessment of Affinity-Based Techniques for Oriented Antibody Immobilization towards Immunosensor Performance Optimization. *J. Sens.* **2019**, *2019*. [CrossRef]
114. Mazigi, O.; Schofield, P.; Langley, D.B.; Christ, D. Protein A Superantigen: Structure, Engineering and Molecular Basis of Antibody Recognition. *Protein Eng. Des. Sel.* **2019**, *32*, 359–366. [CrossRef]

115. Sjobring, U.; Bjorck, L.; Kastern, W. Streptococcal Protein G. Gene Structure and Protein Binding Properties. *J. Biol. Chem.* **1991**, *266*, 399–405. [CrossRef]
116. Bergström, G.; Mandenius, C.F. Orientation and Capturing of Antibody Affinity Ligands: Applications to Surface Plasmon Resonance Biochips. *Sens. Actuators B Chem.* **2011**, *158*, 265–270. [CrossRef]
117. Lee, W.; Oh, B.K.; Bae, Y.M.; Paek, S.H.; Lee, W.H.; Choi, J.W. Fabrication of Self-Assembled Protein A Monolayer and Its Application as an Immunosensor. *Biosens. Bioelectron.* **2003**, *19*, 185–192. [CrossRef]
118. Bakhmachuk, A.; Gorbatiuk, O.; Rachkov, A.; Dons'koi, B.; Khristosenko, R.; Ushenin, I.; Peshkova, V.; Soldatkin, A. Surface Plasmon Resonance Investigations of Bioselective Element Based on the Recombinant Protein A for Immunoglobulin Detection. *Nanoscale Res. Lett.* **2017**, *12*, 112. [CrossRef] [PubMed]
119. De Juan-Franco, E.; Caruz, A.; Pedrajas, J.R.; Lechuga, L.M. Site-Directed Antibody Immobilization Using a Protein A-Gold Binding Domain Fusion Protein for Enhanced SPR Immunosensing. *Analyst* **2013**, *138*, 2023–2031. [CrossRef] [PubMed]
120. Schmid, A.H.; Stanca, S.E.; Thakur, M.S.; Thampi, K.R.; Suri, C.R. Site-Directed Antibody Immobilization on Gold Substrate for Surface Plasmon Resonance Sensors. *Sens. Actuators B Chem.* **2006**, *113*, 297–303. [CrossRef]
121. Sohn, Y.-S.; Lee, Y.K. Site-Directed Immobilization of Antibody Using EDC-NHS-Activated Protein A on a Bimetallic-Based Surface Plasmon Resonance Chip. *J. Biomed. Opt.* **2014**, *19*, 51209. [CrossRef]
122. Hu, W.P.; Hsu, H.Y.; Chiou, A.; Tseng, K.Y.; Lin, H.Y.; Chang, G.L.; Chen, S.J. Immunodetection of Pentamer and Modified C-Reactive Protein Using Surface Plasmon Resonance Biosensing. *Biosens. Bioelectron.* **2006**, *21*, 1631–1637. [CrossRef]
123. Paiva, T.O.; Almeida, I.; Marquês, J.T.; Liu, W.; Niu, Y.; Jin, G.; Viana, A.S. Nanostructured Interfaces with Site-Specific Bioreceptors for Immunosensing. *Appl. Surf. Sci.* **2017**, *412*, 455–463. [CrossRef]
124. Niu, Y.; Matos, A.I.; Abrantes, L.M.; Viana, A.S.; Jin, G. Antibody Oriented Immobilization on Gold Using the Reaction between Carbon Disulfide and Amine Groups and Its Application in Immunosensing. *Langmuir* **2012**, *28*, 17718–17725. [CrossRef]
125. Jung, Y.; Jeong, M.L.; Jung, H.; Bong, H.C. Self-Directed and Self-Oriented Immobilization of Antibody by Protein G-DNA Conjugate. *Anal. Chem.* **2007**, *79*, 6534–6541. [CrossRef]
126. Oh, B.K.; Lee, W.; Chun, B.S.; Bae, Y.M.; Lee, W.H.; Choi, J.W. The Fabrication of Protein Chip Based on Surface Plasmon Resonance for Detection of Pathogens. *Biosens. Bioelectron.* **2005**, *20*, 1847–1850. [CrossRef]
127. Mckeating, K.S.; Hinman, S.S.; Rais, N.A.; Zhou, Z.; Cheng, Q. Antifouling Lipid Membranes over Protein a for Orientation-Controlled Immunosensing in Undiluted Serum and Plasma. *ACS Sens.* **2019**, *4*, 1774–1782. [CrossRef] [PubMed]
128. Almeida, I.; Marquês, J.T.; Liu, W.; Niu, Y.; de Almeida, R.F.M.; Jin, G.; Viana, A.S. Phospholipid/cholesterol/decanethiol Mixtures for Direct Assembly of Immunosensing Interfaces. *Colloids Surf. B* **2015**, *136*, 997–1003. [CrossRef] [PubMed]
129. Bichet, M.C.; Chin, W.H.; Richards, W.; Lin, Y.W.; Avellaneda-Franco, L.; Hernandez, C.A.; Oddo, A.; Chernyavskiy, O.; Hilsenstein, V.; Neild, A.; et al. Bacteriophage Uptake by Eukaryotic Cell Layers Represents a Major Sink for Phages during Therapy. *bioRxiv* **2020**. [CrossRef]
130. Moon, J.-S.; Kim, W.-G.; Kim, C.; Park, G.-T.; Heo, J.; Yoo, S.Y.; Oh, J.-W. M13 Bacteriophage-Based Self-Assembly Structures and Their Functional Capabilities. *Mini Rev. Org. Chem.* **2015**, *12*, 271–281. [CrossRef]
131. Ertürk, G.; Lood, R. Bacteriophages as Biorecognition Elements in Capacitive Biosensors: Phage and Host Bacteria Detection. *Sens. Actuators B Chem.* **2018**, *258*, 535–543. [CrossRef]
132. Ahovan, Z.A.; Hashemi, A.; De Plano, L.M.; Gholipourmalekabadi, M.; Seifalian, A. Bacteriophage Based Biosensors: Trends, Outcomes and Challenges. *Nanomaterials* **2020**, *10*, 501. [CrossRef] [PubMed]
133. Peltomaa, R.; Benito-Peña, E.; Barderas, R.; Moreno-Bondi, M.C. Phage Display in the Quest for New Selective Recognition Elements for Biosensors. *ACS Omega* **2019**, *4*, 11569–11580. [CrossRef]
134. Peltomaa, R.; López-Perolio, I.; Benito-Peña, E.; Barderas, R.; Moreno-Bondi, M.C. Application of Bacteriophages in Sensor Development. *Anal. Bioanal. Chem.* **2016**, *408*, 1805–1828. [CrossRef] [PubMed]
135. Lee, J.W.; Song, J.; Hwang, M.P.; Lee, K.H. Nanoscale Bacteriophage Biosensors beyond Phage Display. *Int. J. Nanomed.* **2013**, *8*, 3917–3925. [CrossRef] [PubMed]
136. Nanduri, V.; Balasubramanian, S.; Sista, S.; Vodyanoy, V.J.; Simonian, A.L. Highly Sensitive Phage-Based Biosensor for the Detection of β-Galactosidase. *Anal. Chim. Acta* **2007**, *589*, 166–172. [CrossRef] [PubMed]
137. Nanduri, V.; Bhunia, A.K.; Tu, S.I.; Paoli, G.C.; Brewster, J.D. SPR Biosensor for the Detection of L. Monocytogenes Using Phage-Displayed Antibody. *Biosens. Bioelectron.* **2007**, *23*, 248–252. [CrossRef] [PubMed]
138. Karoonuthaisiri, N.; Charlermroj, R.; Morton, M.J.; Oplatowska-Stachowiak, M.; Grant, I.R.; Elliott, C.T. Development of a M13 Bacteriophage-Based SPR Detection Using Salmonella as a Case Study. *Sens. Actuators B Chem.* **2014**, *190*, 214–220. [CrossRef]
139. Naidoo, R.; Singh, A.; Arya, S.K.; Beadle, B.; Glass, N.; Tanha, J.; Szymanski, C.M.; Evoy, S. Surface-Immobilization of Chromatographically Purified Bacteriophages for the Optimized Capture of Bacteria. *Bacteriophage* **2012**, *2*, 15–24. [CrossRef]
140. Hussain, W.; Ullah, M.W.; Farooq, U.; Aziz, A.; Wang, S. Bacteriophage-Based Advanced Bacterial Detection: Concept, Mechanisms, and Applications. *Biosens. Bioelectron.* **2021**, *177*, 112973. [CrossRef]
141. Han, L.; Wang, D.; Yan, L.; Petrenko, V.A.; Liu, A. Specific Phages-Based Electrochemical Impedimetric Immunosensors for Label-Free and Ultrasensitive Detection of Dual Prostate-Specific Antigens. *Sens. Actuators B Chem.* **2019**, *297*, 126727. [CrossRef]
142. Predonzani, A.; Arnoldi, F.; López-Requena, A.; Burrone, O.R. In Vivo Site-Specific Biotinylation of Proteins within the Secretory Pathway Using a Single Vector System. *BMC Biotechnol.* **2008**, *8*, 41. [CrossRef]

143. Hutsell, S.Q.; Kimple, R.J.; Siderovski, D.P.; Willard, F.S.; Kimple, A.J. High-Affinity Immobilization of Proteins Using Biotin- and GST-Based Coupling Strategies. *Methods Mol. Biol.* **2010**, *627*, 75–90. [CrossRef] [PubMed]
144. Kay, B.K.; Thai, S.; Volgina, V.V. High-Throughput Biotinylation of Proteins. *Methods Mol. Biol.* **2009**, *498*, 185–198. [CrossRef] [PubMed]
145. Dundas, C.M.; Demonte, D.; Park, S. Streptavidin-Biotin Technology: Improvements and Innovations in Chemical and Biological Applications. *Appl. Microbiol. Biotechnol.* **2013**, *97*, 9343–9353. [CrossRef]
146. Jain, A.; Cheng, K. The Principles and Applications of Avidin-Based Nanoparticles in Drug Delivery and Diagnosis. *J. Control. Release* **2017**, *245*, 27–40. [CrossRef]
147. Jain, A.; Barve, A.; Zhao, Z.; Jin, W.; Cheng, K. Comparison of Avidin, Neutravidin, and Streptavidin as Nanocarriers for Efficient siRNA Delivery. *Mol. Pharm.* **2017**, *14*, 1517–1527. [CrossRef]
148. García-Aljaro, C.; Muñoz, F.X.; Baldrich, E. Captavidin: A New Regenerable Biocomponent for Biosensing? *Analyst* **2009**, *134*, 2338–2343. [CrossRef]
149. Knoglinger, C.; Zich, A.; Traxler, L.; Poslední, K.; Friedl, G.; Ruttmann, B.; Schorpp, A.; Müller, K.; Zimmermann, M.; Gruber, H.J. Regenerative Biosensor for Use with Biotinylated Bait Molecules. *Biosens. Bioelectron.* **2018**, *99*, 684–690. [CrossRef]
150. Dutra, R.F.; Kubota, L.T. An SPR Immunosensor for Human Cardiac Troponin T Using Specific Binding Avidin to Biotin at Carboxymethyldextran-Modified Gold Chip. *Clin. Chim. Acta* **2007**, *376*, 114–120. [CrossRef]
151. Mansouri, M.; Fathi, F.; Jalili, R.; Shoeibie, S.; Dastmalchi, S.; Khataee, A.; Rashidi, M.R. SPR Enhanced DNA Biosensor for Sensitive Detection of Donkey Meat Adulteration. *Food Chem.* **2020**, *331*, 127163. [CrossRef]
152. Yu, H.; Muñoz, E.M.; Edens, R.E.; Linhardt, R.J. Kinetic Studies on the Interactions of Heparin and Complement Proteins Using Surface Plasmon Resonance. *Biochim. Biophys. Acta Gen. Subj.* **2005**, *1726*, 168–176. [CrossRef]
153. De Juan-Franco, E.; Rodríguez-Frade, J.M.; Mellado, M.; Lechuga, L.M. Implementation of a SPR Immunosensor for the Simultaneous Detection of the 22K and 20K hGH Isoforms in Human Serum Samples. *Talanta* **2013**, *114*, 268–275. [CrossRef]
154. Bai, H.; Wang, R.; Hargis, B.; Lu, H.; Li, Y. A SPR Aptasensor for Detection of Avian Influenza Virus H5N1. *Sensors* **2012**, *12*, 12506–12518. [CrossRef] [PubMed]
155. Loureiro, F.C.C.L.; Neff, H.; Melcher, E.U.K.; Roque, R.A.; de Figueiredo, R.M.P.; Thirstrup, C.; Borre, M.B.; Lima, A.M.N. Simplified Immunoassay for Rapid Dengue Serotype Diagnosis, Revealing Insensitivity to Non-Specific Binding Interference. *Sens. Bio-Sens. Res.* **2017**, *13*, 96–103. [CrossRef]
156. Jordan, C.E.; Frutos, A.G.; Thiel, A.J.; Corn, R.M. Surface Plasmon Resonance Imaging Measurements of DNA Hybridization Adsorption and streptavidin/DNA Multilayer Formation at Chemically Modified Gold Surfaces. *Anal. Chem.* **1997**, *69*, 4939–4947. [CrossRef]
157. Kang, C.D.; Lee, S.W.; Park, T.H.; Sim, S.J. Performance Enhancement of Real-Time Detection of Protozoan Parasite, Cryptosporidium Oocyst by a Modified Surface Plasmon Resonance (SPR) Biosensor. *Enzym. Microb. Technol.* **2006**, *39*, 387–390. [CrossRef]
158. Pei, R.; Yang, X.; Wang, E. Enhanced Surface Plasmon Resonance Immunosensing Using a Streptavidin-Biotinylated Protein Complex. *Analyst* **2001**, *126*, 4–6. [CrossRef] [PubMed]
159. Ding, X.; Yan, Y.; Li, S.; Zhang, Y.; Cheng, W.; Cheng, Q.; Ding, S. Surface Plasmon Resonance Biosensor for Highly Sensitive Detection of microRNA Based on DNA Super-Sandwich Assemblies and Streptavidin Signal Amplification. *Anal. Chim. Acta* **2015**, *874*, 59–65. [CrossRef]
160. Sun, T.; Zhang, Y.; Zhao, F.; Xia, N.; Liu, L. Self-assembled biotin-phenylalanine nanoparticles for the signal amplification of surface plasmon resonance biosensors. *Microchim. Acta* **2020**, *187*, 473. [CrossRef]
161. Li, Y.J.; Bi, L.J.; Zhang, X.E.; Zhou, Y.F.; Zhang, J.B.; Chen, Y.Y.; Li, W.; Zhang, Z.P. Reversible Immobilization of Proteins with Streptavidin Affinity Tags on a Surface Plasmon Resonance Biosensor Chip. *Anal. Bioanal. Chem.* **2006**, *386*, 1321–1326. [CrossRef]
162. Lamla, T.; Erdmann, V.A. The Nano-Tag, a Streptavidin-Binding Peptide for the Purification and Detection of Recombinant Proteins. *Protein Expr. Purif.* **2004**, *33*, 39–47. [CrossRef] [PubMed]
163. Kim, J.H.; Chang, T.M.; Graham, A.N.; Choo, K.H.; Kalitsis, P.; Hudson, D.F. Streptavidin-Binding Peptide (SBP)-Tagged SMC2 Allows Single-Step Affinity Fluorescence, Blotting or Purification of the Condensin Complex. *BMC Biochem.* **2010**, *11*. [CrossRef] [PubMed]
164. Zauner, D.; Taskinen, B.; Eichinger, D.; Flattinger, C.; Ruttmann, B.; Knoglinger, C.; Traxler, L.; Ebner, A.; Gruber, H.J.; Hytönen, V.P. Regenerative Biosensor Chips Based on Switchable Mutants of Avidin—A Systematic Study. *Sens. Actuators B Chem.* **2016**, *229*, 646–654. [CrossRef]
165. Meyer, R.; Giselbrecht, S.; Rapp, B.E.; Hirtz, M.; Niemeyer, C.M. Advances in DNA-Directed Immobilization. *Curr. Opin. Chem. Biol.* **2014**, *18*, 8–15. [CrossRef]
166. Garai, A.; Ghoshdastidar, D.; Senapati, S.; Maiti, P.K. Ionic Liquids Make DNA Rigid. *J. Chem. Phys.* **2018**, *149*, 045104. [CrossRef]
167. Ladd, J.; Boozer, C.; Yu, Q.; Chen, S.; Homola, J.; Jiang, S. DNA-Directed Protein Immobilization on Mixed Self-Assembled Monolayers via a Streptavidin Bridge. *Langmuir* **2004**, *20*, 8090–8095. [CrossRef]
168. Ladd, J.; Taylor, A.D.; Piliarik, M.; Homola, J.; Jiang, S. Hybrid Surface Platform for the Simultaneous Detection of Proteins and DNAs Using a Surface Plasmon Resonance Imaging Sensor. *Anal. Chem.* **2008**, *80*, 4231–4236. [CrossRef]
169. Bombera, R.; Leroy, L.; Livache, T.; Roupioz, Y. DNA-Directed Capture of Primary Cells from a Complex Mixture and Controlled Orthogonal Release Monitored by SPR Imaging. *Biosens. Bioelectron.* **2012**, *33*, 10–16. [CrossRef]

170. Leroy, L.; Bombera, R.; Engel, E.; Calemczuk, R.; Laplatine, L.; Baganizi, D.D.R.; Marche, P.N.; Roupioz, Y.; Livache, T. Photothermal Effect for Localized Desorption of Primary Lymphocytes Arrayed on an antibody/DNA-Based Biochip. *Lab Chip* **2014**, *14*, 1987–1990. [CrossRef]
171. Piliarik, M.; Bocková, M.; Homola, J. Surface Plasmon Resonance Biosensor for Parallelized Detection of Protein Biomarkers in Diluted Blood Plasma. *Biosens. Bioelectron.* **2010**, *26*, 1656–1661. [CrossRef]
172. Tort, N.; Salvador, J.P.; Aviñó, A.; Eritja, R.; Comelles, J.; Martínez, E.; Samitier, J.; Marco, M.P. Synthesis of Steroid-Oligonucleotide Conjugates for a DNA Site-Encoded SPR Immunosensor. *Bioconjug. Chem.* **2012**, *23*, 2183–2191. [CrossRef]
173. Kim, D.H.; Cho, I.H.; Park, J.N.; Paek, S.H.; Cho, H.M.; Paek, S.H. Semi-Continuous, Real-Time Monitoring of Protein Biomarker Using a Recyclable Surface Plasmon Resonance Sensor. *Biosens. Bioelectron.* **2017**, *88*, 232–239. [CrossRef] [PubMed]
174. Fercher, C.; Jones, M.L.; Mahler, S.M.; Corrie, S.R. Recombinant Antibody Engineering Enables Reversible Binding for Continuous Protein Biosensing. *ACS Sens.* **2021**, *6*, 764–776. [CrossRef]
175. Brambilla, D.; Sola, L.; Chiari, M. Advantageous Antibody Microarray Fabrication through DNA-Directed Immobilization: A Step toward Use of Extracellular Vesicles in Diagnostics. *Talanta* **2021**, *222*, 121542. [CrossRef] [PubMed]
176. Fruk, L.; Müller, J.; Weber, G.; Narváez, A.; Domínguez, E.; Niemeyer, C.M. DNA-Directed Immobilization of Horseradish Peroxidase–DNA Conjugates on Microelectrode Arrays: Towards Electrochemical Screening of Enzyme Libraries. *Chem. A Eur. J.* **2007**, *13*, 5223–5231. [CrossRef] [PubMed]
177. Wiener, J.; Kokotek, D.; Rosowski, S.; Lickert, H.; Meier, M. Preparation of Single- and Double-Oligonucleotide Antibody Conjugates and Their Application for Protein Analytics. *Sci. Rep.* **2020**, *10*, 1–11. [CrossRef]
178. Daub, H.; Traxler, L.; Ismajli, F.; Groitl, B.; Itzen, A.; Rant, U. The Trimer to Monomer Transition of Tumor Necrosis Factor-Alpha Is a Dynamic Process That Is Significantly Altered by Therapeutic Antibodies. *Sci. Rep.* **2020**, *10*, 1–10. [CrossRef]
179. Knecht, S.; Ricklin, D.; Eberle, A.N.; Ernst, B. Oligohis-Tags: Mechanisms of Binding to Ni^{2+}-NTA Surfaces. *J. Mol. Recognit.* **2009**, *22*, 270–279. [CrossRef]
180. Cao, Y.; Griffith, B.; Bhomkar, P.; Wishart, D.S.; McDermott, M.T. Functionalized Gold Nanoparticle-Enhanced Competitive Assay for Sensitive Small-Molecule Metabolite Detection Using Surface Plasmon Resonance. *Analyst* **2018**, *143*, 289–296. [CrossRef]
181. Kimple, A.J.; Muller, R.E.; Siderovski, D.P.; Willard, F.S. A Capture Coupling Method for the Covalent Immobilization of Hexahistidine Tagged Proteins for Surface Plasmon Resonance. *Methods Mol. Biol.* **2010**, *627*, 91–100. [CrossRef] [PubMed]
182. Zhang, L.; Wei, T.T.; Li, Y.; Li, J.; Fan, Y.; Huang, F.Q.; Cai, Y.Y.; Ma, G.; Liu, J.F.; Chen, Q.Q.; et al. Functional Metabolomics Characterizes a Key Role for N-Acetylneuraminic Acid in Coronary Artery Diseases. *Circulation* **2018**, *137*. [CrossRef] [PubMed]
183. Fischer, M.; Leech, A.P.; Hubbard, R.E. Comparative Assessment of Different Histidine-Tags for Immobilization of Protein onto Surface Plasmon Resonance Sensorchips. *Anal. Chem.* **2011**, *83*, 1800–1807. [CrossRef]
184. Chu, R.; Reczek, D.; Brondyk, W. Capture-Stabilize Approach for Membrane Protein SPR Assays. *Sci. Rep.* **2014**, *4*, 7360. [CrossRef] [PubMed]
185. Wang, X.; Liu, Q.; Tan, X.; Liu, L.; Zhou, F. Covalent Affixation of Histidine-Tagged Proteins Tethered onto Ni-Nitrilotriacetic Acid Sensors for Enhanced Surface Plasmon Resonance Detection of Small Molecule Drugs and Kinetic Studies of Antibody/antigen Interactions. *Analyst* **2019**, *144*, 587–593. [CrossRef]
186. Horta, S.; Qu, J.H.; Dekimpe, C.; Bonnez, Q.; Vandenbulcke, A.; Tellier, E.; Kaplanski, G.; Delport, F.; Geukens, N.; Lammertyn, J.; et al. Co(III)-NTA Mediated Antigen Immobilization on a Fiber Optic-SPR Biosensor for Detection of Autoantibodies in Autoimmune Diseases: Application in Immune-Mediated Thrombotic Thrombocytopenic Purpura. *Anal. Chem.* **2020**, *92*, 13880–13887. [CrossRef] [PubMed]
187. Qu, J.-H.; Leirs, K.; Escudero, R.; Strmšek, Ž.; Jerala, R.; Spasic, D.; Lammertyn, J. Novel Regeneration Approach for Creating Reusable FO-SPR Probes with NTA Surface Chemistry. *Nanomaterials* **2021**, *11*, 186. [CrossRef]
188. Könning, D.; Kolmar, H. Beyond Antibody Engineering: Directed Evolution of Alternative Binding Scaffolds and Enzymes Using Yeast Surface Display. *Microb. Cell Fact.* **2018**, *17*, 32. [CrossRef]
189. Rathore, A.S.; Sarker, A.; Gupta, R.D. Recent Developments Toward Antibody Engineering and Affinity Maturation. *Protein Pept. Lett.* **2018**, *25*, 886–896. [CrossRef]
190. Kim, D.H.; Seo, S.M.; Paek, S.H.; Lim, G.S.; Paek, S.H. Premature Antibodies with Rapid Reaction Kinetics and Their Characterization for Diagnostic Applications. *Anal. Biochem.* **2012**, *420*, 54–60. [CrossRef]
191. Hall, E.A.H.; Chen, S.; Chun, J.; Du, Y.; Zhao, Z. A Molecular Biology Approach to Protein Coupling at a Biosensor Interface. *Trends Anal. Chem.* **2016**, *79*, 247–256. [CrossRef]
192. Zou, F.; Wang, X.; Qi, F.; Koh, K.; Lee, J.; Zhou, H.; Chen, H. Magneto-Plamonic Nanoparticles Enhanced Surface Plasmon Resonance TB Sensor Based on Recombinant Gold Binding Antibody. *Sens. Actuators B Chem.* **2017**, *250*, 356–363. [CrossRef]
193. Ha, T.H.; Jung, S.O.; Lee, J.M.; Lee, K.Y.; Lee, Y.; Park, J.S.; Chung, B.H. Oriented Immobilization of Antibodies with GST-Fused Multiple F c-Specific B-Domains on a Gold Surface. *Anal. Chem.* **2007**, *79*, 546–556. [CrossRef]
194. Boonen, A.; Singh, A.K.; Van Hout, A.; Das, K.; Van Loy, T.; Noppen, S.; Schols, D. Development of a Novel SPR Assay to Study CXCR4-Ligand Interactions. *Biosensors* **2020**, *10*, 150. [CrossRef]
195. Hussack, G.; Baral, T.N.; Baardsnes, J.; van Faassen, H.; Raphael, S.; Henry, K.A.; Zhang, J.; MacKenzie, C.R. A Novel Affinity Tag, ABTAG, and Its Application to the Affinity Screening of Single-Domain Antibodies Selected by Phage Display. *Front. Immunol.* **2017**, *8*, 1406. [CrossRef] [PubMed]

196. Sokolowska-Wedzina, A.; Chodaczek, G.; Chudzian, J.; Borek, A.; Zakrzewska, M.; Otlewski, J. High-Affinity Internalizing Human scFv-Fc Antibody for Targeting FGFR1-Overexpressing Lung Cancer. *Mol. Cancer Res.* **2017**, *15*, 1040–1050. [CrossRef] [PubMed]
197. Djender, S.; Schneider, A.; Beugnet, A.; Crepin, R.; Desrumeaux, K.E.; Romani, C.; Moutel, S.; Perez, F.; de Marco, A. Bacterial Cytoplasm as an Effective Cell Compartment for Producing Functional VHH-Based Affinity Reagents and Camelidae IgG-like Recombinant Antibodies. *Microb. Cell Fact.* **2014**, *13*, 140. [CrossRef] [PubMed]
198. Xie, X.Y.; Xu, J.Z.; Luo, Y.; Ou, L.; Gao, L.C.; Gao, C.Y.; Wang, H.X.; Fu, J.; Dong, L.H.; Song, H.F. Development and Application of an Immunogenicity Assay against Thrombopoiesis Stimulating Fusion Protein (TMP-Fc) Based on SPR System. *Chin. J. New Drugs* **2017**, *26*, 2424–2430.
199. Ko, S.; Park, T.J.; Kim, H.S.; Kim, J.H.; Cho, Y.J. Directed Self-Assembly of Gold Binding Polypeptide-Protein A Fusion Proteins for Development of Gold Nanoparticle-Based SPR Immunosensors. *Biosens. Bioelectron.* **2009**, *24*, 2592–2597. [CrossRef] [PubMed]

Publikacja P2:

A Careful Insight into DDI-Type Receptor Layers on the Way to Improvement of Click-Biology-Based Immunosensors

biosensors

MDPI

Article

A Careful Insight into DDI-Type Receptor Layers on the Way to Improvement of Click-Biology-Based Immunosensors

Sylwia Karoń [1,2], Marcin Drozd [1,2,*] and Elżbieta Malinowska [1,2,*]

[1] Department of Medical Diagnostics, Centre for Advanced Materials and Technologies CEZAMAT, Warsaw University of Technology, Poleczki 19, 02-822 Warsaw, Poland; sylwia.karon.dokt@pw.edu.pl
[2] Chair of Medical Biotechnology, Faculty of Chemistry, Warsaw University of Technology, Noakowskiego 3, 00-664 Warsaw, Poland
* Correspondence: marcin.drozd.ch@pw.edu.pl (M.D.); elzbieta.malinowska@pw.edu.pl (E.M.); Tel.: +48-22-1821074 (M.D.); +48-22-1821145 (E.M.)

Abstract: Protein-based microarrays are important tools for high-throughput medical diagnostics, offering versatile platforms for multiplex immunodetection. However, challenges arise in protein microarrays due to the heterogeneous nature of proteins and, thus, differences in their immobilization conditions. This article advocates DNA-directed immobilization (DDI) as a solution, emphasizing its rapid and cost-effective fabrication of biosensing platforms. Thiolated single-stranded DNA and its analogues, such as ZNA® and PNA probes, were used to immobilize model proteins (*anti*-CRP antibodies and SARS-CoV nucleoprotein). The study explores factors influencing DDI-based immunosensor performance, including the purity of protein-DNA conjugates and the stability of their duplexes with DNA and analogues. It also provides insight into backfilling agent type and probe surface density. The research reveals that single-component monolayers lack protection against protein adsorption, while mixing the probes with long-chain ligands may hinder DNA-protein conjugate anchoring. Conventional DNA probes offer slightly higher surface density, while ZNA® probes exhibit better binding efficiency. Despite no enhanced stability in different ionic strength media, the cost-effectiveness of DNA probes led to their preference. The findings contribute to advancing microarray technology, paving the way for new generations of DDI-based multiplex platforms for rapid and robust diagnostics.

Keywords: DNA-directed immobilization; DNA-protein conjugates; self-assembled monolayers; surface plasmon resonance; conjugates purification; receptor layer formation

Citation: Karoń, S.; Drozd, M.; Malinowska, E. A Careful Insight into DDI-Type Receptor Layers on the Way to Improvement of Click-Biology-Based Immunosensors. *Biosensors* **2024**, *14*, 136. https://doi.org/10.3390/bios14030136

Received: 4 January 2024
Revised: 26 February 2024
Accepted: 2 March 2024
Published: 6 March 2024

1. Introduction

Microarrays, or multi-analyte assays, have served as efficient tools for high-throughput diagnostics, involving the miniaturization of various assays on a single substrate. They find applications in genetic diagnostics (DNA/RNA arrays) as well as proteomics and immunodiagnostics (protein/immunoarrays) [1–3]. Nonetheless, the potential of protein microarrays, as opposed to DNA arrays, is still constrained by a number of technological obstacles. While DNA is a relatively stable oligomer with well-defined physicochemical characteristics, practically independent of its sequence, proteins refer to a heterogeneous group of biomolecules that are generally more fragile than DNA [4]. As a result, selecting an optimal immobilization approach that assures protein availability and precise surface orientation is critical. While nucleic acids are commercially accessible with various chemical modifications, allowing for appropriate surface orientation, proteins are more diverse, making it challenging to develop immobilization methods with broad applicability [5].

Nowadays, it is highly desirable to design microarrays that enable numerous measurements in a row with a detection method that can be performed on a routine basis. Such an approach is possible when regeneration is conducted without harming the layer, or when it is possible to remove receptors and rapidly reconstruct the entire receptor layer [6–8].

The ability of complementary oligonucleotide strands to hybridize has been introduced into more complex assemblies, such as protein microarrays obtained via DNA-directed immobilization (DDI). This implementation enables miniaturized, rapid, low-cost, efficient, and site-specific fabrication of biosensing platforms. DDI requires conjugating antibodies with complementary DNA strands to those immobilized on the surface [8]. This functionalization has been employed in label-based [5,9] and label-free [10,11] immunoplatforms.

Directional immobilization of proteins through DNA anchors has been reported in the development of biosensors [12,13], i.e., for profiling of extracellular vesicles [5], detection of hormones [14], circulating cancer biomarkers [15], and viral pathogens [11]. DDI also found applications in protein arrays, as well as in platforms for multiplex kinetic analysis and cell organization [16]. Even though constructing a functional receptor layer in a multiplex format for the analysis of protein samples is much more challenging, several emerging problems are often overlooked in DDI. These include selecting an appropriate anti-fouling agent, optimizing the probe surface density, and purifying the conjugates. The attachment of DNA anchors to protein receptors can be realized by covalent methods and biological affinity [17]. Conjugating the two biomolecules is also quite troublesome to control, regardless of the strategy employed. Nevertheless, conjugate valency (DNA to protein ratio) aspects are also underestimated in constructing DDI-based bioreceptor platforms [4,18].

It should also be noted that negatively charged DNA chains tend to repel each other, resulting in inefficient hybridization, and problems with controlling the surface density of bioreceptors. Using DNA analogues instead of conventional DNA may improve detection accuracy because it can discern a perfect match from a single base-pair-mismatched strand. The interaction of the analogues and DNA is unaffected by the ionic strength of the buffer, and they can hybridize with the corresponding DNA in a low ionic strength environment in the absence of divalent cations [19]. We expect that the properties of new generations of nucleic acid analogues may still have undiscovered advantages for applications in the development of receptor layers via DDI.

In this work, we have thoroughly investigated the importance of the selected factors, such as the quality and purity of DNA-protein conjugates, the composition of the oligonucleotide monolayer, and the type and surface density of anchoring probes for the improvement of the quality of receptor layers for potential applications in label-free, DDI-based immunosensing. For this purpose, thiolated single-stranded DNA and its analogues—ZNA® and PNA probes (sequences of 15 or 48 nt.)—were examined as oligonucleotide probes for the immobilization of two model proteins. Mouse *anti*-CRP antibody and nucleocapsid protein of SARS-CoV were conjugated with ssDNA *ligand strand* sequence of 48 nucleotides, then purified through ion chromatography, and used for the formation of a regenerable DNA-based layer for detection of viral inflammation biomarkers. Based on the results of SPR and SPRi measurements, the influence of purity and stoichiometry of the conjugates on their capability for DDI-based immobilization was investigated. Additionally, the differences in the hybridization kinetics for the conjugates and free DNA and the influence of the type of oligonucleotide probes on hybridization efficiency were examined. The selection of the backfilling agent was carried out to provide the best receptor layer affinity and binding specificity. The relationship between the oligonucleotide probe charge and the protein-DNA conjugates' binding efficiency and stability was also determined. The findings presented in this article explore aspects relevant to the molecular recognition process at interphase for the further improvement of DDI-based immunoplatforms.

2. Materials and Methods

2.1. Reagents and Materials

Gold SPR slides (50 nm gold layer thickness) were purchased from Horiba Scientific (Palaiseau, France) (SPR imaging studies) and BioNavis Ltd. (Tampere, Finland) (multi-parametric SPR kinetic studies). DNA and ZNA® oligonucleotide sequences were purchased from Metabion GmbH (Planegg, Germany). A thiolated *PNA probe* was pur-

chased from Panagene Co., Ltd. (Daejeon, Republic of Korea). The sequences used in this study were as follows:

- *ligand strand* (48 nt.) 5′-NH_2-C_6-ATC AGT ACT TGT CAA CAC GAG CAG CCC GTA TAT TCT CCT ACA GCA CTA-3′
- *DNA probe (long)* (48 nt.) 5′-SH-C_6-TAG TGC TGT AGG AGA ATA TAC GGG CTG CTC GTG TTG ACA AGT ACT GAT-3′
- *DNA probe* (15 nt.) 5′-SH-C_6-TAG TGC TGT AGG AGA-3′
- *PNA probe* (15 nt.) 5′-SH-C_6-TAG TGC TGT AGG AGA-3′
- *ZNA® probe* (15 nt.) 5′-SH-C_6-TAG TGC TGT AGG AGA-(spermine)$_3$-3′

Additionally, 6-mercaptohexanol, poly(ethylene glycol) methyl ether thiol (average M_n = 800 Da) (referred to as *PEG-800*), polyclonal goat *anti*-mouse secondary antibody, polyclonal rabbit IgG antibody, sodium chloride, potassium chloride, sodium hydrogen phosphate, sodium dihydrogen phosphate and potassium dihydrogen phosphate were from Sigma-Merck (Poznań, Poland). Ammonia (25%), hydrogen peroxide (30%), sulfuric acid (96%), hydrochloric acid (35–37%), glycine and sodium hydroxide were from Chempur (Piekary Śląskie, Poland). *α*-hydroxy-*ω*-mercapto PEG (average M_n = 3.0 kDa) (referred to as *PEG-3k*) was from Rapp Polymere GmbH (Tübingen, Germany). Monoclonal mouse *anti*-hCRP antibody, clone line 6405 was from Medix Biochemica (Espoo, Finland). SARS-CoV Nucleocapsid recombinant protein expressed in *Escherichia coli* was from Thermo Fisher Scientific (Warsaw, Poland). proFIRE® Amine Coupling Kit for proteins (>5 kDa) was from Dynamic Biosensors GmbH (Munich, Germany). All solutions were prepared using deionized (DI) water (conductivity < 0.055 µS/cm at 20 °C, TOC < 1.0 ppb).

2.2. Surface Preparation of SPR Gold Slides and Ex Situ Immobilization of Oligonucleotide Probes

SPR gold-coated slides were rinsed with DI water and then cleaned using 15 min immersion in "basic piranha" solution (25% ammonia, 30% hydrogen peroxide, and DI water in volumetric ratios 1:1:3) at 70 °C. Next, slides were rinsed with deionized water, dried under compressed air, and soaked in "acidic piranha" solution (3:1 (*v*/*v*) mixture of conc. sulfuric acid and perhydrol) for 1 min. Subsequently, slides were rinsed with DI water, dried in a compressed air stream, and cleaned under UV/ozone (Ossila Ltd., Sheffield, UK) for 30 min. DNA, PNA, or ZNA® oligo probes were diluted to 0.5 µM solutions in phosphate-buffered saline (PBS) pH = 7.2 (unless stated otherwise). Such solutions (or mixtures with a backfilling agent—typically *PEG-800*—at a molar ratio of 1:4) were dispensed on a clean Au SPR slide by manual spotting (0.5–8 µL per spot) and incubated for 30 min. The whole Au surface was rinsed with DI water and covered with the backfilling agent—typically 50 µM aqueous solution of *PEG-800* for 20 min.

2.3. Conjugation of Receptor Proteins with ssDNA Anchors and Conjugates Purification

The conjugation process was carried out with amine-terminated *ligand strand* DNA oligonucleotide (3 nmol) and 200 µg of the protein: *anti*-hCRP antibody (M_w ~ 130 kDa, 1.54 nmol) or SARS-CoV nucleoprotein (M_w ~ 62.5 kDa, 3.2 nmol) using the proFIRE® Amine Coupling Kit, according to the developed conjugation protocol. In the first step, the *ligand strand* sequence was incubated for 20 min at room temperature with a molar excess of the crosslinker in a 500 mM Na_2HPO_4/NaH_2PO_4 buffer, pH 7.2, with 1.5 M NaCl. After removing the excess of the crosslinker by using Zeba™ spin desalting columns 7 K MWCO, the NHS ester-modified oligonucleotide was incubated overnight with 200 µg of the selected protein at 4 °C. Then, the protein-oligonucleotide conjugate was purified via preparative ionic chromatography using a proFIRE® instrument (Dynamic Biosensors, Munich, Germany). Separation was carried out by the gradient elution method in 50 mM phosphate buffer pH 7.2 with a linear increase of NaCl concentration (from 0.15 M to 1.5 M). After chromatographic purification, 12 fractions (with a volume of ~ 700 µL each) were collected. The concentration of DNA conjugates in each fraction was evaluated by a built-in optical detector operating at a fixed wavelength of 260 nm. In addition, the conjugates and their components were qualitatively characterized based on absorption spectra recorded in

the UV range (200–340 nm) using Lambda25 spectrophotometer (PerkinElmer, Waltham, MA, USA) equipped with quartz cuvettes with an optical path length of 1 cm.

2.4. Ex Situ Immobilization of Protein Conjugates by DNA-Directed Immobilization (DDI)

To immobilize protein-DNA conjugates, SPR slides modified with a selected type of oligonucleotide probe were used according to the protocol described in Section 2.2. Chromatographically purified fractions of the DNA-protein conjugates (in a concentration of ~100 nM in 50 mM phosphate buffer pH 7.2 with 150 mM NaCl) were dispensed as spots of 0.5 µL on the DNA-covered gold chip. After 1 h incubation, slides were rinsed with PBS and dried under compressed air.

2.5. Multi-Parametric SPR Measurements and Kinetic Analysis

Kinetic studies on the immobilization of thiolated oligonucleotide probes and their interactions with *ligand strand* target DNA and DNA-protein conjugates were carried out with an MP-SPR Navi™ 220A NAALI device equipped with an autosampler (BioNavis Ltd., Tampere, Finland). PBS pH 7.4 was employed as a running buffer at a 20 µL/min flow rate. Immobilization of the thiolated oligonucleotide probes and surface blocking was performed directly in a microfluidic system (both injections lasted 10 min at a flow rate of 20 µL/min), using the same reagents as for ex situ immobilization. PBS buffer pH 7.4 was injected into the reference channel as a negative control instead of conjugate. Consecutive injections of increasing concentrations of complementary DNA (*ligand strand*) and its conjugate with *anti*-hCRP antibody were carried out to determine the hybridization kinetics. In the case of the *ligand strand* DNA, the upper concentration level was 10.82 µM (dilution factor = 5), while for the DNA-*anti*-hCRP conjugate, the upper concentration level was 12.52 nM (dilution factor = 2). 100 mM sodium hydroxide (20 µL/min, 4 min) was used for regeneration between target injections. The kinetic evaluation of the complementary *ligand strand* DNA and *anti*-hCRP conjugates interaction with the *DNA probe* was performed with TraceDrawer® software, v 1.8 (Ridgeview Instruments AB, Uppsala, Sweden) and the SPR responses were fitted according to "one to one" kinetic model.

2.6. Surface Plasmon Resonance Imaging Measurements

The gold SPR slide covered with ex situ immobilized DNA/PNA/ZNA® oligonucleotide probes and blocked with a chosen backfilling agent was inserted into the SPRi Lab Plus instrument (Horiba, France). PBS buffer with 0.05% Tween20® (PBST) was employed as a running buffer. The injection of *ligand strand* (2.7 µM in PBST buffer) or the conjugate of DNA with *anti*-CRP antibody (90 nM in 50 mM phosphate buffer pH 7.2 with 150 mM NaCl) enabled real-time monitoring and comparison of different probes' suitability for the DNA-directed immobilization via oligonucleotide duplexes formation (manual injections, flowrate = 80 µL/min, ~5 min). In turn, the injections of unconjugated, polyclonal rabbit *IgG* antibody (10 µg/mL in PBST buffer) were carried out for studies on non-specific protein adsorption. Additionally, 100 mM sodium hydroxide was used for the regeneration between injections (80 µL/min, 4 min).

2.7. Surface ζ-Potential Measurements of Oligonucleotide Receptor Layers

Surface ζ-potential (SZP) measurements of Au substrates and receptor layers composed of self-assembled oligonucleotide probes (DNA, PNA, ZNA®) were carried out employing an indirect approach using a Zetasizer Nano ZS instrument (Malvern Panalytical Ltd., Malvern, UK), according to the manufacturer's protocol [20]. Depending on the expected surface charge, a solution of Malvern transfer standard DTS 1235 (10x diluted) in 10 mM phosphate buffer (pH 7.4) or a diluted solution of fabric softener Lenor® (also known as Downy®) in 10 mM phosphate buffer pH 7.4 was used as an anionic/cationic tracer, respectively. SPR slide fragments were mechanically cut to 5 × 4 nm and used as substrates for SZP measurements. After cleaning and immobilization of various oligonucleotide probes (as in Section 2.2), the substrates were glued to the table between the electrodes of

the measurement cell using cyanoacrylate glue. A series of measurements of the tracer's ζ-potential at increasing distances from the examined layer (in the range of 125–750 µm) enabled the calculation of the ζ-potential directly at the interphase. The calculations were based on the linear fitting and Equation (1) [21]:

$$\text{SZP} = \text{tracer } \zeta\text{-potential} - \text{intercept (d = 0 µm)} \quad (1)$$

3. Results and Discussion

The development of functional and reproducible bioreceptor layers for molecular interaction studies using "click-biology" methodologies (such as DNA-directed immobilization) requires preserving possibly unaffected bioreceptor activity and efficient attachment of DNA anchor tags. The concept of "click biology"—by analogy with the more widely known term "click chemistry"—represents the convenience obtained by effortlessly attaching two moieties through bio-molecular interactions. It often refers to biotransformation processes, DNA ligation, or formation of highly ordered structures via hybridization [22]. Preferably, each bioreceptor molecule is expected to be linked to one molecule of anchor DNA, and the conjugates should be separated from the unbound components. Meeting all the prerequisites allows efficient loading of the transducer's surface binding sites with protein-DNA conjugates. The problem of the quality of DNA-protein conjugates (as well as other receptor layers based on immobilization of tagged receptors) is often overlooked in protocols developed to date, which can negatively affect the analytical performance of as-constructed biosensors. In the case of inadequately purified conjugates, uncontrolled dilution of protein receptors may occur due to the competition of tagged proteins and free tags (e.g., DNA anchors) for binding sites. It negatively affects the sensitivity. In addition to diluting receptor layers by blunt DNA anchors, the presence of multiple-tagged receptors with disturbed stoichiometry (DNA tag to protein ratio >> 1) is also unfavorable. A multiple-tagged protein—especially in analyte-binding regions—may exhibit altered analyte binding capacity. Therefore, it is vital to control the quality of DNA-labeled receptors at the synthesis stage and to carry out the post-synthetic preparative purification of DNA-protein conjugates. The goal is to maximize the fraction of DNA-tagged proteins characterized by a 1:1 DNA-to-protein stoichiometry.

3.1. Purification of DNA-Protein Conjugates and SPR-Based Quality Control for DDI

Amine coupling with the use of various NHS-based linkers, such as DBCO-NHS and maleimide-NHS, is a robust and well-characterized method of covalent conjugation of DNA with proteins [23,24]. Such conjugates are typically characterized by chromatographic methods and gel electrophoresis [25–27]. To provide efficient separation of DNA-protein conjugates, an already established protocol for preparative separation by ion chromatography has been employed. Variation in the retention times of DNA and other components occurs due to differences in the relative charge of the separated biomolecules. The strongly anionic character of DNA allowed for lengthened retention times of their conjugates with proteins on the ion exchange column with respect to native proteins.

In our study, pre-activated, 48-oligonucleotide-long NHS ester-terminated DNA anchors (*ligand strand* sequence) were conjugated with proteins. As model protein receptors were taken: (i) *anti*-hCRP monoclonal antibody (chosen for detection of CRP as inflammatory biomarker) and (ii) SARS-CoV nucleoprotein (receptor for serological biomarkers of COVID-19). The amine coupling reaction mixtures were subjected to preparative chromatographic separation using gradient elution and representative chromatograms are shown in Figure 1. As can be seen, non-conjugated proteins are characterized by the shortest retention times. The attachment of a single DNA strand (1:1-type conjugates) and more (multiple-tagged conjugates) resulted in a significant interaction enhancement, resulting in gradually longer retention times. Unbound DNA leaves the column as the last, as it exhibits the most anionic character. In both cases, shown in Figure 1, DNA-protein conjugates were found in the post-reaction mixture. To confirm the correct assignment of the observed

signals to the respective fractions, chromatograms from the analysis of a sample containing only DNA and a mixture of protein and DNA (unconjugated) are shown in Figure S1a. In addition, the effect of NHS-based crosslinker on DNA ligand strand was examined to rule out the possibility of its spontaneous crosslinking (Figure S1b). A more in-depth discussion on the selectivity of the amine coupling and reactivity of NHS esters with exocyclic amine groups of nucleobases and the differences in coupling efficiency for individual proteins can also be found in Supplementary Material.

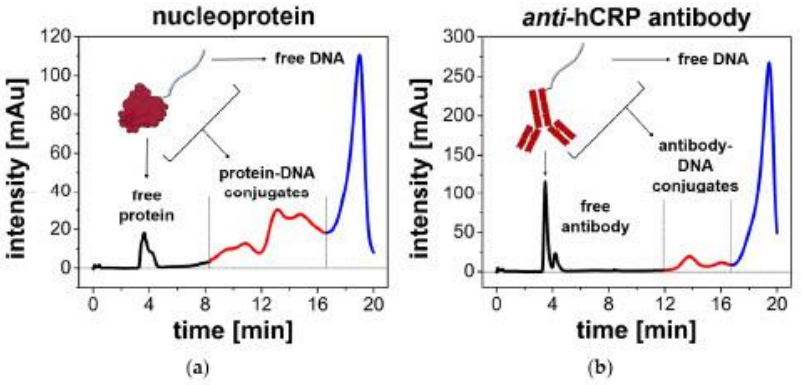

Figure 1. Chromatograms showing the results of separation of DNA-SARS-CoV nucleoprotein conjugates (**a**) and DNA-*anti*-hCRP antibody conjugates (**b**). The colors indicate fractions of free protein (black line), DNA-protein conjugates (red line), and free DNA (blue line). The chromatogram was captured using a spectrophotometric detector at $\lambda = 260$ nm.

Similarly, analysis of subtle differences in the UV absorption spectra allowed us to observe differences in the compositions of the main chromatographic fractions. The normalized absorption spectra of the free DNA *ligand strand*, the free antibody, and the two fractions of their conjugates are shown in Figure S2, and the detailed discussion on applicability of this method for quality control of DNA-protein conjugates was provided in Supplementary Material [24,28].

The relevance of the purification process of DNA-protein conjugates was evaluated in our study by comparing their interaction kinetics with *DNA probes* immobilized on SPR slide (Figure 2a). Normalized sensograms allow a comparison of the binding kinetics of two fractions of DNA-mAb *anti*-hCRP conjugates (with 1:1 stoichiometry and multiply tagged) to a layer of immobilized *DNA probes*. SPR responses were also recorded for the reaction mixture after conjugation but without chromatographic purification and for free *ligand strand* sequence (corresponding to DNA tag) as a reference. As shown in Figure 2a, according to our expectations, the significant difference in the SPR response profile for the conjugates before and after purification indicates a substantial contribution of binding unconjugated DNA strands to the receptor layer. The flat, nearly linear evolution of the SPR signal at the step of conjugate association indicates a noticeably slower kinetics of its binding to the surface, typical for bulky ligands whose binding is further limited by diffusion processes [28]. The apparent difference in the association curves confirms that the hybridization of unconjugated *ligand strand* DNA is additionally favored kinetically due to lower steric constraints.

To further analyze the binding kinetics of free DNA ligands and purified conjugates, association and dissociation rates (k_a, k_d) and equilibrium dissociation constant (K_D) were further determined, as shown in Figure 2b,c. K_D levels of several nM indicate the high affinity of both components to immobilized DNA probes, which will promote their effective binding to the surface at low concentrations. The lower K_D value, which characterizes the binding of *DNA probes* to the free *ligand strand* sequence (1.95 nM) compared to binding

of DNA-*anti*-CRP antibody conjugates (5.91 nM), confirms the thermodynamic preference of binding free ligands over their protein conjugates. The observed, more than 3-fold, difference in K_D values will translate into lower durability of probe DNA complexes with DNA-protein conjugates when compared to regular DNA–DNA duplexes. The detailed parameters of the kinetic model employed as well as the obtained results are summarized in Table S1. Residuals between fitted curves and experimental data for interactions of DNA probe with free ligand strand DNA and DNA-*anti*-CRP antibody conjugate were shown in Figure S3. Given both the relatively low rate of DNA conversion during amine coupling with proteins and the proven preference for binding non-conjugated DNA, ensuring adequate purity of DNA-protein conjugates appears particularly important. Such an approach should be reflected in an improvement of the surface density of protein receptors during DNA-directed immobilization.

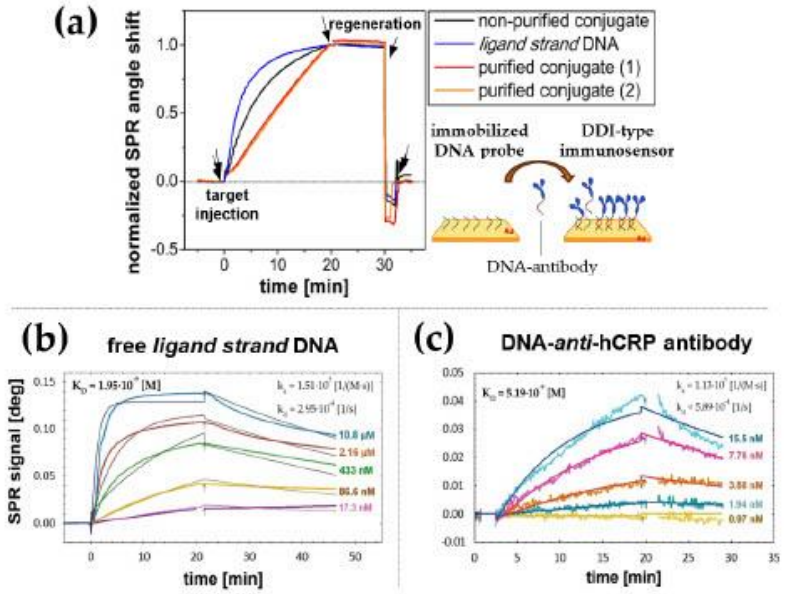

Figure 2. SPR responses representing the binding of targets: free DNA and DNA-antibody conjugates at different purification levels (2 fractions of purified conjugates and a non-purified reaction mixture), by an immobilized *DNA probe* (**a**). SPR responses to injections of a series of *ligand strand* DNA (**b**) and DNA-*anti*-CRP antibody conjugate (**c**) against the immobilized *DNA probe*. Colored curves represent experimental results, and black curves illustrate the fitting according to the 1:1 kinetic model.

3.2. Development of the Oligonucleotide Probe Layer Composition for DDI

3.2.1. Selection of the Oligonucleotide Anchor Type

The formation of oligonucleotide duplexes through DNA-directed immobilization is based on strong and spontaneous Watson–Crick base pair interactions. Nevertheless, a specific activation barrier exists involving electrostatic repulsion of phosphate backbones of complementary DNA strands [29]. This phenomenon negatively affects both the hybridization kinetics and the thermodynamic stability of duplexes of immobilized probes and DNA-protein conjugates. Also, at an earlier stage, electrostatic repulsion may impair self-assembly of thiolated probes on Au substrates. It can result in a reduced effective surface density of protein receptors immobilized by DDI. To overcome the mutual repulsion of DNA strands, buffers with high ionic strength are typically required. These provide screening of the negative charge by the cations present in solution [30]. However, this

approach imposes limitations with respect to the composition of immobilization and hybridization media. Maintaining a high ionic strength can also be troublesome in real-world applications, as it results in the risk of dissociation of DDI-immobilized receptors during washing steps.

With this in mind, we analyzed the possibility of using DNA analogues as immobilized DDI probes. To attenuate the anionic character of oligonucleotide probes, two DNA analogues of the same sequence (15 nb length) were examined: thiol-terminated peptide nucleic acid (PNA-SH) and heterobifunctional DNA with ω-mercaptohexyl and spermine trimer at both terminals, known as zip nucleic acid (ZNA®) [31,32]. With the replacement of DNA with PNA and ZNA® analogues, the polyanionic nature of receptors is expected to be attenuated, which should facilitate the binding of complementary sequences and the persistence of duplexes. As shown in Figure 3a, DNA analogues (ZNA® and PNA) had significantly lower immobilization efficiency than regular DNA. The surface density of ZNA® and PNA reached 17% and 19% of the density observed for the *DNA probe*, respectively [33,34].

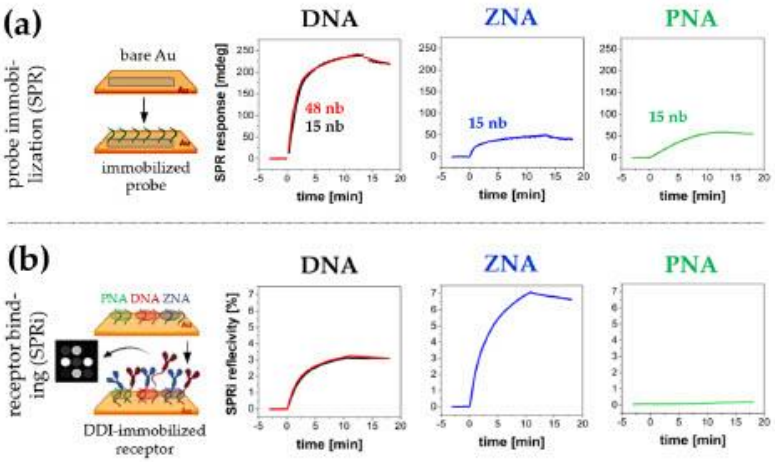

Figure 3. (a) Comparison of SPR responses, which reflect direct chemisorption of thiol-terminated DNA, ZNA® and PNA probes on the surface of a gold SPR transducer during probes immobilization. (b) SPRi responses representing hybridization of the oligonucleotide probes with fully complementary *ligand strand* sequence. In both cases, red sensograms refer to a "long" *DNA probe* (48 nb) and black sensograms refer to a "short" *DNA probe* (15 nb).

A plausible explanation for the observed phenomena lies in the complexity of the interaction mechanism of the probes with the gold surface. The surface density and spatial orientation of probes (especially for relatively long oligonucleotide sequences) are also significantly affected by direct interactions of side chains with the gold surface [35]. Both PNA, rich in electron-donor groups capable of interacting with gold atoms, and DNA labelled with oligoamine tag (ZNA®), promote multidentate tethering. Such a phenomenon results in the horizontal alignment of oligonucleotide strands on the gold surface, thus limiting the maximum achievable surface density and capability of subsequent hybridization. Literature reports suggest that PNA chemisorption is a two-step process and a high probe concentration in the immobilization medium is needed to obtain the desired conformation [33]. Given the reported problems in PNA SAMs formation, as well as their generally high cost and the inconsistency of preparation protocols (some recommend the addition of trifluoroacetic acid and/or organic solvent to improve PNA solubility [34]), we concluded that they were not competitive with classical DNA probes and did not continue further optimization.

In the case of ZNA®, relatively low surface density did not adversely affect the hybridization efficiency in PBS buffer observed by means of SPRi—on the contrary, as can be seen in Figure 3b, the obtained response of the ZNA® receptor layer was nearly twice as high as that observed for the DNA layer. It can be explained by lowering the thermodynamic barrier for the *ligand strand* binding reaction due to the attenuation of electrostatic repulsion of DNA strands at the initial stage of duplex formation. High hybridization efficiency at low surface density makes the *ZNA® probe* a good candidate as an alternative to DNA as high-binding anchors for DNA-directed immobilization. In contrast, the formation of PNA–DNA duplexes was not observed under the examined conditions.

In parallel with the study of DNA analogues, we also verified the impact of the DNA oligonucleotide probe (regular—15 nb vs. long—48 nb) on its ability to self-assemble on gold. As shown in Figure 3a (left graph), both injected sequences (*DNA probe* and *DNA probe (long)*, respectively) underwent spontaneous chemisorption. The similar values of the resonant angle shifts (236 mdeg and 239 mdeg, respectively) at the end of the association stage reflect the similar surface density of the associated mass. However, given the significant difference in molecular weight of regular and long *DNA probes* (mass ratio 1.0: 3.05), the observed values of SPR angle shift indicate an approximately threefold higher (expressed in molar terms) surface density of short *DNA probes* [36]. Given the observed lack of a noticeable difference in the binding capacity of the *ligand strand* sequence (Figure 3b—left graph), probes with a length of 15 nb were used during further studies. Such probes proved equally effective as the full-length complementary sequences for capturing oligonucleotide-tagged proteins in DDI.

To evaluate the influence of the type of oligonucleotide probe on its surface charge, values of surface ζ-potential of Au substrates before and after modification with *DNA* and *ZNA® probes* were determined (Figure 4). As can be seen, the introduction of a terminal polycationic chain into the structure of DNA dramatically alters its surface charge. At near neutral pH (7.4), both bare gold (*via* anions coordinatively bound to the surface) [37], as well as Au modified with *DNA probe*, as expected, are characterized by an anionic surface (represented by a negative surface ζ-potential (ZP), −59.9 mV and −38.2 mV, respectively). In contrast, for ZNA®, the measured ZP value was +47.8 mV. It can be expected that these significant differences in the character of the surface can affect the stability of oligonucleotide duplexes employed in DDI. The surface charge can also affect non-specific interactions of sample components with immobilized probes [38,39].

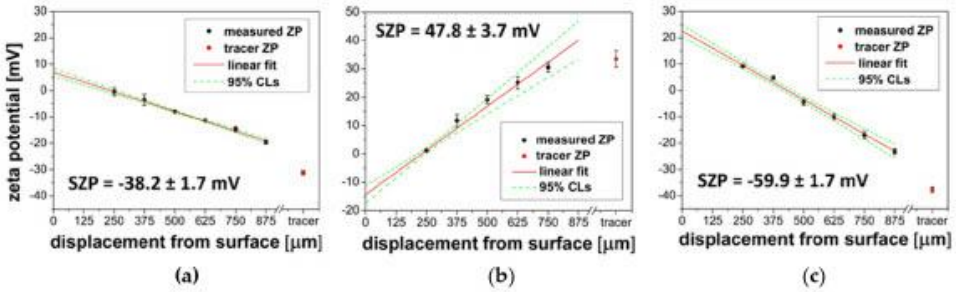

Figure 4. Plots of measured ζ-potential of tracer particles against displacement from the surface of the following: (**a**) Au@DNA probe, (**b**) Au@ZNA® probe, (**c**) bare Au. Red dots represent native ζ-potential of the tracer (undisturbed by the measured surface). Extrapolated ZP values for d = 0 were used to indirect determination of surface ζ-potential.

The stabilities of DNA–DNA and ZNA®–DNA duplexes were compared by SPR studies in a medium with low ionic strength. For this purpose, a series of equimolar *ligand strand* sequence injections in buffer with varying Na^+ concentration (regulated by the concentration of NaCl in phosphate buffer) were carried out. Examples of recorded SPR

responses and SPR signal values as a function of Na^+ concentration for *DNA* and *ZNA® probes* are shown in Figure 5. Contrary to our expectations, beyond the previously observed higher efficiency of duplex formation in PBST buffer, no other advantages of the ZNA® receptor layer over the DNA layer were observed.

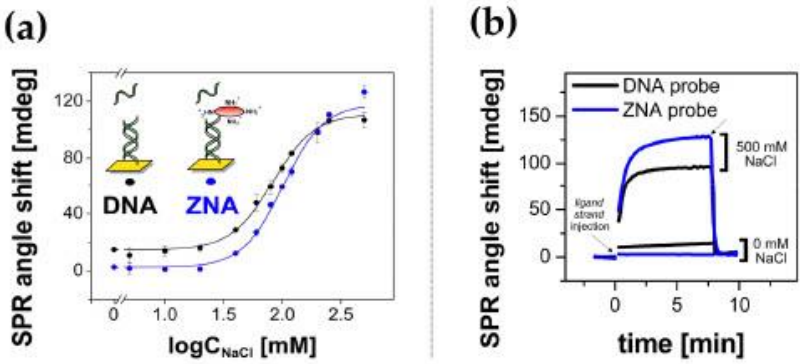

Figure 5. (**a**) The relationship between *ligand strand* target concentration and its hybridization efficiency with immobilized DNA (black dots) and *ZNA® probes* (blue dots). Relative signal values were calculated from differential SPR sensograms after the association equilibrium was reached (n = 2), (**b**) exemplary SPR responses recorded for *ligand strand* injections in high ionic strength medium (10 mM phosphate buffer pH 7.4 with 500 mM NaCl) and low ionic strength medium (10 mM phosphate buffer pH7.4 with 0 mM NaCl). Distilled water was used as the running buffer.

Notably, no enhanced efficiency of ZNA®–DNA duplex formation was observed in low ionic strength media, as evidenced by the similar hybridization efficiency profiles shown in Figure 5a. Likewise, both types of hybrids showed the typical DNA tendency to rapid, water-induced cleavage of the double helix, as can be seen in the sensograms provided in Figure 5b. Given the lack of significant advantages of *ZNA® probes*, it was therefore decided to prefer cheap and readily available *DNA probes* for anchoring DNA-protein conjugates in the framework of further studies. A summary of the applicability of DNA and its analogues as probes for DDI can be found in Table S2. It lists their immobilization and hybridization efficiencies and the benefits of their use.

3.2.2. Selection of Non-Receptor Components

Another aspect determining the application potential of Au substrates with immobilized oligonucleotide probes in DDI-based biosensor design is their resistance to non-specific adsorption of proteins. The origin of such interferences can be both protein conjugates and components of matrices of real samples. For DDI-based biosensors, hybridization via DNA tags should be the only effective way to anchor protein receptors. Therefore, it is necessary to minimize passive adsorption and surface fouling by other proteins. The appropriately designed receptor layer gives a lower background response and ensures comfortable and efficient regeneration under controlled conditions.

As shown in Figure 6a, single-component monolayers composed only of oligonucleotide probes do not protect against the adsorption of native rabbit IgG antibodies chosen as a model interferent. It is evidenced by a significant increase of SPRi signals, indicating fouling of DNA, ZNA®, and PNA monolayers under measurement conditions suitable for DDI-based sensors. Remarkably, the surface charge of the layer does not significantly affect the adsorption process as both *DNA* and *ZNA® probes* are susceptible to protein fouling. In contrast, bare gold was characterized by several times lower IgG adsorption (~10% of the value observed for *DNA probe*—see Figure 6a). The results suggest that electrostatic interac-

tions do not play a dominant role in the adsorption of proteins on oligonucleotide-modified gold surfaces.

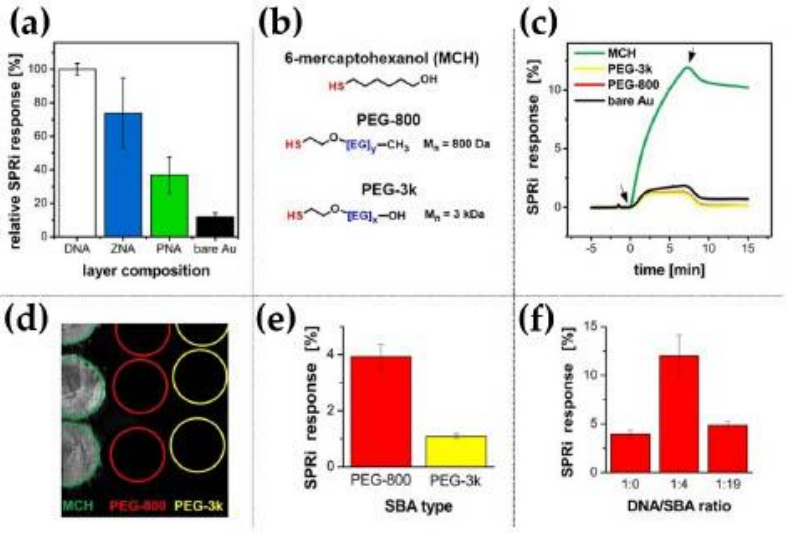

Figure 6. (**a**) Normalized SPRi signals recorded as responses of DNA, PNA, and ZNA® monolayers and bare gold to injection of unconjugated rabbit IgG antibody (10 µg/mL), (**b**) structures of thiolated backfilling agents (BA) used within this study, (**c**) SPRi sensograms (left), (**d**) SPRi differential image depicting the interactions of monolayers composed of backfilling agents (MCH, *PEG-800*, *PEG-3k*) and bare gold with unconjugated rabbit IgG antibody (10 µg/mL), (**e**) and (**f**) SPRi signal values, which represent hybridization efficiencies of mixed monolayers containing immobilized *DNA probe* and *ligand strand* sequence, as a function of (**e**) type of PEG-based backfilling agent used (molar ratio of *DNA probe* to BA = 1:4), (**f**) molar ratio of DNA probe to *PEG-800* in the immobilization mixture (n = 3).

A careful selection of backfilling agents was carried out to ensure better assembly of oligonucleotide probes on the Au substrate. The resulting mixed monolayer is expected to be characterized by an increased ability to capture DNA *ligand strand* together with the improvement of anti-fouling properties of the obtained receptor layer [38–40]. To choose the optimal backfilling agent, three thiol-terminated polar ligands differing in size and structural flexibility were compared: 6-mercaptohexanol, oligo (methyl ether thiol) with a molecular weight of 800 Da (*PEG-800*), and thiolated PEG with a molecular weight of 3 kDa (*PEG-3k*) (Figure 6b). SPRi studies of the interactions between native rabbit IgG antibody and monolayers of individual backfilling agents showed that the tested components have different anti-fouling properties. The effectiveness of the blocking agent increases dramatically with the introduction of flexible and highly hydrophilic polyether segments into its structure, which can be easily observed in the case of *PEG-800* and *PEG-3k*, (sensograms in Figure 6c and SPR image in Figure 6d). PEG derivatives are very effective in suppressing the adsorption of a model protein interferent, in contrast to 6-mercaptohexanol, which is typically employed as a component of DNA biosensors.

Covering the surface of a biosensor with a bulky surface-blocking agent carries the risk of creating a steric hindrance to surface processes. Shielding of oligonucleotide probes by long-chain PEG ligands can hinder the anchoring of DNA-protein conjugates during the DDI process. Therefore, the effect of both PEG-type backfilling agents (in the form of a mixed layer with *DNA probes*) on *ligand strand* sequence binding capacity is shown

in Figure 6e. The significant, nearly 4-fold, decrease in hybridization efficiency for the *PEG-3k*-containing mixed monolayer compared to the analogous *PEG-800*-containing layer confirms the significance of the above-postulated steric effect on the efficiency of DNA-directed immobilization. Therefore, employing *PEG-800* as a component of the receptor layer for immobilizing DNA-protein conjugates appears to be a reasonable compromise that combines receptor binding efficiency and good anti-fouling properties.

Further, the effect of the surface density of *DNA probes* on the binding efficiency of the complementary sequence was also tested. For this purpose, *DNA probes* were co-immobilized with thiolated *PEG-800* as a dilution agent at different molar ratios. It was shown that the "diluted" layer obtained by co-adsorption of *DNA probe* with *PEG-800* at a molar ratio of 1:4 showed more than 120% better binding efficiency than an analogous layer formed by two-step immobilization. In such an approach, surface blocking followed the incubation of the Au substrate with an undiluted *DNA probe*. This effect was observed over a wide range of DNA to *PEG-800* molar ratios. Finally, at a 19-fold excess of the blocking agent, the layer reached a similar binding capacity as the layer fabricated with an undiluted receptor (Figure 6f). At first glance, the surprising result indicates the significant influence of spatial freedom on solid-phase hybridization capacity. As we expect, this effect will be further enhanced when more bulky ligands in the form of DNA-tagged protein receptors are employed. Presumably, dense DNA layers, through their high charge concentration and insufficient freedom to adopt a double-helix conformation, are not conducive to efficient hybridization. For this reason, mixed-type layers (*DNA probe* to *PEG-800* molar ratio = 1:4) were used to further study DNA-based layers.

However, it should be emphasized that the optimal surface density (expressed as the ratio of DNA probe to PEG-800) may vary depending on the length and structure of the specific oligonucleotide probe (including the length of the aliphatic linker or the presence of non-binding spacer). Therefore, given the possibility of individual design of DNA anchor sequences depending on the application, we have given up more detailed optimization in this field. In turn, for *ZNA® probes* (as molecules of partially neutralized global charge and characterized by a relatively low probe surface density—see Figure 3a), backfilling was scheduled as a separate step after the self-assembly of undiluted *ZNA® probes* on the Au surface.

To demonstrate that DNA and ZNA® anchoring layers with a previously optimized composition (mixed layers of oligonucleotide probes and *PEG-800*) provide good quality substrates for DDI, three injections of the components of the receptor layers and the model target were carried out sequentially. As shown in Figure 7, consecutive injections of unconjugated *ligand strand* (500 nM), mouse IgG antibody-DNA conjugate (40 nM—based on DNA concentration), and *anti*-mouse IgG (10 µg/mL) resulted in sensor responses consistent with those expected from previous experiments. The ability to hybridize with free DNA ligands and their conjugates was demonstrated by immobilized *DNA* and *ZNA® probes*. The first provided a slightly higher surface density of hybridized *ligand strand* represented by the observed reflectivity shifts (3.49% for DNA vs. 3.25% for ZNA®), while for DNA-antibody conjugates the binding efficiency was slightly higher for *ZNA® probes* (6.14% for ZNA® vs. 5.48% for DNA). In both cases, the immobilized antibodies showed the capacity for immunoreaction with *anti*-mouse IgG antibodies used as model analytes. The analyte binding efficiency (from a sample containing the target antibody at a concentration of 1 µg/mL) was readily observable in real time using SPRi (see inset in Figure 7).

The observed reflectance changes for both types of layers were very similar (4.6% for DNA and 4.7% for ZNA®) with a complete lack of response for the PNA layer (for which, however, no oligonucleotide and protein receptors bound to the surface after immobilization were detected). It indicates a significant correlation between the surface density of receptors immobilized via DDI and the efficiency of immunoreaction. These conclusions are similar to the findings of Simon et al. for studies of the formation of PNA–DNA and DNA–DNA duplexes in monolayers [41].

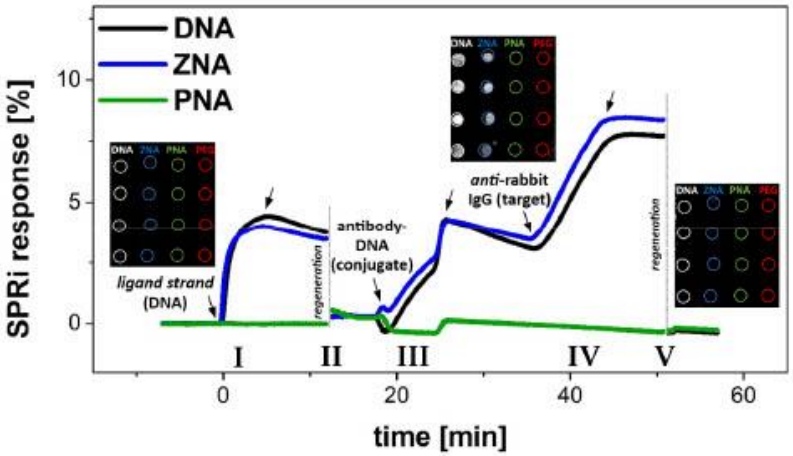

Figure 7. Average values of SPRi signal changes for the optimized composition of DNA-modified layer (co-immobilization of *DNA probe* and *PEG-800* at molar ratio 1:4, (0.1 µM *DNA probe* + 0.4 µM *PEG-800*), PNA- and ZNA®-modified layer (immobilization of *PNA* and *ZNA® probe* followed by surface blocking with *PEG-800*). The sensograms show the subsequent processes: (I) binding of unconjugated *ligand strand* sequence (preliminary quality control of the immobilized probes), (II) surface regeneration by means of injection of 50 mM NaOH, (III) injection of DNA-*anti*-hCRP antibody conjugate, (IV) injection of *anti*-mouse IgG (as model analyte), (V) complete regeneration of DDI-based biosensor. PBST buffer pH 7.4 was used as a running buffer and for all dilutions. Insets show differential SPRi images, which visualize the observed differences in reflectivity for different oligonucleotide probes.

Equally important from the point of view of the reusability of DDI biosensor substrates is the observed excellent regeneration efficiency. Injection of 50 mM NaOH—responsible for the breakdown of the double helix—at the same time ensures very efficient removal of immunocomplexes of antibody-DNA conjugates with the captured secondary antibodies. The signal recovery to the baseline level, i.e., before immobilization of *DNA/ZNA® probes*, is observed after a single regeneration cycle (SPR signal increase does not exceed 0.2% for each of the tested oligonucleotide probe), as shown in Figure 7. It confirms good anti-fouling properties of the developed DDI platforms as well as their stability under immobilization, analyte binding, and regeneration conditions. Notably, the results of a parallel experiment carried out using SARS-CoV nucleoprotein-DNA conjugates and anti-nucleoprotein mAb turned out to be very similar. This observation points to the major advantage of the developed strategy, which is its versatility—the immobilization occurs in a similar manner and conditions, even for receptor proteins of significantly different structures and properties.

The appropriate design of the anchor layer has been shown to provide both efficient "click-biology-based" assembly of receptors on oligonucleotide platforms and enable their interaction with model analytes. Ultimately, matrix-type platforms with receptor proteins of different origin (such as recombinant antigens or monoclonal antibodies) are intended to be used for the construction of multiplex biosensors. They can operate both in a label-free format and as highly sensitive platforms employing additional optical labelling, which is currently the subject of our research studies. Such biosensors can find application in detection of various targets, e.g., viral disease biomarkers (i.e., specific antibodies or biomarker-like antigens) in real samples.

4. Conclusions

DNA-directed immobilization as a strategy for receptor layer assembly has proven to have many advantages over traditional, covalent approaches. It employs only hydrophobic and/or ionic interactions between the biomolecules efficient and reversible coupling. DNA anchors allowed for rapid layer regeneration and re-immobilization without using additional reactants. The immobilization reaction occurs in mild conditions (pH about 7.0, regardless of the pI of the protein). DNA as the anchoring molecule is relatively cheap, readily available, stable, and can be stored for a long time without risk of degradation. The only disadvantages are the need for protein-DNA conjugation, careful and time-consuming conjugate purification, and relatively low coupling efficiency, leading to protein loss at the conjugation stage. We have thoroughly investigated the impact of a number of aspects important to the fabrication of protein biosensors through DDI. The importance of the synergistic effect of factors such as the quality and purity of DNA-protein conjugates, the composition of the oligonucleotide monolayer, and the type and surface density of anchoring probes has received little awareness so far, which may have resulted in suboptimal analytical performance of DDI-based biosensors. Our study demonstrated key differences in the kinetics and thermodynamics of hybridization between unconjugated DNA and its conjugates with *anti*-CRP antibodies and SARS-CoV nucleoprotein. The lower K_D value (1.95 nM) of *ligand strand* binding than that of the conjugates (5.91 nM) confirms the thermodynamic preference for binding free ligands over their protein conjugates. A significantly lower binding rate and increased protein-DNA conjugate volume have been shown to alter its reactivity and binding specificity in hybridization reactions with immobilized, complementary probes. It was reflected in the use of anchor layers with low density of oligonucleotide probes and appropriate backfilling agents with improved anti-fouling properties (preferably based on PEG derivatives). Next, we compared three types of thiolated oligonucleotide anchors (based on regular DNA and their analogues: PNA and ZNA®) for the construction of DDI platforms. We have chosen standard DNA anchors as the most cost-effective and virtually inferior to their ZNA® analogues regarding the facility and efficiency of immobilization on gold and stability of DDI duplexes with protein receptors. Mixed monolayers composed of DNA and ZNA® with an optimized composition have proven to be high-binding and regenerable platforms for constructing immunosensors through a DDI strategy. The appropriate surface density and retained high affinity of the DDI-immobilized receptors allows for the label-free immunodetection of protein analytes of diagnostic significance, while also providing excellent regenerability and reusability of the platforms. We believe that the proposed improvements in DDI technology will enable its widespread implementation in the construction of versatile protein arrays based on platforms routinely employed in conventional DNA arrays.

Supplementary Materials: The following supporting information can be downloaded at https://www.mdpi.com/article/10.3390/bios14030136/s1, Figure S1: (a) Chromatograms showing the results of separation of unconjugated SARS-CoV nucleoprotein (solid black line) and the mixture of unconjugated SARS-CoV nucleoprotein with ligand strand DNA (dashed red line). The arrows indicate fractions of free protein (retention time around 3.5 min) and unconjugated DNA (retention time around 18 min). (b) Chromatograms of ligand strand sequence before (solid black line) and after treatment with NHS-based crosslinker (dashed red line) in the absence of protein. Chromatograms were captured using a spectrophotometric detector at $\lambda = 260$ nm [26,27,42–45]; Figure S2: Normalized absorption spectra of selected fractions of post-conjugation mixture as a result of DNA-anti-hCRP antibody conjugate separation; Figure S3: Residuals between fitted curves and experimental data for interactions of *DNA probe* with fre-e *ligand strand* (a) and DNA-*anti*-CRP antibody conjugate (b); Table S1: Detailed statistics data characterizing the used kinetics binding model; Table S2: A comparison of the different types of oligonucleotide probes examined within this study.

Author Contributions: Conceptualization, S.K. and M.D.; Formal analysis, M.D. and E.M.; Funding acquisition, E.M.; Investigation, S.K. and M.D.; Methodology, S.K. and M.D.; Supervision, M.D. and E.M.; Visualization, S.K. and M.D.; Writing—original draft, S.K. and M.D.; Writing—review & editing, M.D. and E.M. All authors have read and agreed to the published version of the manuscript.

Funding: This work was financially supported by the National Centre for Research and Development in Poland under the Smart Growth Operational Programme co-financed by the European Regional Development Fund (grant no. POIR.01.01.01-00-0638/20 "Development of construction and technology for the production of miniature diagnostic devices for rapid detection of SARS CoV-2 virus in POCT mode") and Warsaw University of Technology. We would like to acknowledge the financial support (MP-SPR platform funding) from the Ministry of Education and Science, Poland, grant number 7015/IA/SP/2019.

Institutional Review Board Statement: Not applicable.

Informed Consent Statement: Not applicable.

Data Availability Statement: The data presented in this study are available on request from the corresponding author.

Conflicts of Interest: The authors declare no conflicts of interest. The funders had no role in the design of the study; in the collection, analyses, or interpretation of data; in the writing of the manuscript; or in the decision to publish the results.

References

1. Aparna, G.M.; Tetala, K.K.R. Recent Progress in Development and Application of DNA, Protein, Peptide, Glycan, Antibody, and Aptamer Microarrays. *Biomolecules* **2023**, *13*, 602. [CrossRef]
2. Li, S.; Song, G.; Bai, Y.; Song, N.; Zhao, J.; Liu, J.; Hu, C. Applications of Protein Microarrays in Biomarker Discovery for Autoimmune Diseases. *Front. Immunol.* **2021**, *12*, 645632. [CrossRef]
3. Walter, J.; Eludin, Z.; Drabovich, A.P. Redefining Serological Diagnostics with Immunoaffinity Proteomics. *Clin. Proteom.* **2023**, *20*, 42. [CrossRef]
4. Watson, E.E.; Winssinger, N. Synthesis of Protein-Oligonucleotide Conjugates. *Biomolecules* **2022**, *12*, 1523. [CrossRef]
5. Brambilla, D.; Sola, L.; Chiari, M. Advantageous Antibody Microarray Fabrication through DNA-Directed Immobilization: A Step toward Use of Extracellular Vesicles in Diagnostics. *Talanta* **2021**, *222*, 121542. [CrossRef]
6. Langer, A.; Hampel, P.A.; Kaiser, W.; Knezevic, J.; Welte, T.; Villa, V.; Maruyama, M.; Svejda, M.; Jähner, S.; Fischer, F.; et al. Protein Analysis by Time-Resolved Measurements with an Electro-Switchable DNA Chip. *Nat. Commun.* **2013**, *4*, 2099. [CrossRef]
7. Cléry, A.; Sohier, T.J.M.; Welte, T.; Langer, A.; Allain, F.H.T. SwitchSENSE: A New Technology to Study Protein-RNA Interactions. *Methods* **2017**, *118–119*, 137–145. [CrossRef]
8. Washburn, A.L.; Gomez, J.; Bailey, R.C. DNA-Encoding to Improve Performance and Allow Parallel Evaluation of the Binding Characteristics of Multiple Antibodies in a Surface-Bound Immunoassay Format. *Anal. Chem.* **2011**, *83*, 3572–3580. [CrossRef]
9. Huang, S.; Wang, W.; Li, J.; Zhang, T.; Liang, Y.; Wang, Q.; Jiang, Z. Multifunctional DNA Mediated Spatially Confined Assembly for Antibody Orientation: Surpassing Sensitivity and Accuracy for Rituximab Detection. *Chem. Eng. J.* **2021**, *419*, 129613. [CrossRef]
10. Ünlü, N.L.; Kanik, F.E.; Seymour, E.; Connor, J.H.; Ünlü, M.S. DNA-Directed Antibody Immobilization. In *Biosensors and Biodetection*; Humana Press: New York, NY, USA, 2017; Volume 1571.
11. Seymour, E.; Daaboul, G.G.; Zhang, X.; Scherr, S.M.; Ünlü, N.L.; Connor, J.H.; Ünlü, M.S. DNA-Directed Antibody Immobilization for Enhanced Detection of Single Viral Pathogens. *Anal. Chem.* **2015**, *87*, 10505–10512. [CrossRef]
12. Bernardinelli, G.; Oloketuyi, S.; Werner, S.F.; Mazzega, E.; Högberg, B.; de Marco, A. A Compact Nanobody-DNAzyme Conjugate Enables Antigen Detection and Signal Amplification. *New Biotechnol.* **2020**, *56*, 1–8. [CrossRef]
13. Al-Amin, R.A.; Muthelo, P.M.; Abdurakhmanov, E.; Vincke, C.; Amin, S.P.; Muyldermans, S.; Danielson, U.H.; Landegren, U. Sensitive Protein Detection Using Site-Specifically Oligonucleotide-Conjugated Nanobodies. *Anal. Chem.* **2022**, *94*, 10054–10061. [CrossRef]
14. Ladd, J.; Taylor, A.D.; Piliarik, M.; Homola, J.; Jiang, S. Hybrid Surface Platform for the Simultaneous Detection of Proteins and DNAs Using a Surface Plasmon Resonance Imaging Sensor. *Anal. Chem.* **2008**, *80*, 4231–4236. [CrossRef]
15. Ambrosetti, E.; Paoletti, P.; Bosco, A.; Parisse, P.; Scaini, D.; Tagliabue, E.; De Marco, A.; Casalis, L. Quantification of Circulating Cancer Biomarkers via Sensitive Topographic Measurements on Single Binder Nanoarrays. *ACS Omega* **2017**, *2*, 2618–2629. [CrossRef] [PubMed]
16. Leroy, L.; Bombera, R.; Engel, E.; Calemczuk, R.; Laplatine, L.; Baganizi, D.-D.R.; Marche, P.N.; Roupioz, Y.; Livache, T. Photothermal Effect for Localized Desorption of Primary Lymphocytes Arrayed on an Antibody/DNA-Based Biochip. *Lab Chip* **2014**, *14*, 1987–1990. [CrossRef] [PubMed]

17. Dovgan, I.; Koniev, O.; Kolodych, S.; Wagner, A. Antibody-Oligonucleotide Conjugates as Therapeutic, Imaging, and Detection Agents. *Bioconjug. Chem.* **2019**, *30*, 2483–2501. [CrossRef]
18. Yan, X.; Zhang, H.; Wang, Z.; Peng, H.; Tao, J.; Li, X.-F.; Chris Le, X. Quantitative Synthesis of Protein-DNA Conjugates with 1:1 Stoichiometry. *Chem. Commun.* **2018**, *54*, 7491–7494. [CrossRef] [PubMed]
19. Simon, L.; Lautner, G.; Gyurcsányi, R.E. Reliable Microspotting Methodology for Peptide-Nucleic Acid Layers with High Hybridization Efficiency on Gold SPR Imaging Chips. *Anal. Methods* **2015**, *7*, 6077–6082. [CrossRef]
20. Nobbmann, U. Measure Surface Zeta Potential. Available online: https://www.materials-talks.com/surface-zeta-potential-what-it-is-and-how-to-measure-it/ (accessed on 6 January 2015).
21. Corbett, J.C.W.; McNeil-Watson, F.; Jack, R.O.; Howarth, M. Measuring Surface Zeta Potential Using Phase Analysis Light Scattering in a Simple Dip Cell Arrangement. *Colloids Surf. A Physicochem. Eng. Asp.* **2012**, *396*, 169–176. [CrossRef]
22. Rodríguez, D.F.; Moglie, Y.; Ramírez-Sarmiento, C.A.; Singh, S.K.; Dua, K.; Zacconi, F.C. Bio-Click Chemistry: A Bridge between Biocatalysis and Click Chemistry. *RSC Adv.* **2022**, *12*, 1932–1949. [CrossRef] [PubMed]
23. El-Sagheer, A.H.; Brown, T. Click Nucleic Acid Ligation: Applications in Biology and Nanotechnology. *Acc. Chem. Res.* **2012**, *45*, 1258–1267. [CrossRef]
24. Wiener, J.; Kokotek, D.; Rosowski, S.; Lickert, H.; Meier, M. Preparation of Single- and Double-Oligonucleotide Antibody Conjugates and Their Application for Protein Analytics. *Sci. Rep.* **2020**, *10*, 1457. [CrossRef] [PubMed]
25. Heerwig, A.; Kick, A.; Sommerfeld, P.; Eimermacher, S.; Hartung, F.; Laube, M.; Fischer, D.; Pietzsch, H.-J.; Pietzsch, J.; Löser, R.; et al. The Impact of N^{ε}-Acryloyllysine Piperazides on the Conformational Dynamics of Transglutaminase 2. *Int. J. Mol. Sci.* **2023**, *24*, 1650. [CrossRef]
26. Frato, K.E.; Schleif, R.F. A DNA-Assisted Binding Assay for Weak Protein-Protein Interactions. *J. Mol. Biol.* **2009**, *394*, 805–814. [CrossRef] [PubMed]
27. Tang, Y.; Cain, P.; Anguiano, V.; Shih, J.J.; Chai, Q.; Feng, Y. Impact of IgG Subclass on Molecular Properties of Monoclonal Antibodies. *MAbs* **2021**, *13*, 1993768. [CrossRef]
28. Marquart, A.; Kuncova-Kallio, J.; Albers, M.; Bombera, R.; Stahlberg, R. *Handbook of Multi-Parametric Surface Plasmon Resonance for Molecular Interaction Analysis—Theory and Practice*, 1st ed.; The Royal Society of Chemistry: Tampere, Finland, 2019.
29. Gong, P.; Levicky, R. DNA Surface Hybridization Regimes. *Proc. Natl. Acad. Sci. USA* **2008**, *105*, 5301–5306. [CrossRef] [PubMed]
30. Bielec, K.; Kowalski, A.; Bubak, G.; Witkowska Nery, E.; Hołyst, R. Ion Complexation Explains Orders of Magnitude Changes in the Equilibrium Constant of Biochemical Reactions in Buffers Crowded by Nonionic Compounds. *J. Phys. Chem. Lett.* **2022**, *13*, 112–117. [CrossRef]
31. Nothisen, M.; Perche-Létuvée, P.; Behr, J.-P.; Remy, J.-S.; Kotera, M. Cationic Oligospermine-Oligonucleotide Conjugates Provide Carrier-Free Splice Switching in Monolayer Cells and Spheroids. *Mol. Ther. Nucleic Acids* **2018**, *13*, 483–492. [CrossRef]
32. Zhu, B.; Travas-Sejdic, J. PNA versus DNA in Electrochemical Gene Sensing Based on Conducting Polymers: Study of Charge and Surface Blocking Effects on the Sensor Signal. *Analyst* **2018**, *143*, 687–694. [CrossRef]
33. Briones, C.; Mateo-Marti, E.; Gómez-Navarro, C.; Parro, V.; Román, E.; Martín-Gago, J.A. Ordered Self-Assembled Monolayers of Peptide Nucleic Acids with DNA Recognition Capability. *Phys. Rev. Lett.* **2004**, *93*, 208103. [CrossRef]
34. Del Bene, A.; D'Aniello, A.; Tomassi, S.; Merlino, F.; Mazzarella, V.; Russo, R.; Chambery, A.; Cosconati, S.; Di Maro, S.; Messere, A. Ultrasound-Assisted Peptide Nucleic Acids Synthesis (US-PNAS). *Ultrason. Sonochem.* **2023**, *95*, 106360. [CrossRef] [PubMed]
35. Drozd, M.; Pietrzak, M.D.; Malinowska, E. SPRi-Based Biosensing Platforms for Detection of Specific DNA Sequences Using Thiolate and Dithiocarbamate Assemblies. *Front. Chem.* **2018**, *6*, 173. [CrossRef]
36. Sarcina, L.; Torsi, L.; Picca, R.A.; Manoli, K.; Macchia, E. Assessment of Gold Bio-Functionalization for Wide-Interface Biosensing Platforms. *Sensors* **2020**, *20*, 3678. [CrossRef]
37. Li, Z.; Ruiz, V.G.; Kanduč, M.; Dzubiella, J. Ion-Specific Adsorption on Bare Gold (Au) Nanoparticles in Aqueous Solutions: Double-Layer Structure and Surface Potentials. *Langmuir* **2020**, *36*, 13457–13468. [CrossRef] [PubMed]
38. Saito, N.; Matsuda, T. Protein Adsorption on Self-Assembled Monolayers with Water-Soluble Non-Ionic Oligomers Using Quartz-Crystal Microbalance. *Mater. Sci. Eng. C* **1998**, *6*, 261–266. [CrossRef]
39. Szymczyk, A.; Soliwodzka, K.; Moskal, M.; Różanowski, K.; Ziółkowski, R. Further Insight into the Possible Influence of Electrode Blocking Agents on the Stem-Loop Based Electrochemical DNA Sensor Parameters. *Sens. Actuators B Chem.* **2022**, *354*, 131086. [CrossRef]
40. Havens, A.; El-Shaer, E.; Garcia, L.; Godino, J.L.; Thompson, R.S. Protein Adsorption on Mixed Self-Assembled Monolayers: Influence of Chain Length and Terminal Group. *Langmuir* **2023**, *39*, 16712–16720. [CrossRef]
41. Simon, L.; Gyurcsányi, R.E. Multiplexed Assessment of the Surface Density of DNA Probes on DNA Microarrays by Surface Plasmon Resonance Imaging. *Anal. Chim. Acta* **2019**, *1047*, 131–138. [CrossRef]
42. Voigt, N.V.; Tørring, T.; Rotaru, A.; Jacobsen, M.F.; Ravnsbæk, J.B.; Subramani, R.; Mamdouh, W.; Kjems, J.; Mokhir, A.; Besenbacher, F.; et al. Single-Molecule Chemical Reactions on DNA Origami. *Nat. Nanotechnol.* **2010**, *5*, 200–203. [CrossRef]
43. Gothelf, K.V. Chemical Modifications and Reactions in DNA Nanostructures. *MRS Bull.* **2017**, *42*, 897–903. [CrossRef]

44. Verdolino, V.; Cammi, R.; Munk, B.H.; Schlegel, H.B. Calculation of PKa Values of Nucleobases and the Guanine Oxidation Products Guanidinohydantoin and Spiroiminodihydantoin Using Density Functional Theory and a Polarizable Continuum Model. *J. Phys. Chem. B* **2008**, *112*, 16860–16873. [CrossRef] [PubMed]
45. Bryantsev, V.S.; Diallo, M.S.; Goddard III, W.A. PKa Calculations of Aliphatic Amines, Diamines, and Aminoamides via Density Functional Theory with a Poisson-Boltzmann Continuum Solvent Model. *J. Phys. Chem. A* **2007**, *111*, 4422–4430. [CrossRef] [PubMed]

Suplement S2 publikacji P2:

A Careful Insight into DDI-Type Receptor Layers on the Way to Improvement of Click-Biology-Based Immunosensors

Supplementary Figures

Figure S1

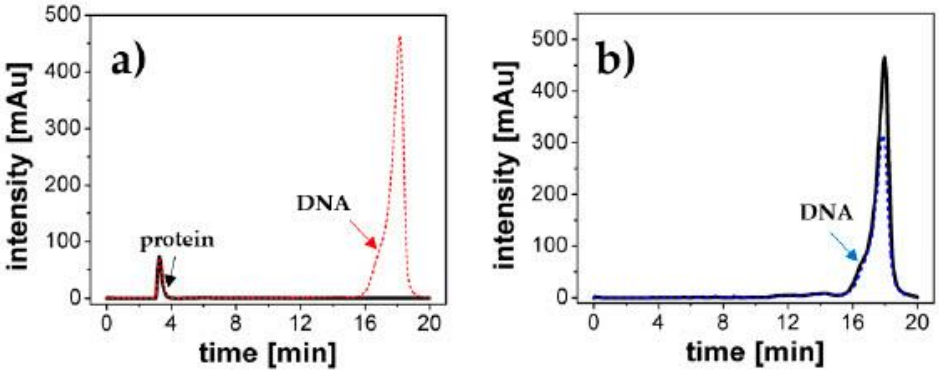

Figure S1. a) Chromatograms showing the results of separation of unconjugated SARS CoV-2 nucleoprotein (solid black line) and the mixture of unconjugated SARS CoV-2 nucleoprotein with *ligand strand* DNA (dashed red line). The arrows indicate fractions of free protein (retention time around 3.5 min) and unconjugated DNA (retention time around 18 min). b) Chromatograms of *ligand strand* sequence before (solid black line) and after treatment with NHS-based crosslinker (dashed red line) in the absence of protein. Chromatograms were captured using a spectrophotometric detector at λ = 260 nm.

Analysis of the chromatograms captured for the free protein and its mixture with DNA confirms that in the absence of a crosslinker, there is no non-covalent interaction between these molecules (See Figure S1a). It is evidenced by the unchanged retention time of the free protein and the absence of additional signals indicating the presence of protein-DNA associates. This observation supports the postulated mechanism of covalent coupling with the participation of protein amino groups as the main reaction responsible for forming protein-DNA conjugates. To confirm the specificity of amino-coupling and to verify the relevance of the influence of the possible side reaction of active NHS esters coupling to primary amine groups within nucleobases (thus crosslinking DNA strands at the activation step), the effect of the amine-reactive crosslinker on the ion chromatogram of the ligand strand DNA was also checked. Such a reaction occurring with noticeable efficiency could significantly disrupt the stoichiometry and homogeneity of the DNA-protein conjugates. As can be seen in Figure S1b, there is no noticeable change in the character of the peak from the unmodified DNA sequence after the incubation with the crosslinker compared to the signal for the same sequence without the crosslinker addition. It demonstrates the absence of signs of reaction between the active NHS ester

and -NH2 groups of DNA nucleobases. The selectivity of the activation reaction can be explained by the significantly attenuated basicity of exocyclic amines compared to aliphatic ones [1,2]. Therefore, the DNA nucleobases show poor reactivity towards NHS esters at room temperature [3,4]. Intensities of signals corresponding to the conjugate fractions of various proteins on the chromatograms (*anti*-SARS CoV-2 nucleoprotein in Figure 1a and *anti*-hCRP antibody in Figure 1b, respectively) were compared. It leads to the conclusion that the efficiency of amine-coupling significantly depends on the type of protein. In the case of nucleocapsid antigen, the average conjugation yield for three independent batches (calculated in relation to the total amount of DNA used in the reaction) amounted to 57.6 % ± 8.3 %. In contrast, the efficiency was significantly lower for antibodies, reaching 12.9 % ± 2.0 %. Both calculations were based on the areas of the obtained signals apparent in the chromatograms. Their complex structure may explain the lower coupling efficiency with antibodies. Antibody as a large glycoprotein presumably shows worse reactive amino group availability than recombinant protein without additional modifications. In addition, the lower pI value of the antibody compared to the SARS CoV-2 nucleoprotein (5.8–7.5 vs. 10.2) impedes the interaction of polyanionic DNA chains with the antibody in the conjugation medium due to more negative charge over a wide pH range and thus increased repulsion of polyanionic DNA tags [5,6]. Noteworthy, to increase the efficiency of conjugation with respect to the protein (which is usually a more expensive and less accessible component), a molar excess of DNA is used. This approach further supports the importance of procedures for the purification and fractionation of protein-DNA conjugates due to the need to remove excess free ligands from the reaction mixture.

Figure S2

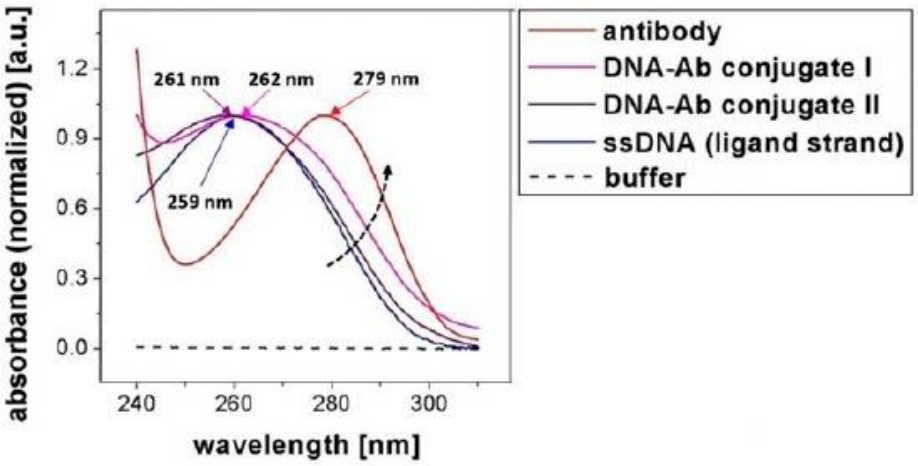

Figure S2. Normalized absorption spectra of selected fractions of post-conjugation mixture as a result of DNA-*anti-h*CRP antibody conjugate separation.

Analysis of UV absorption spectra indicates that DNA-protein conjugates exhibit characteristics of both components. It is evidenced by the observed bathochromic shift relative to free DNA (λ_{max}: 259 nm -> 261 nm for DNA-rich fraction conjugate II and λ_{max}: 259 nm -> 262 nm – for a fraction of 1:1 stoichiometry conjugate I), which can be attributed to the increasing proportion of protein (λ_{max} = 279 nm) in the conjugate. Due to differences in molar extinction, the proximity of the characteristic absorption bands of proteins and DNA, and the low concentration of the tested conjugates, it is impossible to observe independent bands of the two components. Therefore, UV absorption spectra analysis cannot be the only method to validate the efficiency of DNA conjugation with proteins. However, UV absorption analysis can be treated as an auxiliary method to ion chromatography, which does not cause destruction and loss of the sample and allows for the quantitative determination of the conjugate concentration. Despite the limitations mentioned above, UV absorption spectroscopy appears to be an attractive and rapid method for the characterization and quality control of the previously purified DNA-protein conjugates.

Figure S3

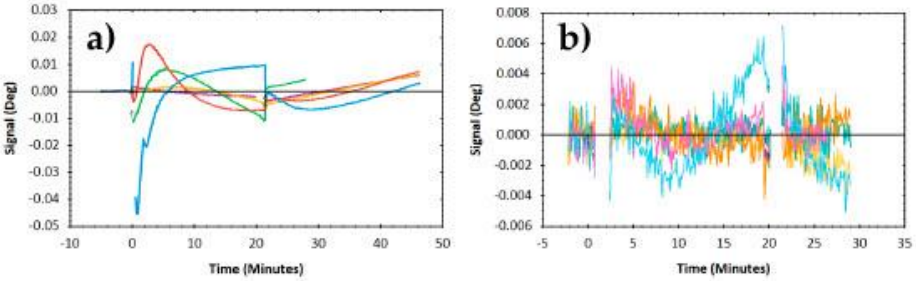

Figure S3. Residuals between fitted curves and experimental data for interactions of *DNA probe* with free *ligand strand* (a) and DNA-*anti*-CRP antibody conjugate (b).

Table S1

Table S1. Detailed statistics data characterizing the used kinetics binding model.

Parameter	Free DNA	DNA-protein conjugate
Fitting model	"one-to-one"	"one-to-one"
Concentration range	17.3 nM – 10.8 μM	0.97 nM – 15.5 nM
B_{max} [mdeg]	140 (± $1.72 \cdot 10^{-1}$)	40.0 (± $8.08 \cdot 10^{-3}$)
k_a [$M^{-1} \cdot s^{-1}$]	$1.51 \cdot 10^{5}$ (± $2.35 \cdot 10^{3}$)	$1.13 \cdot 10^{5}$ (± $1.35 \cdot 10^{1}$)
k_d [s^{-1}]	$2.95 \cdot 10^{-4}$ (± $1.56 \cdot 10^{-6}$)	$5.89 \cdot 10^{-4}$ (± $1.97 \cdot 10^{-7}$)
k_D [M]	$1.95 \cdot 10^{-9}$ (± $4.07 \cdot 10^{-11}$)	$5.19 \cdot 10^{-9}$ (± $2.58 \cdot 10^{-12}$)
Chi^2	0.00	0.00

Table S2

Table S2. A comparison of the different types of oligonucleotide probes examined within this study.

Parameter	DNA	ZNA	PNA
Immobilization efficiency (normalized)	100% (15nb – reference value) 100.0% (48nb)	19.1%	24.5%
Hybridization efficiency (normalized)	46.2% (15nb) 46.8 (48nb)	100% (reference value)	0.1%
Surface charge (zeta potential)	-38.2 mV (+/- 1.7mV)	+ 47.8 mV (+/- 3.7mV)	not measured
Probe synthesis cost	low	moderate	high

References:

1. Voigt, N.V.; Tørring, T.; Rotaru, A.; Jacobsen, M.F.; Ravnsbæk, J.B.; Subramani, R.; Mamdouh, W.; Kjems, J.; Mokhir, A.; Besenbacher, F.; et al. Single-Molecule Chemical Reactions on DNA Origami. *Nat Nanotechnol* **2010**, *5*, 200–203, doi:10.1038/NNANO.2010.5.

2. Gothelf, K.V. Chemical Modifications and Reactions in DNA Nanostructures. *MRS Bull* **2017**, *42*, 897–903, doi:10.1557/mrs.2017.276.

3. Verdolino, V.; Cammi, R.; Munk, B.H.; Schlegel, H.B. Calculation of PKa Values of Nucleobases and the Guanine Oxidation Products Guanidinohydantoin and Spiroiminodihydantoin Using Density Functional Theory and a Polarizable Continuum Model. *Journal of Physical Chemistry B* **2008**, *112*, 16860–16873, doi:10.1021/jp8068877.

4. Bryantsev, V.S.; Diallo, M.S.; Goddard III, W.A. PKa Calculations of Aliphatic Amines, Diamines, and Aminoamides via Density Functional Theory with a Poisson-Boltzmann Continuum Solvent Model. *Journal of Physical Chemistry A* **2007**, *111*, 4422–4430, doi:10.1021/jp071040t.

5. Frato, K.E.; Schleif, R.F. A DNA-Assisted Binding Assay for Weak Protein-Protein Interactions. *J Mol Biol* **2009**, *394*, 805–814, doi:10.1016/j.jmb.2009.09.064.

6. Tang, Y.; Cain, P.; Anguiano, V.; Shih, J.J.; Chai, Q.; Feng, Y. Impact of IgG Subclass on Molecular Properties of Monoclonal Antibodies. *MAbs* **2021**, *13*, doi:10.1080/19420862.2021.1993768.

Publikacja P3:

A versatile approach to quality control of protein-based receptor layers by reversible, nonspecific staining for multiplex SPRi immunosensing

Graphical Abstract

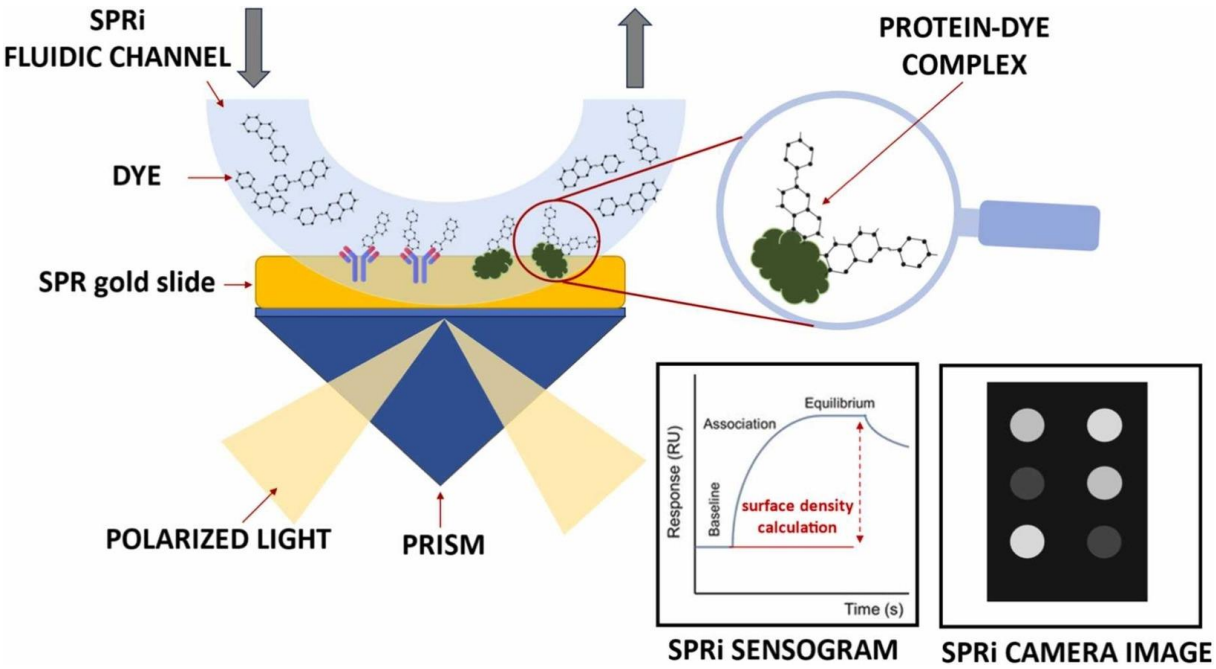

Sensors & Actuators: B. Chemical 421 (2024) 136512

Contents lists available at ScienceDirect

Sensors and Actuators: B. Chemical

journal homepage: www.elsevier.com/locate/snb

A versatile approach to quality control of protein-based receptor layers by reversible, nonspecific staining for multiplex SPRi immunosensing

Sylwia Karoń [a,b], Karolina Porycka [b], Lorico DS Lapitan, Jr [a,c], Marcin Drozd [a,b,*], Mariusz Pietrzak [a,b], Elżbieta Malinowska [a,b]

[a] Department of Medical Diagnostics, Centre for Advanced Materials and Technologies CEZAMAT, Warsaw University of Technology, Warsaw, Poland
[b] Chair of Medical Biotechnology, Faculty of Chemistry, Warsaw University of Technology, Warsaw, Poland
[c] Department of Chemical Engineering and Research Center for the Natural and Applied Sciences, University of Santo Tomas, España Boulevard, Manila, Philippines

ARTICLE INFO

Keywords:
Protein labeling
Protein dyes
Receptor layer quality control
Multiplex immunosensing
Protein mapping
Surface plasmon resonance imaging

ABSTRACT

SPRi protein arrays for rapid, label-free immunodetection offer an attractive approach for high throughput biosensing and analysis of molecular interactions. However, their routine use for quantitative analysis requires adequate reproducibility and homogeneity of receptor assemblies manufactured *ex-situ* using microdispensing techniques. There is also an emerging need to develop versatile and non-destructive methods for the determination of protein surface density for quality control of the immobilization process. Here, we report on a simple, one-step method of surface proteins visualization by their reversible, non-specific staining with anionic dyes: Ponceau S (PS), Amido Black (AB) or Coomassie Brilliant Blue G (CBB-G). Using rabbit IgG antibody and transferrin as model receptors, we demonstrate the possibility of protein surface density determination in a broad range up to ~ 3 ng•mm^{-2} (for a 2D monolayer) and up to at least 12.5 ng•mm^{-2} (for a 3D hydrogel-coated substrate). The ranges of dynamic response for the developed methods cover the typical surface densities required for biosensing and studies of the binding kinetics. It was demonstrated that each of the investigated dyes manifests advantages in specified applications. While CBB-G shows the highest sensitivity of SPRi response, AB requires the gentlest labeling conditions, and PS shows the highest association rate and ease of washing out, even from protein layers of high density. The feasibility of the developed method for the quality control of SPRi microarray was confirmed. The advantages of the new, dye-based, non-specific labeling method over immunolabeling in terms of simplicity of implementation and versatility have also been highlighted.

1. Introduction

Protein microarray technology is an emerging biosensing strategy that allows for high-throughput analysis and simultaneous detection of multiple analytes. This approach involves the direct interaction of target molecules in the sample with protein receptors immobilized on a microarray surface, facilitating simultaneous monitoring of various biochemical interactions. Typically, techniques based on additional labeling, employing fluorescent or enzymatic tags, are used for signal readout [1–6]. In parallel, multiplex label-free formats have also been developed, allowing direct monitoring of intermolecular interactions and biosensing in real time. Label-free, protein-based affinity biosensors in microarray format have been constructed based on various mechanisms for signal transduction, including surface plasmon resonance (SPR) [7], ellipsometry [8], interference-based techniques [9] and atomic force microscopy [10]. Given the well-studied surface chemistry of gold, one of the most widely used solutions is the SPR imaging (SPRi) detection platforms [6,11,12]. A significant challenge in developing these biosensing arrays is the manufacturing of stable and homogeneous receptor layers through high-throughput immobilization techniques like *ex-situ* microspotting. It must be underlined that the receptor surface density is a critical parameter that influences further applicability of the formed receptor layer, and therefore, it should be strictly controlled. Obtaining a uniform receptor layer is challenging in the case of multiplex microarrays due to the need for spatially-resolved immobilization of multiple proteins on the same transducer, where variation can arise from fluctuations in humidity, temperature, and probe concentration [13].

* Corresponding author at: Department of Medical Diagnostics, Centre for Advanced Materials and Technologies CEZAMAT, Warsaw University of Technology, Warsaw, Poland
E-mail address: marcin.drozd.ch@pw.edu.pl (M. Drozd).

https://doi.org/10.1016/j.snb.2024.136512
Received 25 April 2024; Received in revised form 4 August 2024; Accepted 21 August 2024
Available online 22 August 2024

The ideal receptor layer to be used for protein microarray should be characterized by high reproducibility of its manufacturing, which includes controllable receptor surface density and homogeneity of receptor distribution in terms of the shape and size of test fields. There are several ways to check the quality of the receptor layer, but each of them has significant drawbacks. The first and most straightforward method of assessing the quality of the receptor layer is a direct, post-evaluation of the target's binding capacity based on the response to analytical standards of known concentration [14]. However, this approach may preclude biosensor reuse for analysis of real samples due to common problems with its regeneration. Another way to check the receptor layer's quality is the direct monitoring of its formation. It should be noted that the classical SPR format offers controllability of receptor surface densities by tracking immobilization in real time [15]. This, however, is not feasible for SPRi arrays and a variety of other biosensor types in microarray formats. A third possibility is the assessment of the surface density of receptor proteins through specific immunolabeling. This requires specific antibodies, such as secondary antibodies against certain species (e.g., *anti*-mouse or *anti*-goat for immunolabeling of antibodies) or specific antibodies against immobilized proteins (immunolabeling of antigens). Specific immunolabeling by means of antibodies against the receptor protein is expensive, as numerous antibodies of different specificities are required - primarily in the case of antigen/protein-based arrays, for which the use of secondary antibodies is not possible.

Non-specific labeling of proteins employs the binding of a universal marker, allowing their visualization and surface density determination. The ideal non-specific protein marker should interact selectively with a wide range of proteins without its inactivation. Such interaction should be characterized by rapid association and dissociation rate, allowing fast binding and spontaneous washing out without additional stages of regeneration. Dyes commonly used for the visualization of proteins on Western blotting membranes and polyacrylamide gels appear as good candidates for protein markers [16]. However, to date, no studies have been reported on their use for the quality control of protein-based SPRi biosensors [16–18].

The development of *post*-immobilization methods for mapping and determination of protein bioreceptor surface density appears to be an important challenge that can improve the reliability of SPRi-based assays. There are known methods based on DNA microarrays. Simon et al. demonstrated the applicability of hexamine ruthenium(III) complex, which was previously employed for electrochemical quantification of DNA coverage on gold electrodes, for application in SPRi-based determination of the surface density of DNA probes in microarrays [19]. Chiari et al. introduced a label-free method for quality control of DNA probes on microarrays using the Interferometric Reflectance Imaging Sensor (IRIS), enabling real-time monitoring of immobilization and optimal probe concentration assessment [13]. Another approach provided by Duarte et al. employs an open-source protein microarray data processing software to enhance consistency analysis with advanced normalization techniques [20]. As an example of receptor layer quality control in immunoassays, Campanero-Rhodes reported the application of a fluorescent dye to identify printing errors and assess immobilization efficiency [21]. The development of the aforementioned methods highlights the growing focus on the quality assessment of receptor layers in microarrays. However, developing a rapid and non-destructive methodology for visualization and quality control of the protein-based SPRi arrays seems to be a challenge that still needs to be addressed.

This work employs a combination of two SPR formats, classical SPR and SPR imaging, to develop an SPRi-based method for the quality control of protein receptor layers. To our knowledge, there have yet to be any reports on a protocol for the rapid, one-step quality evaluation of multiplexed immunosensing platforms by means of SPRi, which can be applied *in-line* immediately before its use. For this purpose, the possibility of utilizing popular anionic protein dyes has been investigated. Three compounds of different properties were selected as candidates for non-specific protein labels for SPRi. Ponceau S (PS), Amido Black 10B (AB) and Coomassie Brilliant Blue G-250 (CBB-G) exhibit the capacity for reversible binding to protein receptors on the surface. Due to the previously unexplored and significant differences in the nature of dyes binding by protein monolayers on Au transducers, an extended study of dye-protein interactions has been conducted. This research provides a deeper understanding of the mechanisms behind reversible staining using AB and CBB-G, which have so far been considered irreversible in typical, membrane-related applications.

The use of classical SPR made it possible to follow the process of receptor layer formation and determination of the surface density in the case of covalently bound rabbit IgG and transferrin as model receptors. Tracking of dye-protein interactions by means of SPRi enables protein mapping *via* non-specific labeling. It has been demonstrated that the proposed method has a wider linear range, greater versatility, and simplicity than specific immunolabeling. A combination of non-specific protein staining and SPRi resulted in the development of a versatile approach to quality control of protein-based receptor layers for multiplex SPRi immunosensing.

2. Experimental

2.1. Materials and reagents

Human transferrin, immunoglobulin G from rabbit serum (rabbit IgG), goat *anti*-rabbit IgG, TWEEN®20, N-hydroxysuccinimide (NHS), 2-(N-morpholino)ethanesulfonic acid (MES), ethanolamine, sodium hydrogen phosphate dihydrate and potassium dihydrogen phosphate, were purchased from Merck KGaA (Germany). *Anti*-transferrin antibody line HM063 was purchased from Medix Biochemica (Finland). Coomassie Brilliant Blue G-250 (CBB-G), Coomassie Brilliant Blue R-250 (CBB-R), Amido black 10B (AB), Ponceau S (PS), fluorescein and thymolphtalein were from Thermo Scientific Chemicals (United States, MA). Thiol-PEG-CH_2COOH (M_w = 1 kDa) (PEG-COOH) was purchased from BroadPharm (United States, CA). Bare gold SPR slides were from Horiba Scientific (France). CMD hydrogel-coated SPR slides (density: 50 M) and 1-ethyl-3-(3-dimethylaminopropyl)carbodiimide hydrochloride (EDC) were from XanTec Bioanalytics GmbH (Germany). Hydrogen peroxide (30 %), ammonia (25 %), hydrochloric acid (35–37 %), acetic acid (99 %), glycine, sodium chloride, potassium chloride and sodium hydroxide were from Chempur (Poland). Deionized (DI) water (conductivity < 0.055 $\mu S \bullet cm^{-1}$ at 20 °C, TOC < 1.0 ppb) was used for the preparation of all solutions and buffers. pH of buffers was adjusted using 1 M $NaOH_{aq}$ or 1 M HCl_{aq}.

2.2. Apparatus and software

MP-SPR Navi™ 220 A NAALI device equipped with a goniometric resonant angle system, integrated microfluidics and autosampler (BioNavis Ltd., Tampere, Finland) was employed for the covalent immobilization of proteins on the surface of SPR chips and kinetics studies of dye-protein interactions. SPRi Lab Plus device (Horiba Scientific, Palaiseau, France) was used for SPR imaging studies. MP-SPR Navi™ DataViewer software (BioNavis Ltd., Tampere, Finland) and TraceDrawer® software, v 1.8 (Ridgeview Instruments AB, Uppsala, Sweden) were used for analysis of SPR sensograms. OriginPro Software for Graphing&Analysis (Northampton, Massachusetts, USA) was employed for analysis of SPRi sensograms and visualization of results.

2.3. SPRi studies on the interactions of model protein receptors with anionic dyes

The detailed protocol for cleaning gold SPR slides (of universal size, compatible with both classical SPR and SPRi device), their functionalization and proteins immobilization (both in the SPR microfluidic system and *ex-situ* by microspotting) is described in Supplementary Material.

The schematic of a typical procedure of reversible protein staining on the SPRi chip is shown in Fig. 1A. Briefly, the SPR chip with immobilized rabbit IgG and transferrin was assembled into the SPRi instrument. PBS buffer with 0.05 % Tween20 (PBST), pH 7.4 was used as a running buffer throughout all experiments. All injections of protein dyes typically lasted ~5 min and were carried out at the flow rate of 150 μL•min^{-1} at RT (cleanroom conditions). Dye-protein interaction studies employing SPRi were carried out through manual injections of dye solutions. Unless otherwise stated, working solutions of buffered dyes (50 μM each) were prepared in media of optimal composition, *i.e.* 10 mM Glycine/HCl buffer pH 2.0 (PS, CBB-G) or 10 mM Acetate/NaOH buffer pH 4.0 (AB). Stock solutions (1 mM) were prepared by dissolving solids in a minimum volume of 1 M acetic acid, followed by dilution with a dedicated buffer and pH adjusting using 1 M NaOH. Injections of dye solutions were carried out to collect SPRi responses to dye-protein interactions. Areas of the chips non-covered with proteins are defined as a negative control. Unless otherwise stated, differential SPRi sensograms were shown to suppress bulk effects by subtracting the responses from test fields without immobilized protein (blank response). To carry out the immunolabeling, a 5-min injection of a specific antibody against the

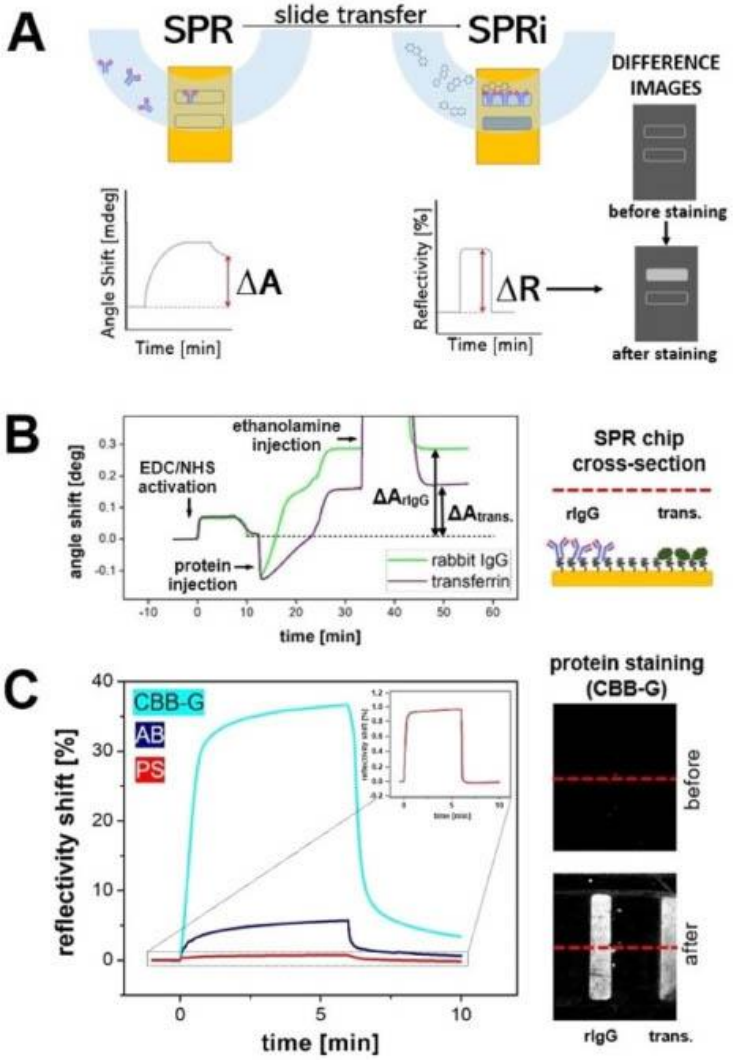

Fig. 1. A) Schematic overview of the measurement procedure carried out in the presented studies. B) Exemplary SPR sensograms illustrating covalent immobilisation of model receptor proteins: transferrin and rabbit IgG, along with the resonant angle shift values (ΔA). A schematic of the longitudinal section (across the SPR cells) can be seen on the right. C) Differential SPRi sensograms illustrating the interaction of different dyes with rabbit IgG layer. On the right, differential CCD camera images of the sensor slide with visible bright fields resulting from the CBB-G association.

immobilized protein (*anti*-rabbit IgG or *anti*-transferrin antibody in PBST buffer, C = 50 $\mu g \bullet mL^{-1}$ each) was performed at the end of each experiment. 10 mM glycine HCl pH 2.0 was used as a regeneration buffer for protein layer stabilization and desorption of specific antibodies. SPRi analysis is based on the monitoring of reflectivity changes (ΔR) in predefined areas. Typically, a minimum of 3 independent spots of min. 400 μm (diameter) for each immobilized protein and a blank (without a protein) were defined. The exception was microarray analysis, in which there was one test spot covering the entire area of the spotted zone. Differential SPR and SPRi sensograms (after subtraction of the reference signal and bulk effects) were used for quantitative studies of protein surface density.

3. Results and discussion

Our study aimed to develop a simple method for quality control of SPRi receptor layers that enables the preservation of the protein biological activity and allows further reuse of biosensing platforms. Therefore, it was necessary to find labels characterized by: i) good selectivity towards proteins, ii) fast association kinetics and iii) capability of spontaneous dissociation without extensive regeneration steps. Six anionic compounds were selected as candidates for non-specific protein staining: Ponceau S (PS), Amido Black 10B (AB), Coomassie Brilliant Blue G-250 (CBB-G), Coomassie Brilliant Blue R-250 (CBB-R), Thymolphthalein and Fluorescein. Sensograms (both raw and differential) illustrating interactions of these compounds with model receptor proteins and SPR sensor substrate as the reference are shown in Fig. S1 and S2. The criteria of affinity towards both rabbit IgG and transferrin (resulting in a measurable SPRi response) and facility of rapid dissociation were met by three of six examined dyes, i.e., PS, AB, and CBB-G. Therefore, such compounds were selected for further research.

The routine protocol employed for the characterization of the developed method of receptor layer quality control involved controlled immobilization of proteins in a microfluidic system of classical 2-channel SPR device and then the transfer of the SPR slide to the SPRi device, as depicted in Fig. 1A. Fig. 1B shows SPR sensograms illustrating the process of covalent immobilization, during which the observable change of the baseline angle shift confirms the effective and stable coupling of rabbit IgG and transferrin to the surface via EDC/NHS chemistry. Firstly, the injection of EDC/NHS occurs to activate carboxyl groups on the surface. The protein of interest, which contains primary amine groups, is injected after activation. The surface is treated with ethanolamine to block any remaining reactive sites and prevent non-specific binding. This step quenches unreacted NHS esters by converting them to inert amide groups. In turn, SPRi sensograms and images captured by the CDD camera of the SPRi instrument illustrate the concept of protein visualization (Fig. 1C). In a differential image, the non-labeled proteins bound to the surface are not visible. After injection of a given dye leading to non-specific labeling, it is possible to observe the brightening of the microfluidic cell outlines due to dye binding. This phenomenon is indicated in SPRi sensograms as a measurable change in reflectivity. Specific labeling of surface proteins with antibodies was used as a reference strategy for their mapping. A noticeable difference in the course of sensograms obtained in the case of immunolabeling (shown in Fig. S1) and non-specific labeling with dyes reflects the differences in the stability of the resulting immunocomplexes and dye-protein complexes. In the case of non-specific staining, no layer regeneration is required because molecules of all types of dyes wash out over time under the influence of running buffer injection, while the interaction of receptors with antibodies leads to stable immunocomplexes and thus requires a subsequent regeneration cycle. Moreover, immunolabeling with a single antibody allows for obtaining a signal for only one of the immobilized proteins, and the SPR response is then noticeably smaller than the one resulting from the dyes.

The observed significant changes in the reflectance of the test fields shown in Fig. 1C can be attributed to the high efficiency of the labeling with dyes, which is favored by its non-specific and multidentate character due to the presence of multiple binding sites within a protein, as well as the small size of dyes molecules. Due to the lack of spatial and diffusion constraints, equilibrium can be achieved in a relatively short time, as best illustrated by the SPRi response to PS dye. Due to the rapid dissociation of dyes, for quantitative studies, it was assumed that the change in reflectivity recorded at the association stage, i.e., for a time corresponding to 90 % of the total injection time, will be taken as the analytical signal (as shown in Fig. 1A. Thanks to the observed features of their interactions with proteins, the selected dyes meet the prerequisites for being effective non-specific markers for mapping SPRi protein arrays.

In the next step, the effect of pH and buffer ionic strength on the SPRi responses was examined to maximize the efficiency of dye binding to proteins. For pH selection, SPRi responses were compared for three selected pH buffers, i.e., pH 7.4 (10 mM phosphate), pH 4.0 (10 mM acetate), and pH 2.0 (10 mM Glycine-HCl). Acidic media was chosen for optimization studies due to the significantly better solubility of all studied dyes in solutions of low pH [22,23]. Interactions of both ionic and hydrophobic nature were recognized as crucial for the intended purpose. Therefore, the binding efficiency strongly depends on the pH and ionic content of the applied solution.

The results presented in Fig. 2A show that the highest binding efficiency was achieved for PS and CBB-G at pH 2.0. At the same time, the highest response was observed for AB at pH 4.0. In contrast, further acidification of the interaction medium to pH 2.0 almost totally suppressed the dye-protein interaction (only 2.1 % of the signal observed for pH 4.0. In the case of CBB-G, pH ~ 2.0 provides the molecule with a slightly anionic character of the ligand molecule at the strongly positive surface charge of both proteins (pH << pI) [24]. Our observations regarding CBB-G confirmed the previous reports that CBB at low pH shows greater binding efficiency to proteins, resulting in more linear assay plots and less color variability. It was also noticed that at neutral pH, the formation of the dye-protein complex is slower, and the dye binds fewer sites. High salt concentrations can lead to demixing and condensate formation in proteins due to the reduction of electrostatic protein-protein interactions [25]. Therefore, the effect of NaCl content in the medium was studied for two dyes with different interaction characteristics, i.e., AB and CBB-G. As shown in Fig. 2B, in the case of AB, as the concentration of NaCl in solution increased up to ~ 200 mM, the sensitivity decreased, which suggests the domination of the ionic-nature attraction of this dye to proteins. Concerning CBB-G, no such relationship could be observed, as the increasing salt concentration did not significantly affect sensitivity, which may indicate a predominance of hydrophobic interactions.

Table S1 provides in-depth characterization of the physico-chemical properties of the dyes examined within presented research. These data, as well as literature reports, support our initial conclusions regarding the interaction mechanisms. Congdon et al. reported the contribution of both basic and aromatic amino acid side chains in the CBB-G binding to proteins. CBB tends to bind to other already bound dye molecules via π-π stacking of the phenyl ring system [26]. This is supported by both our observations and the characteristics of this dye in acidic media. Based on the relation between protein surface density and SPRi response to CBB-G staining it was assumed that the number of nucleation sites for π-π-stacking still depends on the amount of protein on the surface. Thus, this effect only results in signal amplification for prolonged interaction times. In our study, we used relatively short injections, at which we did not notice any significant and negative effect of this phenomenon. The highest hydrophobicity of CBB-G among the analyzed dyes (logD = 7.05), as well as its near-zero net charge ($pI_{CBB\text{-}G} = 2.59$), explains its very efficient association through hydrophobic interactions and thus high SPRi responses. In the case of the remaining dyes, the electrostatic or mixed electrostatic and hydrogen bond-related mechanism dominates due to their anionic nature over the entire range of tested pH (see Table S1) [18].

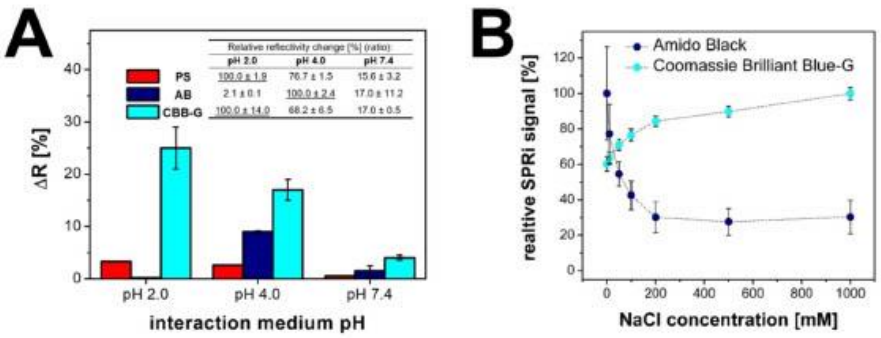

Fig. 2. The effect of the assay medium pH (A) and ionic strength (represented by NaCl concentration) (B) on the SPRi response to PS, AB, and CBB-G dyes in the concentration of 50 μM each. (n = 3). Immobilized rabbit IgG was used as a model protein. Table (Inset of Fig. 2A) shows the normalized reflectivity changes calculated by taking the highest responses for a given dye as 100 %.

Analysis of the dose-response curves (Fig. S3A, S4A) was carried out to further characterize the interaction of dyes with model protein receptors. The profiles of response to injections of dyes at different concentrations (in the optimized composition of interaction medium for each dye) are presented as a function of the logarithm of dye concentration (Fig. S3B, S4B). The lack of fundamental differences between the binding characteristics of dyes to model receptors of different types (protein antigen and IgG antibody) demonstrates the versatility of these compounds as markers for protein mapping. In the case of AB and CBB-G, a linear relationship of SPRi response to the logarithm of dye concentration is observed over a relatively wide range of concentrations (typically in the range of 5–50 μM). In turn, Ponceau S is characterized by a rather abrupt flattening of the response profile for concentrations above 20 μM and relatively narrow dynamic response ranges for both rabbit IgG and transferrin. It indicates the ease of achieving equilibrium for this dye and the relatively efficient saturation of binding sites in the protein structure. These observations stay in accordance with reports on the different characteristics of PS dye, as it is the only compound among the studied group that is considered easily washable (reversible), in opposition to AB and CBB-G, which are considered permanent in membrane blotting applications [27]. Nevertheless, according to our preliminary studies, all three selected dyes can be classified as reversible in the specific application as markers of protein receptor layers of SPRi biosensors.

The binding of dyes to proteins is similar across Western blot membranes, PAGE gels, and SPR/SPRi receptor layers, involving ionic and hydrophobic interactions. The perception of CBB-G and AB dyes as "irreversible" in blotting and electrophoresis is influenced by mass transport limitations in porous structures, with pore sizes ranging from 0.2 to 0.45 micrometers. This can lead to trapped dye-protein complexes characterized by slow diffusion and destaining [28]. Our study shows that substrates with reduced porosity and smaller thickness (up to 700 nm) allow dyes to dissociate more easily, enhancing staining and washing efficiency. The increased dissociation efficiency of AB and CBB-G is conditioned by the different architecture and chemical nature of the SPRi transducer compared to nitrocellulose membranes and acrylamide gels. In particular, the lack of a porous 3D structure prevents local precipitation of dye and its retention [29].

As the developed method of reversible protein mapping should be non-destructive to the immobilized proteins, the impact of the protein staining by means of CBB-G on the stability and antibody binding capacity of the receptor layer was assessed. Previous optimization studies proved that CBB-G dye shows the highest sensitivity at pH 2.0. This medium is considered to effectively impair protein-protein interactions and, therefore, is commonly used in SPR protocols to regenerate receptor layers [30]. In addition, CBB-G is characterized by a slower dissociation rate than PS, whose compatibility with immunolabeling techniques has already been proven through its use in protein pre-staining in Western blotting methods [27]. Therefore, CBB-G was selected as the most potentially damaging to receptor proteins. In the experiment illustrated in Fig. 3, a series of dye injections were carried out toward immobilized rabbit IgG (studied protein) and transferrin (reference), followed by specific immunolabeling with *anti*-rabbit IgG antibody injection and layer regeneration with 10 mM Gly-HCl pH 2.0. As a result of several cycles (n=6), it is noticeable that the rabbit IgG receptor layer only slightly loses its binding capacity.

As it can be seen in Fig. 3B, a slight decrease in SPR response to immunolabeling is noticeable (~ 73 % of the original signal is observed after 6 cycles), which is in correlation with the SPRi response evolution for CBB-G staining (~ 78.5 % of the original signal after 6 cycles), which can be attributed to gradual layer depletion. The analysis of the SPRi response of immobilized transferrin for cycles of regeneration and CBB-G staining indicates a similar level of signal decrease associated with receptor desorption to the IgG layer (~81.7 % of the original signal is observed after 6 cycles). Importantly, no deterioration in binding selectivity was observed along successive cycles, as evidenced by the absence of signs of non-specific adsorption of *anti*-rabbit IgG on immobilized transferrin (purple sensogram) and uncoated surfaces (black sensogram).

To quantitatively analyze the relationships between SPRi responses to nonspecific staining and surface densities of immobilized receptor proteins, calibration curves for individual dyes were determined (Fig. 4). Data for the correlation studies were obtained by performing a series of rabbit IgG and transferrin immobilizations using classical SPR. The surface densities of the proteins (expressed in ng•mm^{-2}) were calculated based on the value of resonant angle shift [31]. The immobilization was carried out in variable conditions to achieve a possibly wide range of surface densities (in the range of 0.80–6.98 ng•mm^{-2} for rabbit IgG and 1.22–5.72 ng•mm^{-2} for transferrin). It was achieved by varying the protein injection time during immobilization (5–20 min) and the use of different protein concentrations in the immobilization buffer (from 0 to 200 μg•mL^{-1}).

Analysis of the correlations described in Fig. 4 indicates that for all the tested dyes, i.e., PS, AB, and CBB-G, it is possible to determine a near-linear relationship indicating the relation of the SPRi response to the surface density of the receptor protein. In the case of immobilized transferrin, it is shown for all applied dyes that the range of linear response covers densities in the window of 0.0–3.0 ng•mm^{-2}, while for rabbit IgG, the range is nearly twice as wide (0.0–5.7 ng•mm^{-2} for PS and AB and 0.0–4.9 ng•mm^{-2} for CBB-G). These surface densities range

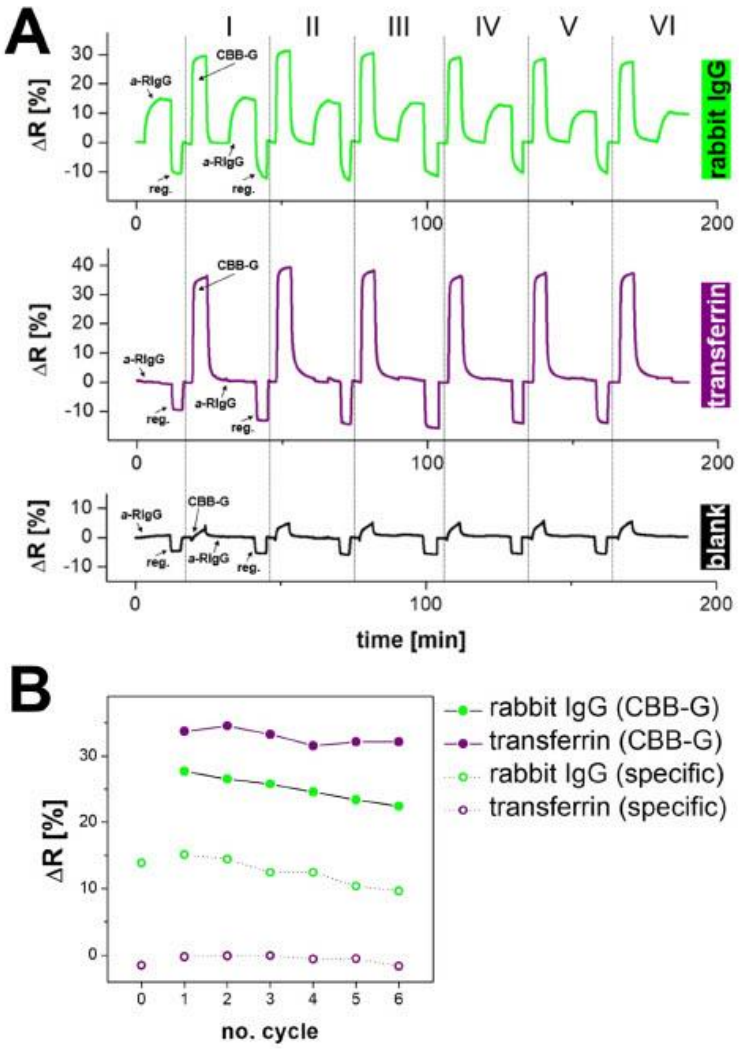

Fig. 8. A) Sensograms showing the evolution of SPRi responses of immobilized rabbit IgG, transferrin, and surface without protein (blank) towards six consecutive cycles of specific labeling (with anti-rabbit IgG), acidic regeneration (with 10 mM Gly-HCl, pH 2.0) and non-specific protein staining with 50 μM CBB-G in 10 mM Gly-HCl, pH 2.0. B) SPRi response values for the immobilized proteins to non-specific CBB-G staining (solid lines) and specific antibody labeling (dotted lines) at individual cycles.

includes typical coverage of protein receptors immobilized via EDC/NHS, which is recommended for kinetic studies (1.5–1.8 ng•mm^{-2}) and biosensor design (2.5–5.0 ng•mm^{-2}) [32–34].

It is worth noting that the ratio of maxima for which linearity of response was observed (3.0 ng•mm^{-2} (transferrin) *vs.* 5.7 ng•mm^{-2} (rabbit IgG)) accurately reflects the ratio of their molecular weights (transferrin ~ 80 kDa, rabbit IgG ~ 150 kDa). Hence, the similarity of the linear ranges expressed as molar surface density (up to 2.26•10^{10} transferrin molecules•mm^{-2} and 2.29•10^{10} IgG molecules•mm^{-2}, respectively) is even more apparent. Comparison of the surface densities obtained within our studies (calculated using Eq. 1) with the values reported in the literature indicates that the organization of proteins in the receptor layer at about 1.5•10^{12} IgG molecules•cm^{-2} corresponds to a single monolayer of physisorbed antibodies [35].

$$\Gamma_{molar} = \frac{\Gamma_{mass}}{M_{W(protein)}} \bullet N_A \quad (1)$$

Although a flexible linker in the form of carboxylated PEG, Mw = 1 kDa, is involved in the construction of our assays, due to its small size compared to the immobilized proteins, we can assume that our receptor layers correspond to the model of 2D monolayer. This conclusion explains both the inability to achieve higher surface densities and the loss

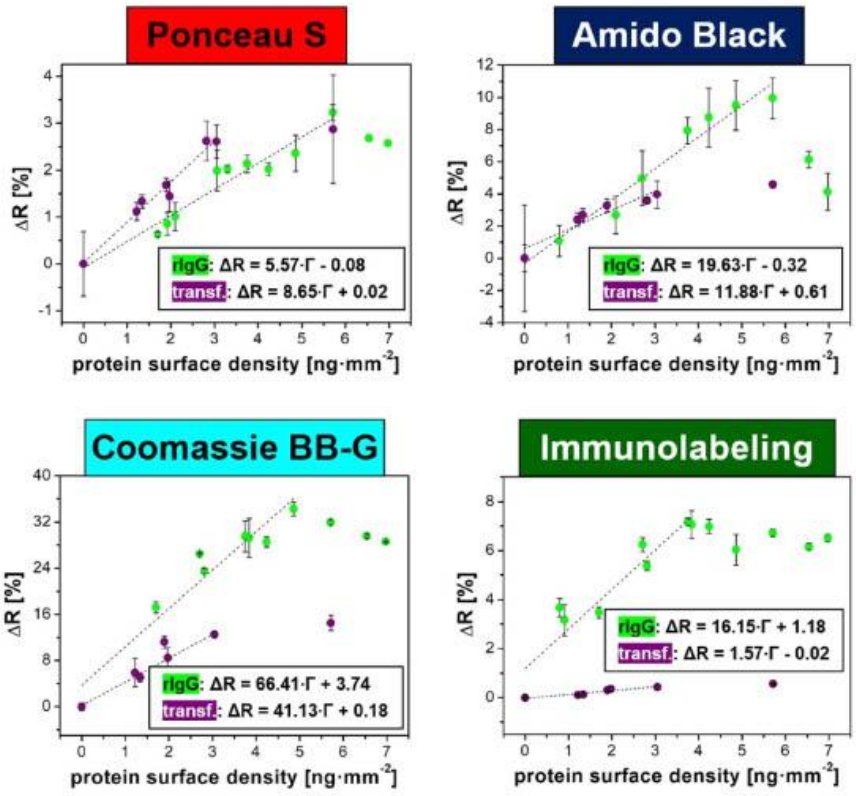

Fig. 4. SPRi reflectivity changes registered for immobilized receptor proteins of various surface densities in response to the injection of the corresponding PS, AB, and CBB dyes (non-specific staining) and anti-rabbit IgG/anti-transferrin antibody (specific immunolabeling). Insets show parameters of linear fitting for rabbit IgG and transferrin.

of linearity of the observed relationships at high surface densities. In both cases, the limitation in the efficiency of protein immobilization and dye binding is primarily due to steric hindrances related to the architecture of the monolayer. Additional support for this hypothesis is the fact that for the specific immunolabeling of surface proteins with *anti*-rabbit IgG and *anti*-transferrin antibodies, the dynamic ranges of the observed SPRi responses were found to be similar for transferrin (0.0–3.0 ng•mm^{-2}) or even narrower (0.0–3.8 ng•mm^{-2}) for rabbit IgG (please refer to Fig. 4 – immunolabeling). Our studies proved that nonspecific protein labeling is a versatile method for quantifying immobilized proteins in a wide range of surface densities. Such a feature is supported by the small size of the used dyes and the lower risk of mass transport limitations compared to specific immunolabeling. The sensitivities of the corresponding assays (expressed by the slopes of the linear sections in Fig. 4) vary and depend on the type of protein tested, i.e., in the case of PS, a higher sensitivity of staining was obtained for transferrin. In contrast, for the remaining dyes, larger SPRi response slopes are observed for rabbit IgG.

By far, the highest sensitivity of quantitative protein mapping was obtained for CBB-G (6.6 RU/ng•mm^{-2} for IgG and 4.4 RU/ng•mm^{-2} for transferrin, respectively). These results demonstrate the observed highest protein binding capacity of CBB-G dye. The variation in the assay's sensitivities towards different proteins was observed for all applied dyes as well as for the immunolabeling method. It indicates the need for preliminary calibration for individual receptor proteins to obtain reliable quantitative results. However, in the case of SPRi bioreceptor arrays, such a calibration will be much easier to carry out due to the possibility of using a single dye as a non-specific marker to visualize all receptor proteins in the SPRi array in a single experiment.

The obtained calibration curves enable the determination of a range for reliable quantitative analyses of protein surface densities, however as shown in Fig. 4, the relationship between SPRi responses and dye staining surface densities exhibits some inaccuracies compared to immunostaining, as evidenced by noticeably larger error bars. These inaccuracies stem from methodological issues in SPR signal analysis and chip transfer rather than intrinsic dye-protein interactions. Calibration curves rely on surface densities derived from SPR sensograms recorded in a small central area, necessitating the assumption of uniform protein density across the flow cell. Furthermore, inaccuracies in dye staining measurements arise because reflectance is read at the end of the association step, unlike immunolabeling. Bulk effects are not always effectively suppressed in SPRi cells, where the medium exchange is less efficient than in narrow SPR microcells, potentially causing differences in interaction times and inhomogeneities across test fields. Immunolabeling signals are unaffected, as they are read after the dye is removed. Despite these challenges, in routine laboratory applications such as

quality control of microfabricated SPRi biochips, comparing responses from corresponding test fields and visually analyzing SPRi images for layer homogeneity can be more valuable than relying solely on absolute surface density values. This approach simplifies result analysis and minimizes inaccuracies associated with surface density determination using SPR. We believe that chip-to-chip comparisons will provide a practical method to assess consistency and quality without being affected by potential measurement errors associated with SPR techniques.

It is worth emphasizing that the presented method can be used to estimate the surface density of immobilized receptors. However, it is unsuitable for determining the protein's viability or available binding sites. The mere presence of a protein on the surface does not ensure its biological functionality. Thus, while the dye-protein interaction confirms that the bioreceptor has successfully immobilized to the surface—highlighting the principal benefit of the presented quality control method—it does not provide insight into potential protein-protein interactions.

The design of sensitive SPRi biosensors and platforms for the reliable characterization of molecular interactions often requires maximizing the measured analytical signal while maintaining the spatial freedom necessary for undisturbed interaction of usually large proteins. Therefore, in routine applications, various SPR substrates with 3D architectures based on carboxymethyl dextran hydrogels have now become preferred for designing protein-based SPR platforms [36]. Thus, in further studies, we investigated the application potential of non-specific staining methods using PS, AB, and CBB-G to quantitatively determine proteins immobilized on a commercial 50 M-type CMD substrate (3D architecture, CMD chain length = 50 nm). Due to the different substrates used for immobilization, the accessibility of the protein to the dye may vary as the spatial architecture of the layer impacts the distance of the protein from the surface. This may be particularly relevant for dyes considered permanent in membrane applications (CBB-G and AB), as they tend to exist in equilibrium with colloidal dye particles, which have limited diffusion capacity [28]. Therefore, the influence of the substrate and topography of immobilized antibodies with varying surface densities has been studied. To obtain different surface densities of proteins within the test zones, rabbit IgG and transferrin solutions of 5 $\mu g \bullet mL^{-1}$ and 100 $\mu g \bullet mL^{-1}$ were used during immobilization. The results of protein immobilization on the CMD-coated slide and their further staining with PS, AB, CBB-G and specific antibodies are depicted in Fig. 5A (rabbit IgG) and 5B (transferrin).

As can be seen, CMD hydrogel substrates enabled much higher protein surface densities than PEG monolayer-based substrates. A protein concentration of 100 $\mu g \bullet mL^{-1}$ in the immobilization buffer allows for obtaining surface densities of about 16 $ng \bullet mm^{-2}$ for rabbit IgG and 12.5 $ng \bullet mm^{-2}$ for transferrin, respectively. For both types of immobilized proteins, an increase in SPRi signals recorded for all dyes was observed as the surface density of the immobilized protein increased. Changing the SPR substrate type from a planar (HS-PEG-COOH) to a 3D CMD hydrogel substrate resulted in a broader range of dynamic responses to protein staining, without a noticeable negative impact of diffusion limitations. It may be assigned to the higher capacity of the hydrogel layer and thus to the reduction in steric crowding of proteins, which hinders their effective interaction with dye molecules.

To better evaluate the quantitative relationships between the surface densities of proteins and the SPRi responses to dye labeling, the signal ratios obtained for both surface densities of each protein were calculated, and the values of the signal ratios are summarized in Table 1. We assumed that the closer the ratio of the SPRi staining response to the ratio of surface densities determined from SPR immobilization sensograms, the more accurately a given dye represents the relationships of the surface densities. As can be seen, the initial relationships between the surface densities of proteins immobilized on 3D CMD substrate were most accurately represented by staining with PS for both rabbit IgG (PS ratio = 92.0 % SPR ratio) and transferrin (PS ratio = 99.6 % SPR ratio). The other dyes, i.e., AB and CBB-G, were characterized by a more noticeable loss of response linearity for high protein surface densities. An even more significant decrease in sensitivity was observed for immunolabeling with polyclonal antibodies (*anti*-rabbit IgG), where the signal ratio (H/L) only slightly exceeds 1. The obtained results support the hypothesis of the presence of significant steric hindrances preventing efficient immunolabeling in the three-dimensional matrix of CMD with high packing of immobilized rabbit IgG. Slightly fewer steric problems were observed for transferrin, which was labeled with a monoclonal antibody. This difference may be explained by the smaller size of transferrin and the limited availability of epitopes to which the antibody

Table 1
Ratios of corresponding SPRi signals of nonspecific staining and immunolabeling for high (H) and low (L) protein surface density. Rabbit IgG and transferrin layers were immobilized on the CMD sensor slide.

	signal ratio (H/L)	
	rabbit IgG	transferrin
SPR	3.61	2.36
PS	3.32±0.46	2.35±0.18
AB	3.25±0.42	1.91±0.10
CBB-G	1.67±0.12	1.57±0.28
immunolabeling	1.16±0.24	1.84±0.23

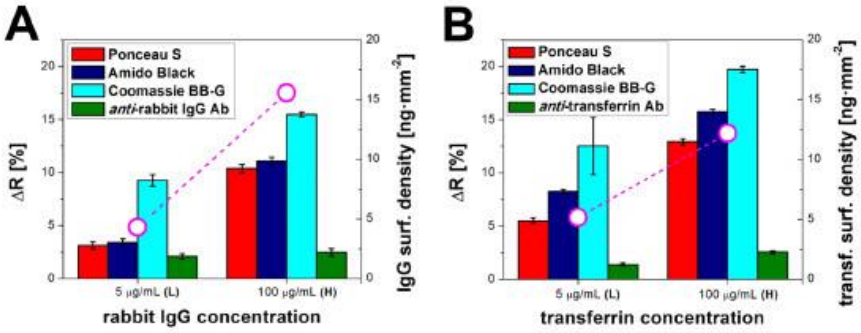

Fig. 5. SPRi response values for rabbit IgG (A) and transferrin (B) to injections of individual dyes and specific antibodies. Proteins were immobilised in-line in the SPR fluidic system at two different concentrations (5 $\mu g \bullet mL^{-1}$ and 100 $\mu g \bullet mL^{-1}$) using a commercial CMD hydrogel substrate with 3D architecture and a thickness of 50 nm (type: 50 M). The auxiliary axis (right axis) shows the protein surface densities calculated from SPR sensograms after immobilization (empty magenta dots with dashed lines).

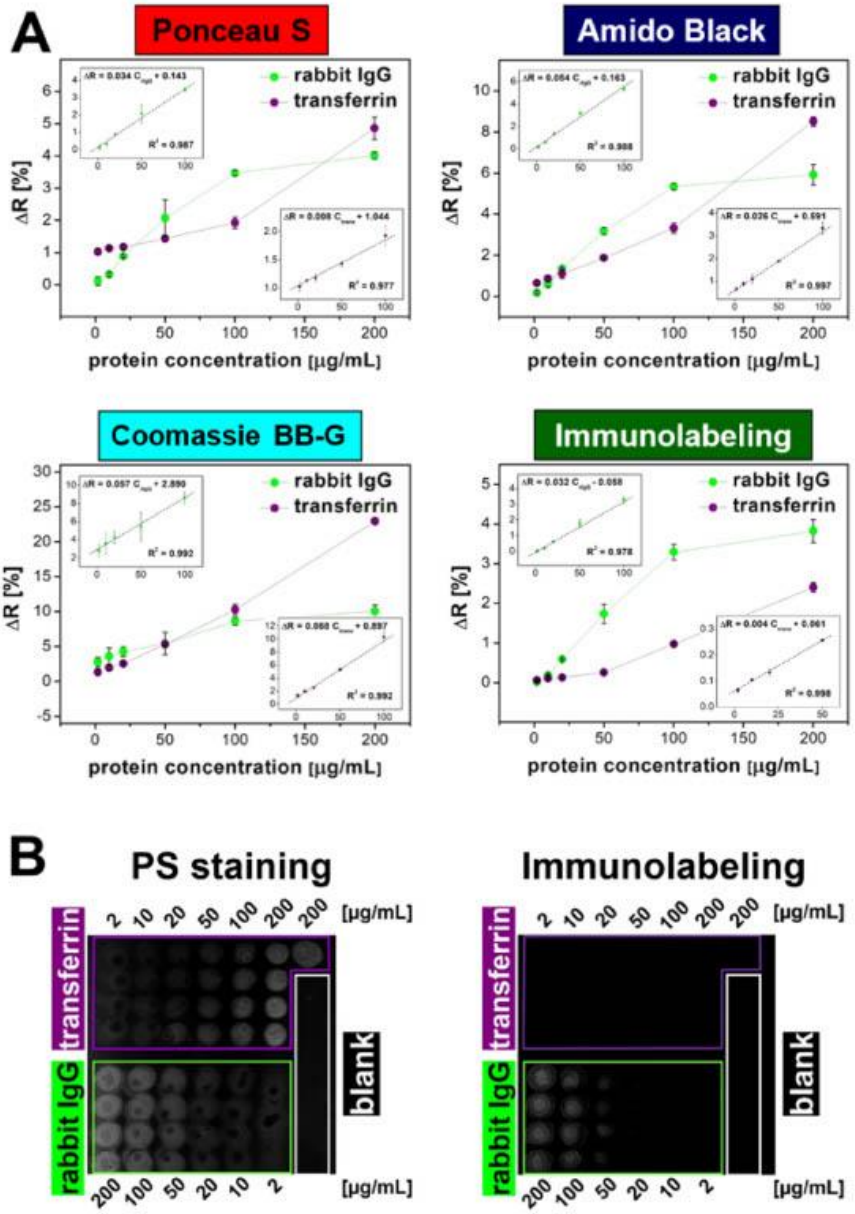

Fig. 6. SPRi reflectivity changes (A) and differential images (B) for the proteins immobilised ex-situ in a microarray format. A series of test fields (n = 4) were manufactured by automatic microdispensing protein solutions in concentrations ranging from 2 to 100 $\mu g \cdot mL^{-1}$. Insets in Fig. 6A show the results of linear fitting along with determined regression parameters. Exemplary images were captured for non-specific staining by Ponceau S and specific immunolabeling by anti-rabbit IgG.

can bind.

The above-commented observations are supported by previous studies and literature reports, which indicated the high reversibility of protein staining with PS and the facility of saturation of protein binding sites with dye molecules. These features of PS promote fast and efficient labeling of proteins in 3D matrices. Therefore, PS appears to be the best candidate for mapping proteins on CMD hydrogel substrates. It offers the highest accuracy for quantitative analysis over a wide range of surface

densities, even despite the lower sensitivity of the recorded SPRi response.

To demonstrate the potential of the developed staining-based methods for receptor layer quality control in SPRi protein microarrays, a platform with covalently immobilized proteins on a CMD-coated SPRi chip was prepared. To validate the feasibility of PS, AB, and CBB-G staining for quantitative evaluation of a wide range of protein surface densities, rabbit IgG and transferrin solutions in the concentration range of 2–100 $\mu g \bullet mL^{-1}$ were automatically spotted by non-contact dispensing. As shown in Fig. 6, Ponceau S, Amido Black, and Coomassie Brilliant Blue G enable visualization and quantitative assessment of the surface densities of proteins immobilized within the protein array. Among these, CBB-G dye demonstrates superior sensitivity, offering pivotal advantages for mapping receptor layers characterized by a low protein surface density. As expected, a monotonic growth in SPRi response to labeling was observed across all dyes, which stands in a good correlation with the increase of receptor protein concentration used for spotting. The linear relationship of SPR responses for all dyes and specific antibodies was observed within an initial part of the concentration range (see insets in Fig. 6). Nevertheless, a distinct observation was that transferrin exhibits enhanced immobilization efficacy at elevated concentrations of spotted proteins, in contrast to rabbit IgG. In the case of antibodies, the equalization of surface density was observed for high protein concentrations in solution. The observed differences in the relationship between protein concentration and surface density may be explained by the different rates of electrostatic preconcentration and immobilization processes accompanying coupling by EDC/NHS chemistry [37].

It is essential to emphasize the fundamental differences in immobilization under fluidic conditions using SPR device (above-commented experiments) and the *ex-situ* microspotting process (herein-discussed experiment). The control of parameters affecting the efficiency and homogeneity of immobilization, such as interaction time, humidity/drying, or local preconcentration processes in tiny droplets, is much more complex, as can also be observed in our case (Fig. 6B). Analysis of the SPRi image resulting from non-specific protein staining with PS allows for rapid visualization and identification of test fields (or their fragments) characterized by low surface density of immobilized proteins of different types during a single dye injection.

The developed method of protein mapping by nonspecific labeling with dyes exhibits significantly higher sensitivity than immunolabelling. In addition, immunolabeling shows substantial variation in sensitivity depending on the labeled protein and antibody used for its visualization. In the case of rabbit IgG, we can observe a higher sensitivity of immunolabeling in comparison to transferrin, and such a discrepancy is not evident with dye-based mapping. Labeling with antibodies involves individual selection of the appropriate antibody concentration, which is problematic for arrays of multiple proteins and consequently complicates the whole procedure. Conversely, dye-based approaches facilitate rapid quality assessment for all receptors at the same time, thus preventing the need for layer regeneration. This advantage overcomes the challenges of establishing suitable regeneration conditions and mitigates the risk of dissociation or inactivation of immobilized receptors. It should be however noted, that the developed method of protein receptor layer quality control using nonspecific dye staining is limited to assays where no additional surface blocking with proteins is applied. Nevertheless, in most of the currently developed SPR/SPRi biosensors, other solutions are used to prevent fouling instead of proteins, such as hydrophilic surface modifiers based on PEG or CMD, which have proven compatibility with the method developed in this work [38].

4. Conclusions

A rapid, low-cost, and versatile method for mapping and quality control of protein-based receptor layers for multiplex SPRi immunosensing has been developed. A single injection of the selected anionic dye: Ponceau S, Amido Black 10B, or Coomassie Brilliant Blue G under optimal conditions allows visualization of the different types of surface-bound proteins on the SPR chip and the quantification of the surface density of receptors previously immobilized on the surface. Due to the ease of spontaneous dissociation of dye molecules from the protein receptor layer on SPR chip, the proposed labeling method does not require additional regeneration steps. It can be used as a routine method to control the efficiency and homogeneity of immobilization in a single experiment immediately before or during the use of the SPRi array for biosensing, which is expected to affect the assay's quality. However, this method does not determine protein viability or functionality, as the dye-protein interaction only confirms surface binding, not potential protein-protein activity. Using proteins with different functions and properties, i.e., rabbit IgG (as a model immunoreceptor) and transferrin (as a model antigen receptor), we demonstrated the versatility of the procedure of non-specific, simultaneous labeling by staining over immunolabeling with antibodies. Given the non-specific nature of dye interactions, the presented method can be adapted for visualizing and characterizing various receptor proteins. Since the dye binding capacity, and consequently the sensitivity of the assay, may vary depending on the structure of the receptor proteins, we recommend individual calibration for quantitative analyses [28]. We proved that the set of methods we developed has a satisfactory sensitivity (depending on the type of dye used) and a wide range of dynamic response: up to at least ~ 3.0–3.8 $ng \bullet mm^{-2}$ for 2D protein monolayers and up to at least ~ 12–15 $ng \bullet mm^{-2}$ for proteins immobilized in commercial CMD hydrogel substrate. The feasibility of the developed methods for post-immobilization mapping and quality control of the model SPRi protein matrix generated by an automated dispenser was also demonstrated. Our studies revealed that each of the tested dyes has unique advantages, predestining its use for specific applications. CBB-G has the highest sensitivity and is recommended for quality control of low surface-density layers. AB offers relatively mild immobilization conditions (pH 4.0) and is therefore recommended for labeling proteins sensitive to acidic media, while PS, due to its fast association kinetics and ease of dissociation, is recommended for quality control of high surface density layers, such as 3D matrices based on CMD hydrogels. We believe that the protein staining method for quality control of SPRi biosensing platforms has excellent potential for further methodology development with different surface modifications and immobilization approaches.

CRediT authorship contribution statement

Marcin Drozd: Writing – original draft, Visualization, Supervision, Methodology, Formal analysis, Data curation, Conceptualization. **Mariusz Pietrzak:** Writing – review & editing, Supervision, Resources, Formal analysis. **Elżbieta Malinowska:** Writing – review & editing, Supervision, Project administration, Formal analysis. **Sylwia Karoń:** Writing – original draft, Visualization, Methodology, Investigation, Formal analysis, Data curation, Conceptualization. **Karolina Porycka:** Investigation, Data curation. **Lorico DS. Lapitan:** Writing – review & editing, Investigation, Data curation.

Declaration of Competing Interest

The authors declare that they have no known competing financial interests or personal relationships that could have appeared to influence the work reported in this paper.

Data availability

Data will be made available on request.

Acknowledgements

This work has been financially supported by Warsaw University of

Technology under the program Excellence Initiative, Research University (IDUB), YOUNG PW, grant number: 504450100067 and IDUB POSTDOC PW Programme, grant number: 1820/126/Z01/2021. We would like to acknowledge the financial support from the Ministry of Education and Science, Poland, grant number 7015/IA/SP/2019.

Appendix A. Supporting information

Supplementary data associated with this article can be found in the online version at doi:10.1016/j.snb.2024.136512.

References

[1] A.D. Stephens, Y. Song, B.L. McClellan, S.-H. Su, S. Xu, K. Chen, M.G. Castro, B. H. Singer, K. Kurabayashi, Miniaturized microarray-format digital ELISA enabled by lithographic protein patterning, Biosens. Bioelectron. 237 (2023), https://doi.org/10.1016/j.bios.2023.115536.

[2] E.N. Savvateeva, M.Yu Yukina, N.F. Nuralieva, M.A. Filippova, D.A. Gryadunov, E. A. Troshina, Multiplex autoantibody detection in patients with autoimmune polyglandular syndromes, Int. J. Mol. Sci. 22 (2021), https://doi.org/10.3390/ijms22115502.

[3] J. Svetlova, D. Gustin, V. Manuvera, D. Shirokov, V. Shokina, K. Prusakov, K. Aldarov, D. Kharlampieva, D. Matyushkina, J. Bespyatykh, V. Lazarev, T. Vedekhina, Microarray profiling of vaccination-induced antibody responses to SARS-CoV-2 variants of interest and concern, Int. J. Mol. Sci. 23 (2022), https://doi.org/10.3390/ijms232113220.

[4] R. Liao, M. Mondal, C.D. Nazaroff, D. Mastroeni, P.D. Coleman, J. Labaer, J. Guo, Highly sensitive and multiplexed protein imaging with cleavable fluorescent tyramide reveals human neuronal heterogeneity, Front Cell Dev. Biol. 8 (2021), https://doi.org/10.3389/fcell.2020.614624.

[5] G. Zhou, S. Bergeron, D. Juncker, High-performance low-cost antibody microarrays using enzyme-mediated silver amplification, J. Proteome Res. 14 (2015) 1872–1879, https://doi.org/10.1021/pr501259e.

[6] B. Wang, B. Park, J. Chen, X. He, Rapid and label-free immunosensing of Shiga toxin subtypes with surface plasmon resonance imaging, Toxins 12 (2020), https://doi.org/10.3390/toxins12050280.

[7] A.S. Malinick, A.S. Lambert, D.D. Stuart, B. Li, E. Puente, Q. Cheng, Detection of multiple sclerosis biomarkers in serum by ganglioside microarrays and surface plasmon resonance imaging, ACS Sens. 5 (2020) 3617–3626, https://doi.org/10.1021/acssensors.0c01935.

[8] Y.-Y. Chen, Z.-H. Wang, Y.-H. Meng, G. Jin, Biosensor with total internal reflection imaging ellipsometry, Int. J. Nanotechnol. 4 (2007) 171–178, https://doi.org/10.1504/IJNT.2007.012322.

[9] H. Zhang, A.M. Klose, B.L. Miller, Label-free, multiplex glycan microarray biosensor for influenza virus detection, Bioconjug Chem. 32 (2021) 533–540, https://doi.org/10.1021/acs.bioconjchem.0c00718.

[10] M. Lynch, C. Mosher, J. Huff, S. Nettikadan, J. Johnson, E. Henderson, Functional protein nanoarrays for biomarker profiling, Proteomics 4 (2004) 1695–1702, https://doi.org/10.1002/pmic.200300701.

[11] A.S. Malinick, D.D. Stuart, A.S. Lambert, Q. Cheng, Surface plasmon resonance imaging (SPRi) in combination with machine learning for microarray analysis of multiple sclerosis biomarkers in whole serum, Biosens. Bioelectron. X 10 (2022), https://doi.org/10.1016/j.biosx.2022.100127.

[12] B. Park, B. Wang, J. Chen, Label-free immunoassay for multiplex detections of foodborne bacteria in chicken carcass rinse with surface plasmon resonance imaging, Foodborne Pathog. Dis. 18 (2021) 202–209, https://doi.org/10.1089/fpd.2020.2850.

[13] E. Chiodi, P. Damin, L. Sola, L. Ferraro, D. Brambilla, M.S. Ünlü, M. Chiari, A reliable, label free quality control method for the production of dna microarrays with clinical applications, Polymers 13 (2021) 1–13, https://doi.org/10.3390/polym13030340.

[14] J.B. Perez, D. Tyagi, M. Yang, L. Calvo, R. Perez, E. Moreno, J. Zhu, Predicting the right spacing between protein immobilization sites on self-assembled monolayers to optimize ligand binding, Anal. Biochem 484 (2015) 133–135, https://doi.org/10.1016/j.ab.2015.05.005.

[15] A.E.M. Wammes, M.J.E. Fischer, N.J. De Mol, M.B. Van Eldijk, F.P.J.T. Rutjes, J.C. M. Van Hest, F.L. Van Delft, Site-specific peptide and protein immobilization on surface plasmon resonance chips via strain-promoted cycloaddition, Lab Chip 13 (2013) 1863–1867, https://doi.org/10.1039/c3lc41338a.

[16] L.-T. Jin, J.-K. Choi, Usefulness of visible dyes for the staining of protein or DNA in electrophoresis, Electrophoresis 25 (2004) 2429–2438, https://doi.org/10.1002/elps.200305995.

[17] T.H. Steinberg, Chapter 31 protein gel staining methods, Introd. Overv. (2009), https://doi.org/10.1016/S0076-6879(09)63031-7.

[18] J.-L. Wang, L. Zhao, M.-Q. Li, W.-G. Chen, C.-J. Xu, A sensitive and reversible staining of proteins on blot membranes, Anal. Biochem 592 (2020), https://doi.org/10.1016/j.ab.2020.113579.

[19] L. Simon, R.E. Gyurcsányi, Multiplexed assessment of the surface density of DNA probes on DNA microarrays by surface plasmon resonance imaging, Anal. Chim. Acta 1047 (2019) 131–138, https://doi.org/10.1016/j.aca.2018.09.048.

[20] J. Da Gama Duarte, R.W. Goosen, P.J. Lawry, J.M. Blackburn, PMA: protein microarray analyser, a user-friendly tool for data processing and normalization, BMC Res Notes 11 (2018), https://doi.org/10.1186/s13104-018-3266-0.

[21] M.A. Campanero-Rhodes, E. Llobet, J.A. Bengoechea, D. Solís, Bacteria microarrays as sensitive tools for exploring pathogen surface epitopes and recognition by host receptors, RSC Adv. 5 (2015) 7173–7181, https://doi.org/10.1039/c4ra14570d.

[22] D. Bickar, P.D. Reid, A high-affinity protein stain for western blots, tissue prints, and electrophoretic gels, Anal. Biochem 203 (1992) 109–115, https://doi.org/10.1016/0003-2697(92)90049-D.

[23] H. Schägger, G. von Jagow, Blue native electrophoresis for isolation of membrane protein complexes in enzymatically active form, Anal. Biochem 199 (1991) 223–231, https://doi.org/10.1016/0003-2697(91)90094-A.

[24] H.J. Chial, A.G. Splittgerber, A comparison of the binding of Coomassie brilliant blue to proteins at low and neutral pH, Anal. Biochem 213 (1993) 362–369, https://doi.org/10.1006/abio.1993.1433.

[25] G. Krainer, T.J. Welsh, J.A. Joseph, J.R. Espinosa, S. Wittmann, E. de Csilléry, A. Sridhar, Z. Toprakcioglu, G. Gudiškytė, M.A. Czekalska, S. Alberti, T.P. J. Knowles, Reentrant liquid condensate phase of proteins is stabilized by hydrophobic and non-ionic interactions, Nat. Commun. 12 (2021), https://doi.org/10.1038/s41467-021-21181-9.

[26] R.W. Congdon, G.W. Muth, A.G. Splittgerber, The binding interaction of coomassie blue with proteins, Anal. Biochem 213 (1993) 407–413, https://doi.org/10.1006/abio.1993.1439.

[27] I. Romero-Calvo, B. Ocón, P. Martínez-Moya, M.D. Suárez, A. Zarzuelo, O. Martínez-Augustin, F.S. de Medina, Reversible Ponceau staining as a loading control alternative to actin in Western blots, Anal. Biochem 401 (2010) 318–320, https://doi.org/10.1016/j.ab.2010.02.036.

[28] V. Neuhoff, N. Arold, D. Taube, W. Ehrhardt, Improved staining of proteins in polyacrylamide gels including isoelectric focusing gels with clear background at nanogram sensitivity using Coomassie Brilliant Blue G-250 and R-250, Electrophoresis 9 (1988) 255–262, https://doi.org/10.1002/elps.1150090603.

[29] F. Chevalier, Analytical Methods: Electrophoresis, 2011. https://doi.org/10.1016/B978-0-12-374407-4.00017-0.

[30] K. Andersson, D. Areskoug, E. Hardenborg, Exploring buffer space for molecular interactions, J. Mol. Recognit. 12 (1999) 310–315, https://doi.org/10.1002/(SICI)1099-1352(199909/10)12:5<310::AID-JMR470>3.0.CO;2-5.

[31] C.S. Schneider, A.G. Bhargav, J.G. Perez, A.S. Wadajkar, J.A. Winkles, G. F. Woodworth, A.J. Kim, Surface plasmon resonance as a high throughput method to evaluate specific and non-specific binding of nanotherapeutics, J. Control. Release 219 (2015) 331–344, https://doi.org/10.1016/j.jconrel.2015.09.048.

[32] P. Gomes, D. Andreu, Direct kinetic assay of interactions between small peptides and immobilized antibodies using a surface plasmon resonance biosensor, J. Immunol. Methods 259 (2002) 217–230, https://doi.org/10.1016/S0022-1759(01)00503-8.

[33] G. Bergström, C.-F. Mandenius, Orientation and capturing of antibody affinity ligands: applications to surface plasmon resonance biochips, Sens Actuators B Chem. 158 (2011) 265–270, https://doi.org/10.1016/j.snb.2011.06.017.

[34] H. Zhao, I.I. Gorshkova, G.L. Pu, P. Schuck, A comparison of binding surfaces for SPR biosensing using an antibody-antigen system and affinity distribution analysis, Methods 59 (2013) 328–335, https://doi.org/10.1016/j.ymeth.2012.12.007.

[35] L. Sarcina, C. Scandurra, C. Di Franco, M. Caputo, M. Catacchio, P. Bollella, G. Scamarcio, E. Macchia, L. Torsi, A stable physisorbed layer of packed capture antibodies for high-performance sensing applications, J. Mater. Chem. C. Mater. 11 (2023) 9093–9106, https://doi.org/10.1039/d3tc01123b.

[36] M. Drozd, E. Kobylska, M. Żmieńko, M. Chudy, Sensitive and label-free SPR biosensing platforms for high-throughput screening of plasma membrane receptors interactions with insulin-like targets of hypoglycaemic activity, Talanta 274 (2024), https://doi.org/10.1016/j.talanta.2024.125914.

[37] F. Risse, E.T. Gedig, J.S. Gutmann, Carbodiimide-mediated immobilization of acidic biomolecules on reversed-charge zwitterionic sensor chip surfaces, Anal. Bioanal. Chem. 410 (2018) 4109–4122, https://doi.org/10.1007/s00216-018-1048-0.

[38] S. Domínguez-Medina, L. Kisley, P. Swanglap, J. Olson, C.F. Landes, S. Link, Adsorption and unfolding of a single protein triggers nanoparticle aggregation, Acta Biomater. 30 (2016) 287–297, https://doi.org/10.1016/j.actbio.2016.02.035.

Sylwia Karoń is a Ph.D candidate of Warsaw University of Technology (WUT). She is a graduate of two universities – Warsaw University of Life Sciences (Bachelor of Engineering, studies on biologically active particles responsible for inflammation signaling in mammals) and WUT (Master's degree, studies on inactivation and separation of bacteriophages). She works at the Centre for Advanced Materials and Technologies (CEZAMAT, WUT). Her ongoing research interests include developing novel constructions for multiplex immunosensors in medical diagnostics and characterizing molecular interactions and biosensing using surface plasmon resonance.

Karolina Porycka received her BSc Eng in Biotechnology from Warsaw University of Technology in 2023, defending the thesis entitled "Application of DNA-labelled antibodies in the design of universal immunosensor platforms for detection of antibodies and biomarkers of viral diseases". Now she is MSc Eng student and her research interest is the development of Lab-on-a-Foil diagnostic systems.

Lorico DS. Lapitan Jr. is a post-doctoral fellow at the Warsaw University of Technology. Particularly, he works for Centre for Advanced Materials and Technologies CEZAMAT. His research interests involve the development of electrochemical and optical biosensors for

label-free techniques, early diagnostics of cancer, and determination/detection of biomarkers. His research has recently focused on surface plasmon resonance (SPR)-based biosensors on developing novel strategies for early cancer diagnostics.

Marcin Drozd is an assistant professor, received his Ph.D. in chemistry from the Faculty of Chemistry, Warsaw University of Technology (WUT) in 2018. Now he works in the Chair of Medical Biotechnology (WUT) and Centre for Advanced Materials and Technologies (CEZAMAT, WUT). His current research interests include synthesis and functionalization of magnetic and plasmonic nanomaterials for bioanalytical applications and development of miniaturized immunoassays. He focuses also on the characterization of molecular interactions and biosensing using surface plasmon resonance.

Mariusz Pietrzak is an associate professor at the Warsaw University of Technology (Faculty of Chemistry, Chair of Medical Biotechnology). He also works for Centre for Advanced Materials and Technologies CEZAMAT, where he is the head of the Medical Diagnostics Department. His research interests concern the development of new electrochemical and optical biosensors and biotests, as well as the synthesis, surface modification, and application of nanoparticles. Recently, the works on nanozymes of noble metals have become his main focus. Particularly, he works on conjugates of catalytic nanoparticles with receptors, which can be used to develop novel tools for detecting various types of biomarkers.

Elżbieta Malinowska is a professor at the Warsaw University of Technology (Faculty of Chemistry, Chair of Medical Biotechnology). She also works at Centre for Advanced Materials and Technologies CEZAMAT WUT as Deputy Director for Research and Development. Her primary research interest is the design of receptor layers for chemical sensors and biosensors. Recently, she has been involved in projects related to PoCT systems for the detection of clinically relevant biomarkers.

Suplement S3 publikacji P3:

A versatile approach to quality control of protein-based receptor layers by reversible, nonspecific staining for multiplex SPRi immunosensing

Supplementary material

A versatile approach to quality control of protein-based receptor layers by reversible, nonspecific staining for multiplex SPRi immunosensing

*Sylwia Karoń[1,2], Karolina Porycka[2], Lorico Jr DS. Lapitan[1,3], Marcin Drozd[*1,2], Mariusz Pietrzak[1,2], Elżbieta Malinowska[1,2]*

1. Department of Medical Diagnostics, Centre for Advanced Materials and Technologies CEZAMAT, Warsaw University of Technology, Warsaw, 02-822, Poland

2. Chair of Medical Biotechnology, Faculty of Chemistry, Warsaw University of Technology, Warsaw, 00-664, Poland

3. Department of Chemical Engineering and Research Center for the Natural and Applied Sciences, University of Santo Tomas, España Boulevard, Manila, Philippines

*corresponding author

e-mail: marcin.drozd.ch@pw.edu.pl

tel.: +48 182 10 74

1. Experimental

1.1. Preparation of surface-modified SPR slides for covalent immobilization

Au-coated SPR slides were cleaned using a mixture of distilled water, 30% H_2O_{2aq}, and ammonia (3:1:1 v/v) at 70°C for 20 minutes, then treated with UV-ozone cleaner (Ossila Ltd, UK) for 30 minutes. For covalent immobilization using EDC-NHS chemistry, the sensor slides were pre-coated with 1 mM PEG-COOH in 1M KH_2PO_4 and left overnight at 4°C. Then, the slides were rinsed with DI water, air-dried, and placed in the SPR apparatus for protein immobilization.

1.2. Covalent immobilization of receptor proteins in a microfluidic SPR system

The immobilization of rabbit IgG and transferrin was performed using the MP-SPR Navi™ 220A NAALI device (BioNavis Ltd, Finland). SPR measurements were conducted parallelly in two microfluidic channels using angular scan mode (60-74°) at wavelength 670 nm. During immobilization in the microfluidic system of the SPR apparatus, the flow cell and prism were thermostated to maintain a constant temperature of 22°C. Dedicated MP-SPR Data Viewer software (BioNavis) was used for data processing. Unless otherwise stated, one channel was used to immobilize rabbit IgG and the second to immobilize transferrin. PBST buffer (PBS with 0.05% TWEEN®20) pH 7.4 was used as the running buffer, and all injections were done parallelly at the flowrate of 20 $\mu L \cdot min^{-1}$, and the maximum volume of the injection loop was 250 µL. The immobilization protocol was as follows: when stable baseline signals were observed, a conditioning solution (100 mM NaOH + 2 M NaCl) was injected for 4 minutes. Then, a freshly prepared solution of 20 mM EDC hydrochloride and 5 mM NHS in 50 mM MES/NaOH buffer pH 5.0 was applied for 9 minutes to activate carboxyl groups. Immediately after activation, solutions of rabbit IgG and transferrin (in concentrations from 0 up to 200 $\mu g \cdot mL^{1}$) were injected for 10-20 minutes (both depending on the specific experiment). The

immobilization medium was 5 mM acetate buffer (pH 4.5 for rabbit IgG and pH 4.0 for transferrin). Lastly, 1M ethanolamine hydrochloride/NaOH pH 8.5 was injected for 4 min to deactivate unreacted NHS-esters. The obtained protein surface densities were calculated from the measured resonant angle shifts, assuming a sensitivity of 10 $ng \cdot mm^{-2} \cdot deg^{-1}$ [1-3]. Conversion from deg to $ng \cdot mm^{-2}$ assumes the refractive index of running buffer close to 1.33 and the use of BK7 prism. After protein immobilization, the SPR chip was transferred to the SPRi Lab Plus instrument (Horiba, France) for further studies on protein-dye interactions.

1.3. *Ex-situ* immobilization on CMD-coated slide

A CMD-coated SPR slide was employed for microarray fabrication. The SPR slide was sequentially immersed in 100 mM NaOH + 2 M NaCl for 2 minutes (conditioning), 0.2 M EDC hydrochloride and 0.05 M N-hydroxysuccinimide (NHS) in 50 mM MES/NaOH buffer pH 5.0 for 9 minutes (activation) followed by rinsing in DI water and air drying. Rabbit IgG and transferrin at different concentrations (2, 10, 20, 50, 100, and 200 $\mu g \cdot mL^{-1}$) in 10 mM acetate buffer (pH 4.0) were automatically spotted (50 nL per drop) using Nano-Plotter NP2.1 (GeSiM Bioinstruments and Microfluidics, Germany) and left overnight in a humid atmosphere. The next day, the slide was blocked by immersion in 1M ethanolamine hydrochloride/NaOH pH 8.5 for 4 minutes, rinsed with water and air-dried. The chip was then inserted into the SPRi instrument for further experiments.

1.4. Determination of dose-response profiles

Injections of 12 concentrations of anionic dyes against immobilized rabbit IgG and transferrin were carried out at the flowrate of 20 $uL \cdot min^{-1}$ for 8 min using SPR device equipped with autosampler. 30-minute post-injection delay was applied to enable the dissociation of the dye. The typical dye concentration window was in the range of 0.2 – 50 $ug \cdot mL^{-1}$.

Table S1

Table S1. Comparison of physico-chemical parameters of the studied dyes.

Dye:	Ponceau S:	Amido Black:	Coomassie BB-G:
Hydrogen bond donor count	5	4	1
Hydrogen bond acceptor count	17	14	9
Isoelectric point	-	-	2.59
Dominant form:			
pH 2.0	Trianionic	Monoanionic	Neutral
pH 4.0	Tetranionic	Monoanionic	Monoanionic
pH 7.4	Tetranionic	Dianionic	Monoanionic
Lipophilicity [logD]:			
pH 2.0	-6.784	-1.924	7.054
pH 4.0	-7.507	-2.001	6.725
pH 7.4	-7.798	-2.941	5.857

* structure-based predictions for chemical properties were provided by Chemicalize platform chemicalize.com (ChemAxon, Budapest, Hungary) (Accessed 22.04.2024)

Figure S1

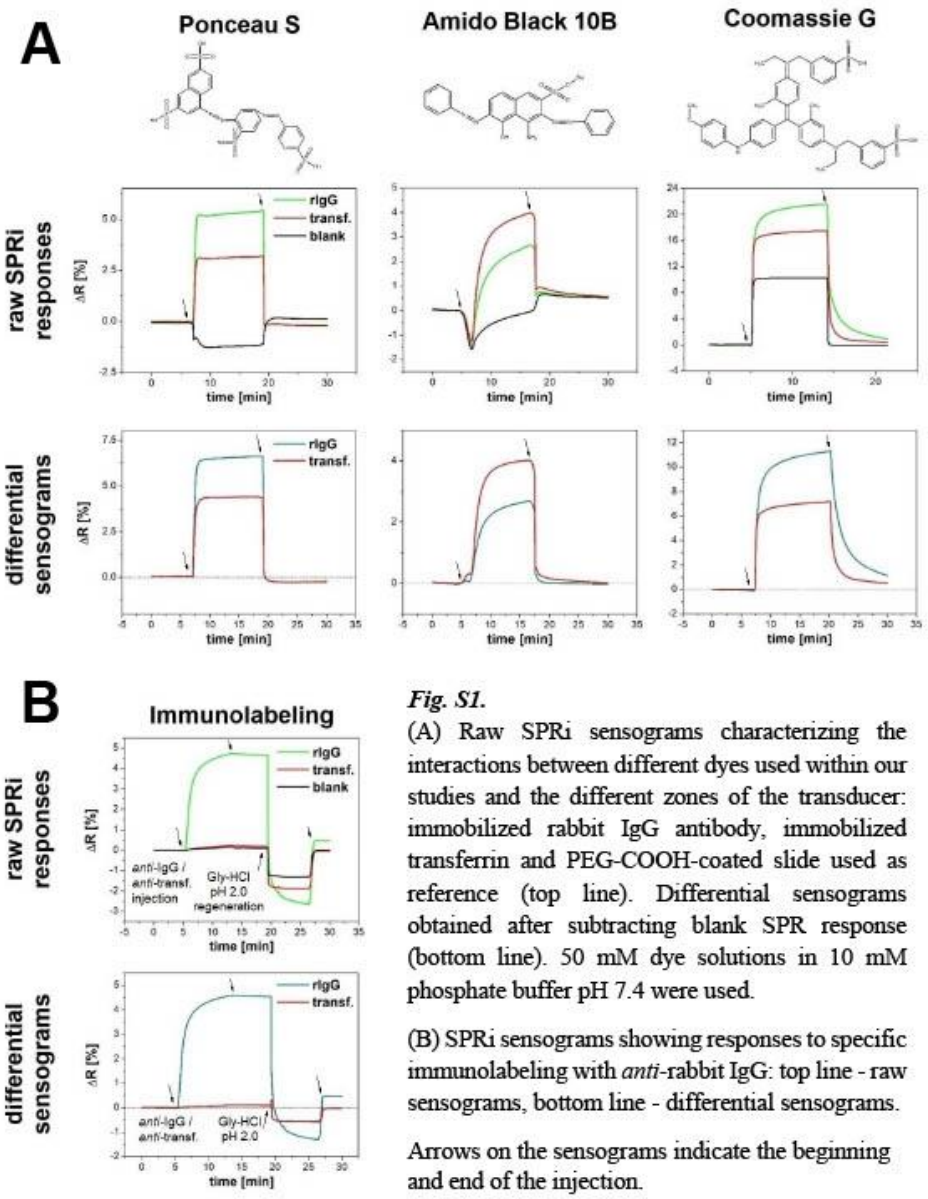

Fig. S1.

(A) Raw SPRi sensograms characterizing the interactions between different dyes used within our studies and the different zones of the transducer: immobilized rabbit IgG antibody, immobilized transferrin and PEG-COOH-coated slide used as reference (top line). Differential sensograms obtained after subtracting blank SPR response (bottom line). 50 mM dye solutions in 10 mM phosphate buffer pH 7.4 were used.

(B) SPRi sensograms showing responses to specific immunolabeling with *anti*-rabbit IgG: top line - raw sensograms, bottom line - differential sensograms.

Arrows on the sensograms indicate the beginning and end of the injection.

In the raw sensograms (top line in Fig. S1), SPRi responses to the injection of dye solutions selected for further study are shown. Both for immobilized transferrin and IgG, an increase in SPRi signal associated with the association of the dye molecules can be observed. The observed differences in reflectivity for blank surfaces without immobilized proteins (black curves) represent the "bulk effect" resulting from the different composition of the dye solution (10 mM Gly-HCl buffer / 10 mM acetate buffer, respectively) compared to the running buffer (PBST with 0.05% Tween®20). Only in the case of Amido Black 10B is a slight non-specific adsorption of the dye on the blank surface (without protein) observed. However, for all dyes selected for further study, there is an evident return to baseline a few minutes after the injection of the running buffer, indicating the reversibility of the staining process for all the chosen dyes. By using differential sensograms (Fig. S1 – bottom line), it is possible to compensate for bulk effects resulting from injecting a buffer of different compositions as well as any potential non-specific adsorption of the AB dye.

Figure S2

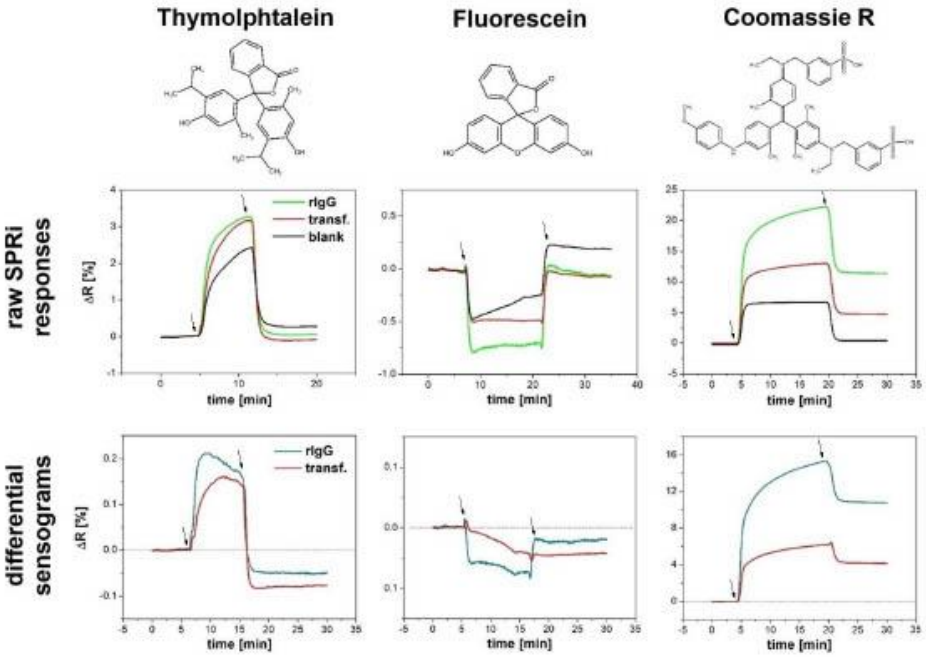

Fig. S2. Top line: Raw SPRi sensograms characterizing the interactions of dyes considered unsuitable for specific and reversible protein staining and the different zones of the transducer: immobilized rabbit IgG antibody, immobilized transferrin and PEG-COOH-coated slide used as reference. 50 mM dye solutions in 10 mM phosphate buffer pH 7.4 were used. Bottom line: differential sensograms obtained after subtracting blank SPR response. Arrows on the sensograms indicate the beginning and end of the injection.

Thymolphthalein was found to be unsuitable for protein staining due to its high level of non-specific binding and difficulty in washing off from the PEG-COOH substrate. Fluorescein showed no ability to interact with proteins. Coomassie Brilliant Blue R, despite its very good sensitivity and selectivity of protein staining, proved to be unsuitable due to the difficulty of washing off the associated dye (lack of reversibility).

Figure S3

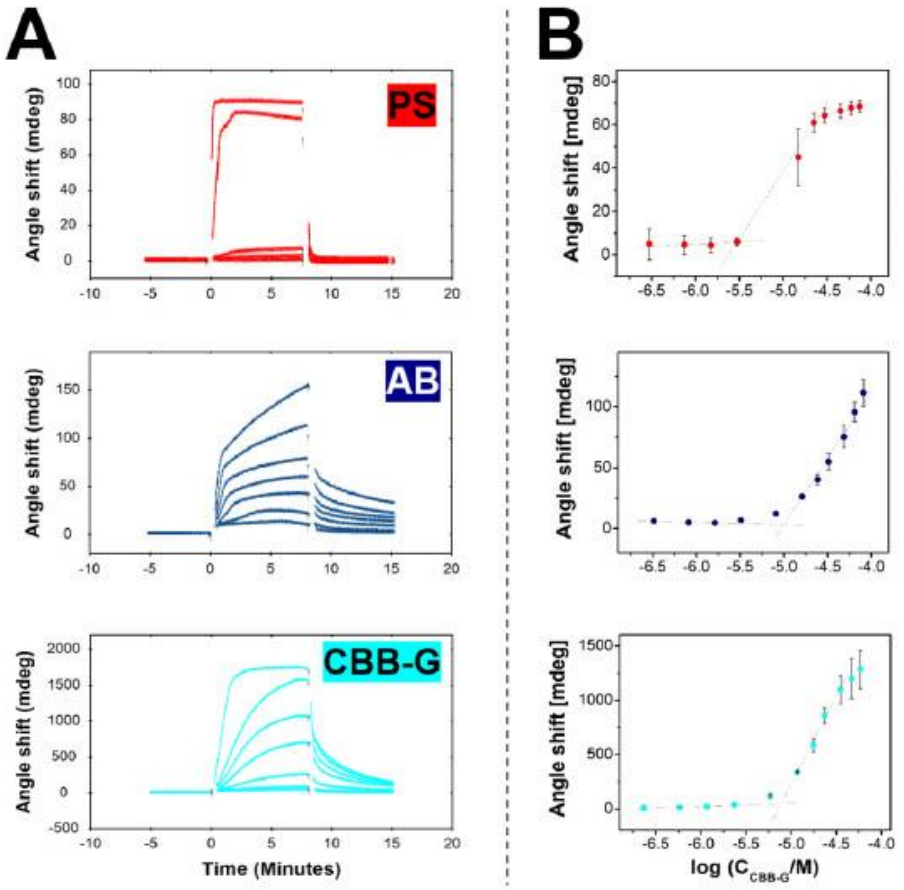

Fig. S3. A) Real-time SPR responses of rabbit IgG to injections of different concentrations of various anionic dyes. Top line: Ponceau S, middle line: Amido Black 10B, bottom line: Coomassie Brilliant Blue G. B) SPR response profiles for immobilized rabbit IgG plotted as a function of the logarithm of dye concentration. Signal values were determined from the sensograms, taking the value of angle shift after 90% of the association time.

Figure S4

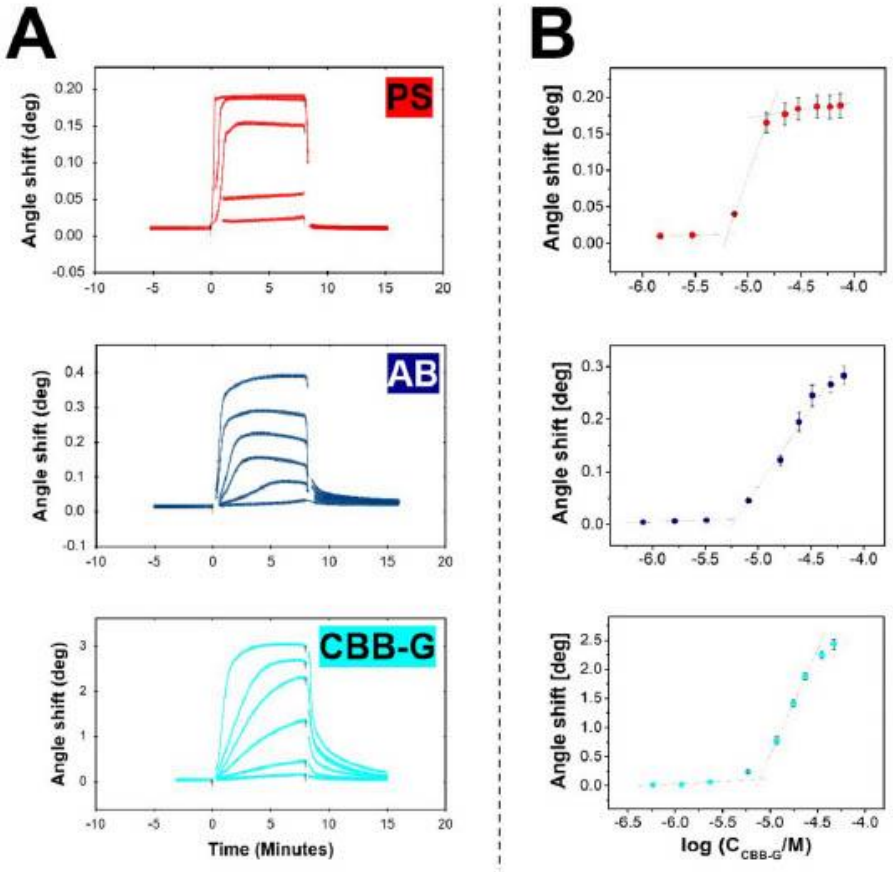

Fig. S4. A) Real-time SPR responses of transferrin to injections of different concentrations of various anionic dyes. Top line: Ponceau S, middle line: Amido Black 10B, bottom line: Coomassie Brilliant Blue G. B) SPR response profiles for immobilized transferrin plotted as a function of the logarithm of dye concentration. Signal values were determined from the sensograms, taking the value of angle shift after 90% of the association time.

References

[1] C.S. Schneider, A.G. Bhargav, J.G. Perez, A.S. Wadajkar, J.A. Winkles, G.F. Woodworth, A.J. Kim, Surface plasmon resonance as a high throughput method to evaluate specific and non-specific binding of nanotherapeutics, J. Control. Release 219 (2015) 331-344. https://doi.org/10.1016/j.jconrel.2015.09.048.

[2] M. Leeman, W.M. Albers, R. Bombera, J. Kuncova-Kallio, J. Tuppurainen, L. Nilsson, Correction to: Asymmetric flow field-flow fractionation coupled to surface plasmon resonance detection for analysis of therapeutic proteins in blood serum, Anal. Bioanal. Chem. 414 (2022) 1741. https://doi.org/10.1007/s00216-021-03793-8. Erratum in: Anal. Bioanal. Chem. 413 (2021) 117-127.

[3] R. Karlsson, A. Michaelsson, L. Mattsson, Kinetic analysis of monoclonal antibody-antigen interactions with a new biosensor-based analytical system, J. Immunol. Methods 145 (1991) 229-240. https://doi.org/10.1016/0022-1759(91)90331-9.

Publikacja P4:

PET Foils Functionalized with Reactive Copolymers as Adaptable Microvolume ELISA Spot Array Platforms for Multiplex Serological Analysis of SARS-CoV-2 Infections

sensors

MDPI

Article

PET Foils Functionalized with Reactive Copolymers as Adaptable Microvolume ELISA Spot Array Platforms for Multiplex Serological Analysis of SARS-CoV-2 Infections

Sylwia Pniewska [1,2], Marcin Drozd [1,2,*], Alessandro Mussida [3], Dario Brambilla [3], Marcella Chiari [3], Waldemar Rastawicki [4] and Elżbieta Malinowska [1,2]

[1] Department of Medical Diagnostics, Centre for Advanced Materials and Technologies CEZAMAT, Warsaw University of Technology, 02822 Warsaw, Poland
[2] Chair of Medical Biotechnology, Faculty of Chemistry, Warsaw University of Technology, 00664 Warsaw, Poland
[3] Institute of Chemical and Technological Science "Giulio Natta", National Research Council of Italy, 20131 Milan, Italy
[4] Department of Bacteriology and Biocontamination, National Institute of Public Health NIH—National Research Institute, 00791 Warsaw, Poland
* Correspondence: marcin.drozd.ch@pw.edu.pl; Tel.: +48-182-10-74

Abstract: Microvolume ELISA platforms have become vital in diagnostics for their high-throughput capabilities and minimal sample requirements. High-quality substrates with advanced surface properties are essential for these applications. They enable both efficient biomolecule immobilization and antifouling properties, which are critical for assay sensitivity and specificity. This study presents PET-based microvolume ELISA spot arrays coated with amine- and DBCO-reactive copolymers MCP-2 and Copoly Azide. The platforms were designed for the sensitive and specific detection of specific antibodies such as COVID-19 biomarkers. Supporting robust attachment of the SARS-CoV-2 nucleoprotein (NP), these arrays outperform traditional approaches. It was demonstrated that covalent attachment methods proved more efficient than passive adsorption, together with the reduction of non-specific binding. Analytical performance was verified with classical ELISA and real-time Surface Plasmon Resonance (SPR) analysis. It enables sensitive detection of IgG and IgA antibodies, including IgG subclasses, in human serum. Clinically, the platform achieved 100.0% sensitivity and 92.9% specificity for anti-NP antibody detection in COVID-19-positive and negative samples. Additionally, DNA-directed immobilization extended the platform's utility to multiplex serological measurements. These findings underscore the potential of PET-based microvolume ELISA arrays as scalable, high-throughput diagnostic tools suitable for detecting multiple biomarkers in a single assay and easily integrated into microfluidic devices.

Keywords: microvolume ELISA; PET; flexible substrate; multiplexing; protein microarray; immunoassay; COVID-19; serological biomarkers; IgG; nucleoprotein

Citation: Pniewska, S.; Drozd, M.; Mussida, A.; Brambilla, D.; Chiari, M.; Rastawicki, W.; Malinowska, E. PET Foils Functionalized with Reactive Copolymers as Adaptable Microvolume ELISA Spot Array Platforms for Multiplex Serological Analysis of SARS-CoV-2 Infections. *Sensors* **2024**, *24*, 7766. https://doi.org/10.3390/s24237766

Received: 18 October 2024
Revised: 15 November 2024
Accepted: 2 December 2024
Published: 4 December 2024

1. Introduction

Biomarker detection is vital in medical diagnostics. It provides critical insights into physiological or pathological processes and responses to treatments. Traditional single-analyte assays like ELISA are highly sensitive. However, they are limited by relatively low throughput, large sample consumption, and the inability to simultaneously detect multiple biomarkers [1]. The growing demand for miniaturized and multiplex detection platforms addresses this limitation. They enable parallel analysis of various biomarkers, providing a more comprehensive disease profile while reducing reagent use and cost [2]. Recent advances in microarrays and microfluidics have revolutionized biomarker

detection [3–6], allowing high-throughput, automated assays. However, challenges in ensuring reliability and sensitivity and managing issues like bioreceptor immobilization, signal interference, and background noise still need to be carefully considered.

Viral infections induce the production of various biomarkers, including viral genetic material, proteins, and host-derived antibodies across different isotypes and subclasses, which indicate an immune response [7]. The N and S proteins are primary targets of the humoral response [8], making them suitable as receptors for antibody detection in diagnostic platforms. Differentiating antibody classes and subclasses provides insight into infection progression and immune response [9]. The IgM antibody isotype is the first to respond, while IgG is the most abundant, with IgG1 and IgG3 crucial for viral defense [10]. In SARS-CoV-2 infection, IgM, IgA, and IgG are detectable soon after seroconversion [11,12].

To accurately reflect the complexity of biological processes, such as the progression of infection, systems capable of detecting multiple biomarkers in a single assay are essential. Established methods, such as lateral flow immunoassays [13,14], fluorescence-based colorimetric sensing [15,16], and label-free biosensors [17,18] are crucial in advancing multiplex biosensing. They enable rapid and sensitive detection across a range of applications. Research on SARS-CoV-2 antibody detection and distribution has been extensive due to its vital role in developing serological diagnostics [19–21]. However, developing multiplex analytical platforms presents distinct challenges. The effectiveness depends on accommodating a wide range of receptors, including recombinant proteins, antibodies, etc., and ensuring their proper binding with the assay substrate. Selecting an appropriate strategy for protein immobilization on solid supports is challenging due to the structural diversity of receptor proteins and the complexity of their interaction with surfaces [22]. For example, physical adsorption is simple but highly dependent on the protein's structure, charge, and hydrophilicity, making it less reliable and prone to probe loss over time [23]. Covalent immobilization offers stronger attachment but requires more complex chemistries [24]. Affinity-based methods, like His-Tag [25] or Avidin-Biotin [26], ensure oriented attachment but are expensive and complicated. As a result, ongoing efforts focus on developing efficient one-step protein coupling methods that also prevent nonspecific adsorption. In turn, the ideal substrate for multiplex assays should support stable, specific immobilization of diverse bioreceptors while preserving their activity. Such a substrate has reactive groups for easy conjugation and antifouling properties, ensuring high sensitivity and specificity. Compatibility with various detection methods, such as electrochemical and optical, is also essential for high-throughput point-of-care treatment (POCT) devices.

A promising solution is the development of microvolume assays on transparent polyester substrates, known as lab-on-a-foil platforms. This miniaturized, adaptable format offers several advantages, including cost-effectiveness through reduced reagent use and seamless integration with microfluidic channels and microarrays on the same substrate. It enables facile sample processing and analysis. Adapting PET-based arrays into microfluidic cassettes is relatively straightforward. It allows for the fabrication of sample-to-answer platforms [27]. The transparency of polyester foils facilitates the usage of optical detection methods such as fluorescence and colorimetry. Lab-on-a-foil devices are portable, making them ideal for POCT applications. PET foils can be coated with reactive copolymers to provide functional surfaces dedicated to bioreceptor immobilization, enhancing their application in multiplex assays. Such polymers and copolymers are typically equipped with reactive groups, like azides, amines, or quinones, to enable efficient "click" chemistry for stable, oriented biomolecule attachment [28,29]. Incorporating antifouling elements into the copolymer coating further enhances surface quality by reducing nonspecific binding from complex biological samples. This improvement increases assay sensitivity and specificity by minimizing background interference.

This work explored the feasibility of using reactive copolymers, MCP-2 and Copoly Azide, to coat PET substrates for developing flexible serological microvolume ELISA spot arrays. Two immobilization strategies (e.g., covalent amine coupling and DNA-directed

immobilization (DDI)) were applied to immobilize receptor proteins, with conventional passive adsorption as a reference. The PET-based platforms were assessed for their ability to detect different immunoglobulin classes and subclasses in sera from SARS-CoV-2 patients. The developed solution offers an effective distinction between positive and negative samples. The clinical potential of these immunoassays was also evaluated. Furthermore, immunoassays based on DDI for multiplex detection of viral biomarkers were designed, demonstrating the adaptability of the platform. Methods such as ELISA and Surface Plasmon Resonance (SPR) were employed to investigate the mechanisms of layer formation and immunoreaction pathways. We believe that the designed platforms possess high potential for further development and application in biosensing and microfluidics-integrated diagnostics.

2. Materials and Methods

A detailed list of basic chemical and biochemical reagents, as well as detailed oligonucleotide sequences used within this study, can be found in the Supplementary Materials.

MCP-2 and Copoly Azide copolymers were synthesized as reported elsewhere [30]. Transparent poly(ethylene terephthalate) foils for laser printers (Diamax, A4, d = 100 μm) were sourced from Argo (Warsaw, Poland). ARcare® 90445Q transparent, flexible adhesive tape was sourced from Adhesives Research Inc. (Glen Rock, PA, USA). Gold SPR slides (50 nm gold layer thickness) were purchased from Horiba Scientific (Palaiseau, France). DNA oligonucleotide sequences were purchased from Metabion GmbH (Planegg, Germany). All solutions were prepared using deionized (DI) water (conductivity < 0.055 μS/cm at 20 °C, TOC < 1.0 ppb). Human serum samples were obtained through a scientific collaboration with the National Institute of Public Health NIH—National Research Institute (Warsaw, Poland). "Positive" sera were collected from individuals infected at the time with the SARS-CoV-2 virus or had either recovered from COVID-19, while "negative" sera were sourced from healthy individuals before the outbreak of the pandemic. The Bioethics Committee of NIPH-NIH approved the study. Participants were informed about the study and gave consent to use the sample. Reference analyses of serum samples, classifying them as positive or negative, were conducted using standard serological ELISA and RT-PCR tests. Detailed protocols for conjugating receptor proteins with ssDNA anchors, purification of the conjugates, and procedures for classic ELISA assays and SPRi studies are provided in the Supplementary Materials.

2.1. Fabrication of Polymer-Coated PET Foils

Prior to MCP-2/Copoly Azide polymer coating, hydrophilization of the bare PET foil surface was performed using a 10 min treatment with UV/ozone cleaner (Ossila, Sheffield, UK). Copoly (DMA-NAS-MAPS), whose commercial name is MCP-2, is a copolymer obtained by free radical polymerization of N,N-dimethylacrylamide (DMA, 97% molar fraction), N-acryloyloxysuccinimide (NAS, 2% molar fraction), and 3-(trimethoxysilyl)propyl methacrylate (MAPS, 1% molar fraction). The principal constituent of Copoly (DMA-NAS-MAPS), dimethylacrylamide (DMA), forms the polymer backbone and ensures strong passive adsorption to variety of materials. NAS is the chemically reactive monomer responsible for probe immobilization through nucleophilic substitution with amine groups on biomolecules. The same monomer is exploited in post-polymerization modifications. In these reactions, NAS is reacted with linkers that contain amine groups to introduce novel functionalities into the polymer backbone. Using this strategy, Copoly Azide was synthesized. Specifically, after the polymerization of DMA, NAS, and MAPS (95, 4, and 1% molar fraction, respectively) the obtained polymer was reacted with 2.5 equivalents of 11-azido-3,6,9-trioxaundecan-1-amine, as described elsewhere. The MCP-2 and Copoly Azide structures are shown in Figure S1. The layer obtained with reactive copolymers has a dual role: antifouling properties due to blocking surface sites via hydrogen

bonds, and bearing reactive groups that enable controlled interactions with biomolecules. The functional groups of the copolymers were characterized using FT-IR and NMR analysis [30].

For coatings, copolymers were dissolved in DI water to a final concentration of 2% *w/v* and then diluted 1:1 with a solution of 1.6 M ammonium sulfate. The MCP-2 polymer was used for the direct covalent immobilization of receptor proteins. The Copoly Azide polymer is capable of click-chemistry reactions with DBCO-conjugated DNA probes. This enables DNA-directed immobilization of protein–oligonucleotide conjugates. The foil was dip-coated for 1 h with the chosen copolymer, then rinsed with DI water, dried under compressed air, and cured under vacuum at 80 °C for 15 min. The immobilization in predefined spots was possible thanks to the adhesive tape used to produce the rims of microwells. Holes, 5 mm in diameter, positioned in 96-well plate format, were cut with a VLS2.30 CO_2 laser plotter (Universal Laser Systems, Vienna, Austria).

The coating of PET foil coating with MCP-2 and Copoly Azide involves the passive attachment of the copolymers through weak, non-covalent interactions such as hydrogen bonding, Van der Waals, and hydrophobic interactions with the surface. Following dip coating, polymerization occurs, forming a stable and robust polymer layer that enables further immobilization of biomolecules. The morphological and chemical properties of passive coating have already been examined by means of atomic force microscopy and X-ray photoemission spectroscopy [31].

2.2. Protein Immobilization on PET

Protein receptor immobilization on modified PET substrates was achieved in two ways: through direct coupling to amine-reactive MCP-2 and indirectly via DNA-directed immobilization using oligonucleotide probes tethered to Copoly Azide [30]. For covalent attachment of proteins on MCP-2-coated foil, a 20 µg/mL solution of SARS-CoV Nucleocapsid recombinant protein (or another SARS-CoV-2 antigen) in PBS was dispensed onto microarray spots (11 µL each) and incubated overnight at 4 °C in a humid atmosphere. The remaining reactive sites were then blocked by applying 20 µL of PBST with 3% BSA for 30 min, followed by rinsing with PBST and drying under compressed air. For DDI on Copoly Azide-coated foil, a 20 µg/mL solution of DBCO-modified DNA in DI was dispensed onto microarray spots (11 µL each) and incubated overnight at 4 °C in a humid atmosphere. Chromatographically purified fractions of ssDNA conjugates with recombinant SARS-CoV-2 nucleoprotein or monoclonal anti-human IgG antibody (~150 nM in 50 mM phosphate buffer, pH 7.2, with 150 mM NaCl) were then dispensed as 11 µL spots onto the DNA-coated foil. After 1 h of incubation, the substrate was rinsed with PBS containing 10 mM $Mg(NO_3)_2$ and dried under compressed air. The blocking steps were identical to those used for covalent immobilization.

2.3. ELISA-like Assays on PET Foils

Two types of immunoreactions were performed in the prepared microwells on PET foils. Indirect immunolabeling was used to detect immunoglobulin subclasses in human sera, utilizing specific monoclonal mouse antibodies and an anti-mouse IgG–alkaline phosphatase conjugate. In contrast, direct immunolabeling with an anti-human IgG/IgA–alkaline phosphatase (ALP) conjugate was employed to detect total IgG and IgG/IgA classes of anti-NP antibodies in human sera. The detailed composition of each assay is provided in Section 3. According to the general protocol, 11 µL of the diluted serum or appropriate target antibody was incubated for 1 h at room temperature in a humid atmosphere, rinsed with PBST, and dried under compressed air. Then, 11 µL of the antibody–ALP conjugate (direct assay) or appropriate secondary antibodies (indirect assay) in PBST buffer with 3% BSA were added to each well, incubated for 1 h at room temperature in a humid atmosphere, rinsed with PBST, and dried under compressed air. Proper antibodies were used at 1 µg/mL, and the antibody–ALP conjugate at 3 µg/mL. For the indirect assay, the antibody–ALP conjugate was added in the third step (incubation and dilution

procedure the same as for the direct assay). For quantitative analysis, 10 mM freshly prepared *p*-nitrophenyl phosphate (PNNP) in 50 mM carbonate buffer pH 9.6 was used as the ALP substrate. An enzymatic reaction was initiated by dispensing 11 µL of PNNP substrate into each microwell, followed by incubation in a humid atmosphere for 12 min. Subsequently, 8 µL of substrate solution was collected from each spot and transferred to a multi-well plate containing 150 µL of 50 mM carbonate buffer (pH 9.6). Absorbance was measured at 405 nm using a Multiskan Go microplate reader (Thermo Scientific, Waltham, MA, USA).

3. Results and Discussion

To achieve the maximum recognition capacity of immunosensors and guarantee the long-term stability of the receptor proteins on the substrate, efficient immobilization in a well-defined orientation is of great value. However, immobilizing protein receptors for rapid diagnostic platforms remains a complex challenge. Antibodies, due to their larger size and structural complexity, are generally easier to immobilize. Their multiple functional groups, such as amines, carboxyl groups, and hydrophobic domains, enable stable and oriented surface attachment [32]. Antibodies also exhibit greater stability and robustness under various conditions compared to antigens. Their structural and functional similarity ensures a consistent, repeatable immobilization. This uniformity allows for standardized protocols to be applied universally and supports reliable and reproducible immobilization across different immunoplatforms [33]. In contrast, the structural and physicochemical diversity of antigens makes developing immobilization protocols more challenging.

To illustrate the impact of substrate type on serological immunoassay sensitivity and non-specific adsorption of serum components, response profiles for assays on standard multi-well plates (Figure 1A) and PET-based miniaturized substrates (Figure 1B) were compared. The efficiency of passive immobilization of nucleoprotein (NP) was evaluated using a classical untreated polystyrene plate and a commercial MediSorp® plate designed for protein binding. Additionally, the contribution of non-specific binding of serum proteins to the ELISA signal was assessed. It can be seen in Figure 1A that the MediSorp®-modified plate exhibited approximately 16 times higher assay sensitivity with minimal non-specific binding compared to the untreated polystyrene plate. The unmodified polystyrene showed low antigen coating capacity and high non-specific protein adsorption, with non-specific interactions contributing up to 70% of the total response at higher serum concentrations. These results highlight the strong dependence of passive adsorption efficiency on surface properties, especially its hydrophilicity [34].

The results obtained for the MediSorp® plates are widely regarded as the gold standard for immunoplatform design. However, adapting this type of substrate to other applications, such as microfluidics, is challenging. To address this limitation, the use of PET foil as a flexible substrate for protein immobilization was investigated. Flexible substrates provide more versatility for incorporating immunoplatforms into complex diagnostic devices. For this purpose, two immobilization methods on PET foil were tested: passive adsorption and covalent attachment. Covalent binding was achieved by coating the foil with the amine-reactive copolymer MCP-2, which enables stable protein attachment. Both MCP-2 and its N_3-functionalized derivative Copoly Azide are distinguished by ease of coating on solid surfaces without requiring an activation step.

As shown in Figure 1B, using the amine-reactive MCP-2 polymer improved protein immobilization efficiency over twofold compared to passive adsorption. Additionally, non-specific binding remained low and stable across higher serum dilutions. At the highest serum concentration, non-specific signals accounted for only 30.1% of the total response, compared to 46.5% for passive adsorption, demonstrating the effective antifouling properties of the MCP-2 layer against serum components.

The effectiveness of the MCP-2 polymer for covalent immobilization is especially evident with recombinant protein attachment. As illustrated by the heat map and graph in

Figure 1C, covalent immobilization of NP on the MCP-2 polymer shows approximately 50% higher efficiency (measured as increased immunoassay signal) compared to passive adsorption on unmodified PET, with similar levels of non-specific adsorption. This effect is less pronounced for antibody immobilization, with a difference of under 9% in favor of MCP-2. This is presumably due to the large contribution of hydrophobic interactions affecting the efficient adsorption of immunoglobulins on PET and other hydrophobic materials [35].

The results indicate that covalent immobilization via an amine-reactive polymer is particularly well suited for the effective immobilization of antigens in developing serological assays. The practical advantages of coating with reactive copolymers over traditional surface modifications like APTES silanization are also significant. Copolymer coatings provide greater flexibility in modifying surface properties and enable more controlled and uniform layers. Additionally, the single-step process is easier to scale up and automate, ensuring better consistency and reproducibility. In contrast, widely employed ω-functionalized silanes require a complex two-step process (coating and glutaraldehyde activation) with strict humidity and reaction time requirements. It makes them labor-intensive and challenging to scale up for microfluidic and other technological applications [36].

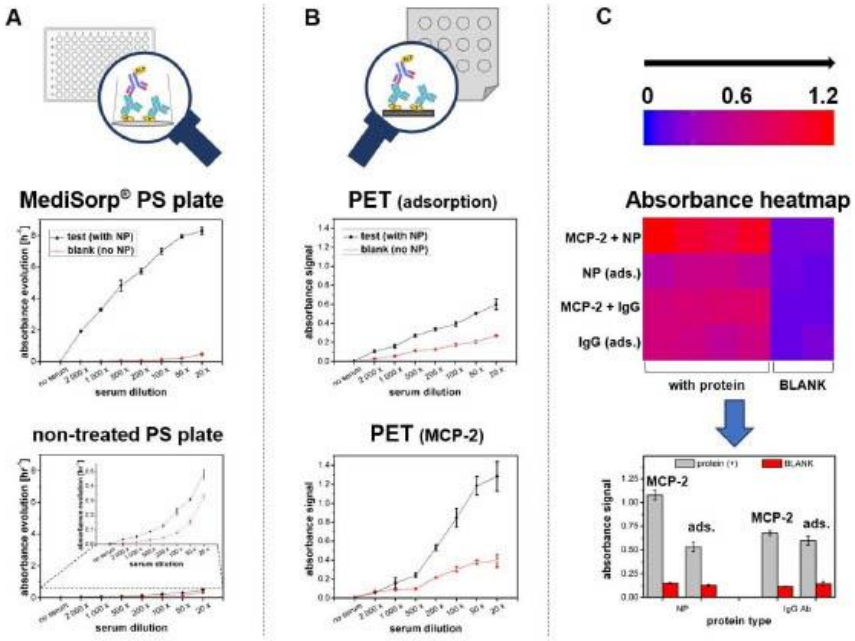

Figure 1. The effect of the substrate type ((**A**)—polystyrene, (**B**,**C**)—PET foils) on NP immobilization efficiency and non-specific adsorption of human serum. The red points (**A**,**B**) represent immunoassay responses obtained for the control wells (without the immobilized receptor protein), and the black points correspond to the total responses obtained for the test wells. Heat map (**C**) represents raw absorbance signals obtained for assays performed with two immobilized receptor proteins (two first rows—NP, two bottom rows—anti-human IgG). The first row for each protein represents covalent immobilization on MCP-2, and the second corresponds to passive adsorption. The layout on the plate is shown as 4 test wells + 2 wells of BLANK (without immobilized receptor protein). Mean signal values were summarized as a bar graph in (**C**).

Simultaneous detection of multiple viral biomarkers is essential for understanding infection dynamics. Inflammation triggers complex immune responses, with viral proteins and host antibodies appearing at different stages. Multiplex assays facilitate the identification of viral antigens and a broad range of antibody classes and subclasses, providing insights into viral load and immune activity. This comprehensive approach enables more accurate diagnostics, differentiation between acute and past infections, and improved monitoring of disease progression or treatment efficacy. Therefore, flexible serological platforms should support detecting various antibodies against diverse antigens and employ multiple assay formats. To this end, MCP-2-coated substrates were thoroughly evaluated for their suitability in diverse serological immunoassays. The experiments began with selecting a suitable model antigen (Figure S2). Results showed that platforms using NP and RBD proteins as receptors offer comparable serum antibody detection sensitivity, with RBD showing only a 3% lower response than NP for the same sample. In contrast, the S1 antigen exhibited nearly 48% lower sensitivity compared to NP and a noticeably higher non-specific signal. These findings confirm the compatibility of MCP-2 with various recombinant antigens. The lack of response for the S1/S2 protein-based assay was attributed to the poor antibody–antigen affinity, as confirmed by a reference test on the MediSorp® polystyrene substrate.

NP was selected as the model antigen to detect specific antibodies. The experiment shown in Figure 2 compared immobilization efficiency via MCP-2 vs. passive adsorption for two assay formats: direct and indirect. The choice of format depends on the availability of specific antibody conjugates. Indirect assays are generally more versatile and sensitive due to additional signal amplification during the secondary labeling but require an additional step, which complicates the entire process. We anticipate that the developed PET-based platforms will support versatile detection, regardless of the chosen assay format. The expectations described above were validated by assay results for both immobilization methods—passive and covalent attachment. A similar trend was observed across both formats: the highest signals were detected for monoclonal anti-NP IgG compared to human serum anti-NP IgG, with the indirect assay format providing over 30% greater sensitivity than the direct format. Non-specific adsorption remained low for both methods. These findings confirm the superiority of covalent NP immobilization using MCP-2 over passive adsorption across various serological immunoassay formats. Covalent immobilization provides robust attachment of receptor proteins. However, it usually requires complex surface modification that poses technological difficulties. Passive adsorption, while simple, often shows immobilization efficiency limitations [37]. PET foils are compatible with various detection strategies, but maintaining their structural integrity may be challenging. Already described methods of their chemical modification usually require harsh conditions such as high temperatures [38], involve multiple reagents [39–41], and are time- and labor-consuming [42,43]. Coating with reactive copolymer MCP-2 is a simple procedure that occurs under mild conditions and allows for one-step covalent attachment of receptor proteins while preserving the good mechanical properties of the PET substrate.

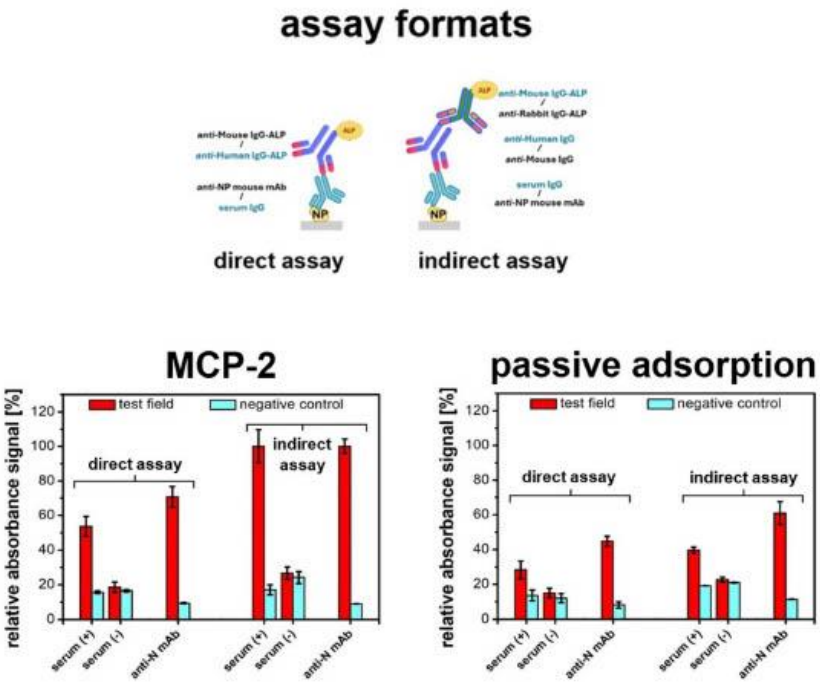

Figure 2. Comparison of direct vs. indirect assays for two protein immobilization methods on PET foil: covalent (MCP-2) and passive adsorption. Assays were conducted using human samples (SARS-CoV-2-positive and -negative sera) and anti-SARS-CoV-2 NP monoclonal antibodies. Red bars show the results of test wells ("positive" serum or monoclonal antibody solution), and blue bars represent control wells (negative serum or buffer). Values are expressed as normalized absorbance signals. Black labels in the graphical schematic refer to serum IgG assays, while blue labels indicate the detection of monoclonal anti-NP IgG.

In serological assays, the complexity of biological samples poses significant challenges due to the potential for non-specific adsorption of proteins and other biomolecules to the surface of diagnostic platforms. This non-specific binding can lead to elevated background signals, reduced assay sensitivity, and compromised specificity, resulting in false positive results, ultimately affecting the reliability and accuracy of diagnostic results [44–46]. Studies on possible blocking agents in immunoassays showed polymeric compounds' superiority in reducing background noise [47]. *N,N*-dimethylacrylamide-derived copolymers such as MCP-2 have been used in microarrays and biosensors, demonstrating rapid surface adhesion, effective covalent biomolecule attachment, and antifouling properties [48]. Compared to traditional surface functionalization methods, covalent attachment to polymer-coated surfaces enhances binding efficiency and reduces non-specific interactions [49].

Further studies have validated the use of the MCP-2-based PET immunoplatform for quantitative analysis. As shown in Figure 3, covalently immobilized NP proteins on polymer-coated substrates enabled quantitative detection of both human anti-SARS-CoV-2 NP antibodies in serum (Figure 3A) and mouse monoclonal anti-NP antibodies (Figure 3B). The response profile to increasing serum dilutions showed a dynamic range of 20× to

1000×. It covers typical working dilutions used in routine serological ELISAs [50,51]. Based on the calibration curve shown in Figure 3B, the analytical parameters of the direct immunoassay for anti-NP monoclonal antibodies as a model target were evaluated. Linearity of the concentration-response curve was observed within the range of 5–200 ng/mL, with a lower detection limit of 2.73 ng/mL. The presented analytical characteristics of MCP-2-based immunoplatforms confirm their suitability for serological quantitative analysis. However, as with classical ELISA formats, the assay's sensitivity can be adjusted at the expense of analysis time, for example, by modifying incubation durations or enzymatic reaction times (currently set to 12 min).

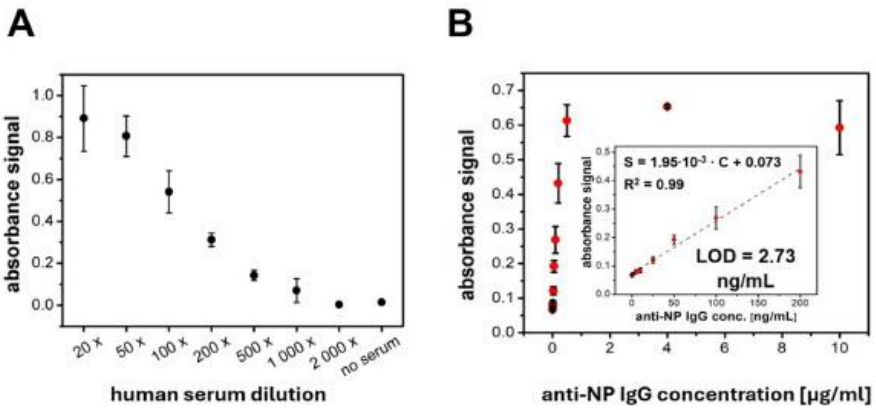

Figure 3. The plot of immunoassay response vs. dilutions of COVID-19-positive human serum (**A**) and concentration of mouse monoclonal anti-NP antibodies (**B**). The inset provides a magnified view highlighting the linear response range and key analytical parameters.

The occurrence of specific IgG subclasses (IgG1, IgG2, IgG3, and IgG4) in human sera was examined using an indirect assay. SARS-CoV-2 NP was immobilized on two substrates: the ELISA-dedicated MediSorp® plate (Figure 4A) and PET foil coated with MCP-2 (Figure 4B). These platforms were used to capture and identify subclass-specific IgG responses. The indirect format allows differentiation of each IgG subclass. It provides not only confirmation of antibody presence but also detailed insights into their specific subclass distribution.

Two randomly selected COVID-19-positive sera (named F and H) with recent infection and well-characterized antibody profiles were analyzed. The results showed a dominant presence of IgG1, significantly lower levels of IgG3, and minimal amounts of IgG2 and IgG4 (in one serum sample IgG2 and IgG4 were barely detectable). The COVID-19-negative serum (named a) and blank (no serum) both exhibit minimal absorbance across all IgG subclasses, which confirms the specificity of the assay. These findings align with the typical distribution of IgG subclasses in human serum, where IgG1 accounts for approximately 60–70% of the total IgG [52]. IgG1 and IgG3 are the main subclasses produced in response to viral infections, while IgG2 and IgG4 are less abundant. IgG2 typically responds to polysaccharide antigens linked to bacterial infections. The dominance of IgG1 and, to a lesser extent, IgG3 in the assay aligns with the expected immune response to viral infections. Differences in subclass profiles among positive sera reflect variability in individual immune responses. While both positive sera show a strong presence of IgG1, the relative levels of IgG3, IgG2, and IgG4 differ between the two samples. However, the trend in the distribution of individual subclasses is noticeable regardless of the type of immunoassay (PS plate vs. flexible substrate). This variability can be attributed to factors

such as the timing of sample collection, individual differences in immune system function, or varying levels of exposure to the virus [53,54]. The distinct profiles of these IgG subclasses underscore the importance of personalized immunological assessments.

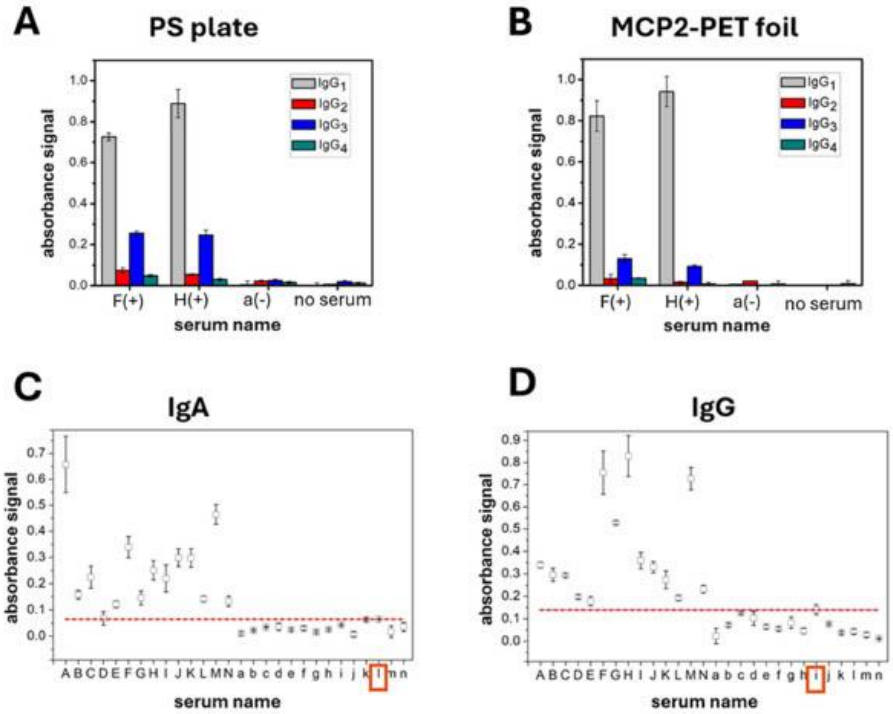

Figure 4. Analysis of antibody subclasses in human sera using standard ELISA (**A**) and PET foil-based ELISA with MCP-2 coating (**B**). The bar graph shows absorbance signals for IgG1, IgG2, IgG3, and IgG4 subclasses in positive, negative, and control samples using an indirect assay. Detection of antibody classes: IgA (**C**) and IgG (**D**) against SARS-CoV-2 NP in human sera. Boxplots show absorbance signals for various sera samples, with uppercase letters representing "positive" sera and lowercase letters representing "negative" sera. The red dashed line indicates the cutoff value differentiating positive and negative samples.

To validate the diagnostic performance, the immunoplatform was used to test a large pool of serum samples from COVID-19-positive and -negative patients. Two antibody classes—IgA (Figure 4C) and IgG (Figure 4D)—with proven diagnostic value were selected. Analyzing both provides insight into the immune response and infection stage: IgG indicates a long-term, mature response, while IgA is key for mucosal immunity [55]. The platform differentiates between positive and negative samples using a cutoff value defined by Equation (1) [56].

$$\text{Cutoff} = \text{Mean of Negative Samples} + (2 \times \text{SD}) \quad (1)$$

The boxplots in Figure 4 show that absorbance signals for positive sera are significantly higher than those for negative samples, exceeding the cutoff value. This confirms that the MCP-2-based immunoplatform effectively evaluates IgG and IgA antibody levels

against NP in serum samples. Variability in signal intensity among COVID-19-positive sera reflects differences in antibody concentrations between patients. The IgG/IgA ratio also varies, indicating different infection stages at the time of biological material collection [57]. COVID-19-negative sera generally showed signals below the cutoff, indicating low or absent IgA/IgG antibody levels compared to positive samples. Sensitivity, specificity, positive predictive value (PPV), negative predictive value (NPV), and assay accuracy are summarized in Table 1. MCP-2-based immunoassays demonstrated identical diagnostic parameters for both IgA and IgG classes. All 14 COVID-19-positive samples were correctly identified, yielding 100% sensitivity. For the 14 COVID-19-negative samples, one false positive was recorded (IgA sample "l" and IgG sample "i"), resulting in 92.9% specificity. These results suggest that the developed platforms are highly suitable for the immunodetection of SARS-CoV-2 serological biomarkers.

Table 1. Main diagnostic parameters of the assay for the detection of anti-NP IgA and IgG. Results were obtained on the basis of 28 actual samples (sera), including 14 positive and 14 negative samples. MedCalc® Statistical Software version 23.0.2 (MedCalc, Ostend, Belgium) was used for the calculation.

Metric	Value
Sensitivity	100.0%
Specificity	92.9%
Positive Predictive Value (PPV)	93.3%
Negative Predictive Value (NPV)	100.0%
Accuracy	96.4%

Although covalent immobilization is generally more efficient than passive adsorption, it does not fully address the challenges arising from antigen structural diversity. Both methods rely on direct interactions between protein functional groups and the surface, making successful binding highly dependent on protein structure and the availability of reactive groups. In contrast, DNA-directed immobilization (DDI) overcomes these limitations by using the hybridization of complementary DNA strands. It enables stable and straightforward immobilization of receptor proteins conjugated with single-stranded DNA onto pre-immobilized complementary ssDNA probes. The DDI strategy demonstrates significant potential for the precise construction of protein arrays with high selectivity and spatial resolution. Two effective approaches can be employed: one using DNA-conjugated receptor proteins with distinct DNA anchors for simultaneous immobilization through specific hybridization, and the other utilizing a unified DNA anchor with controlled spotting for spatial alignment. The first approach ensures selective and simultaneous immobilization of multiple proteins in a single flow step, while the second provides precise spatial control by directly depositing conjugates onto the surface. Both methods effectively prevent cross-interference during immobilization, guaranteeing high specificity and reproducibility. These solutions are particularly valuable for high-throughput biosensor array fabrication, facilitating advanced multiplex detection applications.

The initial step of our studies involved comparing the efficiency of one-step covalent immobilization of ssDNA probes on reactive Copoly Azide polymer to passive adsorption using Surface Plasmon Resonance imaging (SPRi). For this purpose, half of the SPR slide was coated with Copoly Azide. The other half of the slide was left uncoated, and modified DNA probes were passively adsorbed onto bare gold. A schematic representation of the SPRi chip topography, along with a CCD image of the actual SPRi slide, is shown in Figure 5A.

SPRi measurements enable real-time monitoring of the immobilization of protein conjugates and their subsequent immunolabeling with antibodies. Additionally, SPRi facilitates the visualization of differential images, which reveal non-specific protein adsorption on the unmodified gold surface. The Copoly Azide polymer, visible on the upper part of the chip, demonstrates excellent antifouling properties and supports efficient covalent

attachment of DNA probes for subsequent DNA-directed immobilization of protein conjugates. This is confirmed by the absence of brightening in the differential image and no change in reflectance for the polymer-coated area without immobilized DNA (red dashed line). Brightening is observed only at the specific spot where ssDNA was pre-immobilized (solid red line), indicating high specificity of receptor binding. In the case of bare gold, the brightening of the differential image and the significant change in reflectance (black dashed line) are significantly due to the non-specific adsorption of antibodies to the uncoated surface. The critical advantage of the DDI-based platforms is the possibility of rapid and effective layer regeneration which allows for its renewed usage [58]. As can be seen in the final section of the sensogram, DDI-based immunocomplexes on Copoly Azide can be quickly and efficiently removed from the surface by the injection of 50 mM NaOH. After regeneration, the DNA probes can be successfully reused to construct subsequent receptor layers via DDI.

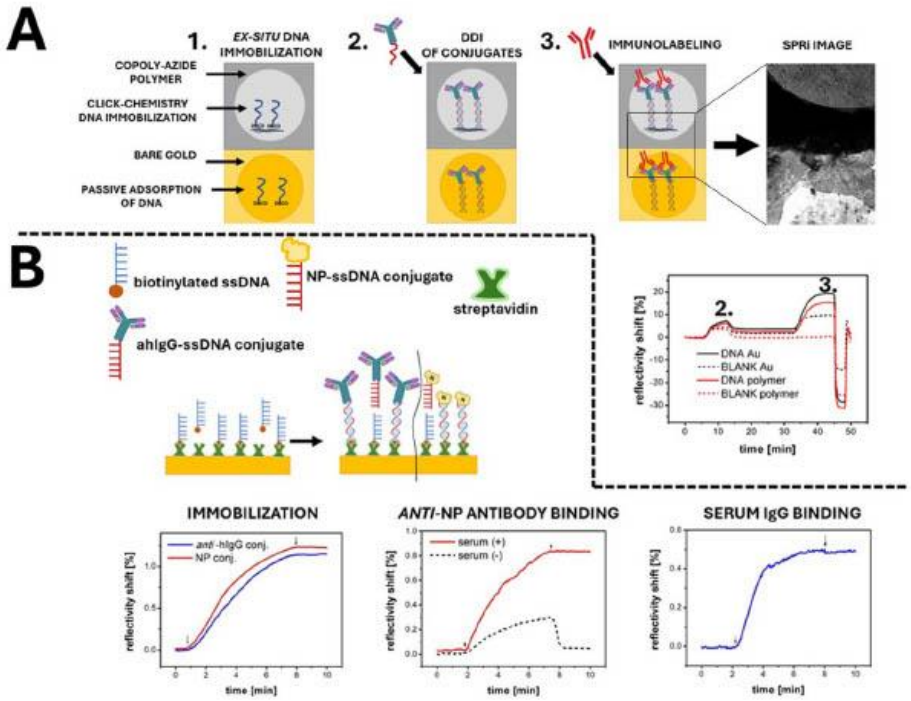

Figure 5. (**A**) Schematic and SPRi analysis of DNA-directed immobilization of antibody–DNA conjugates on Copoly Azide polymer. The upper half of the slide was coated with polymer, while the lower half remained uncoated as a reference (1). The SPRi sensogram shows real-time reflectivity shifts for antibody–DNA conjugate immobilization (2), immunolabeling with secondary antibodies (3), and layer regeneration. (**B**) SPRi responses for DNA-directed immobilization of nucleoprotein (NP) and anti-human IgG conjugates. The left graph compares anti-human IgG (blue) and NP (red) conjugate immobilization. The middle graph shows human anti-NP antibody binding from COVID-19-positive (red) and -negative (black dashed) serum. The right graph depicts human IgG binding from a COVID-19-negative serum.

In the next step, DDI was used to immobilize two DNA–protein conjugates (NP and anti-human IgG antibody) onto the surface of a gold SPR transducer (Figure 5B). The immobilization sensograms showed distinct responses corresponding to the surface density of the immobilized proteins. Notably, protein loading was similar for both conjugates and could be regulated by adjusting the density of DNA probes on the transducer surface [59]. The anti-human IgG antibody conjugate in the receptor layer allowed the capture of various IgG antibodies from COVID-19-negative human serum. Stable binding of the serum IgG antibody can be seen in the sensogram, with no apparent dissociation. In turn, immobilized NP conjugate effectively captured specific antibodies from the COVID-19-positive serum. No binding was observed with the negative serum, indicating high specificity of the DDI-based serological assay. The negative serum exhibited only a reversible, non-specific interaction during the association stage, with immediate dissociation upon returning to the running buffer. This confirms that the surface layer is not entirely resistant to biofouling; however, this does not negatively affect its potential application in serological biosensing. In contrast, the positive serum showed a stable increase in reflectivity. This confirms antibody capture by the immobilized antigen. DDI enabled rapid, stable immobilization of both protein receptors and differentiation of actual samples.

The use of SPR allowed for comprehensive testing of all components involved in DDI, providing real-time monitoring of the assembly process. This approach enabled the tracking of each step and supported the transition from substrates designed for label-free detection to flexible PET foils adapted for label-based detection. As shown in Figure 1C, the reactive MCP-2 copolymer enables easy and efficient covalent immobilization of recombinant proteins, although the efficiency for antibodies was moderate. The DDI approach is expected to eliminate dependence on receptor protein structure during immobilization.

To assess the potential of PET foil coated with Copoly Azide for constructing flexible, easily adjustable immunoassays via DDI, the NP–DNA conjugate was immobilized on the coated substrate. DBCO-modified DNA on the polymer-coated foil enabled hybridization with complementary strands, allowing rapid attachment of the DNA-labeled receptor protein. A quantitative serological assay was then conducted using human serum at various dilutions (Figure 6A). As can be observed, the signal increases with decreasing serum dilution. It indicates a higher concentration of antibodies in the serum, thus confirming the feasibility of the receptor layer obtained by means of DDI. No significant non-specific binding occurred for controls without receptor proteins on the surface. The obtained blank signals (Figure 6A, red line) remained low and showed only a slight increase as the serum protein concentration increased, confirming the high specificity of the assay. A detailed study of the specificity of immunoplatform formation via DDI (Figure S3) showed that protein receptor immobilization on Copoly Azide occurs almost exclusively through DNA–DNA duplex formation. Non-specific adsorption contributes less than 10% to the total signal in all tested cases. The antifouling properties of Copoly Azide are satisfactory, which supports the construction of DDI-based platforms for sensitive and specific serological assays. Most importantly, these platforms enable the development of multiplex assays using various protein-based receptors immobilized through a straightforward single-step process. This was demonstrated by the simultaneous immobilization of two distinct protein conjugates (NP as a recombinant antigen and anti-human IgG as an antibody representative) within a single immunoplatform (Figure 6B). The developed immunoassays were used to detect specific anti-NP antibodies and total IgG antibodies in two human serum samples (COVID-19-positive and -negative). The designed assay allows distinguishing between samples and confirms the absence of non-specific binding. The demonstrated potential of multiplexing is crucial for developing more comprehensive diagnostic assays to detect multiple biomarkers in a single test.

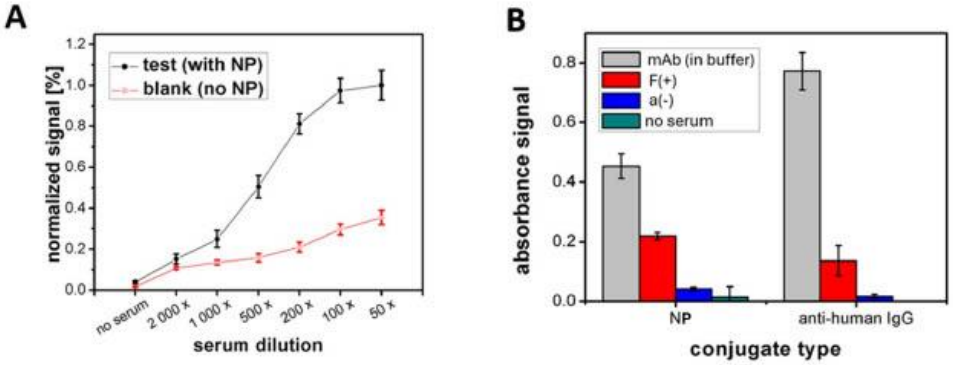

Figure 6. Serological assay results using DNA-directed immobilization on PET foil coated with Copoly Azide. (**A**) Normalized absorbance as a function of serum dilution for anti-NP antibody detection. The black line shows test wells with the NP conjugate, while the red line represents control wells without receptor proteins. (**B**) Multiplex assay showing absorbance signals for anti-NP antibodies and human IgG from various sources, including monoclonal antibodies, COVID-19-positive serum, and COVID-19-negative serum.

To understand the strengths and limitations of antigen immobilization in micro-spot ELISA, analyzing their mechanisms and challenges is essential. Covalent immobilization on MCP-2-coated PET involves the reaction between amine groups of the protein and NAS groups in the copolymer, forming stable amide bonds that ensure robust attachment and minimize protein loss during washing. Despite its simplicity, this method can partially affect sensitive proteins, and attachment efficiency depends on receptor structure [60]. Passive adsorption relies on non-covalent π–π hydrophobic interactions, making it easy to implement but variable due to protein and surface properties [61]. Proteins bound this way may desorb or rearrange, impacting assay reliability. DDI uses affinity-based attachment by hybridizing complementary probes, providing precise orientation and multiplexing capability. However, DNA duplex stability is affected by ionic strength and temperature, making washing with low-ionic solutions problematic and requiring consistent conditions to maintain attachment integrity [62].

The potential of the developed platform extends beyond SARS-CoV-2 detection and holds promise for broader use in multiplex diagnostics. Its adaptability for integrating various protein bioreceptors suggests that this platform could be tailored to determine different biomarkers rapidly, supporting POCT where timely and accurate results are critical. The robust binding properties and minimal non-specific interactions make it an attractive tool for multi-analyte screening. PET foil-based immunoplatforms can be easily integrated with microfluidic systems to further develop high throughput diagnostic tools [63,64]. The inherent properties of these flexible substrates, such as ease of cutting and reshaping, and wide working temperature and pressure range, make them highly adaptable for such applications [65]. The platform can be transformed into a fully functional microfluidic device by incorporating laser-cut microchannels and bonding methods such as thermal lamination or adhesive tapes. These techniques allow the fabrication of sealed cassettes with embedded microchannels, facilitating controlled reagent flow and supporting automated sample processing [27]. The possibility of integration and the compatibility with common optical detection methods leverage potential of the developed platform for the construction of multiplexed diagnostic assays. Exploring these capabilities in further studies should demonstrate the versatility of the immunoplatforms and enhance scalable and sensitive immunodiagnostics.

4. Conclusions

In this work, we have systematically studied the impact of receptor protein characteristics on immobilization strategies and evaluated the suitability of reactive copolymer-coated PET as a substrate for constructing flexible, microvolume ELISA platforms. Passive adsorption was effective for antibody immobilization, while the amino-reactive MCP-2 copolymer ensured stable and functional covalent attachment of protein antigens. DNA-directed immobilization (DDI) demonstrated high versatility. It enables the immobilization of a diverse range of receptors using the Copoly Azide copolymer, which facilitates DBCO-modified DNA attachment for subsequent protein conjugate binding. This strategy allowed the reliable immobilization of complex proteins, expanding the range of usable receptors on a platform. The copolymers also exhibited antifouling properties, minimizing non-specific binding and enhancing assay sensitivity. Designed serological platforms effectively distinguished between COVID-19-positive and -negative serum samples. Quantitative measurements and differentiation between antibody subclasses were also possible. Flexible PET foils increased platform versatility and enable further integration into complex systems, such as microfluidic devices for sophisticated miniaturized diagnostics. Combining DDI with flexible substrates broadens the scope of applications. It facilitates the development of compact, multifunctional platforms suitable for multiplex biosensing and point-of-care diagnostics. The impact of the current study could be broadened by further investigation of the platform's potential for detecting a wider range of biomarkers, making it applicable to other infectious diseases. The usage of the DDI strategy for different antigens would result in the improvement of the platform's versatility and adaptability, supporting high-throughput analytical applications. Further development could also focus on enhancing the integration of this platform into portable and field-deployable diagnostic tools, enabling rapid, on-site testing in diverse scenarios.

Supplementary Materials: The following supporting information can be downloaded at: https://www.mdpi.com/article/10.3390/s24237766/s1, Supplementary Experimental (Reagents, Materials, and Methods), Figure S1: Copolymers composition. A—Chemical structure of MCP-2 and Copoly Azide. B—Monomer molar ratios for MCP-2 and Copoly Azide; Figure S2: Results of SARS CoV-2 antigen selection studies; Figure S3: Results of specificity studies for DDI-type immobilization. Reference [66] is cited in the Supplementary Materials.

Author Contributions: Conceptualization, S.P. and M.D.; methodology, S.P, M.D. A.M., and D.B.; validation, S.P., M.D., and W.R.; formal analysis, M.C., D.B., W.R. and E.M.; investigation, S.P. and A.M.; resources, M.C., W.R. and E.M.; writing—original draft preparation, S.P. and M.D.; writing—review and editing, M.D., D.B., M.C., and E.M.; visualization, S.P., D.B. and M.D.; supervision, M.D. and E.M.; project administration, M.D.; funding acquisition, S.P. and M.D. All authors have read and agreed to the published version of the manuscript.

Funding: This work has been financially supported by the Warsaw University of Technology under the program Excellence Initiative, Research University (IDUB), YOUNG PW 2 (CPR-IDUB/42/Z01/2024 grant number: 504/04496/2530/45.010013). We would like to acknowledge the financial support from the Ministry of Education and Science, Poland, grant number 7015/IA/SP/2019. S.P. acknowledges financial support from Polish National Agency for Academic Exchange—NAWA (scholarship exchange within the project "Smart Education for Engineering Doctors" under the STER program—Internalization of Doctoral Schools).

Institutional Review Board Statement: The study was conducted in accordance with the Declaration of Helsinki, and approved by the Ethics Committee of National Institute of Public Health NIH—National Research Institute (opinion number 2/2021, 02.02.2021).

Informed Consent Statement: Informed consent was obtained from all subjects involved in the study.

Data Availability Statement: Data are contained within the article and supplementary materials

Conflicts of Interest: The authors declare no conflicts of interest.

References

1. Rai, G.; Venkateswaran, K. Limitations and practical problems in enzyme linked immunosorbent assays. *Def. Sci. J.* **1992**, *42*, 71–84. https://doi.org/10.14429/dsj.42.4353.
2. Liu, D.; Wang, J.; Wu, L.; Huang, Y.; Zhang, Y.; Zhu, M.; Wang, Y.; Zhu, Z.; Yang, C. Trends in miniaturized biosensors for point-of-care testing. *TrAC Trends Anal. Chem.* **2020**, *122*, 115701. https://doi.org/10.1016/j.trac.2019.115701.
3. Aggarwal, R.; Ferris, B.; Li, H. Compartmentalized linker array: A scalable and transferrable microarray format for multiplexed immunoassays. *Anal. Chem.* **2023**, *95*, 9068–9075. https://doi.org/10.1021/acs.analchem.3c01442.
4. Jimenez-Valdes, R.J.; Rodriguez-Moncayo, R.; Cedillo-Alcantar, D.F.; Garcia-Cordero, J.L. Massive parallel analysis of single cells in an integrated microfluidic platform. *Anal. Chem.* **2017**, *89*, 5210–5220. https://doi.org/10.1021/acs.analchem.6b04485.
5. Volpetti, F.; Garcia-Cordero, J.; Maerkl, S.J. A microfluidic platform for high-throughput multiplexed protein quantitation. *PLoS ONE* **2015**, *10*, e0117744. https://doi.org/10.1371/journal.pone.0117744.
6. Li, N.; Shen, M.; Xu, Y. A Portable microfluidic system for point-of-care detection of multiple protein biomarkers. *Micromachines* **2021**, *12*, 347. https://doi.org/10.3390/mi12040347.
7. Brown, B.; Ojha, V.; Fricke, I.; Al-Sheboul, S.A.; Imarogbe, C.; Gravier, T.; Green, M.; Peterson, L.; Koutsaroff, I.P.; Demir, A.; et al. Innate and adaptive immunity during SARS-CoV-2 infection: Biomolecular cellular markers and mechanisms. *Vaccines* **2023**, *11*, 408. https://doi.org/10.3390/vaccines11020408.
8. Anand, S.P.; Prévost, J.; Nayrac, M.; Beaudoin-Bussières, G.; Benlarbi, M.; Gasser, R.; Brassard, N.; Laumaea, A.; Gong, S.Y.; Bourassa, C.; Brunet-Ratnasingham, E.; Medjahed, H.; Gendron-Lepage, G.; Goyette, G.; Gokool, L.; Morrisseau, C.; Bégin, P.; Martel-Laferrière, V.; Tremblay, C.; Richard, J.; Bazin, R.; Duerr, R.; Kaufmann, D.E.; Finzi, A. Longitudinal Analysis of Humoral Immunity against SARS-CoV-2 Spike in Convalescent Individuals up to 8 Months Post-Symptom Onset. *Cell Rep. Med.* 2021, 2, 100290. https://doi.org/10.1016/j.xcrm.2021.100290.
9. Lou, B.; Li, T.-D.; Zheng, S.-F.; Su, Y.-Y.; Li, Z.-Y.; Liu, W.; Yu, F.; Ge, S.-X.; Zou, Q.-D.; Yuan, Q.; et al. Serology characteristics of SARS-CoV-2 infection since exposure and post-symptom onset. *Eur. Respir. J.* **2020**, *56*, 2000763. https://doi.org/10.1183/13993003.00763-2020.
10. Woof, J.M.; Russell, M.W. Structure and function relationships in IgA. *Mucosal Immunol.* **2011**, *4*, 590–597. https://doi.org/10.1038/mi.2011.39.
11. Ndzouboukou, J.-L.B.; Zhang, Y.-D.; Fan, X.-L. Recent developments in SARS-CoV-2 Neutralizing antibody detection methods. *Curr. Med. Sci.* **2021**, *41*, 1052–1064. https://doi.org/10.1007/s11596-021-2470-7.
12. Guo, Y.; Li, T.; Xia, X.; Su, B.; Li, H.; Feng, Y.; Han, J.; Wang, X.; Jia, L.; Bao, Z.; et al. Different profiles of antibodies and Cytokines were found between severe and moderate COVID-19 patients. *Front. Immunol.* **2021**, *12*, 723585. https://doi.org/10.3389/fimmu.2021.723585.
13. Wu, P.; Xue, F.; Zuo, W.; Yang, J.; Liu, X.; Jiang, H.; Dai, J.; Ju, Y. A Universal Bacterial Catcher Au–PMBA-Nanocrab-Based Lateral Flow Immunoassay for Rapid Pathogens Detection. *Anal. Chem.* **2022**, *94*, 4277–4285. https://doi.org/10.1021/acs.analchem.1c04909.
14. Huang, L.; Tian, S.; Zhao, W.; Liu, K.; Ma, X.; Guo, J. Multiplexed detection of biomarkers in lateral-flow immunoassays. *Anal.* **2020**, *145*, 2828–2840. https://doi.org/10.1039/c9an02485a.
15. Herbáth, M.; Papp, K.; Balogh, A.; Matkó, J.; Prechl, J. Exploiting fluorescence for multiplex immunoassays on protein microarrays. *Methods Appl. Fluoresc.* **2014**, *2*, 032001. https://doi.org/10.1088/2050-6120/2/3/032001.
16. Zuo, W.; Wu, P.; He, W.; Xiao, Q.; Yang, J.; Liu, X.; Jiang, H.; Dai, J.; Ju, Y. A fluorescent and ratiometric colorimetric biosensor for detection of different hazard contaminants in dairy products. *Sens. Actuators B Chem.* **2023**, *374*, *132816*. https://doi.org/10.1016/j.snb.2022.132816.
17. Soler, M.; Huertas, C.S.; Lechuga, L.M. Label-free plasmonic biosensors for point-of-care diagnostics: A review. *Expert Rev. Mol. Diagn.* **2019**, *19*, 71–81. https://doi.org/10.1080/14737159.2019.1554435.
18. Johnson, S.; Krauss, T.F. Label-free affinity biosensor arrays: Novel technology for molecular diagnostics. *Expert Rev. Med. Devices* **2017**, *14*, 177–179. https://doi.org/10.1080/17434440.2017.1283982.
19. Wasiluk, T.; Sredzinska, M.; Rogowska, A.; Zebrowska, A.; Boczkowska-Radziwon, B.; Stasiak-Barmuta, A.; Radziwon, P. Analysis of the IgG subclass profile and IgG sum-total discrepancy in COVID-19 convalescent plasma donors: A single-centre prospective cohort study. *Transfus. Apher. Sci.* **2022**, *62*, 103527. https://doi.org/10.1016/j.transci.2022.103527.
20. Korobova, Z.R.; Zueva, E.V.; Arsentieva, N.A.; Batsunov, O.K.; Liubimova, N.E.; Khamitova, I.V.; Kuznetsova, R.N.; Rubinstein, A.A.; Savin, T.V.; Stanevich, O.V.; et al. Changes in Anti-SARS-CoV-2 IgG Subclasses over Time and in Association with Disease Severity. *Viruses* **2022**, *14*, 941. https://doi.org/10.3390/v14050941.
21. Xu, J.; Chen, J.; Wen, F.; Liu, K.; Chen, Y. Detection methods and dynamic characteristics of specific antibodies in patients with COVID-19: A review of the early literature. *Heliyon* **2024**, *10*, e24580. https://doi.org/10.1016/j.heliyon.2024.e24580.
22. Rusmini, F.; Zhong, Z.; Feijen, J. Protein immobilization strategies for protein biochips. *Biomacromolecules* **2007**, *8*, 1775–1789. https://doi.org/10.1021/bm061197b.
23. Kim, D.; Herr, A.E. Protein immobilization techniques for microfluidic assays. *Biomicrofluidics* **2013**, *7*, 041501. https://doi.org/10.1063/1.4816934.
24. Lin, P.; Weinrich, D.; Waldmann, H. Protein biochips: Oriented surface immobilization of proteins. *Macromol. Chem. Phys.* **2010**, *211*, 136–144. https://doi.org/10.1002/macp.200900539.

25. Chavan, S.G.; Yagati, A.K.; Koyappayil, A.; Go, A.; Yeon, S.; Lee, M.-H. Recombinant histidine-tagged nano-protein-based highly sensitive electro-sensing device for salivary cortisol. *Bioelectrochemistry* **2022**, *144*, 108046. https://doi.org/10.1016/j.bioelechem.2021.108046.
26. Zhang, H.; Klose, A.M.; Miller, B.L. label-free, multiplex glycan microarray biosensor for influenza virus detection. *Bioconjug. Chem.* **2021**, *32*, 533–540. https://doi.org/10.1021/acs.bioconjchem.0c00718.
27. Drozd, M.; Ivanova, P.; Żukowski, K.; Tokarska, K.; Pietrzak, M.; Brzózka, Z.; Malinowska, E. Printer toner-assisted immobilization of antibodies on PET for genuinely-2D, flexible ELISA spot arrays. *Sens. Actuators B Chem.* **2024**, *403*, 135173. https://doi.org/10.1016/j.snb.2023.135173.
28. Makhneva, E.; Farka, Z.; Skládal, P.; Zajíčková, L. Cyclopropylamine plasma polymer surfaces for label-free SPR and QCM immunosensing of Salmonella. *Sens. Actuators B Chem.* **2018**, *276*, 447–455. https://doi.org/10.1016/j.snb.2018.08.055.
29. Chen, D.; Mei, Y.; Hu, W.; Li, C.M. Electrochemically enhanced antibody immobilization on polydopamine thin film for sensitive surface plasmon resonance immunoassay. *Talanta* **2018**, *182*, 470–475. https://doi.org/10.1016/j.talanta.2018.02.038.
30. Sola, L.; Mallak, L.A.; Damin, F.; Mussida, A.; Brambilla, D.; Chiari, M. Optimization of functional group concentration of N, N-dimethylacrylamide-based polymeric coatings and probe immobilization for DNA and protein microarray applications. *Micromachines* **2023**, *14*, 302. https://doi.org/10.3390/mi14020302.
31. Petti, D.; Torti, A.; Damin, F.; Sola, L.; Rusnati, M.; Albisetti, E.; Bugatti, A.; Bertacco, R.; Chiari, M. Functionalization of gold surfaces with copoly(DMA-NAS-MAPS) by dip coating: Surface characterization and hybridization tests. *Sens. Actuators B Chem.* **2014**, *190*, 234–242. https://doi.org/10.1016/j.snb.2013.08.077.
32. Sharma, S.; Byrne, H.; O'Kennedy, R.J. Antibodies and antibody-derived analytical biosensors. *Essays Biochem.* **2016**, *60*, 9–18. https://doi.org/10.1042/ebc20150002.
33. Gao, S.; Guisán, J.M.; Rocha-Martin, J. Oriented immobilization of antibodies onto sensing platforms—A critical review. *Anal. Chim. Acta* **2021**, *1189*, 338907. https://doi.org/10.1016/j.aca.2021.338907.
34. Does Thermo Fisher Scientific Have an Immunoassay Plate That Is Optimized for Research on SARS-CoV-2 Testing? Smart Notes n.d. Available online: https://assets.thermofisher.com/TFS-Assets/LPD/Application-Notes/elisa-smartnote.pdf (accessed on 13 September 2024).
35. Drozd, M.; Ivanova, P.; Tokarska, K.; Żukowski, K.; Kramarska, A.; Nowiński, A.; Kobylska, E.; Pietrzak, M.; Brzózka, Z.; Malinowska, E. Versatile and easily designable polyester-laser toner interfaces for site-oriented adsorption of antibodies. *Int. J. Mol. Sci.* **2022**, *23*, 3771. https://doi.org/10.3390/ijms23073771.
36. Shakeri, A.; Khan, S.; Didar, T.F. Conventional and emerging strategies for the fabrication and functionalization of PDMS-based microfluidic devices. *Lab Chip* **2021**, *21*, 3053–3075. https://doi.org/10.1039/d1lc00288k.
37. Novo, P.; Prazeres, D.M.F.; Chu, V.; Conde, J.P. Microspot-based ELISA in microfluidics: Chemiluminescence and colorimetry detection using integrated thin-film hydrogenated amorphous silicon photodiodes. *Lab Chip* **2011**, *11*, 4063–4071. https://doi.org/10.1039/c1lc20362b.
38. Wei, W.; Zhang, C.; Qian, J.; Liu, S. Multianalyte immunoassay chip for detection of tumor markers by chemiluminescent and colorimetric methods. *Anal. Bioanal. Chem.* **2011**, *401*, 3269–3274. https://doi.org/10.1007/s00216-011-5400-x.
39. Rodriguez-Moncayo, R.; Cedillo-Alcantar, D.F.; Guevara-Pantoja, P.E.; Chavez-Pineda, O.G.; Hernandez-Ortiz, J.A.; Amador-Hernandez, J.U.; Rojas-Velasco, G.; Sanchez-Muñoz, F.; Manzur-Sandoval, D.; Patino-Lopez, L.D.; et al. A high-throughput multiplexed microfluidic device for COVID-19 serology assays. *Lab Chip* **2020**, *21*, 93–104. https://doi.org/10.1039/d0lc01068e.
40. Irena, G.; Jolanta, B.; Karolina, Z. Chemical modification of poly(ethylene terephthalate) and immobilization of the selected enzymes on the modified film. *Appl. Surf. Sci.* **2009**, *255*, 8293–8298. https://doi.org/10.1016/j.apsusc.2009.05.126.
41. Golshaei, P.; Güven, O. Chemical modification of PET surface and subsequent graft copolymerization with poly(N-isopropylacrylamide). *React. Funct. Polym.* **2017**, *118*, 26–34. https://doi.org/10.1016/j.reactfunctpolym.2017.06.015.
42. Bùi, L.N.; Thompson, M.; McKeown, N.B.; Romaschin, A.D.; Kalman, P.G. Surface modification of the biomedical polymer poly(ethylene terephthalate). *Analyst* **1993**, *118*, 463–474. https://doi.org/10.1039/an9931800463.
43. Song, D.; Liu, J.; Xu, W.; Han, X.; Wang, H.; Cheng, Y.; Zhuo, Y.; Long, F. Rapid and quantitative detection of SARS-CoV-2 IgG antibody in serum using optofluidic point-of-care testing fluorescence biosensor. *Talanta* **2021**, *235*, 122800. https://doi.org/10.1016/j.talanta.2021.122800.
44. Kim, W.; Nishizawa, T.; Yoshimizu, M. Non-specific adsorption of fish immunoglobulin M (IgM) to blocking reagents on ELISA plate wells. *Dis. Aquat. Org.* **2007**, *78*, 55–59. https://doi.org/10.3354/dao01843.
45. Farajollahi, M.M.; Cook, D.B.; Hamzehlou, S.; Self, C.H. Reduction of non-specific binding in immunoassays requiring long incubations. *Scand. J. Clin. Lab. Investig.* **2012**, 72, 531–539. https://doi.org/10.3109/00365513.2012.702352.
46. Jiang, X.; Wu, M.; Albo, J.; Rao, Q. Non-Specific Binding and Cross-Reaction of ELISA: A Case Study of Porcine Hemoglobin Detection. *Foods* **2021**, *10*, 1708. https://doi.org/10.3390/foods10081708.
47. Ren, Z.M.; Nie, X.; Ai, S.S. Influence of Blocking Agents on Non-Specific Background of Polystyrene Microbeads in Serum Immunoassay. *Adv. Mater. Res.* **2013**, *641–642*, 858–861. https://doi.org/10.4028/www.scientific.net/amr.641-642.858.
48. Galbiati, S.; Damin, F.; Ferraro, L.; Soriani, N.; Burgio, V.; Ronzoni, M.; Gianni, L.; Ferrari, M.; Chiari, M. Microarray Approach Combined with ddPCR: A Useful Pipeline for the Detection and Quantification of Circulating Tumour DNA Mutations. *Cells* **2019**, *8*, 769. https://doi.org/10.3390/cells8080769.

49. Brambilla, D.; Panico, F.; Zarini, L.; Mussida, A.; Ferretti, A.M.; Aslan, M.; Ünlü, M.S.; Chiari, M. Copolymer-Coated Gold Nanoparticles: Enhanced Stability and Customizable Functionalization for Biological Assays. *Biosensors* **2024**, *14*, 319. https://doi.org/10.3390/bios14070319.
50. Mazzini, L.; Martinuzzi, D.; Hyseni, I.; Benincasa, L.; Molesti, E.; Casa, E.; Lapini, G.; Piu, P.; Trombetta, C.M.; Marchi, S.; et al. Comparative analyses of SARS-CoV-2 binding (IgG, IgM, IgA) and neutralizing antibodies from human serum samples. *J. Immunol. Methods* **2020**, *489*, 112937. https://doi.org/10.1016/j.jim.2020.112937.
51. Lee, P.; Plavina, T.; Castro, A.; Berman, M.; Jaiswal, D.; Rivas, S.; Schlain, B.; Subramanyam, M. A second-generation ELISA (STRATIFY JCV™ DxSelect™) for detection of JC virus antibodies in human serum and plasma to support progressive multifocal leukoencephalopathy risk stratification. *J. Clin. Virol.* **2013**, *57*, 141–146. https://doi.org/10.1016/j.jcv.2013.02.002.
52. Schroeder, H.W., Jr.; Cavacini, L. Structure and function of immunoglobulins. *J. Allergy Clin. Immunol.* **2010**, *125* (Suppl. 2), S41–S52. https://doi.org/10.1016/j.jaci.2009.09.046.
53. Luo, H.; Jia, T.; Chen, J.; Zeng, S.; Qiu, Z.; Wu, S.; Li, X.; Lei, Y.; Wang, X.; Wu, W.; et al. The Characterization of Disease Severity Associated IgG Subclasses Response in COVID-19 Patients. *Front. Immunol.* **2021**, *12*, 632814. https://doi.org/10.3389/fimmu.2021.632814.
54. Ma, H.; Zeng, W.; He, H.; Zhao, D.; Jiang, D.; Zhou, P.; Cheng, L.; Li, Y.; Ma, X.; Jin, T. Serum IgA, IgM, and IgG responses in COVID-19. *Cell. Mol. Immunol.* **2020**, *17*, 773–775. https://doi.org/10.1038/s41423-020-0474-z.
55. Quinti, I.; Mortari, E.P.; Salinas, A.F.; Milito, C.; Carsetti, R. IgA antibodies and IgA deficiency in SARS-CoV-2 infection. *Front. Cell. Infect. Microbiol.* **2021**, *11*, 655896. https://doi.org/10.3389/fcimb.2021.655896.
56. Oluka, G.K.; Namubiru, P.; Kato, L.; Ankunda, V.; Gombe, B.; Cotten, M.; The COVID-19 Immunoprofiling Team; Musenero, M.; Kaleebu, P.; Fox, J.; et al. Optimisation and validation of a conventional ELISA and cut-offs for detecting and quantifying anti-SARS-CoV-2 Spike, RBD, and Nucleoprotein IgG, IgM, and IgA antibodies in Uganda. *Front. Immunol.* **2023**, *14*, 1113194. https://doi.org/10.3389/fimmu.2023.1113194.
57. Rastawicki, W.; Juszczyk, G.; Gierczyński, R.; Zasada, A.A. Comparison of anti-SARS-CoV-2 IgG and IgA antibody responses post complete vaccination, 7 months later and after 3rd dose of the BNT162b2 vaccine in healthy adults. *J. Clin. Virol.* **2022**, *152*, 105193. https://doi.org/10.1016/j.jcv.2022.105193.
58. Boozer, C.; Ladd, J.; Chen, S.; Jiang, S. DNA-directed protein immobilization for simultaneous detection of multiple analytes by surface plasmon resonance biosensor. *Anal. Chem.* **2006**, *78*, 1515–1519. https://doi.org/10.1021/ac051923l.
59. Karoń, S.; Drozd, M.; Malinowska, E. A careful insight into DDI-type receptor layers on the way to improvement of click-biology-based immunosensors. *Biosensors* **2024**, *14*, 136. https://doi.org/10.3390/bios14030136.
60. Johnsson, B.; Löfås, S.; Lindquist, G.; Edström, Å.; Hillgren, R.M.; Hansson, A. Comparison of methods for immobilization to carboxymethyl dextran sensor surfaces by analysis of the specific activity of monoclonal antibodies. *J. Mol. Recognit.* **1995**, *8*, 125–131. https://doi.org/10.1002/jmr.300080122.
61. Butler, J.E. Solid Supports in Enzyme-Linked Immunosorbent Assay and Other Solid-Phase Immunoassays. *Methods* **2000**, *22*, 4–23. https://doi.org/10.1006/meth.2000.1031.
62. Niemeyer, C.M. Functional devices from DNA and proteins. *Nano Today* **2007**, *2*, 42–52. https://doi.org/10.1016/s1748-0132(07)70058-0.
63. Loo, J.F.; Ho, A.H.; Turner, A.P.; Mak, W.C. Integrated Printed Microfluidic Biosensors. *Trends Biotechnol.* **2019**, *37*, 1104–1120. https://doi.org/10.1016/j.tibtech.2019.03.009.
64. Shahriari, S.; Selvaganapathy, P.R. A Fully Integrated Microfluidic Device with Immobilized Dyes for Simultaneous Detection of Cell-Free DNA and Histones from Plasma Using Dehydrated Agarose Gates. *Gels* **2024**, *10*, 186. https://doi.org/10.3390/gels10030186.
65. Agarwal, A.; Salahuddin, A.; Ahamed, M.J. Demonstration of a Transparent and Adhesive Sealing Top for Microfluidic Lab-Chip Applications. *Sensors* **2024**, *24*, 1797. https://doi.org/10.3390/s24061797.
66. Karoń, S.; Porycka, K.; Lapitan, L.D.S., Jr.; Drozd, M.; Pietrzak, M.; Malinowska, E. A versatile approach to quality control of protein-based receptor layers by reversible, nonspecific staining for multiplex SPRi immunosensing. *Sens. Actuators B Chem.* **2024**, *421*, 136512. https://doi.org/10.1016/j.snb.2024.136512.

Suplement S4 publikacji P4:

PET Foils Functionalized with Reactive Copolymers as Adaptable Microvolume ELISA Spot Array Platforms for Multiplex Serological Analysis of SARS-CoV-2 Infections

Supplementary Material

PET Foils Functionalized with Reactive Copolymers as Adaptable Microvolume ELISA Spot Array Platforms for Multiplex Serological Analysis of SARS-CoV-2 Infections

Experimental

1. Reagents and Materials

Sodium chloride, potassium chloride, sodium hydrogen phosphate, sodium dihydrogen phosphate, magnesium nitrate, ammonium sulfate, and potassium dihydrogen phosphate were obtained from Sigma-Merck (Poznań, Poland). Ammonia (25%), hydrogen peroxide (30%), sulfuric acid (96%), and sodium hydroxide were obtained from Chempur (Piekary Śląskie, Poland). *p*-nitrophenyl phosphate (PNNP) was obtained from Glentham Life Sciences (Corsham, UK). Anti-human IgG clone line 7701, anti-human IgA clone line 8203 and monoclonal mouse anti-nucleoprotein antibody clone line 1143 were obtained from Medix Biochemica (Espoo, Finland). SARS-CoV Nucleocapsid recombinant protein expressed in *Escherichia coli*, goat anti-human IgG antibody conjugated with alkaline phosphatase, mouse anti-human IgG1, IgG2, IgG3, and IgG4 Fc secondary antibodies, and streptavidin were obtained from Thermo Fisher Scientific (Warsaw, Poland). Rabbit anti-mouse IgG antibody, and goat anti-mouse IgG antibody conjugated with alkaline phosphatase were obtained from Sigma-Aldrich (St. Louis, MO, USA). The proFIRE® Amine Coupling Kit for proteins (>5 kDa) was obtained from Dynamic Biosensors GmbH (Munich, Germany).

DNA oligonucleotide sequences

-NH_2 ligand strand (48 nt.) 5′-NH_2-C_6-ATC AGT ACT TGT CAA CAC GAG CAG CCC GTA TAT TCT CCT ACA GCA CTA-3′

- DBCO DNA probe (15 nt.) 5′-DBCO-TEG-TAG TGC TGT AGG AGA-3′

- NH_2 DNA probe (15 nt.) 5′-NH_2-TAG TGC TGT AGG AGA-3′

- biotin–DNA probe (15 nt.) 5′-biotin-(TEG)-TAG TGC TGT AGG AGA-3′

- ligand strand (48 nt.) 5′ -ATC AGT ACT TGT CAA CAC GAG CAG CCC GTA TAT TCT CCT ACA GCA CTA-3′

2. Methods

2.1 Conjugation of Receptor Proteins with ssDNA Anchors and Conjugates Purification

The conjugation process was performed using a DNA oligonucleotide with an amine-terminated ligand (3 nmol) and 200 μg of SARS-CoV-2 nucleoprotein or mouse monoclonal antibody against human IgG using the proFIRE® Amine Coupling Kit according to a previously developed protocol [36].

2.2 Protein immobilization on polystyrene plates for classic ELISA

To perform standard ELISA, antigens were immobilized onto 96-well polystyrene plates (either non-treated or MediSorp® plates) by adding 50 μL of a 10 μg/mL antigen solution prepared in 50 mM carbonate buffer (pH 9.6) to each well. Wells containing only carbonate buffer were used as references. The plates were incubated overnight at 4°C to allow protein adsorption. After incubation, plates were washed three times with PBST. To block nonspecific binding sites, 50 μL of 3% BSA in PBST was added to each well and incubated for 30 minutes at room temperature. All subsequent antibody or serum dilutions were prepared in PBST containing 3% BSA, and 50 μL of the appropriate solution was incubated in each well for 1 hour at room temperature (antibody concentration ~1 μg/mL unless otherwise specified). Actual sera samples after thawing were diluted 200 times (unless otherwise stated). Each incubation step was followed by three washes with PBST. Subsequently, 50 μL of an antibody-alkaline phosphatase conjugate, diluted to 3 μg/mL in PBST with 3% BSA, was added and

incubated for 1 hour at room temperature. The plate was then washed four times with PBST to remove unbound conjugate. Then, 10 mM freshly prepared PNNP in 50 mM carbonate buffer (pH 9.6) was used as the ALP substrate. The reaction was initiated by dispensing 90 µL of PNNP into each microwell, and detection was performed immediately after substrate addition. Absorbance was measured at 405 nm using a Multiskan Go microplate reader (Thermo Scientific, USA).

2.3 SPR slides preparation

SPR gold-coated slides were cleaned under UV/ozone (Ossila Ltd., Sheffield, UK) for 30 minutes, rinsed with deionized (DI) water, and then immersed in a "basic piranha" solution (25% ammonia, 30% hydrogen peroxide, and DI water in a 1:1:3 volumetric ratio) at 70°C for 15 minutes. After rinsing with DI water and drying under compressed air, the slides were soaked in an "acidic piranha" solution (3:1 v/v mixture of concentrated sulfuric acid and perhydrol) for 1 minute. The slides were then rinsed again with DI water and dried.

2.4 SPR slide modification

Bare gold-coated slides were treated with a UV/ozone cleaner (Ossila, UK) for 10 minutes and then dip-coated overnight at room temperature with an aqueous solution of Copoly Azide, as described previously. After coating, the slides were rinsed with DI water, dried under compressed air, and cured under vacuum at 80°C for 15 minutes. The Copoly Azide-coated slides were then manually covered with 100 µL of a 0.5 µM DBCO-modified DNA solution and incubated overnight at 4°C in a humid atmosphere. Slides were then rinsed with DI water, dried under compressed air, and prepared for SPR measurements.

For label-free studies and DDI immunoassay design, SPR transducers were covalently modified with streptavidin and coated with a biotin–DNA probe. Streptavidin was immobilized on the PEG-COOH-coated slide by injecting a 50 µg/mL solution in 5 mM acetate buffer (pH 5.0) for 20 minutes, following a previously described protocol [37]. Subsequently, 1 µM

biotin–DNA probe solution in PBST was injected for 20 minutes to immobilize ssDNA, followed by washing with PBST until a stable signal was achieved.

2.5 Immobilization of Protein Conjugates and Surface Plasmon Resonance Imaging Measurements

Kinetic studies on the immobilization of ligand strand and protein conjugates were carried out with SPRi Lab Plus instrument (Horiba, France). PBS buffer with 0.05% Tween® 20 (PBST) was used as the running buffer at a flow rate of 80 µL/min. The ligand strand (2.7 µM in PBST) or protein conjugate (~20 nM in 50 mM phosphate buffer, pH 7.2, with 150 mM NaCl) was injected manually (flow rate: 80 µL/min, ~5 min) to monitor DNA-directed protein immobilization in real-time. For regeneration between injections, 50 mM sodium hydroxide was applied at 80 µL/min for 4 minutes. Immunolabeling was performed at the end of each experiment by injecting a 5-minute solution of a specific antibody (anti-mouse IgG or anti-SARS-CoV-2 NP antibodies, 50 µg/mL in PBST).

Figure S1

A

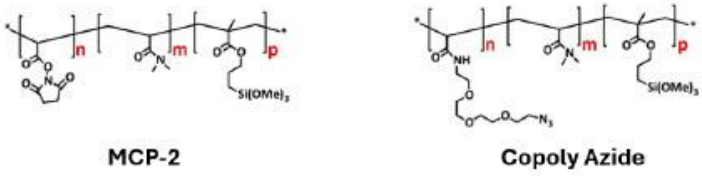

MCP-2 Copoly Azide

B

Copolymer	Monomer molar ratio		
	DMA (m)	NAS/N_3 (n)	MAPS (p)
MCP-2	97	2	1
Copoly Azide	95	4	1

C

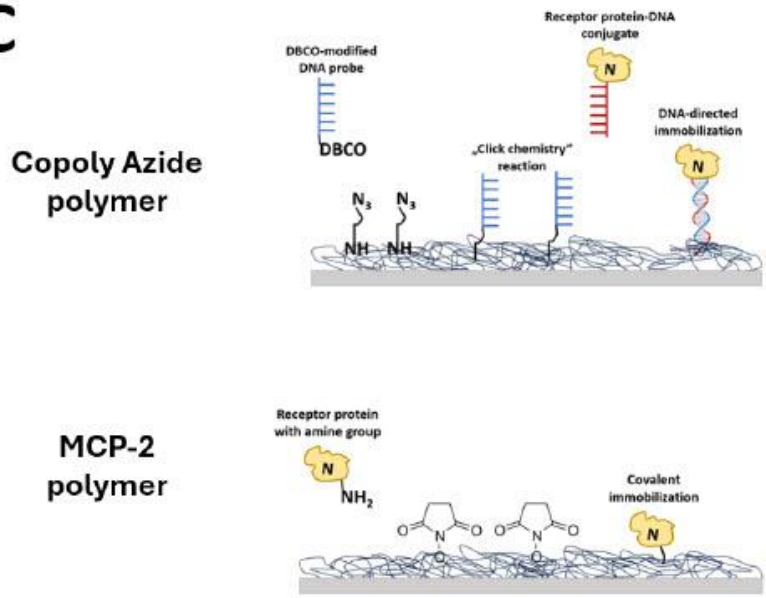

Fig. S1. Copolymers composition. A – Chemical structure of MCP-2 and Copoly Azide. B – Monomer molar ratios for MCP-2 and Copoly Azide. C – Schematic mechanism of receptor protein immobilization on PET foil coated with Copoly Azide and MCP-2.

Figure S2

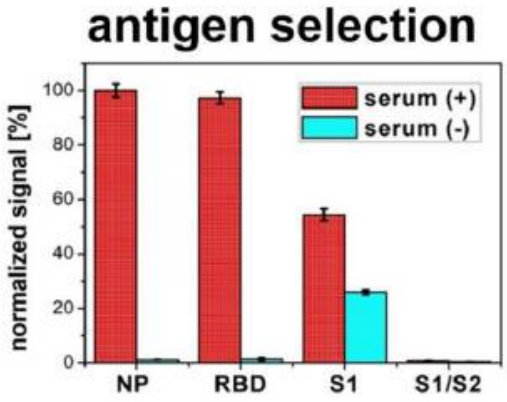

Fig. S2. Specific (red) and non-specific (light blue) signals for various SARS-CoV-2 protein receptors.

Figure S3

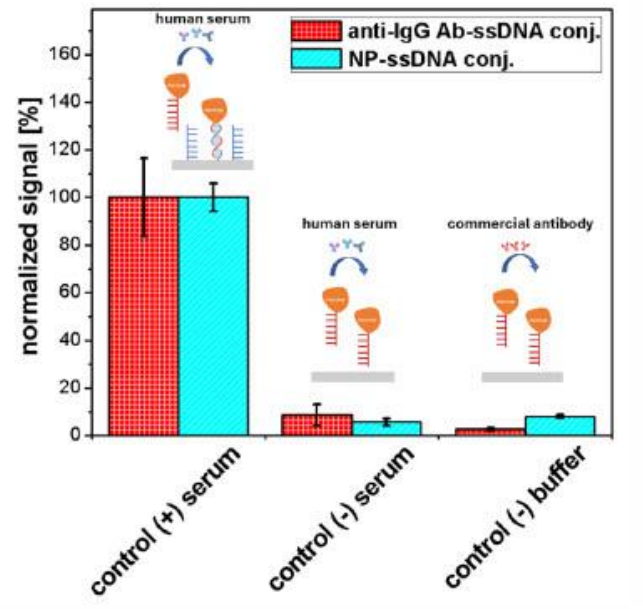

Fig. S3. Results of specificity studies for DDI-type immobilization.

References

[59] **Karoń, S., Drozd, M., & Malinowska, E.** (2024). A Careful Insight into DDI-Type Receptor Layers on the Way to Improvement of Click-Biology-Based Immunosensors. Biosensors, 14(3), 136. https://doi.org/10.3390/bios14030136

[66] **Karoń, S., Porycka, K., Lapitan, L. D. S. Jr., Drozd, M., Pietrzak, M., & Malinowska, E.** (2024). A Versatile Approach to Quality Control of Protein-Based Receptor Layers by Reversible, Nonspecific Staining for Multiplex SPRi Immunosensing. Sensors and Actuators B: Chemical, 136512. https://doi.org/10.1016/j.snb.2024.136512

Dorobek naukowy autorki

Artykuły naukowe

- Raza, S., Matuła, K., **Karoń, S.**, Paczesny, J. Resistance and adaptation of bacteria to non-antibiotic antibacterial agents: Physical stressors, nanoparticles, and bacteriophages. Antibiotics, 2021, 10(4), 435

- Drozd, M., **Karoń, S.**, Malinowska, E. Recent advancements in receptor layer engineering for applications in spr-based immunodiagnostics. Sensors, 2021, 21(11), 3781

- Ivanova, P., Drozd, M., Michrowski, K., **Karoń, S.**, Mazurkiewicz-Pawlicka, M., Pietrzak, M. Au-X (X=Pt/Ru)-decorated magnetic nanocubes as bifunctional nanozyme labels in colorimetric, magnetically-enhanced, one-step sandwich CRP immunoassay. Biosensors and Bioelectronics, 2023, 237, 115511

- **Karoń, S.**, Drozd, M., Malinowska, E. A Careful Insight into DDI-Type Receptor Layers on the Way to Improvement of Click-Biology-Based Immunosensors. Biosensors, 2024, 14(3), 136

- **Karoń, S.**, Porycka, K., Lapitan, Jr, L.D., Pietrzak, M., Malinowska, E. A versatile approach to quality control of protein-based receptor layers by reversible, nonspecific staining for multiplex SPRi immunosensing. Sensors and Actuators B: Chemical, 2024, 421, 136512

- **Pniewska, S.**, Drozd, M., Mussida, A., Brambilla D., Chiari M., Rastawicki, W., Malinowska, E. PET Foils Functionalized with Reactive Copolymers as Adaptable Microvolume ELISA Spot Array Platforms for Multiplex Serological Analysis of SARS-CoV-2 Infections. Sensors, 2024, 24(23), 7766

Udział w projektach badawczych

- Opracowanie konstrukcji i technologii wytwarzania miniaturowych urządzeń diagnostycznych do szybkiego wykrywania wirusa SARS-CoV-2 w trybie POCT, projekt Narodowego Centrum Badań i Rozwoju (POIR.01.01.01-00-0638/20), **wykonawczyni projektu**

- Opracowanie kompozycji metaliczno-polimerowych oraz technologii wytwarzania na ich bazie włóknin warstwowych o właściwościach przeciwdrobnoustrojowych i filtracyjnych dla produktów sanitarnych lub ochrony medycznej, projekt Narodowego Centrum Badań i Rozwoju ((POIR.01.01.01-00-1246/20), **wykonawczyni projektu**

- Konstrukcja uniwersalnego, przenośnego urządzenia mikrofluidycznego działającego w formacie pasywnego przepływu do szybkiej immunodetekcji zakażeń wirusowych i monitorowania wybranych biomarkerów odpowiedzi immunologicznej, projekt „Inicjatywa Doskonałości - Uczelnia Badawcza" (1820/102/Z01/2023), **wnioskodawczyni i wykonawczyni projektu**

Udział w konferencjach naukowych w kraju i zagranicą

- M. Drozd, P. Ivanova, K. Tokarska, K. Żukowski, **S. Karoń**, A. Duszczyk, M. Pietrzak, A. Nowiński, Z. Brzózka, E. Malinowska. „Flexible polymeric substrates as versatile platforms for rapid POCT immunodiagnostics", 13th Annual Next Generation Summit, konferencja online, sierpień 2021, **współautorstwo posteru**

- **S. Karoń**, M. Drozd, E. Malinowska. „Simple design of antibody-based microarrays via DNA- directed immobilization in multiplex diagnostics of viral infection, NanoMedicine 2021, Mediolan, październik 2021, **prezentacja posteru**

- **S. Karoń**, M. Drozd, E. Malinowska. “Development of functional receptor layers based on DNA-directed immobilization for the SPR immunosensing of viral infection biomarkers, 9th International Symposium on Sensor Science, Warszawa, czerwiec 2022, **prezentacja posteru**

- M. Drozd, P. Ivanova, **S. Karoń**, A. Duszczyk, K. Tokarska, E. Malinowska. “Miniaturized Immunoplatforms Supporting the Diagnosis of Lung Cancer Biomarkers and Immunotherapies”, 9th International Symposium on Sensor Science, Warszawa, czerwiec 2022, **współautorstwo posteru**

- **S. Karoń**, M. Drozd, E. Malinowska. “Analogues-directed immobilization in fabrication of microarrays for immunodiagnostic of viral infections, Sensors, Ateny, październik 2022, **prezentacja posteru**

- M. Lelit, M. Słowikowski, M. Juchniewicz, B. Stonio, B. Michalak, K. Pavłov, M. Filipiak, M. Myśliwiec, P. Wiśniewski, K. P. Anders, S. T. Stopiński, A. Duszczyk, **S. Karoń**, R. B. Beck, R. Piramidowicz. „Functionalized photonic silicon-nitride-based integrated circuits operating in visible wavelengths for biosensing applications”, 17th Conference Integrated Optics - Sensors, Sensing Structures and Methods, Szczyrk, luty 2023, **współautorstwo prezentacji**

- M. Drozd, K. Tokarska, Z. Tylenda, **S. Karoń**, K. Żukowski, M. Pietrzak, E. Malinowska, Z. Brzózka. “Disposable, flexible microfluidic system for rapid, pre-analytical separation of IgG antibodies from serum samples”, The 27th International Conference on Miniaturized Systems for Chemistry and Life Sciences (μTAS), Katowice, październik 2023, **współautorstwo posteru**

- **S. Karoń**, K. Porycka, LDS Lapitan, M. Drozd, M. Pietrzak, E. Malinowska. „Nonspecific staining of protein receptor layers as a quality control method for SPRi-based multiplexed biosensing”, 4th International Electronic Conference on Biosensors, konferencja online maj 2024, **prezentacja posteru**

- K. Porycka, **S. Karoń**, M. Drozd, K. Tokarska, K. Żukowski, E. Malinowska. "Development of the microfluidic Lab-on-a-Foil platform for pre-analytical separation of human IgG", 4th International Electronic Conference on Biosensors, konferencja online maj 2024, **współautorstwo posteru**

- K. Porycka, **S. Karoń**, M. Drozd, K. Tokarska, K. Żukowski, E. Malinowska. "A/G protein-based, microfluidic system for the small-scale, preparative separation of IgG from human serum", STER Summer School of Redox Processes, Warszawa, czerwiec 2024, **współautorstwo posteru**

- **S. Pniewska**, M. Drozd, LDS Lapitan, E. Malinowska. „Malinowska The development of customizable biosensing platforms for multiplex immunodetection of various infection-related biomarkers based on DNA-directed immobilization", The 1st International Conference on AI Sensors and 10th International Symposium on Sensor Science, Singapur, sierpień 2024, **prezentacja ustna**

Nagrody

- A. Duszczyk A., B. Bałamut, **S. Karoń**, Lelit M., P. Rękas, A. Szymczyk.
  II miejsce w konkursie MedTech-Athon – inżynierowie dla medycyny (wygrana grupowa), finansowanie w ramach programu „Inicjatywa Doskonałości – Uczelnia Badawcza", Warszawa, maj 2022

Wyjazdy naukowe

- Trzymiesięczny wyjazd naukowy (kwiecień-czerwiec 2023) w ramach pogramu Mobility i NAWA STER do instytutu badawczego w Mediolanie - Instituto di Scienze e Tecnologie Chimiche CNR – SCITEC, grupa profesor Marcelli Chiari

Rola Opiekuna Naukowego

- Praca dyplomowa inżynierska Karoliny Poryckiej pt. *Zastosowanie przeciwciał znakowanych DNA w projektowaniu uniwersalnych podłoży immunosensorowych do detekcji przeciwciał i biomarkerów chorób wirusowych*, kierunek Biotechnologia, numer pracy według wydziałowej ewidencji prac: 102C-ISP-BI/307108/1202328, promotor: dr inż. Marcin Drozd

- Praca dyplomowa magisterka Karoliny Poryckiej pt. *Uniwersalne warstwy immunoreceptorowe dla systemów diagnostycznych Lab-on-a-Foil*, kierunek Biotechnologia, numer pracy według wydziałowej ewidencji prac: 102D-MSP-BI/307108/1290445, promotor: dr inż. Marcin Drozd